ACTA UNIVERSITATIS SZEGEDIENSIS

ACTA MINERALOGICA-PETROGRAPHICA

Tomus XLI.

SZEGED, HUNGARIA
2000

NOTE TO CONTRIBUTORS

General

The Acta Mineralogica–Petrographica publishes original studies on the field of geochemistry mineralogy and petrology, first of all studies Hungarian researches, papers resulted in by cooperation of Hungarian researches and those of other countries and, in a limited volume, papers from abroad on topics of global interest.

Manuscripts should be written in English and submitted to the Editor-in-chief, Institute of Mineralogy, Geochemistry and Petrography, Attila József University, H–6701 Szeged, Pf. 651 Hungary.

The authors are responsible for the accuracy of their data, references and quotations from other sources.

Manuscript

Manuscript should be typewritten with double spacing, 25 lines on a page and space for 50 letter in a line. Each new paragraph should begin with an indented line. Underline only words that should be typed in italics.

Manuscript should be generally be organized in the following order:

Title
Name(s) of author(s) and their affiliations, in foot-note the address of the author to whom the correspondence should be sent
Abstract
Introduction
Methods, techniques, material studied, description of the area investigated, etc.
Results
Discussion or conclusions
Acknowledgement
Explanation of plates (if any)
Tables
Captions of figures (drawings, photomicrographs, etc.)

Abstract

The abstract cannot be longer than 500 words.

Tables

The tables should be typewritten on separate sheets and numbered according to their sequence in the text, which refers to all tables.

The title of the table as well as the column headings must be brief, but sufficiently explanatory.

The tables generally should not exceed the type-area of the journal, i.e. 12,5x18,5 cm. Foldouts can only exceptionally be accepted.

(continuation on the inner side of verso)

ACTA UNIVERSITATIS SZEGEDIENSIS

ACTA MINERALOGICA-PETROGRAPHICA

Tomus XLI.

SZEGED, HUNGARIA
2000

HU ISSN 0365-8066

SERIES NOSTRA AB INSTITUTIS MINERALOGICIS, GEOCHEMICIS PETROGRAPHICS UNIVERSITATUM HUNGARICUM ADIUVATUR

Adjuvantibus

IMRE KUBOVICS
FRIGYES EGERER
GYULA SZÖÖR
BÉLA KLEB

Regidit

TIBOR SZEDERKÉNYI

Editor

Institut Mineralogicum, Geochemicum et Petrographicum
Universitatis Szegediensis

Nota

Acta Miner. Petr., Szeged

Szerkeszti

SZEDERKÉNYI TIBOR

a szerkesztőbizottság tagjai

KUBOVICS IMRE
EGERER FRIGYES
SZÖÖR GYULA
KLEB BÉLA

Kiadja

a Szegedi Tudományegyetem Ásványtani, Geokémiai és Kőzettani Tanszéke
H–6722 Szeged, Egyetem u. 2–6.

Kiadványunk címének rövidítése
Acta Miner. Petr., Szeged

SOROZATUNK A MAGYARORSZÁGI EGYETEMEK ROKON TANSZÉKEINEK TÁMOGATÁSÁVAL JELENIK MEG

Printed in JUHÁSZ NYOMDA, Szeged

Acta Mineralogica-Petrographica, Szeged, XLI, 3–8, 2000

HOGBOMITE FROM Fe-Ti OXIDE DEPOSIT, BOULA-NAUSAHI IGNEOUS COMPLEX, KEONJHAR DISTRICT, ORISSA, INDIA

J. K. MOHANTY*, S. KHAOASH** AND A. K. PAUL**

* Regional Research Laboratory
** Utkal University

ABSTRACT

Primary and secondary hogbomites occurs both as well developed crystals and anhedral grains in Fe-Ti oxide ores of Boula-Nausahi igneous complex. Primary hogbomite is pyrogenic in nature having formed from the magma at a low temperature. The secondary hogbomite has formed at the expense of spinel by the substitution of Ti^{2+} for Mg^{2+} and Fe^{3+} for Al^{3+}. EPMA of hogbomite showed 6-9.59 wt% TiO_2, 57.51 – 59 wt% Al_2O_3, 0-1.99 wt%, Cr_2O_3, 21.43-29.93 wt%, FeO(t), 0.02-0.23 wt%, MnO, 2.46-8.17 wt%, MgO and 1.03-1.84 wt% ZnO. The stoichiometric formula, $Fe^{2+}_{(2.7\text{-}5.09)}Mg_{(0.81\text{-}2.66)}Ti_{(1\text{-}1.156)}Fe^{3+}_{(0.432\text{-}1.124)}Al_{(14.86\text{-}15.345)}O_{32}$ suggests that hogbomite has an open structure as compared to associated magnetite and ilmenite.

Key words: Hogbomite, Fe-Ti oxide ores, Boula-Nausahi complex, India.

INTRODUCTION

Hogbomite has been reported from different parts of world and in a wide spectrum of igneous and metamorphic associations (NEL, 1949; FRIEDMAN, 1952; WOODFORD and WILSON, 1976; ZAKRZEWSKI, 1977; GATEHOUSE and GREY, 1982; ANGUS and MIDDLETON, 1985 and GREW et al., 1990). However, in India, occurrence of hogbomite was first reported by DEVRAJU et al., (1981). Subsequently, JAYARAY et al, (1995) have recorded widespread distribution of the mineral in the Ti-V magnetite deposits in Shimoga and Uttara Kannada districts of Karnataka. In this paper, an attempt has been made to study the textural characters, mineral chemistry and origin of the hogbomite from Boula-Nausahi igneous complex, Orissa, India.

GEOLOGICAL SETTING

Boula-Nausahi Igneous complex (21°15'-21°18'N: 86°18'-86°20'E) is intruded into the Precambrian metamorphics of Iron Ore Group and the age of emplacement is around 2200 Ma (SAHA, 1994). This complex consists of the ultramafics, the mafics and the felsic rock units. The ultramafic rocks (now altered to serpentinites) host chromite ore bodies whereas the mafic rocks represented by gabbro, norite, anorthosite host titaniferous magnetite ore bodies.

* Bhubaneswar-751 013, Orissa, India
** Bhubaneswar, Orissa, India

MINERALOGY

The Ti-V-magnetite ore consists of titanomagnetite (magnetite), ilmenite, spinel, hematite, rutile, hogbomite, goethite, martite, lepidocrocite etc., in varied proportions. Chalcopyrite, covellite and pyrite are present in very minor amounts. Magnetite occurs in coarse, irregular to subhedral grains making upto 70% of the ore. Besides being intergrown with ilmenite, it also occurs as small granules in ilmenite grains, minute platelets in ilmenite along fractures and at the ilmenite grain boundaries. Ilmenite occurs as broad and fine lamellae and as discrete euhedral to irregular grains. Spinel is present as fine rod-like exsolution in magnetite and as tiny dots along ilmenite boundaries. Hematite occurs as exsolved lamellae in ilmenite.

Magnetite exhibits a characteristic polycrystalline granular texture in which the grain boundaries meet at triple points with an interfacial angle of 120°. Ilmenite occurs in juxtapositon with magnetite developing non-interfering boundary relationship. Besides, several textures such as (1) crystallographic intergrowth viz. ilmenite in (111) and (100) planes of magnetite, spinel in (111) plane of magnetite, hematite in (0001) plane of ilmenite, (2) graphic intergrowth between magnetite and ilmenite, (3) eutectoid like intergrowth between rutile and hematite, (4) external and internal granular intergrowth of ilmenite and (5) replacement texture (viz., replacement of magnetite by martite, goethite and lepidocrocite and ilmenite by rutile) are noted. The oriented intergrowths appear to have resulted due to exsolution above magnetite-ulvospinel solvus and exsolution-oxidation below magnetite-ulvospinel solvus (REYNOLDS, 1985).

TABLE 1

EPMA of Magnetite and Ilmenite grains in the Ti-V magnetite ores

	1	2	3	4	5	6	7	8	9	10
FeO	74.43	75.87	73.95	76.16	73.26	45.68	44.31	43.84	45.64	43.61
TiO2	12.93	13.92	13.75	17.86	14.81	53.11	54.11	54.38	50.88	53.38
MgO	0.19	0.05	0.06	0.65	0.33	0.16	0.36	1.56	0.15	1.30
Al_2O_3	0.76	1.37	0.32	0.19	0.19	0.01	0.15	0.02	0.09	0.03
MnO	0.14	0.20	0.11	0.26	0.32	0.87	1.02	0.91	0.81	0.93
Cr_2O_3	1.35	1.27	1.19	0.05	0.22	0.13	0.11	0.05	0.20	0
ZnO	0.09	0.13	0.01	0.08	0	0.12	0.09	0	0.12	0
V_2O_3	0.06	0.08	0.08	0.08	0.08	0.29	0.28	0.28	0.28	0.29
Total	89.95	92.87	89.47	95.34	89.21	100.38	100.42	101.04	98.16	99.53
	Cations on the basis of 4 (O)					Cations on the basis of 3 (O)				
Fe	2.923	2.860	2.921	2.76	2.883	0.977	0.921	0.902	0.984	0.913
Ti	0.457	0.472	0.488	0.582	0.524	1.001	1.012	1.006	0.986	1.005
Mg	0.013	0.003	0.003	0.042	0.023	0.006	0.013	0.057	0.006	0.048
Al	0.042	0.073	0.018	0.028	0.01	0	0.004	0.001	0.003	0.001
Mn	0.006	0.008	0.004	0.01	0.013	0.019	0.021	0.019	0.018	0.02
Cr	0.05	0.045	0.044	0.002	0.008	0.003	0.002	0.001	0.004	0
Zn	0.003	0.004	0	0.003	0	0.002	0.002	0	0.002	0
V	0.002	0.003	0.003	0.003	0.003	0.006	0.006	0.006	0.006	0.006
Total	3.496	3.468	3.482	3.428	3.465	2.013	1.981	1.991	2.008	1.992

Sample: 1-5 Magnetite; 6-10 Ilmenite

Chemical composition and structural formula of magnetite and ilmenite are presented in Table 1. In this ore, chlorite is the major silicate mineral. Except for somewhat higher alumina and lower silica (Table 2), chemically it is comparable with sheridanite reported by WILSON (1977) and DEVRAJU et al., (1981).

TABLE 2

EPMA of the associated chlorites

	1	2	3	4
FeO	9.02	10.69	9.44	10.82
TiO2	0.31	0.16	0.64	1.65
MgO	26.13	26.36	25.23	24.93
Al_2O_3	31.66	31.57	32.37	29.90
MnO	0	0.03	0.09	0.08
Cr_2O_3	0	0	0.08	0.10
ZnO	0.05	0	0.09	0
V_2O_3	0	0	0.01	0.01
SiO_2	21.05	21.79	21.32	22.64
Total	88.21	90.61	89.24	90.13
Cations on the basis of 10 (O)				
Fe	0.520	0.605	0.539	0.617
Ti	0.016	0.008	0.033	0.086
Mg	2.686	2.657	2.566	2.525
Al	2.572	2.516	2.853	2.394
Mn	0	0.002	0.005	0.004
Cr	0	0	0.004	0.008
Zn	0.003	0	0.005	0
V	0	0	0	0
Si	1.450	1.473	1.455	1.540
Total	7.247	7.260	7.459	7.174

Hogbomite

This is a minor mineral in the magnetite ore. It shows deep brown colour, feeble pleochroism, one set longitudinal cleavage and irregular cracks under transmitted light. Under reflected light, it is characterized by grey colour with or without pinkish tinge, feeble bireflectance, very low reflectivity (around 8%), distinct anisotropism, reddish brown internal reflection and high microhardness (VHN = 1000 to 1250 newton). Presence of hogbomite is also confirmed by d values of 2.438, 1.427 and 2.098 Å in XRD pattern.

Textural characters

Textural hogbomite occurs as (a) idiomorphic (rhombohedral, bipyramidal, hexagonal), hypidiomorphic (prismatic, pinacoidal, tabular, platy and cylindrical) and irregular shaped disseminations, (b) irregular grains intergrown with spinel, (c) partial overgrowth in spinel in a matrix of magnetite and in the interface between ilmenite and magnetite, (d) mosaic aggregates showing scalloped boundaries against magnetite and (e) subhedral grains partially rimmed by dark chlorite. Rows of hogbomite disseminations are

crystallo-graphically oriented along both cubic and octahedral cleavages in magnetite. It is observed that highly martitised ores contain more hogbomite which can be explained by removal of alumina from spinel concurrently with oxidation of Fe during martitisation (ZAKRZEWSKI, 1977). Moreover, well developed crystals of hogbomite have been found to occur in ores containing higher modal percentage of hogbomite.

Mineral chemistry

Electronprobe analyses of a few hogbomite grains are carried out by JEOL JXA-8600 M Superprobe using SPI standards with an accelerating voltage of 15 KV, specimen current of 2 mA and online oxide ZAF correction programme. The elemental composition and the cation contents obtained are given in Table 3. Selected analyses of hogbomites from different parts of world are also presented for comparison.

TABLE 3

EPMA of hogbomite of Boula-Nausahi complex compared with hogbomites from other parts of world

	1	2	3	4	5	6	7	8	9
FeO	29.93	28.63	29.20	21.42	22.39	20.27	24.78	21.02	12.36
TiO_2	6.21	6.92	6.01	9.59	8	6.19	7.41	6.01	6.42
MgO	2.51	2.46	2.6	7.59	8.17	9.96	5	9.66	16.6
Al_2O_3	57.51	58.14	58.5	59	57.72	59.86	58.53	59.94	63.75
MnO	0.23	0.17	0.23	0.03	0.02	0.13	0.26	0.14	0.13
Cr_2O_3	1.88	1.99	1.77	0	0.08	0.29	0	0	0.31
ZnO	1.27	1.04	1.03	1.47	1.84	0.87	2.74	1.06	0.46
V_2O_3	0.03	0.04	0.04	0.05	0.04	0.13	0	0.21	0
Total	99.57	99.39	99.38	99.51	98.26	97.64	98.72	98.04	100.03
Cations of the basis of 32 (O)									
Fe^{2+}	5.078	4.884	5.09	2.706	2.97	2.929	4.343	3.136	1.04
Fe^{3+}	0.518	0.432	0.342	1.124	1.12	0.724		0.66	1
Ti	1.045	1.156	1.004	1.542	1.314	0.994	1.168	0.976	0.96
Mg	0.835	0.813	0.863	2.533	2.662	3.2	1.562	3.108	4.92
Al	15.152	15.219	15.345	14.868	14.86	15.205	14.457	15.304	14.96
Mn	0.043	0.032	0.041	0.005	0.004	0.02	0.05	0.004	0.04
Cr	0.33	0.347	0.31	0	0.013	0.049	0	0	0.04
Zn	0.208	0.171	0.168	0.233	0.295	0.14	0.424	0.168	0.08
V	0.003	0.003	0.003	0.008	0.006	0.021	0	0.036	0
Total	23.212	23.056	23.167	23.019	23.244	23.282	22.414	23.352	23.04

Samples: 1-5 Boula-Nausahi complex, 6: JAYARAJ et al., (1995), 7: GREW et al., (1990), 8: DEVRAJU et al. (1981), 9: ZAKRZEWSKI (1977)

From the Table 3, it is observed that hogbomite grains show considerable compositional variation in respect of FeO, TiO_2, MgO, MnO and Cr_2O_3. Average chemical data when compared with the analyses from other parts of the world show that the hogbomites of the present area are rich in FeO, TiO_2, Cr_2O_3 and ZnO and impoverished in MgO. TiO_2, MgO and ZnO show inverse relation with FeO where as MnO and Cr_2O_3

exhibit a positive relation with FeO. As compared to the hogbomites of Tanzania, the hogbomites of present area are rich in FeO, Cr_2O_3 and poor in MgO and Al_2O_3. Compared to the hogbomite from Karnataka, India these are richer in Fe, Cr, Ti and Zn but poorer in Mg and V (JAYARAJ, et al., 1995). Negative relationships between Fe and Ti (r = -0.94), Fe and Mg (r = -0.98) and Fe and Al (r = -0.40) indicate that Ti, Mg and Al replace Fe2+ and Fe3+ in the hogbomite structure. Higher {Fe(t)/Fe(t)+Mg} ratio of 0.78 to 0.94 is attributable to very low concentration of Mg in the mineral derived rom the magma having very-low MgO content (MANCKTELOW, 1981, ANGUS and MIDDLETON, 1985, RAMMLMAIR et al., 1988, GREW et al., 1990; JAYARAJ et al, 1995). From the chemical analyses, it is seen that the structure of hogbomite is more open than the co-existing magnetite and ilmenite and can admit a variety of substitution.

A generalized stoichiometric formula calculated according to ZAKRZEWSKI (1977) is as follows:

$$Fe^{2+}_{(2.7\text{-}5.09)}\ Mg_{(0.81\text{-}2.66)}\ Ti_{(1\text{-}1.156)}\ Fe^{3+}_{(0.432\text{-}1.124)}\ Al_{(14.86\text{-}15.345)}\ O_{32}$$

DISCUSSION AND CONCLUSION

Based on textural features and the pattern of association with magnetite, chlorite and spinel, hogbomite formation in Fe-Ti ores of Boula-Nausahi complex can be put into two categories i e., (1) primary or pyrogenic eg., those formed directly from the magma either as external granule exsolution or as oxidation-exsolution at a slightly low temperature and (2) secondary eg., those formed after spinel as alteration product.

Isolated hogbomite grains of varied morphology may have formed by external granule exsolution skin to formation of coarse grained euhedral ilmenite in most titanomagnetite ore bodies (BUDDINGTON and LINDSLEY, 1964, GREW et al., 1990). These alongwith very fine grained hogbomite grains found enclosed within the titanomagnetite ore under electron microscope and exsolved blebs of hogbomite found oriented along (111) cleavage in magnetite can be termed as primary having formed directly from the magma at falling temperature.

Association with spinel and chlorite points to the secondary nature of hogbomite. Spinel-hercynite can alter to hogbomite (GREW et al., 1990). Scanning Electron Microscopic study of hogbomite grain in association with spinel-hercynite and mutual textural and interface boundary relationship indicate the secondary nature of a few hogbomite grains. The hogbomite associated with spinel is formed at the expense of spinel by the substitution of Ti^{2+} for (Mg^{2+}, Fe^{2+}) and Fe^{3+} for Al^{3+} under silica undersaturation and high oxygen fugacity condition. The scooping/scalloping of boundaries of hogbomite suggest late stage replacement of spinel/hogbomite by magnetite.

Fe-Ti oxide ore bodies in this area are formed around 700-900 °C temperature and oxygen fugacity of 10^{-9} to 10^{-17} (TUGARINOV et al., 1973, MOHANTY, 1994.) Previous works suggest that primary hogbomite can be formed at a low temperature of 400-500 °C (SOUTHWICK, 1968; MICLKE AND SCHREYER, 1972; RUMBLE, 1976; BRAUN and RAITH, 1985). Though direct estimation of temperature and oxygen fugacity of hogbomite formation could not be determined in the present case, based on textural relation it may be surmised that hogbomite at Boula-Nausahi igneous complex has formed at low temperature, and high oxygen fugacity and in the presence of water.

ACKNOWLEDGEMENTS

The authors are thankful to the Director for his permission to publish this paper. Thanks are also due to Director, USIC, Roorkee and Dr. B. K. Mohapatra, scientist, RRL, Bhubaneswar for providing EPMA and SEM facility respectively

REFERENCES

ANGUS, N. S. and MIDDLETON, R. (1985): Compositional variation in hogbomites from North Connemara, Ireland. Min. Mag. 49, 649-654.

BRAUN, E. and RAITH, M. (1985): Fe-Ti oxides in metamorphic basites from the eastern Alps, Austria: A contribution to the formation of solid solutions of natural Fe-Ti oxide assemblages. Contr. Miner. Petrol. 90, 199-213.

DEVARAJU, T. C.; UTTANGI, V. H. and COOLEN, J. J. M. M. M. (1981): Hogbomite from Fe-Ti deposit of Madangere, Ankola Taluk, Karnataka. J. Geol. Soc. India, 22, 439-443.

FRIEDMAN, G. M. (1952): Study of Hogbomite. Am. Minerl., v. 37, pp. 600–608.

GATEHOUSE, B. M. and GREY, L. E. (1982): The crystal structure of hogbomite-8H. Am. Miner. 67, 373-380.

GREW, E. S.; HIROI, Y. and SHIRAISHI, K. (1990): Hogbomite from the Prince Olav Coast, East Antarctica: An example of oxidation-exsolution of a complex magnetite solid solution? V. 75, 589-600.

JAYARAJ, K. R.; KHANADALI, S. D.; DEVARAJU, T. C. and SPIERING, B. (1995): A study of hogbomite in the V-Ti-Fe deposits of Karnataka. J. Geol. Soc. India, 45, 57-64.

MANCKTELOW, N. S. (1981): Hogbomite of unusal composition from Reedy Creek, S. Africa. Min. Mag. 44, 91-94.

MIELKE, H. and SCHREYER, W. (1972): Magnetite-rutile-assemblages in metapelites of the Fichtelgebrige, Germany. Earth and Planetary Sci. Lett. 16, 423-428.

MOHANTY, J. K. (1994): Geology, mineralogy and geochemistry of Boula-Nausahi Igneous Complex with special reference to the associated economic ore minerals. Unpublished Ph.D Thesis, Utkal University, Orissa, India.

NEL, H. J. (1949): Hogbomite from the corundum fields of Eastern Transvaal, S. Afr. Geol. Surv. Mem, 43, 1-7.

RAMLMAIR, D.; MOGESSIE, A.; PURTSCHELLER, F. and TESSADRI, R. (1988): Hogbomite from the Vumba schist belt, Botswana, Am. . Miner. 73, 651-656.

REYNOLDS, I. M. (1985): Contrasted mineralogy and textural relationships in the uppermost titaniferous magnetite layers of the Bushveld complex in the Bierkraal area, North of Rustenburg. Econ. Geol. 80, 1027-1048.

RUMBLE, D. III (1976): Oxide minerals in metamorphic rocks. In Mineralogical Society of America, Reviews in Mineralogy, 3, R1-R24.

SAHA, A. K. (1994): Crustal evolution of Singhbhum, N. Orissa, E. India. Mem. Geol. Soc. India, 27, 1-34.

SOUTHWICK, D. I. (1968): Mineralogy of a rutile- and apatite bearing ultramafic chlorite rock, Harford Country, Maryland. U.S.G.S. Prof. Paper 600-C, C38-C44.

TUGARINOV, A. I.; LAKTIONOVA, N. V. and MOHANTI, R. C. (1973): Distribution of V, Cr, Ni, Co and Cu in titanomagnetites from some Indian deposits. Geochemistry International, 10, 1326-1336.

WILSON, A. F. (1977): A zincian hogbomite and some other hogbomites from Strangways Range, Central Australia. Min. Mag. 41, 337-344.

WOODFORD, P. J. and WILSON, A. F. (1976): Sapphirine, hogbomite, Kornerupine and Surinamite from aluminous granulites, North Eastern Strangeways range, C. Australia. Neues. Jb. Miner. Mh. H-1, 15-25.

ZAKRZEWSKI, M. A. (1977): Hogbomite from the Fe-Ti deposit of Liganga (Tanzania). N.Jb.Min.Mh. H-8, 273-280.

Manuscript received: 18. Aug. 2000.

Acta Mineralogica-Petrographica, Szeged, XLI, 9–29, 2000

CLAY MINERALS OF A GERMAN-TYPE MIDDLE TRIASSIC SEQUENCE, BORE HOLE NAGYKOZÁR 2, MECSEK MTS., S. HUNGARY

I. VICZIÁN*

Hungarian Institute of Geology

ABSTRACT

The mineralogical composition of Middle Triassic sedimentary rocks in the bore hole sequence Nagykozár-2 and in few surface outcrops in the western Mecsek Mts. was investigated by X-ray diffraction methods. The composition of the bulk rock, insoluble residue and the <2 μm fraction was considered. Triassic sediments of the Mecsek Mts. Show remarkably analogous features with those of the German-type Triassic. Middle Triassic was deposited in a transgressive period of evolution of a flat coastal plain and later of a carbonate ramp environment.

Buntsandstein-type sandstones of Schythian age are overlain by Röt-type sediments. Red to green laminated siltstones of tidal flat facies contain the detrital clay assemblage of *illite (mica), Fe-Mg-chlorite*, and the detrital feldspars *K-feldspar* and *plagioclase*. Anhydritic evaporites alternating with dolomite and siltstone beds of coastal sabkha origin are characterised by illite and *Mg-rich chlorite* or *mixed-layer chlorite/smectite* of presumably neoformational origin. The carbonate mineral of the evaporites is dolomite sometimes associated by *magnesite. Corrensite, Mg-chlorite* and *illite* occur in the overlying marly limestones and dolomites of inner and mid ramp, periodically dysaerobic carbonate environment. The genesis of corrensite is connected with the restricted nature of this sedimentary basin.

Carbonate sediments analogous to Germanic Muschelkalk are represented by Middle Anisian to Middle Ladinian formations. They are mostly characterised by the dominance of the single clay mineral *illite-1Md* and by presumably authigenic *K-feldspar*. In lower part of the sequence a dolomitised variegated peritidal facies exists in which sometimes *kaolinite* may be enriched indicating subaerial weathering on the top of periodically emerging small carbonate sand bars. Another kaolinitic weathering seems to have taken place during the Middle Muschelkalk emersion.

In contrast to the Germanic Triassic, the Mecsek Mts. rocks underwent relatively strong burial diagenetic transformation which is reflected by the widths of the illite basal reflections (KÜBLER indexes). Another reason of sharpening of the illite reflections is the reorganisation in the evaporitic environment.

Analogies with the clay mineralogy of a formerly studied bore hole sequence in the Mecsek Mts., Pécs-IX. and with that of Triassic formations of the Germanic basin are discussed.

INTRODUCTION

Mineralogy of Middle Triassic clastic, evaporitic and carbonate formations of the Mecsek Mts. was studied by the present author using the material of the bore hole Pécs-IX (VICZIÁN 1990, 1992, 1993). X-ray diffraction analysis and microscopic petrographic observations revealed that facies relations are reflected by the clay mineralogy of these formations: in clastic siltstones a detrital illite + chlorite assemblage predominates, anhydrites and restricted basin marly limestones contain the Mg-rich assemblage of Mg-

* H-1143 Budapest, Stefánia út 14.

chlorite, corrensite and illite while other carbonate rocks are characterised almost solely by illite. Neoformations were interpreted using the low-temperature phase diagrams of LIPPMANN and analogies with sedimentary formations of the Germanic Basin were indicated.

Recently the similarity between the Triassic sedimentation of the Mecsek Mts. and of German-type basins of Europe was stressed by the detailed sedimentological and paleontological studies of TÖRÖK (1997b, 1998) and KONRÁD (1997, 1998). It was shown that the Lower Triassic conglomerate and sandstone sequence of the Mecsek corresponds to the Buntsandstein unit of the Germanic Triassic while Middle Triassic formations in Mecsek are analogous with the Röt and Muschelkalk units. There are much larger differences in the Upper Triassic formations of Mecsek and Keuper of the Germanic basin.

The aim of the present study is to analyse the mineralogical variations in another Triassic bore hole sequence in the Mecsek Mts, that of the well Nagykozár-2 in order to prove the relations observed in the bore hole Pécs-IX in another facies sequence of the same character. In addition, in view of the new sedimentological results, a more detailed comparison with the clay mineralogy of the Germanic Triassic is made possible by these studies.

GEOLOGICAL RELATIONS

The geological map of the Mecsek and Villány Mts. is shown in *Fig. 1.* The bore hole Pécs-IX is located in the main block of the western Mecsek Mts., a few km northwards from the city of Pécs. Bore hole Nagykozár-2 lies about 10 km SE from the bore hole Pécs-IX. Although there are important structural lines in between, the Triassic sequences in both bore holes are very similar. In the sequence of Nagykozár-2 Triassic is covered by Tertiary, Cretaceous and Jurassic sediments and fills the 675.0 to 1704.3 m depth interval. Triassic is underlain by Paleozoic formations.

The stratigraphic succession of the Nagykozár-2 sequence including the names of local lithostratigraphic units is shown in *Figs 3* and *4*, following the first description of the core material by BARABÁS-STUHL (1988). The definitions and descriptions of the lithostratigraphic units were made by RÁLISCH-FELGENHAUER and TÖRÖK (1993). BARABÁS-STUHL (1993) studied the stratigraphy of the sequence. In the bore hole Nagykozár-2 samples were taken only from the generally transgressive part of the sequence, from the *Patacs* until the *Zuhánya Formations.* TÖRÖK (1997b, 1998) interpreted the Middle Triassic evolution in the Mecsek Mts. as stages of the development of a carbonate ramp. According to this interpretation the pre-ramp stage is represented by the *Patacs Siltstone Formation,* the initial ramp by the *Magyarürög Evaporite Member. Hetvehely Dolomite Mb.* corresponds to inner ramp, *Viganvár Limestone Mb.* to mid-ramp while *Rókahegy Dolomite Fm.* again to inner ramp situation. The deepening started again during the deposition of the mid-ramp *Lapis Limestone Fm.*, the deepest outer ramp facies was that of the *Zuhánya Limestone Fm.* According to Konrád (1997, 1998) the deposition of the Zuhánya Fm. was followed by a sea level drop and temporary emersion as a consequence of tectonic movements. After this unconformity, members of the *Csukma Fm., Kozár Limestone* and *Kán Dolomite* were formed in the territory of western Mecsek. These members are partly covered by the *Mánfa Siderite Mb.*, which indicates another period of emersion and subaerial weathering.

For comparison with the results of the above sequence, a few samples were analysed from surface localities in the western Mecsek area.

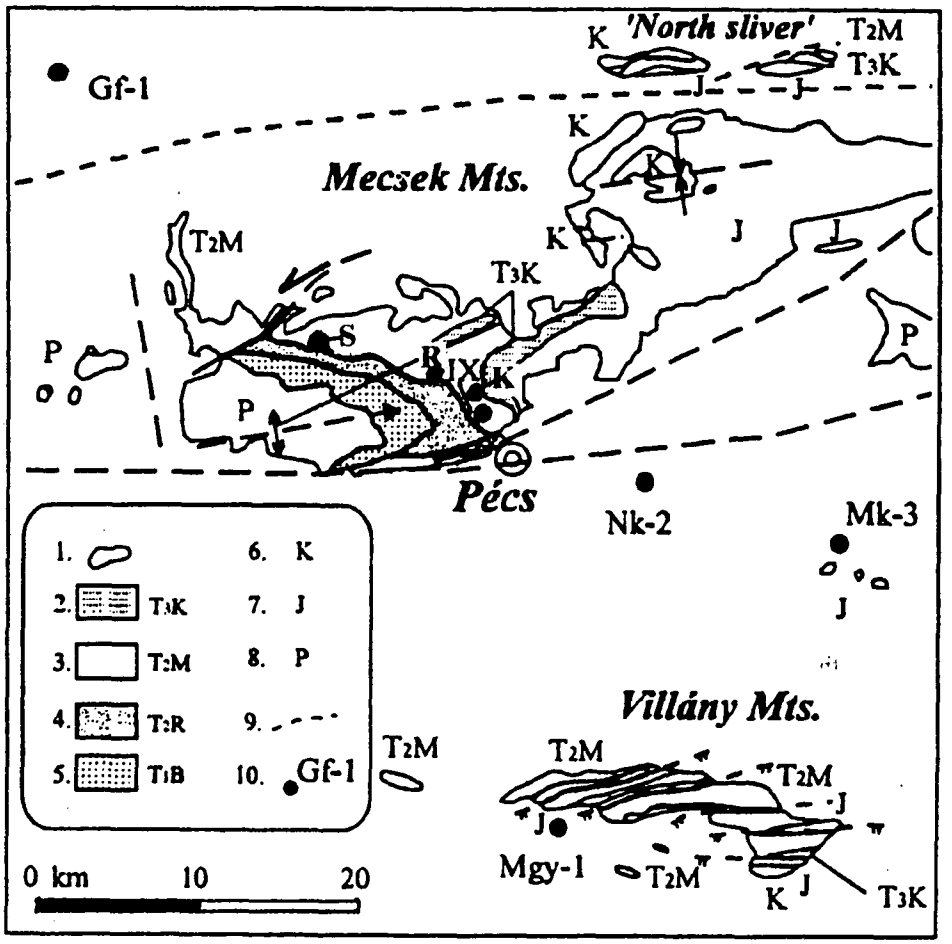

Fig. 1. Geological map of the surrounding of bore hole Nagykozár-2 (Nk-2) according to KONRÁD (1998). Some important bore holes and localities mentioned in the present study are shown.
IX: bore hole Pécs-IX; R: Remete-rét, K: Kis-rét, near the hill Misina at Pécs; S: Sás-völgy at Hetvehely. 1. Boundary of outcrop of Paleozoic and Mesozoic formations; 2. Upper Triassic detrital sediments; 3. Middle Triassic Muschelkalk-type carbonates; 4. Middle Triassic Röt-type formations; 5.Lower Triassic Buntsandstein-type Jakabhegy Sandstone; 6. Cretaceous; 7. Jurassic; 8. Paleozoic; 9. important structural line; 10. site of deep drillings and outcrop localities.

- One oncoidal limestone sample was taken from the locality *Kis-rét, Misina*, from the *Kozár Limestone Mb.* which is the uppermost member of the Mecsek Middle Triassic and a member of the Csukma Fm.

- Two samples were taken from the locality *Remete-rét, Misina*, from a special facies of the Rókahegy Dolomite Fm. containing branching stromatolitic forms. The occurrence was extensively studied and described by KONRÁD (1997).

- Three samples were taken from the locality *Sás-völgy* at the village Hetvehely, from an outcrop of the Hetvehely Dolomite and Viganvár Limestone Members.

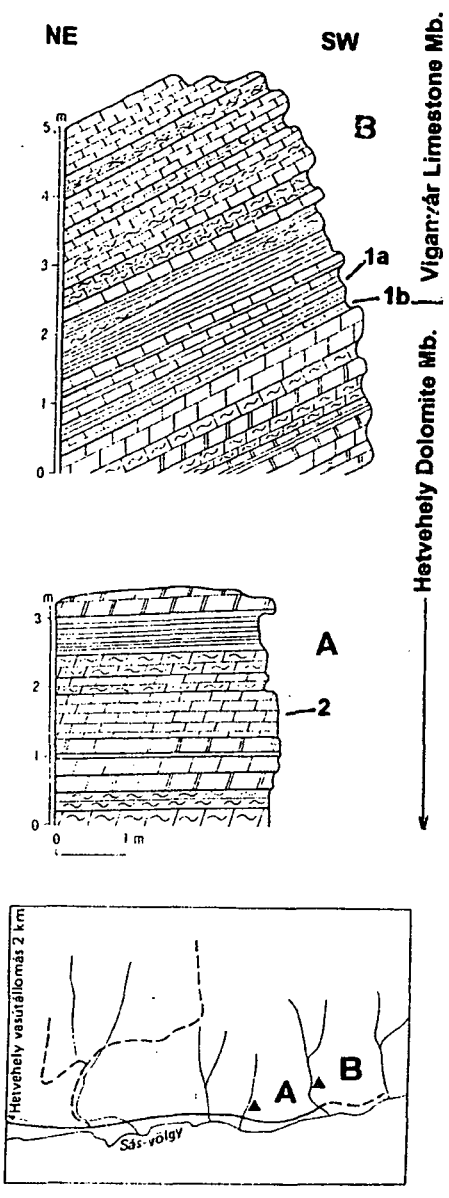

Fig. 2. Geological profiles of the outcrops A and B in Sás-völgy at Hetvehely, according to RÁLISCH-FELGENHAUER (1988a). The stratigraphic position of the samples taken is shown.

The geological relations of these localities, which are also stratigraphic key section, were described by RÁLISCH-FELGENHAUER (1987, 1988a,b). *Fig. 2* shows the profile and the sampling points of the locality Sás-völgy at Hetvehely.

SAMPLES AND METHODS

Field descriptions and microscopic examinations were made by RÁLISCH-FELGENHAUER. A total of 24 samples were taken for X-ray diffraction analysis, both bulk rock and the 3 % HCl insoluble residue were analysed.

Another set of samples was selected for detailed XRD study of the clay minerals in the <2 μm fraction. For the clay mineral analyses 9 samples were taken from the bore hole Nagykozár-2 and 6 samples from the outrcops mentioned above. Brief description and stratigraphic position of these samples is listed in Table 1. In each case, the <2 μm fraction was obtained by sedimentation after removal of the carbonate content by 3 % HCl. It was attempted to obtain the clay fraction of an anhydrite rock by repeated dissolution in distilled water, in a similar way as described by LIPPMANN and PANKAU (1988, p. 264). The complete dissolution of anhydrite was not achieved, however, it was possible to obtain a sufficiently enriched silicate fraction from which the <2 μm fraction was separated. Clay minerals were identified in oriented specimens of the < 2 μm fraction, in untreated and in ethylene gylcol treated form.

Semi quantitative XRD analysis was carried out by weighing selected reflections of the phases by intensity factors, according to standard methods used in the Hungarian Institute of Geology (RISCHÁK and VICZIÁN 1974, SZEMEREY-SZEMETHY 1976, KOMKOV et al. 1989, SIDORENKO et al. 1992). The width at half height of the first basal reflection of illite at 10 Å and of kaolinite at 7.2 Å was measured on smoothed curves after background

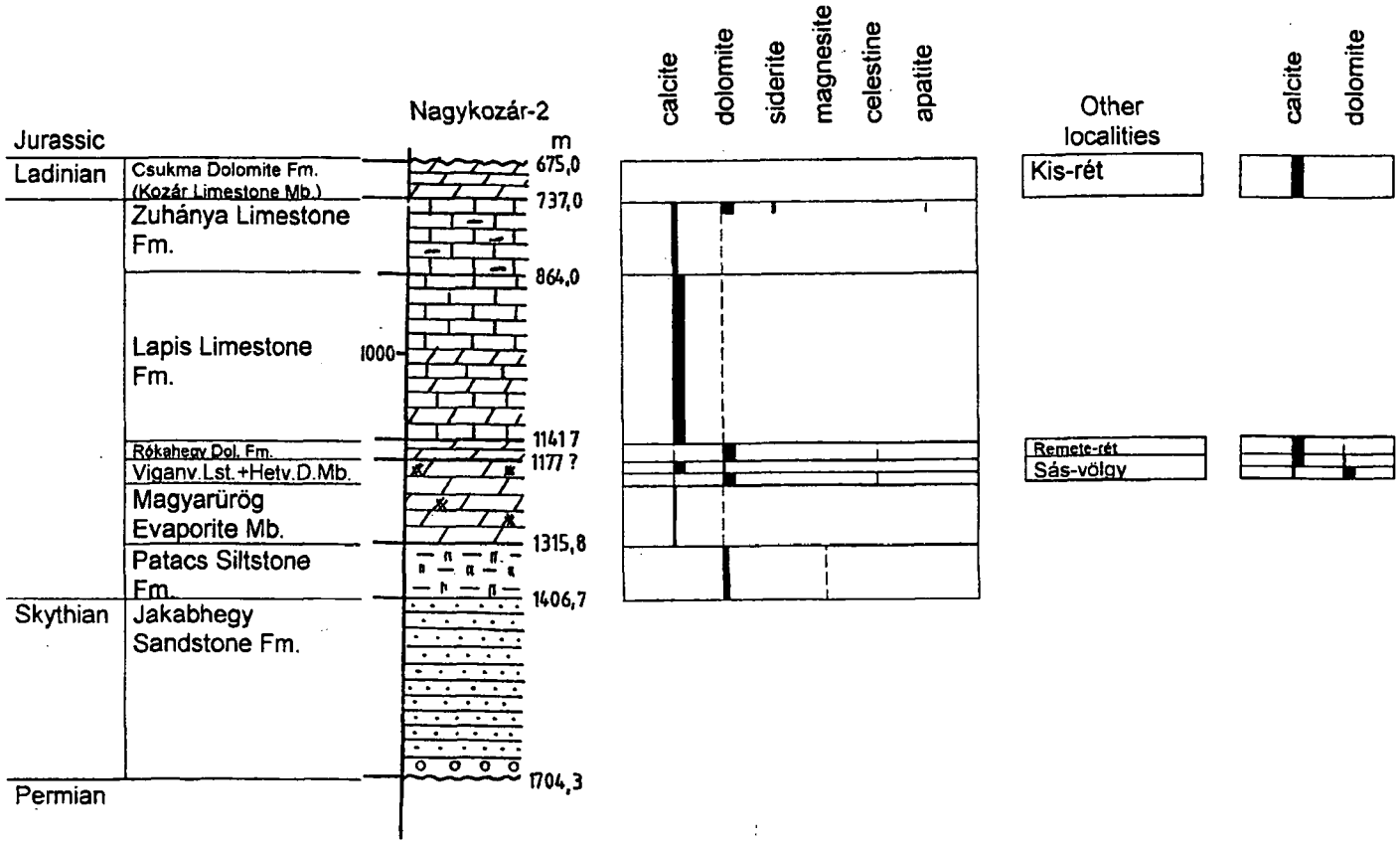

Fig. 3. Frequency of carbonate and related minerals in stratigraphic units of the Triassic sequence in bore hole Nagykozár-2 and in other localities in Mecsek Mts. Semi-quantitative abundance of the minerals is shown by the thickness of the corresponding line, see the legend to fig. 4. Stratigraphic succession and lithology according to BARABÁS-STUHL (1988).

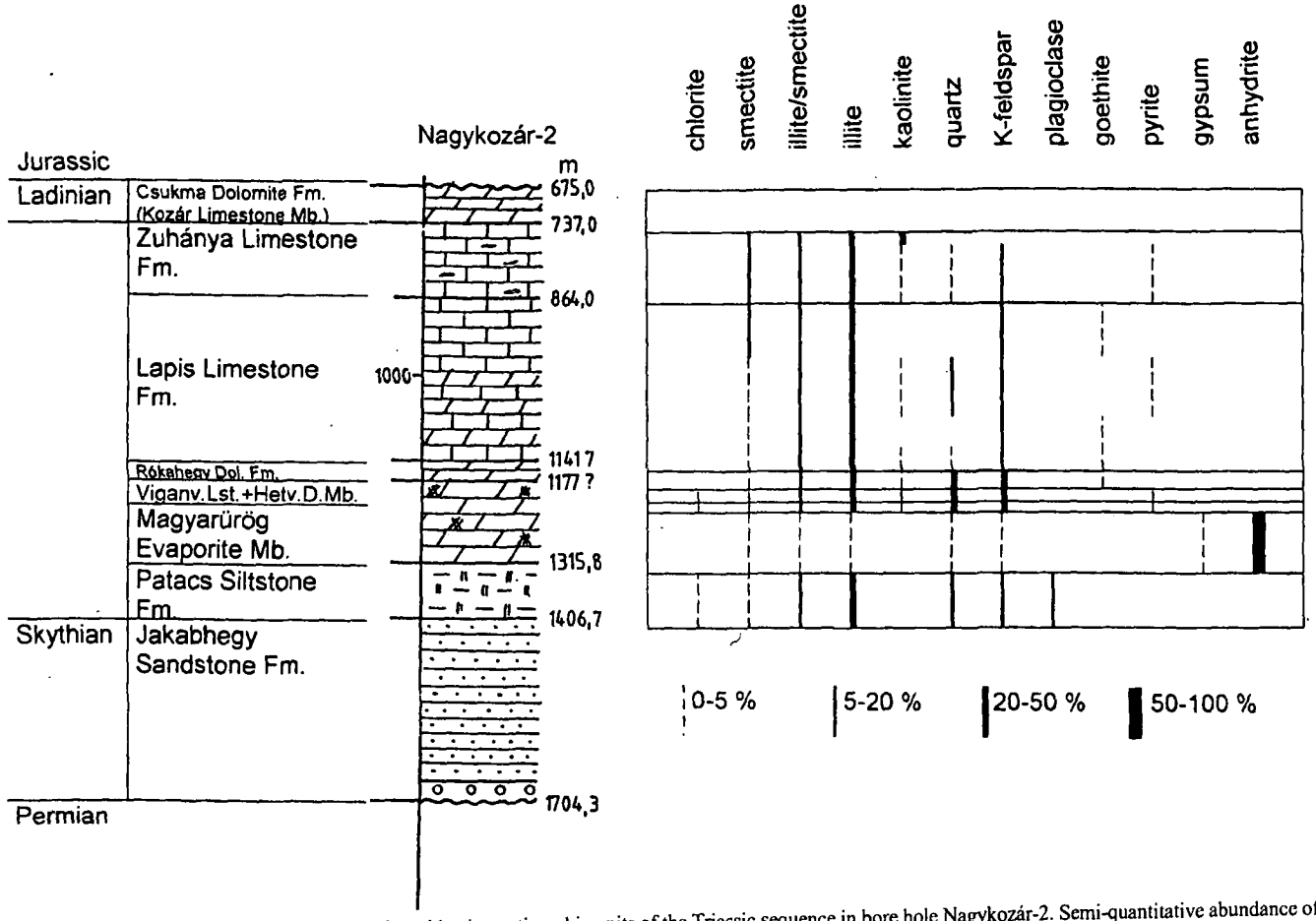

Fig. 4. Frequency of minerals in the insoluble residue in stratigraphic units of the Triassic sequence in bore hole Nagykozár-2. Semi-quantitative abundance of the minerals is shown by the thickness of the corresponding line. Stratigraphic succession and lithology according to BARABÁS-STUHL (1988).

correction. Normally, the polytypism of illite was determined on random powder specimens of the insoluble residue and of the <2 μm fraction, in some cases special side-filled sample holder was used in order to enhance non-basal reflections.

The XRD analyses of the samples from Remete-rét and Kis-rét were made by P. KOVÁCS-PÁLFFY and K. BARÁTH (1996), the others by I. VICZIÁN and Á. ÉNEKES (1993). M. FÖLDVÁRI (1996) analysed the Remete-rét and Kis-rét bulk samples by thermal methods (unpublished reports).

RESULTS

The variation of the carbonate minerals in the Middle Triassic section of the Nagykozár-2 sequence and of other localities in Mecsek Mts. is shown in *Fig. 3.* The composition of the insoluble residue in Nagykozár-2 is shown in *Fig. 4.* The figures are generalisations of the primary semi-quantitative data for a particular stratigraphic units.

Carbonate minerals

Considering the *Röt-type* formations, the carbonate mineral is exclusively dolomite, in the Lower Anisian Patacs Siltstone Fm. and Magyarürög Evaporite Mb. In the Magyarürög Mb., however, anhydrite may be accompanied by magnesite instead of dolomite. The occurrence of magnesite in analogous horizons of the bore hole Pécs-IX was discussed in detail by VICZIÁN (1992). Dominantly *dolomite* occurs in the Hetvehely Dolomite Mb., there is, however, a little calcite, both in the bore hole samples and at Sás-völgy.

Within the *Muschelkalk-type* formations the dominant carbonate minerals are calcite in the Lapis and Zuhánya Limestone Fms and alternatively calcite or dolomite in the Viganvár Mb. and Rókahegy Fm. According to TÖRÖK (1998) "the dolomitized beds are peritidal inner ramp deposits" whereas limestones were formed in deeper, mid or outer ramp environment. No carbonate mineral was found in one red siltstone sample from the Rókahegy Fm. which is probably the product of temporary emersion. At Remete-rét, the textural elements of the stromatolite-like structures in the Rókahegy Fm. always contain a few per cents of dolomite in addition to about 80 % calcite. The carbonate phase of the oncoidal Kozár Limestone at Kis-rét consists only of pure calcite.

There are interbeddings in the Lapis and Zuhánya Limestone Fms where the total carbonate contents are only 40 to 70 % and the carbonate phase consists of both calcite and dolomite. Such rocks may be called dolomitic calcareous marlstones. Frequently *dolomites* are *Fe-varieties* in those marly layers. Thin marlstone films were considered by TÖRÖK (1998) as products of 'background' sedimentation. There are also relatively pure carbonate rocks which consist partly of calcite and partly of dolomite, both of practically stoichiometric composition. Dolomitisation and dedolomitisation processes in dolomite-mottled limestones of the Zuhánya Limestone Fm. were studied in detail by TÖRÖK (1997a). A special *calcite + dolomite + siderite* carbonate assemblage was found in the uppermost sample of the Zuhánya Fm (751.5 m).

Minerals in the insoluble residue

The variation of non-carbonate minerals (silicates, sulphates) will be considered in the composition of the 3 % HCl insoluble residue.

Quartz reveals peculiar distribution. In the lower clastic formations of Röt type, up to the Hetvehely Dolomite Mb., quartz makes 20 to 40 % of the insoluble residue which is the normal composition of detrital terrigeneous sediments. In the Muschelkalk-type

sediments, however, quartz is very low or even missing in the carbonate-free fraction (see e. g. *fig. 5*).

In most cases *K-feldspar* exceeds quartz, its amount being about 20 % of the insoluble residue throughout the section. The unusual, relatively even intensity distribution of the main reflections shows that there is no tendency of preferred orientation, unlike the most detrital K-feldspars which usually exhibit a strong 3.24 Å line (*Fig. 5*). *Plagioclase* is restricted only to the lowermost clastic Patacs Siltstone Fm., it is missing in other formations.

Clay minerals are the most frequent minerals in the silicate fraction. 40 to 60 % of the silicate fraction in Röt-type sediments and 60 to 80 % of silicate fraction of quartz-poor Muschelkalk-type rocks are clay minerals. Their composition is rather uniform: the dominant clay mineral is almost exceptionally *illite*. The broadening of the illite basal reflection toward higher d values is interpreted as mixed-layer illite/smectite and smectite. The polytypic modification 1Md always dominates over a minor portion of 2M, 2M being sometimes completely missing (*Fig. 5*). It has to be emphasised that this is the case in the insoluble residue of the rocks which means that the abundance of illite-1Md is not the product of the laboratory enrichment of the fine size fractions, but the property of the bulk rock itself. There is more regular variation in the distribution of other clay minerals: *chlorite* occurs in the lower detrital formations up to the Hetvehely Dolomite Mb. Higher on in the sequence chlorite is replaced by kaolinite but its amount is usually low. There are

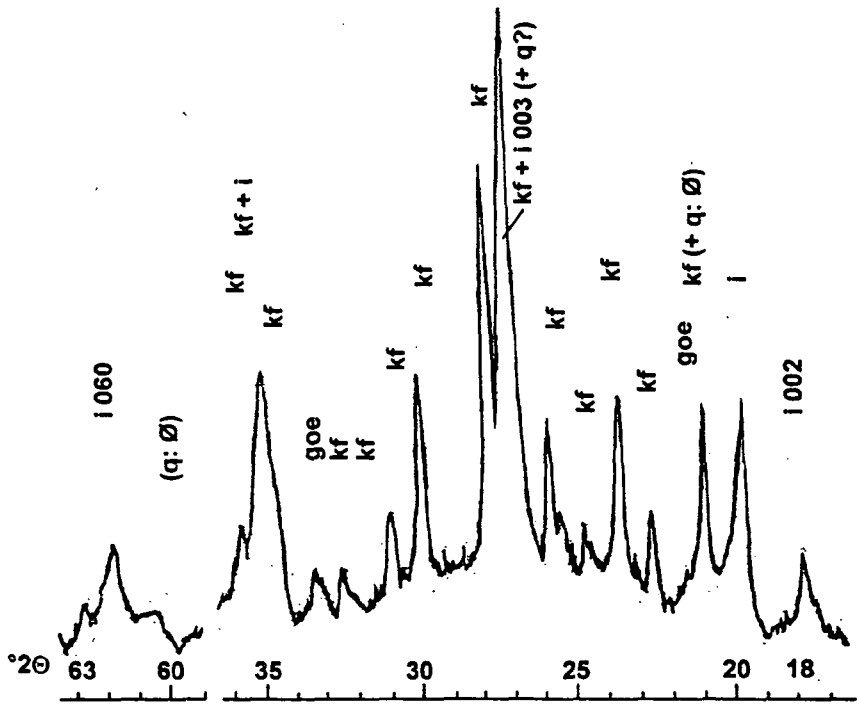

Fig. 5. X-ray diffraction pattern of non-oriented powder specimen showing the non-basal reflections and weak 002 and 003 basal reflections of illite-1Md and the strong reflections of potassium feldspar in the ranges 17 to 36 and 59 to 63 °2Θ. The presence of little goethite and the absence of quartz lines is indicated. Nagykozár-2, 884.7 m, 3 % HCl insoluble residue of dolomitic calcareous marl, Lapis Fm.

few exceptionally high *kaolinite* contents, the maximum is 40 % in the uppermost sample of Zuhánya Fm. (Nk-2. 751.5 m).

There is indication of *corrensite* in the bulk composition of a carbonate-free anhydritic siltstone at 1192.3 m depth but it could not be detected in the insoluble residue. Corrensite was found also in the bulk composition of a dolomite at 1191 m and in two bulk limestone samples of the Sás-völgy locality (Hetvehely and Viganvár Mbs, respectively).

Goethite and *pyrite* occur in alternating intervals in the carbonate rocks and in their marly and silty intercalations. Usually their presence is shown by the yellowish, brownish or grey colour of the rocks, respectively. The abundance of goethite seems to correlate with the quartz-poor and quartz-free and – surprisingly – also with the kaolinite-poor intervals of the Muschelkalk-type sequence.

Sulphate minerals, especially *anhydrite* and minor portions of *gypsum* are concentrated in the Magyarürög Mb. Almost pure anhydrite rocks of more than 80 % anhydrite content may occur. It is interesting that sporadic occurrences of *celestine* are restricted to the overlying Hetvehely Dolomite Fm.

Clay minerals in the <2 μm fraction

Table 2 contains the composition of the <2 μm fraction. The following clay minerals can be distinguished:

Smectite. Smectite was identified by the expansion to 17.0 Å upon treatment with ethylene glycol. There are only subordinate quantities in the Viganvár Mb. and Rókahegy Fm., the most being 9 % of the <2 μm fraction in the stromatolitic limestone at Remete-rét.

Illite. The dominant clay mineral in the whole section of Middle Triassic is illite. In most cases the clay mineral fraction is parctically monomineralic consisting only of illite. Similarly to the bulk rock and to the insoluble residue, illite is mostly of the disordered 1Md polytypic modification. Illite-1Md was identified by the strong reflections at d = 4.5 Å and 2.6 Å and by the absence of other non-basal reflections. Weak non-basal reflections indicate minor amounts of modificaton 2M in most samples an 1M in a few cases. The 001 basal reflection has some broadening towards lower °2Θ values which can be interpreted as a few per cent of smectite interlayering in addition to stacking disorder. Broadening was expressed by the „illite crystallinity" (IC) values according to KÜBLER (1990). IC values vary in the range of 0.50 to 0.90 °2Θ, expectionally low values were found in the anhydritic evaporite rock (Nk-2. 1343 m, 0.40 °2Θ) and in the highly kaolinitic clay fraction of a dolomite in the Rókahegy Fm. (Nk-2. 1150 m, 0.34 °2Θ).

Kaolinite. Kaolinite is missing in the lower clastic units (Patacs Siltstone Fm. and Magyarürög Evaporite Mb.) and is a minor component (0-2 %) in the carbonate rock units. The only expection is a dolomite sample in the Rókahegy Dolomite Fm. where kaolinite amounts to 35 % of the <2 μm fraction (Nk-2. 1150 m). Kaolinite is here well crystallised, it has very sharp basal reflection (width of 001 at half height: 0.34 °2Θ), similarly to the low IC value of illite.

Chlorite. Chlorite is normal Fe-Mg-chlorite. Mg-chlorites, typical in the bore hole Pécs-IX, were not found here. In the bore hole Nagykozár-2 chlorite is a minor component throughout the section, it seems to be a little more abundant in the lower clastic horizons. It is enriched in a single case, in silty fraction of the magnesite-bearing anhydrite rock in the Magyarürög Mb. (Nk-2. 1343 m). In the lower clastic horizons chlorite is accompanied by irregular mixed-layer chlorite/smectite.

Irregular mixed-layer chlorite/smectite. The mineral occurs in the anhydrite (Nk-2. 1343 m), in minor amounts also in a similar rock in the Patacs Fm. (Nk-2. 1346 m), as well as in the clay fraction of a Hetvehely Mb. dolomite sample at the outcrop Sás-völgy.

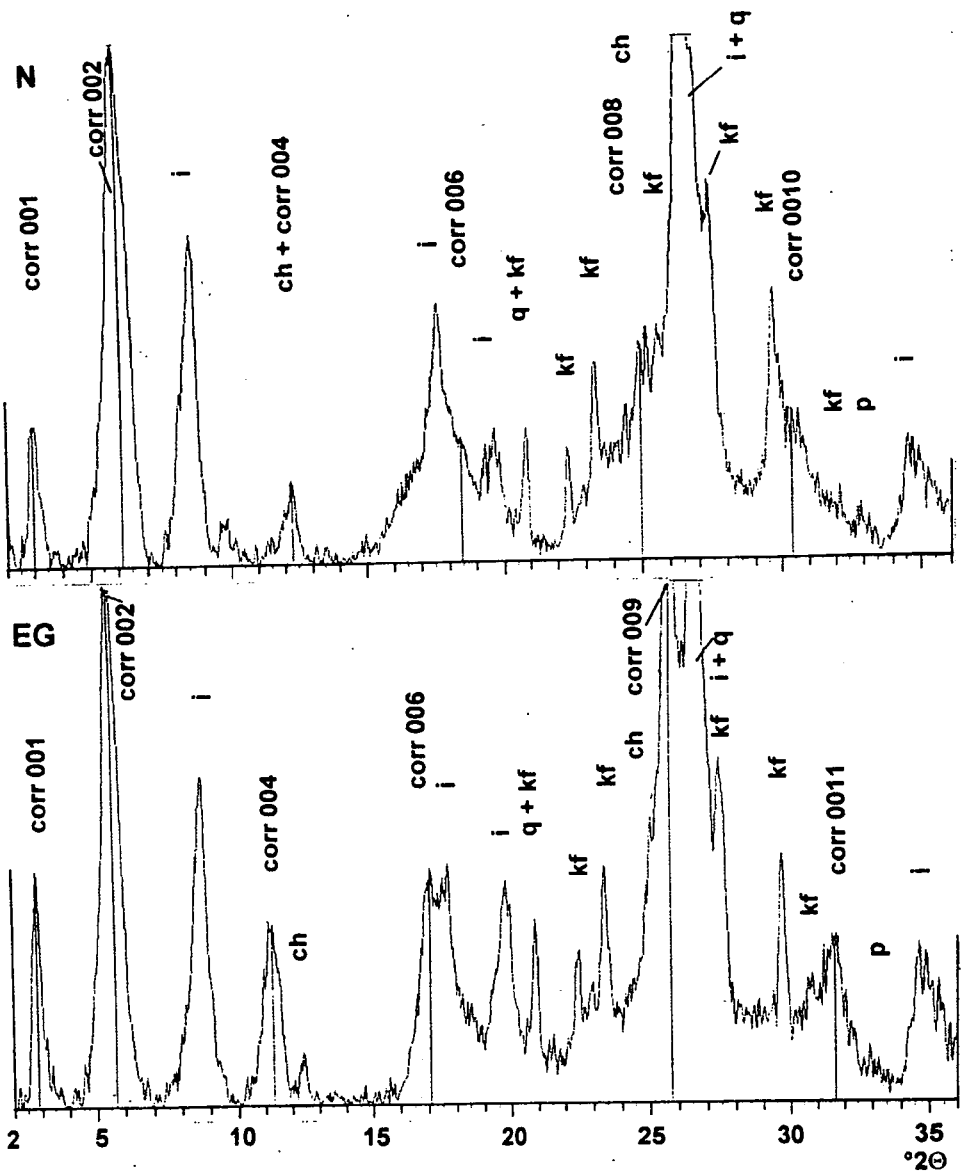

Fig. 6. Background corrected X-ray diffraction pattern of a corrensite-bearing mineral assemblage. Oriented specimen of untreted material („N") and after ethylene glycol treatment („EG"). Nagykozár-2, 1191 m, <2 μm fraction of clayey dolomite, Hetvehely Mb. Legend: corr: corrensite, ch: chlorite, i: illite, q: quartz, goe: goethite, kf: potassium feldspar, p: pyrite.

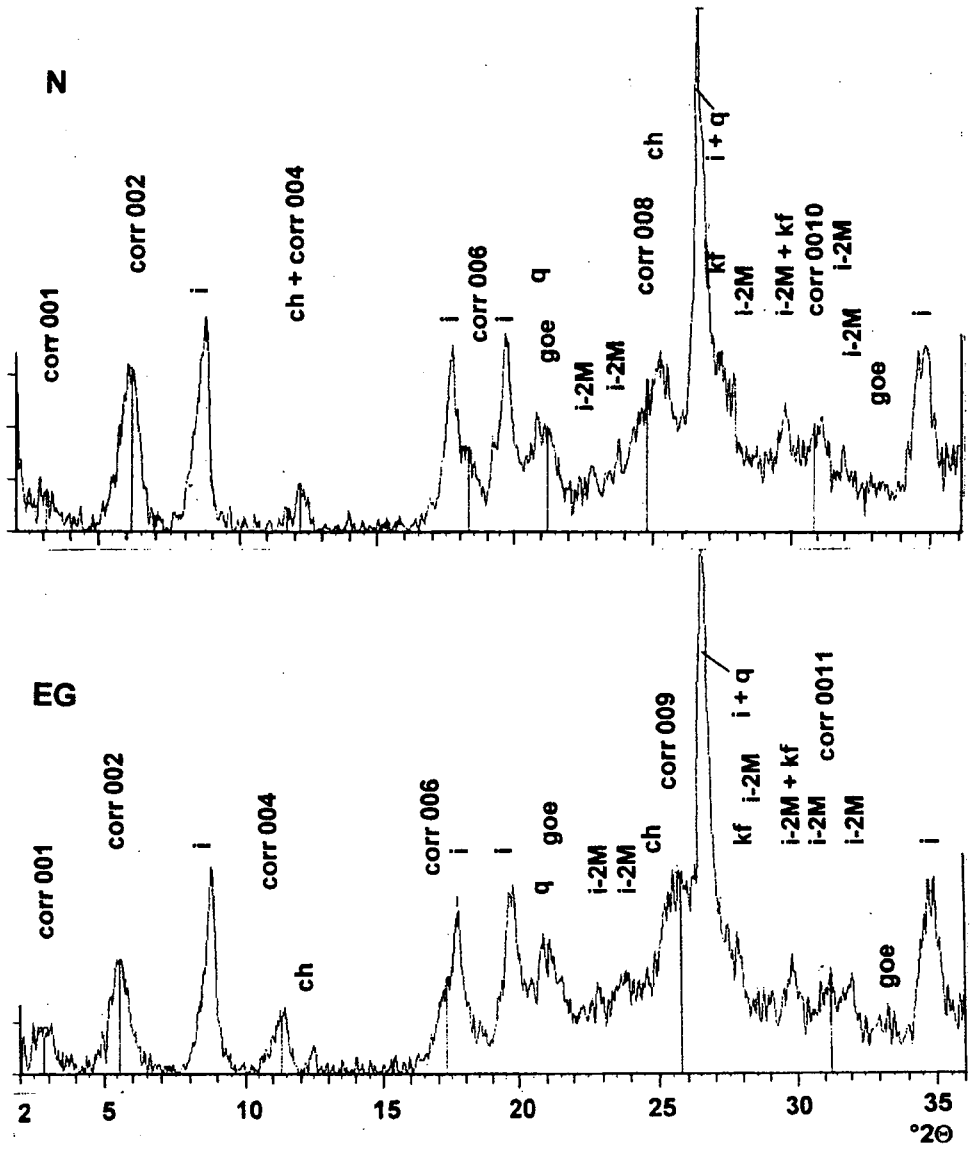

Fig. 7. Background corrected X-ray diffraction pattern of a corrensite-bearing mineral assemblage. Oriented specimen of untreated material ("N") and after ethylene glycol treatment ("EG"). Sás-völgy at Hetvehely, sample 1a, <2μm fraction of dark grey clayey limestone, Viganvár Mb. Legend: see fig. 6.

Mixed-layer chlorite/smectite in the sample Nk-2. 1343 m can be recognised by shifting of the first basal reflection from 14.5 Å to 15.7 Å and of the second basal reflection from 7.1 Å to 7.8 Å upon glycolation. The Sás-völgy sample contains a more disordered variety: in the glycolated sample there is a broad transition between the basal reflection of chlorite at 14.5 Å and that of smectite at 17.0 Å. It seems so that there are several transitional steps from irregular chlorite/smectites to well ordered corrensite.

Corrensite. This regular variety of mixed-layer chlorite/smectite occurs in a grey dolomite sample in the Hetvehely Mb. (Nagykozár-2 = Nk-2. 1191 m) and in a dark grey limestone sample of the Viganvár Mb. at the locality Sás-völgy. Corrensite can be recognised by the integral sequence of the basal reflections (BAILEY 1982) as it is shown in *figs 6* and *7* and in Tables 3 and 4.

K-feldspar. In each case, clay minerals are accompanied by relatively high contents of K-feldspar in the <2 μm fraction. Its abundance in the fine fraction shows that the mineral itself is generally fine-grained.

TABLE 1

Description and stratigraphic position of samples taken for analysis of the <2 μm fraction

Locality Depth, m or Sample No.	Formation or Member	Rock
Nagykozár-2		
1143	Rókahegy Dolomite	*Limestone,* light grey, with thin, yellowish marly interbeddings
1145	Rókahegy Dolomite	*Dolomite* marl, dark brownish red, thin lamination
1150	Rókahegy Dolomite	*Dolomite,* yellowish grey, in voids rhombohedral crystals and white dusty material
1177	Viganvár Limestone	*Limestone,* grey, with thin, wavy, dark grey marly interbeddings
1179	Viganvár Limestone	*Dolomitic* calcareous marl, with many thin, wavy, dark grey marly interbeddings
1181	Hetvehely Dolomite	*Dolomite,* grey, with thin, dark grey marly interbeddings
1191	Hetvehely Dolomite	*Dolomite,* dark grey, homogeneous, thin lamination, with smooth layer smooth layer surface
1343	Magyarürög Evaporite	*Magnestic* anhydrite, contorted beds of pink anhydrite, dark grey marl and light carbonate
1346	Patacs Siltstone	*Dolomitic, anhydritic siltstone,* thin, light dolomite, anhydrite and ark grey silty layers
Kis-rét		
1.	Kozár Limestone	*Ocoidal limestone,* dark grey oncoids of cm size, between oncoids: dark brown
Remete-rét		
1.	Rókahegy Dolomite	*Stromatolitic limestone,* „lower layer": dark grey, massive, homogenous
2.	Rókahegy Dolomite	*Stromatolitic limestone,* „upper layer": bright black biogene structures, light brown matrix
Sás-völgy		
1a.	Viganvár Limestone	*Limestone,* dark grey, homogeneous, layered
1b.	Hetvehely Dolomite/ Viganvár Limestone	*Limestone,* light grey, thin layers with even surface
2.	Hetvehely Dolomite	*Dolomite,* grey, with dark grey marly layers and spots, authigenic breccia (?)

TABLE 2

Clay mineral composition (%) and IC values of the <2 μm fraction

Locality Depth, m or Sample No.	Smectite	Illite (+Illite/ Smectite)	Kaolinite	Chlorite	Chlorite/ Smectite	Corrensite	IC, °2Θ
Nagykozár-2							
1143	1	99	tr.				0.79
1145	tr.	98	1	1			0.56
1150	tr.	65	35				0.34
1177	tr.	98	1	1			0.78
1179	tr.	97	2	1			0.72
1181		98	2				0.86
1191		61		6		33	0.68
1343[1]		64		23	13		0.40
1346		95		4	1		0.79
Kis-rét							
1.		97		3			0.49
Remete-rét							
1.		98		2			0.66
2.	9	89		2			0.68
Sás-völgy							
1a.		75		6		19	0.53
1b.	2	98					0.58
2.		90		7	3		0.54

[1] Dissolved in distilled water

TABLE 3

lx d(001) (Å) values for corrensite, sample Nk-2. 1191 m, <2 μm fraction

001	*l x d(001) (Å)* Untreated	*l x d(001) (Å)* Ethylene glycol
001	29.4	30.7
002	2 x 14.54 = 29.08	2 x 15.55 = 31.10
004	4 x 7.23 = 28.92	4 x 7.81 = 31.24
006	6 x 4. 81 = 28.86	6 x 5.19 = 31.14
008	8 x 3.57 = 28.56	
009		9 x 3.456 = 31.10
0010	10 x 2.938 = 29.38	
0011		11 x 2.822 = 31.04

TABLE 4

lx d(001) (Å) values for corrensite, sample Sás-völgy 1a, <2 μm fraction

001	*l x d(001) (Å)* Untreated	*l x d(001) (Å)* Ethylene glycol
001	29.0	31.1
002	2 x 14.43 = 28.86	2 x 15.88 = 31.76
004	4 x 7.25 = 29.00	4 x 7.78 = 31.12
006	6 x 4.84 = 29.04	6 x 5.15 = 30.90
008	8 x 3.59 = 28.70	
009		9 x 3.456 = 31.10
0010	10 x 2.897 = 28.97	
0011		11 x 2.813 = 30.94

DISCUSSION

Clay mineral zones

Considering the composition and that of the insoluble residue, the following clay mineral associations can be distinguished in the sequence of Nagykozár-2:

Illite + chlorite + chlorite/smectite: This is typical in clastic rocks of the Patacs Siltstone and Magyarürög Evaporite Fms. Mg-rich chlorites found at Pécs-IX did not occur in the present study. Perhaps they correspond here to mixed-layer chlorite/smectites.

Corrensite + illite + chlorite: Corrensite is restricted to some layers of the Hetvehely, Viganvár Mbs, in each case occurring in "unclean" clayey limestones or dolomites.

Illite + illite/smectite (+ smectite), with minor kaolinite and chlorite: This illite dominated association is typical in all carbonate rock formations from the corrensite-free layers of the Hetvehely Dolomite and Viganvár Limestone upwards, in the Rókahegy, Lapis and Zuhánya Fms.

Illite + kaolinite: There are relatively high kaolinite contents in some layers of the Rókahegy Dolomite Fm. and in the uppermost sample of the Zuhánya Limestone Fm. In the latter case kaolinite seems to replace the otherwise abundant K-feldspar.

The composition of the samples taken from surface outcrops fits well into this scheme:

At *Sás-völgy* the Hetvehely Dolomite sample seems to belong to the lower clastic clay assemblage, the limestone at the Hetvehely/Viganvár boundary to the illite-dominated association and the Viganvár Limestone to the corrensite-bearing one.

The stromatolitic limestone samples of Rókahegy Fm. at *Remete-rét* belong to the illite-dominated association.

The composition of the oncoidal limestone sample at *Kis-rét* shows that the illite-dominated association continues up to the Middle Ladinian Csukma Fm., i. e. up to the uppermost Triassic formation represented in the bore hole Nagykozár-2.

Comparison with the bore hole Pécs-IX and with other Middle Triassic occurrences in Mecsek Mts.

The data obtained in the present study are in full agreement with the results received from the bore hole Pécs-IX (VICZIÁN 1992, 1993). The stratigraphic range is slightly different. The sequence starts in both cases with Lower Anisian, but at Pécs-IX the lower clastic members are more pronounced while in the present study the carbonate-rich upper formations up to the Middle Ladinian are more represented.

Similar features in both bore holes are the absence of *calcite*, the permanent presence of *dolomite* in the evaporitic members, the occurrences of *magnesite* in these evaporitic rocks and of *celestine* in the Hetvehely Dolomite Mb. Similar are the *clay mineral* zones. Illite crystallinity (IC) values found in evaporitic and normal-salinity formations vary in the same range in both profiles.

Among the *feldspars* the K-feldspar is dominant in almost the whole sequence in the present study while at Pécs-IX neoformation of albite was observed in the lower part of the sequence.

The absence or low concentration of quartz in the Muschelkalk-type carbonate rocks is a new result.

The enrichment of *kaolinite* in the Rókahegy Fm. was not observed before. The appearance of *siderite* and *kaolinite* in the uppermost sample of the Upper Anisian

Zuhánya Fm. resembles the occurrence of kaolin, siderite-bearing kaolin in the bore hole Komló K-LXXII (NAGY and RAVASZ-BARANYAI 1968). These special kaolinite-bearing rocks belong to the stratigraphic unit Mánfa Siderite Mb. which immediately overlies the Kozár Limestone Fm. (RÁLISCH-FELGENHAUER and TÖRÖK 1993), however, no corresponding stratigraphic horizons occur in the well Nagykozár-2. Similarly, kaolinite-rich "green clay" interbeddings are known from other Upper Anisian occurrences in the western Mecsek Mts. (WÉBER 1965, 1978). In spite of the lithologic similarity, these formations are not contemporaneous. All these occurrences belong to a stratigraphically higher level, the top of the Kozár Fm., while the sample of the present study represents a former emersion period after the deposition of the Zuhánya Fm.

Comparison with the German Triassic basin

Mineralogy provides further evidences of the similarity between the facies and stratigraphic relations of Mecsek Mts. Lower and Middle Triassic formations and the German-type basins which was discussed in detail by KONRÁD (1997, 1998) and TÖRÖK (1997b, 1998). Mineralogical data were collected from the literature and the typical clay mineral assemblages were determined for stratigraphic horizons in the German Triassic basin (*Fig. 8*).

Middle to Upper Buntsandstein and silty clastic members of *Röt (Upper Buntsandstein)* contain the detrital illite+chlorite assemblage, similarly to the Mecsek Mts. clastic formations. *Evaporitic* members of the Röt contain normally corrensite but corrensites have been found also in other restricted basin sediments in Germany. In Hungary, corrensites were found only in restricted basin marly limestones and dolomites while true evaporitic anhydrite rocks seem to contain Mg-chlorite or chlorite/smectite. Authigenic quartz and albite were found in carbonates in Mecsek Mts.

Lower and Upper Muschelkalk is always characterised by dominant illite and authigenic neoformations of potassium feldspar and to a lesser amount albite. It was shown first by FÜCHTBAUER as early as in 1950. Kaolinite and chlorite contents are normally subordinate in limestones of the basin, there are higher kaolinite and chlorite contents in the untypical marginal formations in Luxemburg and adjacent areas. The authigenic feldspars and the illitic clay minerals of the Silesian Muschelkalk are well documented by MICHALIK (1991). Corresponding limestone members of the Mecsek sequence contain practically only illite and the authigenic formation of potassium feldspar is suspected. Middle Muschelkalk is evaporitic in many places in Germany containing corrensite, similarly to the Röt saline formations. KONRÁD supposes that there is an unconformity in the same horizon in Mecsek which is possibly shown by the elevated kaolinite content in the uppermost underlying sample.

Genesis of clay minerals

Genetical problems were extensively studied by the present author in connection with the bore hole Pécs-IX (VICZIÁN 1990, 1992, 1993). In the present study, the similarity between the two sequences was found. It is not necessary, therefore, to repeat the whole argumentation of the previous papers. In the following only new aspects of composition and the results of recent sedimentological analyses are discussed in detail.

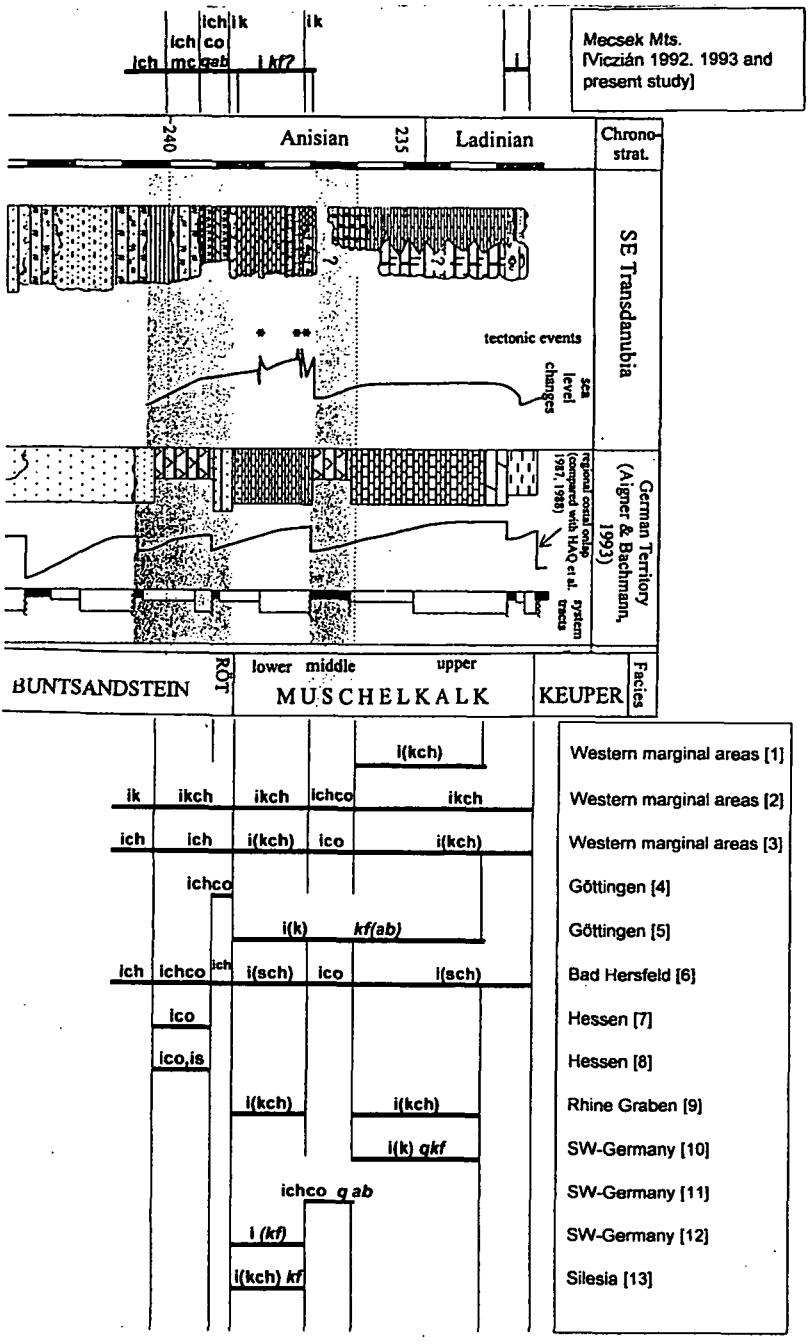
Mecsek Mts.
[Viczián 1992. 1993 and present study]
Anisian
Ladinian
Chrono-strat.
SE Transdanubia
tectonic events
sea level changes
German Territory (Aigner & Bachmann, 1993)
BUNTSANDSTEIN
ROT
lower middle upper
MUSCHELKALK
KEUPER
Facies
Western marginal areas [1]
Western marginal areas [2]
Western marginal areas [3]
Göttingen [4]
Göttingen [5]
Bad Hersfeld [6]
Hessen [7]
Hessen [8]
Rhine Graben [9]
SW-Germany [10]
SW-Germany [11]
SW-Germany [12]
Silesia [13]

Fig. 8.

Fig. 8. Comparison of typical clay and authigenic minerals in Lower to Middle Triassic rocks of Mecsek Mts. and of the German and adjacent Triassic basins. Stratigraphic correlation according to KONRÁD (1998).
Abbreviations of clay minerals: i: illite, ch: chlorite, mc: Mg-chlorite, co: corrensite, k: kaolinite, s: smectite. Authigenic minerals are written in *italics: q:* quartz, *kf:* K-feldspar, *ab:* albite. Minerals in brackets: about 10 to 20 % of total clay minerals.
References: [1]: MULLER et al. (1977) and MULLER (1978), [2]: SCHRADER in BERNERS et al. (1984), [3]:WAGNER (1989), [4]: LIPPMANN (1956), [5]: FÜCHTBAUER (1950), [6]: STROUHAL, HENDRIKS (1988), [7]: BÜHMANN, RAMBOW (1979), [8]: DOUBINGER, BÜHMANN (1981), [9]: GENG et al. (1996), [10]: LIPPMANN, SCHLENKER (1970), [11]: LIPPMANN, PANKAU (1988), [12]: LIPPMANN, BERTHOLD (1992), [13]: MICHALIK (1991).

I. Diagenesis

The degree of burial diagenetic transformation can be determined considering the mineral assemblage and the IC values. The scarcity of expanding smectites points *to medium to deep zones of burial.* Corrensites are typical diagenetic products. They are formed in the shallow burial stage in German Triassic-type environment, stable in the medium stage and may persist in the deep burial stage (LIPPMANN 1987, KÜBLER 1973, 1984).

Relatively high IC values in non-evaporitic formations (see Table 1), irregularly mixed-layer illite/smectites and chlorite/smectites exclude the onset of the anchizone. IC values are much higher than 0.42 °2Θ, which is the limit between diagenesis and anchizone (KÜBLER 1990).

The predominance of the illite-1Md polytipic from in the bulk rocks (*fig. 5*) shows that illites are not simply fine-grained detrital 2M micas. Much more probably they were partly expandable illitic weathering products which were reorganised in a potassium rich diagenetic environment. The nature and abundance of K-feldspar in carbonate rocks makes probable its authigenic origin (*Fig. 5*) which is another indication of a potassium-rich diagenetic environment. Lower IC values in evaporitic rocks show that the transformation started in these rocks during sedimentation or during early burial. The abundance of *illite* and *potassium feldspar* in the silicatic phase of carbonate rocks seems to be typical for the whole Muschelkalk-type upper half of the sequence. The transformation of illites may have lasted until the medium to deep zones of diagenesis. Authigenic potassium feldspars are considered to have been formed in Muschelkalk-type limestones from diagenetic pore waters enriched in K+ ions, after burial, without direct contact with the sea water (FÜCHTBAUER 1950, MICHALIK 1991).

Very probably the high *kaolinite* content of the dolomite sample from Nk-2, 1150 m is a diagenetic feature. Kaolinite is very well crystallised and even illite has sharper basal reflection then otherwise. Kaolinite might have crystallised from solutions *in open space* of abundant voids of this very porous dolomite.

II. Environment of deposition

The evolution of clay minerals of the French part of German Triassic basin and related basins in western Europe and Morocco was subject of the discussion given by MILLOT (1964) based on classical studies of LUCAS. He considered a continuous aggradational transformation of degraded illites both in time, from Lower Triassic to Keuper, and in space, from coastal facies to central areas of the basin. Now we can give a more differentiated picture of these relations in time, space and in terms of depositional

environments within the German basin. This is true also for the Mecsek area, however, lateral variations cannot be recognised due to its very limited extent.

The *illite + chlorite* assemblage in lower clastic and members of the sequence seem to be normal terrigeneous detrital sediments derived from the nearby continent. The lack of kaolinite in the material indicates the lack of deeply weathered soil profiles in the source area. In view of the possible diagenetic transformation, it is possible, that there was a relatively high proportion of expanded clay minerals in the transported load.

Irregularly mixed-layer chlorite/smectites and Mg-chlorites occur in evaporites of coastal sabkha and marine lagoonal environments as products of chemical transformation in Mg-rich solutions.

According to experiences obtained so far from the Mecsek Mts., *corrensites* are typical chemical neoformations of less saline environments of restricted circulation, such as the carbonatic formations of the Hetvehely and Viganvár Members. According to LIPPMANN (1987) and LIPPMANN and PANKAU (1988), the crystallisation of corrensite needs solutions enriched in both Mg^{2+} and $(OH)^-$ ions. Its formation is favoured by the conditions of a restricted basin, which is a collector of alkaline waters derived from adjacent source areas.

According to the sedimentological analysis of TÖRÖK (1998) these formations were deposited on the northern margin of the Tethys in a mid- to outer-ramp setting in normal salinity marine environment. The carbonate ramp was very broad, at least several hundreds of kilometres away from continent and from the 'shelf edge' of the open Tethys ocean. The primary source area of the detrital sediments seems to have been the present territory of the Bohemian massif, both the continental and the marine areas were very flat, levelled terrains. Fossils and sediment types indicate warm and rather dry climate, close to 30°N paleo-latitude. The carbonate ramp lasted for a long time, for about 14 million years. All these conditions may explain the production of a terrigeneous, moderately weathered, fine-grained detrital material which contained primarily partly expanded illitic minerals, with a little kaolinite and quartz. LIPPMANN and BERTHOLD (1992) came to similar conclusions concerning the provenance of illite in the Muschelkalk of SW Germany. An earlier study (STÖRR et al. 1977) concluded that the development of a kaolinitic weathering crust on the surface of the Bohemian-Vindelician Massif started in the Upper Triassic and continued further in the Jurassic. In addition, the poverty in kaolinite and quartz and enrichment of illite in the Muschelkalk sediments in Mecsek Mts. may be due to the long transporting distance from the source area.

An important result of the sedimentological analysis is that hard reef-building organisms were missing and the dominant type of carbonate sedimentation was the accumulation of carbonate mud which remained soft relatively long due to the stirring action of storms. Storms stirred the whole water column both in inner and mid-ramp conditions. Goethite and pyrite containing beds probably indicate primary oxidation-reduction conditions of sedimentation.

The relative enrichment of *kaolinite* in the Rókahegy and in the uppermost Zuhánya Fms (except the diagenetic formation in pores of Rókahegy dolomite mentioned above) may be due to subaerial weathering during temporary emersion periods and inner ramp setting which was stressed by KONRÁD (1997b, 1998).

CONCLUSIONS

1. In the Mecsek Mts., during the Lower Anisian, evaporitic sabkha and restricted basin shallow marine conditions were favourable for the formation of irregular and regular mixed-layer smectite/chlorites. Corrensites occur in the marly carbonate rocks of the Hetvehely Dolomite and Viganvár Limestone Members.

2. From Middle Anisian till Middle Ladinian Muschelkalk-type carbonate sedimentation prevailed. The clay mineral of the limestones is illite accompanied by K-feldspar. Both minerals have been formed or reorganised in a potassium-rich diagenetic environment.

3. On the adjacent continent essentially illitic weathering crust developed in a levelled, relatively flat surface. The conditions for the development of a kaolinitic crust of weathering were first favourable in the Upper Triassic, however, during shorter elevation periods during the Middle Triassic partly kaolinitic weathering products may have developed (Rókahegy Fm. and top of Zuhánya Fm.).

4. The present investigations confirm the former results of the author regarding the clay mineralogy and diagenetic neoformations in a similar Middle Triassic rock suite in Mecsek Mts., the sequence of the bore hole Pécs-IX.

5. The typical clay minerals of the Mecsek Mts. Middle Triassic are very similar to the corresponding formations of the Triassic of German and adjacent basins which is another proof of the close genetic relations of both terrains. The difference is in the degree of diagenesis, which is weak in the German basin and reaches deep burial in Mecsek Mts.

ACKNOWLEDGEMENTS

This paper is devoted to the memory of professor Friedrich LIPPMANN (1928-1998), who has inspired the present investigations during the stay of the author in his laboratory in Tübingen, Germany.

The author expresses his gratitude to dr. Erzsébet RÁLISCH-FELGENHAUER for valuable discussions on field and petrographic relations of the rocks studied. Thanks are due to Mrs. Mariann HÓZER for laboratory preparation of the samples, to dr. Mária FÖLDVÁRI for thermal analysis and to dr. Péter KOVÁCS-PÁLFFY, Mrs. Katalin BARÁTH and Ágnes ÉNEKES for their help in X-ray diffraction analysis.

REFERENCES

BAILEY, S. W. (1982): Nomenclature for regular interstratifications. A report of the AIPEA Nomenclature Committee. Clays Clay Min. **30**, 1, 76-78. and Clay Min. **17**, 2, 243-248.

BARABÁS-STUHL, Á. (1988): Outline of stratigraphy of old formations in bore hole Nagykozár 2. Unpublished report, Archives of Hungarian Geological Survey, Budapest. (in Hungarian).

BARABÁS-STUHL, Á. (1993): Palynological reevaluation of Lower Triassic and Lower Anisian formations of Southeast Transdanubia. Acta Geol. Hung. **36**, 4, 405-458.

BERNERS, H.-P., BOCK, H., COUREL, L., DEMONAFAUCON, A., HARY, A., HENDRIKS, F., MÜLLER, E., MULLER, A., SCHRADER, E., WAGNER, J. F. (1984): Vom Westrand des Germanischen Trias-Beckens zum Ostrand des Pariser Lias-Beckens: Aspekte der Sedimentationsgeschichte. Jber. Mitt. oberrhein. geol. Ver., N. F. **66**, 357-395.

BÜHMANN D., RAMBOW, D. (1979): Der Obere Buntsandstein (Röt) bei Borken/Hessen, Stratigraphie und Tonmineralogie. Geol. Jb. Hessen **107**, 125-138.

DOUBINGER, J., BÜHMANN, D. (1981): Röt bei Borken und bei Schlüchtern (Hessen, Deutschland). Palynologie und Tonmineralogie. Z. dt. geol. Ges. **132**, 421-449.

FÜCHTBAUER, H. (1950): Die nichtkarbonatischen Bestandteile des Göttinger Muschelkalkes mit besonderer Berücksichtigung der Mineralneubildungen. Beitr. Min. Petr. **2**, 235-254.

GENG, A., WARR, L. N., BECHSTÄDT, T. (1996): Clay mineral crystallinity of diagenetic grade Middle Triassic Muschelkalk of the Rhine Graben, southwest Germany. 13th Conf. Clay Min. Petr., Praha, 1994. Acta Univ. Carol., Geol. **38**, 2-4, 193-201.

KOMKOV, A. I., DYAKONOV, YU, S., MISCHENKO, K. S., RAYNOV, N., CECHLAROVA, I., RISCHÁK, G., UNGER, H., HERING, A. (1989): Application of quantitative X-ray diffraction phase analysis in the geological survey. I. A methodological guide. Scientific Commission of Analytical Methods, Scientific Commission of Methods of Mineralogical Research, VIMS, Moskva (in Russian).

KONRÁD, Gy. (1997): Sedimentology of Lower and Middle Triassic formations in SO Transdanubia. C. Sc. Thesis, Budapest. (in Hungarian).

KONRÁD, Gy. (1998): Synsedimentary tectonic events in the Middle Triassic evolution of the SE Transdanubian part of the Tisza Unit. Acta Geol. Hung. **41**, 3, 327-341.

KÜBLER, B. (1973): La correnside, indicateur possible de milieux de sédimentation et du degré de transformation d'un sédiment. Bull. Rech. Pau - SNPA **7**, 2, 543-556.

KÜBLER, B. (1984): Les indicateurs des transformations physiques et chimiques dans la diagenèse. Températures et calorimétrie. In Lagache, M. (ed.): Thermométrie et barométrie géologiques vol. **2**, Ch. 14. Soc. Franç. Min. Crist., Paris.

KÜBLER, B. (1990): "Cristallinité" de l'illite et mixed-layers: brève révision. Schw. Min. Petr. Mitt. **70**, 89-93.

LIPPMANN, F. (1956): Clay minerals from the Röt Member of the Triassic near Göttingen, Germany. J. Sed. Petr. **26**, 2, 125-139.

LIPPMANN, F. (1987): Mode of formation of Mg-bearing clay minerals (abstract). 6th Meeting of the European Clay Groups, Sevilla, 1987, Summaries, Proceedings 338.

LIPPMAN, F., BERTHOLD, C. (1992): Der Mineralbestand des Unteren Muschelkalkes von Geislingen bei Schwäbisch Hall (Deutschland). N. Jb. Min. Abh. **164**, 2-3, 183-209.

LIPPMANN, F., PANKAU, H.-G. (1988): Der Mineralbestand des Mittleren Muschelkalkes von Nagold, Württemberg. N. Jb. Min. Abh. **158**, 3, 257-292.

LIPPMANN, F., SCHENKLER, B. (1970): Mineralogische Untersuchungen am Oberen Muschelkalk von Haigerloch (Hohenzollern). N. Jb. Min. Abh. **113**, 1, 68-90.

MICHALIK, M. (1991): Authigenic K-feldspars from Gogolin Limestones (Lower Muschelkalk) of the Cracow-Silesian region. Min. Polonica **22**, 2, 3-10.

MILLOT, G. (1964): Géologie des argiles. Masson et Cie., Paris.

MULLER, A. (1978): Oberer Muschelkalk, Eicks. Lettenkohle, Oberer Muschelkalk, Irnicher Berg (N. Eifel). Sedimentologisches Geländepraktikum, S. S. 1978 (manuscript).

MULLER, A., PAPAIOANOU, J., SCHRADER, E. (1977): Der Mittlere und Obere Trias der Nordeifel. Publ. Serv. Géol. Luxembourg, Bull. **8**, 23-36.

NAGY, E., RAVASZ-BARANYAI, L. (1968): Tuffaceous kaolinite and siderite deposits on the base Mecsek Ladinian complex. Földt. Közl. (Bull. Hung. Geol. Soc.) **98**, 2, 213-217. (in Hungarian).

RÁLISCH-FELGENHAUER, E. (1987): Kisrét, park-lane to Dömörkapu, "U" bend of Misina road, Pécs. Misina Formation, Kozár Limestone Member. – Magyarország geológiai alapszelvényei (Geological Key Sections of Hungary) No. 87/254. Hungarian Institute of Geology, Budapest.

RÁLISCH-FELGENHAUER, E. (1988a): Mecsek Mountains, Hetvehely, Sás-völgy. Hetvehely Dolomite Formation. – Magyarország geológiai alapszelvényei (Geological Key Sections of Hungary) No. 88/211. Hungarian Institute of Geology, Budapest.

RÁLISCH-FELGENHAUER, E. (1988b): Remete-rét, S slope of Vörös-hegy, Pécs, Mecsek Mountains. Vöröshegy Dolomite Member. Magyarország geológiai alapszelvényei (Geological Key Sections of Hungary) No. 88/49. – Hungarian Institute of Geology, Budapest.

RÁLISCH-FELGENHAUER, E., TÖRÖK, Á. (1993): Mecsek and Villány Mountains. In: Haas, J. (ed.): Triassic lithostratigraphic units in Hungary. Hungarian Geological Survey MOL, Budapest 232-260. (in Hungarian).

RISCHÁK, G., VICZIÁN, I. (1974): Mineralogical factors determining the intensity of basal reflections of clay minerals. Annual Rept. of Hung. Geol. Inst. **1972**, 229-256.

SIDORENKO, G. A., VOLKOV, M. A., DYAKONOV, YU, S., MISCHENKO, K. S., RAYNOV, N., CECHLAROVA, I., RISCHÁK, G., MELKA, K., KORECKY, J., UNGER, H., HERING, A. (1992): Application of quantitative X-

ray diffraction phase analysis in the geological survey. II. 1-28. A methodological guide. Scientific Commission of Methods of Mineralogical Research, VIMS, Moskva (in Russian).

STÖRR, M., KÖSTER, H. M., KUZVART, M., SZPILA, K., WIEDEN, P. (1977): Kaolin deposits in Central Europe. IGCP Working Group "Genesis of Kaolins". Proc. 8th Int. Kaolin Symposium and Meeting on Alunite, Madrid-Rome K-20, 1-21.

STROUHAL, A., HENDRIKS, F. (1988): Die Tonmineralassoziationen in der Trias von Bad Hersfeld und von Eschwege, unter besonderer Berücksichtigung der Avicula-Schichten (Mittlerer Buntsandstein). Bochumer Geol. Geotechn. Arb. **29**, 216-219.

SZEMEREY-SZEMETHY, A. (1976): Quantitative determination of carbonate minerals by X-ray diffraction method. Annual Rept. Hung. Geol. Inst. **1973**, 475-482.

TÖRÖK, Á. (1997a): Dolomitization and karst-related dedolomitization of Muschelkalk carbonates in South Hungary. Acta Geol. Hung. **40**, 4, 441-462.

TÖRÖK, Á. (1997b): Triassic ramp evolution in Southern Hungary and its similarities to the Germano-type Triassic. Acta Geol. Hung. **40**, 4, 367-390.

TÖRÖK, Á. (1998): Controls on development of Mid-Triassic ramps: examples from southern Hungary. In: Wright, V. P. & Burchette, T. P. (eds): Carbonate Ramps. Geological Society, London. Special Publications **149**, 339-367.

VICZIÁN, I. (1990): Transformation of corrensite in deep zones of diagenesis, Mecsek Mts., S. Hungary (abstract). IGCP Project 294: Very Low Grade Metamorphism. Phyllosilicates as indicators of very low grade metamorphism and diagenesis. A conference in Manchester, 1990.

VICZIÁN, I. (1992): Diagenetic neoformations in Middle Triassic evaporitic and carbonate rocks, Mecsek Mts. (S. Hungary). Acta Min. Petr. Szeged **33**, 13-24.

VICZIÁN, I. (1993): Clay mineralogy of Middle Triassic evaporitic and carbonate rocks, Mecsek Mts. (southern Hungary). 11th Conference on Clay Mineralogy and Petrology, Č. Budějovice, 1990, 135-144. Univerzita Karlova, Praha.

WAGNER, J.-F. (1989): Paläeogeographische Entwicklung der triadischen Randfazies Luxemburgs. Z. dt. geol. Ges. **140**, 311-331.

WÉBER, B. (1965): Green clay intercalation in the Upper Anisian dolomite complex of western Mecsek Mts. Földt. Közl. (Bull. Hung. Geol. Soc.) **95**, 4, 442-444 (in Hungarian).

WÉBER, B. (1978): Contributions to the knowledge of Anisian and Ladinian beds in Mecsek Mts. Földt. Közl. (Bull. Hung. Geol. Soc.) **108**, 2, 137-148. (in Hungarian).

Manuscript received: 3. March. 2000.

Acta Mineralogica-Petrographica, Szeged, XLI, 31–62, 2000

ANTIMONY OXIDE MINERALS FROM HUNGARY

SÁNDOR SZAKÁLL*, GÁBOR PAPP**, ISTVÁN SAJÓ, ÁRPÁD KOVÁCS***

* Department of Mineralogy, Herman Ottó Museum
** Department of Mineralogy and Petrography, Hungarian Natural History Museum
*** Department of Metallography, University of Miskolc

ABSTRACT

Most of the Hungarian stibnite and fahlore occurrences contain antimony-bearing weathering products that earlier were either unidentified or their identification was doubtful. All these occurrences were investigated by using XRPD and EDS for the identification of the substances in question.

The results of investigations are reported here together with a brief description of the Hungarian stibnite occurrences, the antimony-bearing weathering products and their mineral assemblages. Occurrences of stibnite and antimony oxides are shown in *Fig. 1*. A list of Hungarian stibnite localities arranged according to mountains is given in Table 1 and a list of antimony oxide minerals is given in Table 2

Cervantite, in spite of being reported most frequently from this mineral group in the Hungarian mineralogical literature, has been found to occur only in Gyöngyösoroszi. On the other hand, stibiconite proved to be ubiquitous, and several new occurrences of bindheimite were also found. Our investigations confirmed the occurrences of valentinite and tripuhyite in Hungary and the first occurrence of partzite is also described.

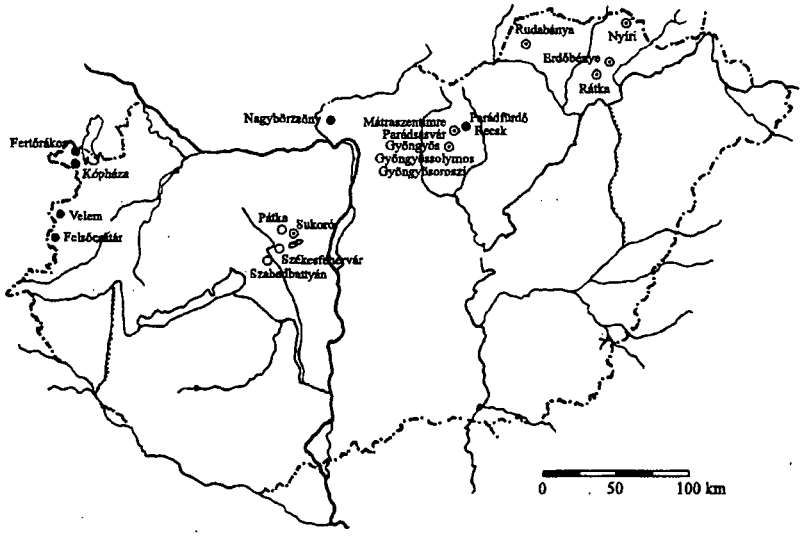

Fig. 1. Occurrences of stibnite and "antimony ochres" in Hungary
Symbols: ● stibnite, ⊙ stibnite and antimony ochre, O antimony ochre

* H–3525 Miskolc, Kossuth u. 13.
** H–1083 Budapest, Ludovika tér 2.
*** Miskolc, Egyetemváros

TABLE 1

Stibnite occurrences of Hungary (arranged by mountains from the west)

	LOCALITY	AREA	REFERENCES (other than this paper)
2.1.1	* Felsőcsatár: talc mine	Kőszeg–Vashegy	HOM collection
2.1.2	? Velem: Szent Vid Hill	Kőszeg–Vashegy	Földvári et al. (1949); Bendefy (1963, 1968); Vendel (1969)
2.1.3	* Velem: V-3, 4, 5, 6 boreholes	Kőszeg–Vashegy	Nagy (1972)
2.2.1	* Kópháza: Kő Hill	Sopron Hills	HOM collection
2.2.2	* Fertőrákos: Gödölye Hill	Sopron Hills	Fazekas et al. (1972)
2.3.2	* Székesfehérvár II inclined borehole	Velence Hills	Mikó (1964)
2.3.3	Pátka: Kőrakás Hill	Velence Hills	Jantsky (1952); Kiss (1954); Kaszanitzky (1959)
2.3.5	Lovasberény: Meleg Hill	Velence Hills	Jantsky (1952, 1957); Kubovics (1958)
2.4.1b	* Nagybörzsöny: Nb-13 borehole	Börzsöny Mts.	Nagy (1984)
2.5.1	* Recsk: –900 m level	Mátra Mts.	HOM collection
2.5.2	* Parádfürdő: Fehér-kő Hill / Hegyes Hill	Mátra Mts.	HOM collection / Nagy (1985)
2.5.3a	Gyöngyösoroszi: Aranybánya-bérc, Arany-Péter, Bányabérc, Hidegkút, Károly, Kiskút, Új-Károly veins	Mátra Mts.	Vidacs (1961a); Koch (1966); Kun (1985); Dódony (1986); Nagy (1986)
2.5.3b	Mátraszentimre: Mátraszentimre vein / outcrops on the Teréz Hill	Mátra Mts.	Koch (1966); Nagy and Barbácsi (1966); Csongrádi (1969); Kun (1985) / MÁFI Collection
2.5.4	Gyöngyössolymos: Asztag Kő Hill	Mátra Mts.	Szurovy (1940); Kiss (1960); Koch (1966); Szakáll (1989)
2.5.5	Parádsasvár: road cut	Mátra Mts.	Nagy and Szentes (1969)
2.5.6	Gyöngyös–Mátraháza road cut	Mátra Mts.	HOM collection
2.6.1	Rudabánya: Polyánka and Andrássy III. mines	Rudabánya Mts.	Szakáll et al. (in press)
2.6.2.	? Martonyi	Rudabánya Mts.	Maderspach (1880)
2.7.1	Erdőbénye: Ligetmajor and Mogyorósok areas / Sás stream valley	Tokaj Mts.	Endes (1988); Szakáll (1991) / Szabó (1870); Papp (1992)
2.7.2	Rátka: Hercegköves / Koldu open pits	Tokaj Mts.	Jánosi and Papp (1985) / MÁFI collection
2.7.3a	? Telkibánya: old references	Tokaj Mts.	Zipser (1817); Cotta and Fellenberg (1862); Szakáll et al. (1994)
2.7.3b	Telkibánya: Nyíri gallery	Tokaj Mts.	HOM collection

Symbols: ? – uncertain information; * – without antimony oxides

Abbrevations: MÁFI – Hungarian Geological Institute, Budapest; HOM – Herman Ottó Museum, Miskolc

TABLE 2

Antimony oxide minerals of Hungary (arranged by mountains and localitites within)

	stibiconite	bindheimite	partzite	tripuhyite	cervantite	sénarmonite	valentinite
Localities	$SbSb_2O_6OH$	$Pb_2Sb_2O_6(O,OH)$	$CuSb_2(O,OH)_7(?)$	$FeSb_2O_6$	Sb_2O_4	Sb_2O_3	Sb_2O_3
Szabadbattyán							
Pátka, Kőrakás Hill							
Pátka, Szűzvár							
Lovasberény, Meleg Hill							
Parádfürdő							
Gyöngyösoroszi							
Mátraszentimre							
Gyöngyössolymos, Asztag-kő Hill							
Parádsasvár							
Gyöngyös-Mátraháza							
Rudabánya							
Erdőbénye							
Rátka, Hercegköves							
Rátka, Koldu							

INTRODUCTION

Antimony oxides – or "antimony ochres" as they have usually been called – are formed in the oxidation zone of ore deposits and showings as weathering products of stibnite or occasionally of other antimony-bearing sulphides. Weathering of stibnite starts at the cleavage planes and can easily proceed turning the whole mass of the crystal into antimony oxides. Therefore antimony oxides (first of all stibiconite) frequently appear as pseudomorphs after stibnite. Bindheimite and (less commonly) stibiconite are formed by the weathering of Pb, Sb, sulphides (usually tetrahedrite or Pb, Sb, sulphosalts). They appear first in scattered grains, later in small aggregates and finally turn the sulphide into a spongy mass. Since bindheimite is usually formed during the weathering of different, tightly intergrown sulphides, it is as a rule accompanied by other secondary minerals (mainly cerussite and jarosite).

"Antimony ochres" are difficult to identify due to their fine-grained habit and frequent presence of admixed minerals. Despite this fact species names were assigned to such substances in the past without adequate research. In some cases a re-examination of the mineral in question proved that the earlier identification was false. In addition to these misinterpreted old occurrences, some new unknown ones were discovered in the last decade. This is why we undertook a comprehensive survey of antimony oxide minerals of Hungary.

X-ray powder diffraction (XRPED) and electron microprobe (SEM-EDS) was used for the identification of the minerals. Unfortunately, weathering products of stibnite frequently show a low degree of crystallinity (cf. Vitaliano and Mason, 1952). The interpretation of the XRPD pattern may be difficult even if the degree of crystallinity is sufficient, when the sample is an unseparable mixture. The strongest reflections of some antimony oxide minerals are close to each other (in addition to those belonging to the same structural

group). For example the two most intensive reflections of cervantite almost coincide with two strong peaks of stibiconite. VITALIANO and MASON (1952) have already pointed out the difficulties of the detection of small quanitites of valentinite associated with stibiconite. Some frequent associated minerals (stibnite, quartz etc.) may also cause problems; an example is the detection of subordinate tripuhyte in the presence of quartz and stibiconite.

In this paper only the minerals that were detected reliably, i.e. at least three or four characteristic reflections were present on the X-ray pattern of the specimen (some 70 to 80 samples were studied by XRPD), are discussed. The XRPD studies were completed with semi-quantitative EDS analyses. Chemical data helped us to detect antimony oxides and to distinguish structurally related but chemically different phases (e. g. stibiconite, bindheimite and partzite).

EXPERIMENTAL

X-ray powder diffraction (XRPD) investigations:

Dept. of Mineralogy, Eötvös L. University (hereafter reffered to as ELTE): Siemens 500 D diffractometer, CuK_α radiation, accelerating voltage 40 kV, tube current 20 mA, graphite monochromator, scan speed 1 or 2°20/min.

X-ray laboratory, MOL Rt. Philips PW 1820 diffractometer, CuK_α radiation, accelerating voltage 40 kV, tube current 30 mA, graphite monochromator, scan speed 0,05° 20/sec.

X-ray laboratory, Bay Zoltán Institute of Materials Science and Technology: Philips PW/1820 diffractometer, CuK_α radiation, accelerating voltage 45 kV, tube current 30 mA, graphite monchromator, scan speed 0.04°20/sec.

Electron microprobe (SEM-EDS) investigations:

Dept. of Metallurgy, University of Miskolc: AMRAY 1830i scanning electron microscope, EDAX 9900 energy dispersive X-ray spectrometer, accelerating voltage 20 kV, sample current 10–10 A, SiLi detector.

SURVEY OF STIBNITE AND ANTIMONY OXIDE OCCURENCES BY AREAS

Occurrences are described by mountains approximately in a west to east order. Stibnite localities without antimony-containing weathering products are also included for the sake of completeness. For every area a brief geological outline is given first on the basis of BÉRCZI and JÁMBOR (1998), CSÁSZÁR (1998), MOLNÁR et al. (1999) and other handbooks. More detailed information about the localities themselves based mainly on the data of JANTSKY (1966) and MOLNÁR et al. (1999) is included in the relevant entries.

Kőszeg–Vashegy area

Metamorphic rocks of the small Kőszeg Hills and Vashegy areas belong to the Rechnitz and Eisenberg tectonic windows of the Eastern Alps, respectively. They are made up by Penninian formations, metasediments and metamorphosed ophiolites. Sulphide mineralisations are scarse and little known, but stibnite is present in some occurrences.

Felsőcsatár, tale mine, stibnite occurrence

In a presumably Jurassic greensicht formation serpentinite, talc schist, chlorite schist, tremolite schist etc. are found at Felsőcsatár. A mine between 1952–1995 exploited the talc deposit. Quartz veins in the schists host late galena- and sphalerite-bearing sulphide showings. A stibnite sample from this paragenesis is stored in the Herman Ottó Museum (hereafter referred to as HOM) collection (inv. # 21 871). Acicular aggregates of stibnite are associated with an unidentified Pb, Sb sulphosalt. Weathering products of stibnite have not been observed yet.

Szent Vid Hill, Velem, doubtful stibnite occurrence

BENDEFY (1963, 1968) claimed that Bronze Age inhabitants of the settlement on Szent Vid Hill had mined antimony, iron and manganese. He found stibnite-bearing quartzite pebbles on the hill and observed outcrops of stibnite-bearing quartz veins. Geologists who mapped the area (FÖLDVÁRI et al, 1948; LENGYEL, 1953; VENDEL, 1969) have never found such outcrops and, therefore, they supposed that the stibnite-bearing material had been transported from the nearby stibnite deposit at Schlaining or the actually occurring pyrolusite was confused with stibnite. The newest geoarcheological studies (CZAJLIK et al, 1995) proved that the source of ore for production of antimony-bearing bronze tools is from ancient mines close to Salzburg or from the Carpathians. Our repeated attempts to find stibnite specimens were also unsuccessful, moreover, there are no such specimens in any public collection. By this reason we think that the data on the occurrence of stibnite on the Szent Vid Hill are false.

Velem, boreholes, ore showings

Disseminated pyrite and marcasite grains were found in a presumably Jurassic greenschist-facies calc-phyllite formation (NAGY, 1972). The ore microscopic studies of cores from V–3, 4, 5, 6 boreholes by Béla Nagy revealed magnetite, chalcopyrite, native gold, stibnite, galena and sphalerite in addition to the iron sulphides. Stibnite is the latest precipitation product of the latest post-tectonic ore-forming phase. No weathering products have been reported so far.

Sopron Hills

Metamorphic rocks of Sopron Hills belong to the Lower Austroalpine "Grobgneis" complex. This polymetamorphic crystalline complex is made up by metamorphosed sedimentary and magmatic rocks. Only one occurrence is known among the rare sulphide mineralisations where stibnite was found. Metamorphic rocks of the nearby "Fertőrákos Schist Isle" (the Hungarian aprt of the "Mörbisch Schist Isle") have been formed by polymetamorphism of sedimentary and igneous rocks of varied composition ranging from acidic to basic. It is correlated with the Wechsel series. Different levels of the series contain sulphide ore mineralisations (KOCH, 1985).

Kő Hill, Kópháza, stibnite occurrence

A stibnite sample from an outcrop of the Palaeozoic Sopron gneiss at the Kő Hill near Kópháza is found in the HOM collection (inv. # 21702). Rare sulphide clusters up to 0.5–1 cm) contain acicular stibnite crystals (up to 0.1–0.5 mm) associated with marcasite, galena and sphalerite. Weathering products have not been observed yet.

Gödölye Hill, Fertőrákos, ore showings

Uraniferous schists outcrop in the vicinity of Fertőrákos near the Austrian boundary. The prospect boreholes discovered a sequence of mica schists, gneisses, amphibolites, amphibole schists etc. Different levels of the series contain peculiar polymetallic ore showings with pyrite, arsenopyrite, Co, Ni arsenides, pyrrhotite, chalcopyrite, galena, sphalerite, fahlore, U, Ti oxides etc. as main components (FAZEKAS et al., 1972; KOCH, 1985). Stibnite was found by Károly Várszegi along a veinlet in a pegmatoid body (KOCH, 1985).

Velence Hills and their surroundings

From the Szabadbattyán area, SW from the Velence Hills, Lower Carboniferous limestones are known from galleries and boreholes, having tectonic contacts with underlying Ordovician slates and overlying metamorphosed Devonian limestones. The Devonian limestones show hydrothermal metasomatic alterations and host a fahlore-containing galena deposit.

The Velence Hills are made up by Carboniferous biotite orthoclase granite that intruded an anchimetamorphic Lower Paleozoic slate series. In the eastern part the grainite body is bordered by Eocene andesite rocks. In some places the Velence granite shows considerable post-magmatic and hydrothermal alterations. Hydrothermal quartz-fluorite and quartz-barite veins with polymetallic mineralisation are frequent and in two areas near Pátka form small ore deposits with stibnite and/or fahlore as antimony minerals.

Szár Hill, Szabadbattyán, lead deposit

In the Szár Hill a metasomatic lead deposit is found in Devonian crystalline limestone along a NW–SE striking faulted zone. The limestone itself suffered a strong iron metasomatism. The most important ore mineral is galena with some fahlore, sphalerite and chalcopyrite; the main secondary minerals are cerussite, malachite, azurite and yellow, bindheimite-like ochre. A small-sclae lead mine was in operation between 1938–46 and 1949–54 (JANTSKY, 1966).

KOCH (1943) found minor amounts of a yellow, pulverulent material in close connection with cerussite. He detected Al, Fe, Pb and Si by wet tests in the mineral, which was then classified as a hydrous Al silicate with Fe and Pb as impurities. The "bindheimite-like" mineral that was described by ZSIVNY (1951) is very likely the same substance. It occurred as lemon to orange yellow, pulverulent, earthy fracture fillings in strongly cerussitised ore samples. XRPD analyses of several samples from the collections of the ELTE and the HOM justified that the yellow powdery aggregates are composed of bindheimite. Bindheimite was found not only in the cavities and fissures of the cerussitised galena but also in the accompanying limonite. It should be mentioned that due to sample preparation problems the detection of bindheimite was difficult, because most of its reflections were overlapped by those of cerussite. However, some of the samples (e.g. C97) have low cerussite content and every important reflection of bindheimite could easily be identified: 3.005 (100), 2.612 (30), 1.843 (55), 1.571 (30) [d(Å) (I_{rel})] (Fig. 2). Bindheimite is always accompanied by cerussite, other close associates are quartz and a jarosite-group mineral. XRF analyses prove a persistent iron content.

Recalling Zsivny's paper, the uncertainty of his identification of the Kőrakás Hill bindheimite was due to the difficulties in the interpretation of wet chemical data (PbO 63.42, Fe_2O_3 2.78, Sb_2O_5 24.55, H_2O 7.00, Al_2O_3 0.26, SiO_2 1.43, total 99.33%), showing excess lead and less antimony as compared to the theoretical values of bindheimite.

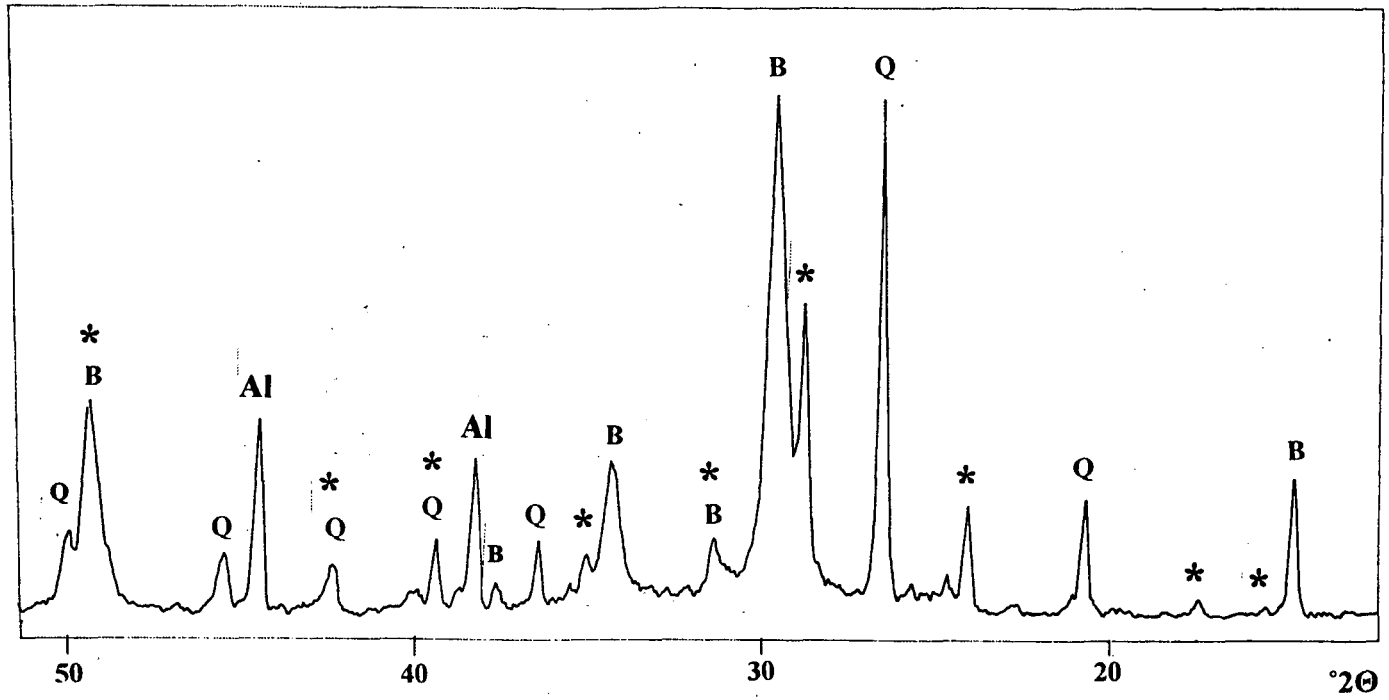

Fig. 2. XRPD pattern of bindheimite from Szár Hill, Szabadbattyán (C97)
Symbols: Al: sample holder, B: bindheimite, Q: quartz, * jarosite-group mineral

Unfortunately, the analytical details have not been published but the contradiction can be resolved if we assign some 5% of H_2O, presumably calculated from weight loss, to cerussite as CO_2. This explanation is in line with our experiences; namely we were practically unable to prepare a cerussite-free sample for XRPD analysis.

Székesfehérvár II inclined borehole

The Székesfehérvár II inclined borehole that was drilled to prospect the quartz vein of the Székesfehérvári szőlők area traversed a 2 cm thick quartz string as 199 m relative depth. The quartz string was bordered by a sphalerite I – galena – sphalerite II – stibnite – pyrite paragenesis associated with unspecified secondary minerals (MIKÓ, 1964).

Kőrakás Hill, Pátka, polymetallic ore deposit

On the Kőrakás Hill 4 km SSW from Pátka hydrothermal veins are found in silicified granite. The main components of the brecciated, banded and cockade ore are sphaleriteand galena with some chalcopyrite, stibnite and fahlore. The most important gangue minerals are quartz and fluorite; secondary minerals include cerussite, azurite, malachite, cinnabar, antimony ochre etc. (JANTSKY, 1966). The Kőrakás Hill mine operated from 1951 until 1973.

The occurrence of stibnite was first reported by JANTSKY (1952). According to KISS (1954), stibnite was found in the upper zone of the ore deposit uncovered by the first exploratory shaft (also called Földvári shaft), as radiated aggregates in vugs and fissures of the siliceous veins in granite. It was frequently replaced by antimony ochre pseudomorphs. Kiss also reported "rare powdery coatings composed of cinnabar and Pb, Sb ochre" associated with azurite and malachite (the unaltered ore was galena with microscopic sphalerite, chalcopyrite and fahlore grains). Stibnite was also found in quartz veins at the contact zone of granite and schist exposed by the north-eastern drift. According to KISS (1954) the Szűzvár stibnite forms striated aggregates composed of crystals few mm to few cm long, the crystals are rimmed or occasionally fully replaced by a yellowish weathering product. KASZANITZKY (1959) referred to this materials as cervantite although it has not been studied up to the present.

XRPD study of specimen # BE 21755 (collected by János Kiss and stored at the ELTE revealed that this substance is a well-crystallised stibiconite (sample # H145). All characteristic reflections of stibiconite appear on the record (*Fig. 3*): 5.92 (35), 3.09 (35), 2.963 (100), 2.568 (30), 1.979 (+ quartz), 1.817 (+ quartz), 1.737 (10), 1.568 (10), 1.550 (30) [d(Å) (I_{rel})]. Samples 4997, 4998 and 4999 of the MÁFI (collected by Béla Jantsky) came from the exploration workings driven on the Kőrakás Hill. These specimens contain thin stibnite bands in weathered, argillised granite. Stibnite may also form clusters of 0.5–1.5 cm in diameter along thin quartz veinlets in silicified granite. In the marginal zones of the veins and clusters, stibnite is always covered by yellowish brown, light brown weathering products, froming crusts or earthy aggregates. An XRPD pattern (sample D11) indicated the presence of stibiconite on the basis of the reflections: 5.95 (10), 3.09 (30), 2.99 (100), 2.589 (25), 1.819 (+quartz) [d(Å) (I_{rel})].

Szűzvár, Pátka, polymetallic ore deposit

The base metal vein-type mineralisation was discovered in 1951. The veins are characterised by a chalcopyrite-sphalerite-galena+tetrahedrite succession. Gangue minerals are fluorite and/or quartz with some barite. In most parts the lode is characterised by fluorite gangue, and the main products of the Szűzvár mine (operated from 1951 until

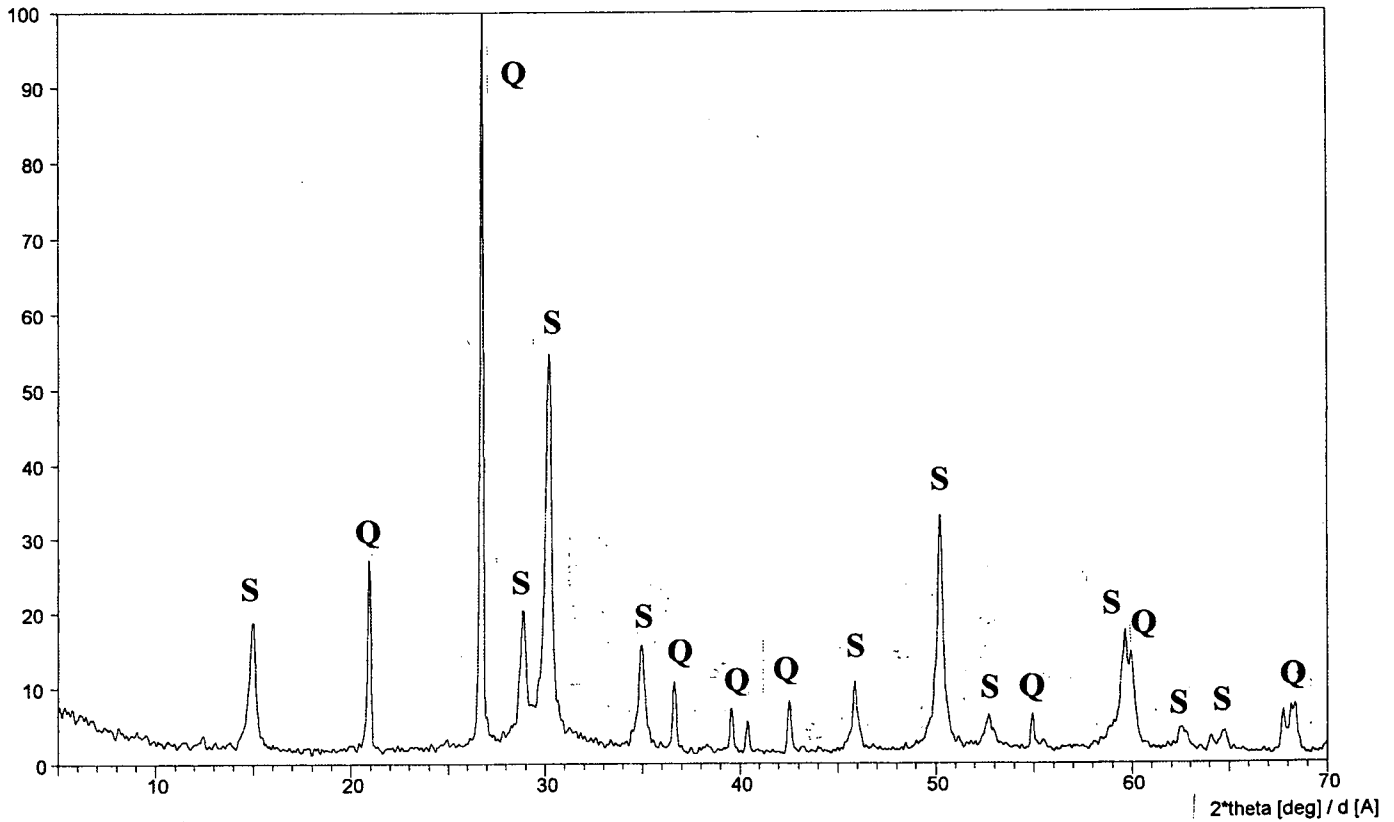

Fig. 3. XRPD pattern of stibiconite from Kőrakás Hil, Pátka (H145). Symbols: Q: quartz, S: stibiconite

1967) was in fact fluorite. Main secondary minerals are cerussite, pyromorphite, cinnabar, malachite and azurite (JANTSKY, 1966).

A "bindheimite-like" material accompanied by covellite, azurite, malachite, cerussite and cinnabar in altered fahlore-bearing galena ore was first mentioned by KISS (1954). We have also detedted this weathering product as yellow, fine-grained masses and early aggregates 1-5 mm in size on ore samples. It occurred most frequently in strongly weathered, spongy, cerussite- and pyromorphite-bearing fillings of siliceous vein outcrops above the adit. All characteristic reflections of bindheimite were identifiable on the XRPD pattern (H103) in spite of the presence of cerussite. EDS detected both antimony and lead. Associated minerals are malachite, azurite, cinnabar, linarite and cuprite.

A pale yellow pulverulent material proved to contain only antimony by EDS, the XRPD investigation of the probable antimony ochre mineral has not been completed yet.

Meleg Hill, Lovasberény, antimony showings in siliceous formations

JANTSKY (1952, 1957) found small prisms and radiating aggregates of stibnite and "yellow coatings after stibnite" together with limonite and secondary copper minerals on the SE slope of the Meleg Hill in hydrothermally silicified zones of granite. It is to be noted that some of the stibnite occurrences (viz. those on the W part of the hill) mentioned by JANTSKY (1952) are actually those of enargite. The Sb-rich zone is located as "antimonite–ochre-of-antimony area" on the map published as Fig. 1 in KUBOVICS (1958). According to ore microscopic observations of KUBOVICS (1958) stibnite forms zoned intergrowths with bismuthinite and the originally euhedral crystals are usually corroded by siliceous fluids. Stibnite is frequently replaced by unidentified antimony ochre. It is worth mentioning that we found Sb, Pb, Bi- and Pb, Bi, Ag-bearing minerals during the microprobe study of the lately collected samples. Recent studies by MOLNÁR (1995) have shown that the mineralization on the Meleg Hill is genetically connected to the Tertiary magmatic-volcanic complex bounding the area from east.

There is a stibnite-containing specimen labelled "hydroquartzite" in the collection of the Hungarian Geological Institute (hereafter referred to as MÁFI) from the eastern slope of the Meleg Hill (inv. # 4995, collected by Béla Jantsky). Columnar and needle-like stibnite crystals form aggregates 0.5 to 2 cm in size. They give a dark grey to black colour to the rock. Stibnite crystals are usually coated by a light yellow to yellowish brown weathering product, which proved to be a mixture of bindheimite and a jarosite-group mineral according the XRPD analysis (sample D47). EDS analysis (presence of K, Fe, S) suggest the presence of jarosite.

Description of recently collected samples from the eastern slope of the Meleg Hill is summarised as follows. Stibnite crystals, which are embedded in the silicified rock just as in the museum samples, reach 0.5–1 cm length and form radial-fibrous aggregates. The rim of the individual crystals is altered to white and/or light yellow antimony oxides. XRPD and EDS studies revealed the presence of stibiconite and bindheimite (samples K87–89). Associated minerals are acanthite (crusts and clusters few mm in size), jarosite (yellow, powdery aggregates), barium-pharmacosiderite (hexahedra 0.01–0.03 mm in size), segnitite and/or beudantite (dark brown crusts) and goethite.

Börzsöny Mts.

Early Middle Miocene submarine andesite extrusive domes and related volcanoclastic rocks overlain by remnants of andesite stratovolcano with andesite and diorite porphyry intrusions are exposed in the eroded central zone. Intrusion-related Cu (Mo) porphyry

showings, base-metal stockworks and low-sulphidation type epithermal. Au occurrences are known. The base metal and gold rich ore veins at Nagybörzsöny were intensively mined during the Middle Ages.

a) Rózsa Hill mineralised area, Nagybörzsöny

In the central part of the Rózsa Hill area a precious metal-containing pyrrhotite–arsenopyrite ore deposit is known as stockwork impregnation in a propylitised dacite breccia pipe. The main ore minerals of the first ore-bearing phase are pyrrhotite, galena, sphalerite, pyrite and chalcopyrite, those of the second phase are arsenopyrite with native bismuth, bismuth sulphides, Pb, Bi sulphosalts and native gold. The southern part is characterised by thin polymetallic veins with the products of the first ore-bearing phase in clayey gangue. (NAGY, 1983; KOCH, 1985)

The siliceous vein fillings of the Felső Rózsa gallery in the central part of the Rózsa Hill area contain many secondary minerals. During the preliminary study a small amount of as yet unidentified antimony oxides was found by EDS in white to pale yellow pulverulent aggregates.

b) Zálog-bérc Hill, Nagybörzsöny

Stibnite grains up to 1 mm showing twin lamellae, associated with pyrite or as inclusions in the latter were found by NAGY (1984) in polished sections of the material of the Nb-13 borehole that was drilled on the Zálog-bérc Hill, SSW from the Rózsa Hill mineralised area.

Mátra Mts.

Two major volcanic units make up the Mátra Mts. The Palaeogene Unit covers 25 km^2 in the NE part of the mountains in the environs of Recsk. There an Upper Eocene calc-alkaline volcanic sequence is intercalated with sedimentary rocks. The ore complex around Recsk contains high and low sulphidation type epithermal, porphyry copper, skarn and metasomatic replacement deposits.

The Neogene Unit extends over some 350 km2. It is formed by a Miocene calc-alkaline volcanic activity. In the Western Mátra this unit has a stratovolcanic structure with caldera and subvolcanic diorite porphyry intrusions, plus several rhyolite domes and dikes. Post-caldera andesites cover highest ridges. Volcanic rocks lie on Early Miocene sediments and tuffs. The volcanic sequence was formed in three major eruption cycles during the Lower and Middle Miocene. There are several base-metal rich low-sulphidation epithermal veins in the mountains. Low-sulphidation epithermal mineralisation related to Badenian volcanic activity occurs in two parts of the caldera structure of the Western Mátra Mts. The Gyöngyösoroszi-Mátraszentimre deposit is located in the central part and the Parádsasvár-Gyöngyössolymos mineralised zone along its eastern boundary. See MOLNÁR et al., 1999 for details and further references.

Recsk, deep levels of the deposit

At Recsk (Palaeogene Unit) a near-surface enargite-luzonite deposit in the Lahóca Hill at Recsk was minedfrom the 19th century until 1980. A subvolcanic diorite intrusion, which intruded Mesozoic sedimentary rocks during the Palaeogene volcanism, hosts another, deep-seated ore deposit. The deep deposit has been discovered by boreholes in the 1960s. During the 1970–1980s it was prospected in detail by further boreholes, two shafts and drifts. In the deep-seated ore zone a typical porphyry Cu + Mo mineralisation

developed in the intrusion and skarn (Cu, Zn, and Fe) mineralisation formed along the exo/endocontacts. The carbonate host rocks contain replacement Zn, Cu, Fe ore.

Stibnite was found in the –900 m level, on the drift face of the West 3 gallery in a serpentinite-brucite-calcite (aposkarn) rock (SZABOLCS TÓTH, personal communication). Acicular aggregates up to 1–2 mm are embedded in massive coarse crystalline calcite occasionally giving a grey colour to calcite. Antimony oxides have not been found.

Parádfürdő, polymetallic mineralisations

The locality is situated in the NW and SE parts of the Palaeogene Unit of the Mátra Mts. The epithermal mineralisation of this zone is spatially related to dacite domes that intruded into the andesitic stratovolcanic sequence. The dacitic host rocks (lava flows and pyroclastics) are variably silicified. These bodies occur as flat lenses and vein-like vertical-subvertical bodies. They are surrounded by a quartz stockwork. The ore is confined to the silicified and argillic zones and formed in three stages (galena+sphalerite with some Pb, Se and Ag, Sb sulphosalts – tetrahedrite – pyrite with rare Au, Ag, Bi, Te and Sb minerals, e. g. stibnite). See MOLNÁR et al. (1999) for details and further references.

A paragenesis rich in secondary minerals has been found recently on the southern slope of the Fehér-kő Hill, in the cavities of intensively leached siliceous-baritic vein fillings above the Egyesség gallery. Antimony oxides present are stibiconite and bindheimite according to the XRPD and EDS studies. Characteristic reflections of stibiconite are 5.96 (55), 3.11 (+barite), 2.978 (100), 2.581 (20), 1.820 (+quartz) and 1.545 (+quartz) [d(Å) (I_{rel})]. Stibiconite forms yellowish white to light brown, firable, porous coatings on the cavities of the quartz veins. Bindheimite appears in yellow, porous, earthy coating. Based on XRPD and EDS analyses, the secondary minerals of the paragenesis are as follows: jarosite, scorodite, mimetite, malachite, cornubite, richelsdorfite, olivenite, azurite, gypsum, goethite, beudantite/segnitite and smithsonite (?). Antimony oxides and arsenates have been formed by weathering of tetrahedrite and tennantite.

NAGY (1985) reported the occurrence of stibnite grains few mm in size on the rim of pyrite and as inclusions in pyrite-bearing samples collected on the waste dump of the Hegyes Hill Gallery and studied by microprobe.

a) Gyöngyösoroszi, polymetallic lead-zine deposit

The Gyöngyösoroszi–Mátraszentimre deposit crops out over a 12 km^2 area between the two villages. Some 20 hydrohtermal veins are hosted by andesitic lava flows and pyroclastic rocks of the Middle Andesite Sequence. The predominant trends of the veins are NNW–SSE, NNE–SSW and N–S. The (siliceous-carbonate) veins show symmetrical infillings with a variety of textures. The veins developed in seven stages with pyrite, marcasite, sphalerite, wurtzite, galena, and chalcopyrite as main products in the most important sulphide-bearing periods (2–4 stages). See MOLNÁR et al., 1999 for details and further references.

In Hungarian stibnite is the most frequent and the most varied in appearance in Gyöngyösoroszi. The oxidation zone of the deposit is shallow; therefore secondary antimony oxides appear only in minor amounts. Cervantite (NAGY, 1986) and valentinite (KOCH, 1966) have been reported so far.

Before describing the antimony oxides of the deposit, we give a list of the workings where stibnite was found according to KUN (1985). Stibnite is known from vein fissures at the +465 m level of the Károly vein as acicular aggregates on quartz or inclusions in

calcite crystals. In the northern part of the Károly vein, above the +430 m level, stibnite was found in several places as mm- or cm-sized globular aggregates, which were usually embedded in calcite or in clay. The radial-fibrous structure of these dull aggregates could be observed on the fractures. Stibnite in vein fissures of the +470 m level of the Károly vein was accompanied by cinnabar.

Stibnite occurrences of the Új-Károly vein were very similar to those of the Károly vein. In the southern and central sections of the Northern Aranybánya-bérc vein stibnite-rich vugs of amethyst and calcite were found in the cementation zone above the +460 m level. Finally, in the Hidegkút vein stibnite was found associated with barite in the exploration adit and in the workings above the +400 m level.

According to KÁROLY NAGY (personal communication, 1996) stibnite was frequently found in the upper levels of the mine, in the adit until Mátraszentimre, in the Bányabérc, Kiskút and Hidegkút veins and in the compressor hall grown on or within quartz (amethyst). On the +350 m level at about 300 from the shaft a cavity was found during the abandonment of the workings, with an egg-sized, plumose mass of stibnite. In 1980, a dip heading was driven from the +150 m level and a mine working was introduced on the +100 m level for the Arany-Péter vein. Here some cavities contained plumose stibnite aggregates 3–5 cm in diameter (studied by DÓDONY, 1986) on white or colourless calcite. Calcite was sometimes nearly black due to the stibnite inclusions (also reported by KUN, 1985). Stibnite has also been observed in the exploration adit above the Károly gallery on the +560 m level. The mineral was enclosed in quartz and covered by limonite.

According to KUN (1985) rhe greatest amount of antimony ochre was found around the +510 m level in the rise driven to the surface along the Károly vein. Another parageneses that have been observed on the samples of the HOM collection include:

Radial-fibrous stibnite spherules 2–5 mm in diameter with a pyrite-marcasite coating, the latter altered to different sulphates (rozenite, gypsum, and jarosite), on a quartz crust.

Radial-fibrous stibnite aggregates with siderite spherules ("spherosiderite") 0.5–2 mm in diameter, in quartz veins. Sometimes siderite forms coatings on the stibnite aggregate, similarly to the classical stibnite–spherosiderite paragenesis of Baia Sprie (Felsőbánya).

It can be concluded that stibnite occurs frequently in the upper horizons of the Gyöngyösoroszi ore deposit and this paragenesis is related to the final stages of the ore formation (VIDACS, 1961a, GATTER, 1986; MOLNÁR et al., 1999). Associated minerals are calcite, quartz, barite, marcasite/pyrite, siderite, cinnabar; secondary minerals include sulphur, rozenite, gypsum, jarosite, stibiconite and rarely cervantite (see below).

Analytical results of antimony oxides from the ore deposit of Gyöngyösoroszi can be summarised as follows. Usually diffuse peaks of poorly crystallised phases appear on the records; however, stibiconite can be proved in several cases. HOM 18671 specimen deserves special attention. The cream-coloured, thin crust on stibnite is composed of stibiconite with some cervantite. All major reflections of stibiconite appear on the XRPD record (sample D15, Table III), which makes its identification certain. A few small peaks corresponding to medium-intensity reflections of cervantite (Table III) suggest that cervantite may also present in the sample, although the two highest peaks of cervantite are overlapped by two strong reflections of stibiconite. This is the first occurrence of cervantite in Hungary that is supported by XRPD data. It is to be noted that we were unable to detect valentinite although KOCH (1966) had reported it from the Károly vein.

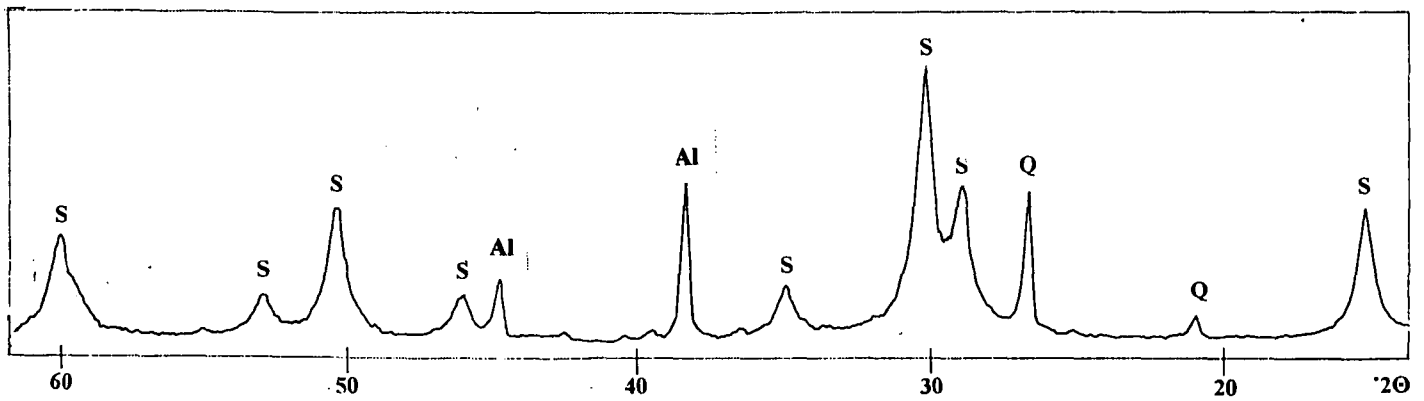

Fig. 4. XRPD pattern of stibiconite from Teréz Hill, Mátraszentimre (C3)
Symbols: Al: sample holder, Q: quartz, S: stibiconite

TABLE 3

XRPD data of an antimony ochre sample from Gyöngyösoroszi (D15)

HOM 18 671 (sample D15)		stibiconite JCPDS 10-388		cervantite JCPDS 11-694		Quartz JCPDS 5-490	
d (Å)	I/I_{max}	*d* (Å)	I	*d* (Å)	I	*d* (Å)	I
5.922	45	5.93	90				
4.254	15					4.260	34
3.567	2						
3.470	8			3.443	35		
3.346	70					3.342	100
3.225	6						
3.097	57	3.09	70	3.073	100		
2.966	100	2.96	100	2.942	45		
2.666	3			2.650	25		
2.569	19	2.57	40				
2.461	7					2.458	12
2.413	1			2.404	17		
2.357	3						
2.284	4					2.282	12
2.241	3			2.235	11	2.237	6
2.130	5					2.127	9
2.097	1						
1.977	15	1.98	30			1.979	6
1.869	2			1.862	25		
1.816	4	1.81	80	1.781	20	1.816	17
1.736	12	1.74	30	1.723	20		
1.707	3			1.697	11		
1.673	2					1.672	7
				1.636	11		
1.566	6	1.57	20				
1.549	27	1.55	60			1.541	15
1.482	6	1.48	30	1.487	13		
1.456	2			1.469	11	1.453	3

(Registered in the X-ray Laboratory of MOL Rt. Budapest, by É. MARGITICS-SIPŐTZ. Remarks: Reflections exceeding 10% relative intensity only are listed from the cervantite JCPDS pattern. Observed d values are corrested using quartz as internal standard.)

b) Mátraszentimre, polymetallic lead zinc deposit

According to NAGY and BARBÁCSI (1966) stibnite occurs here in radial fibrous aggregates and acicular crystals in the vein quartz, associated with pyrite and less sphalerite and galena. In the near-surface samples stibnite is replaced by antimony ochres along the cleavage planes. KOCH (1966) regarded the oxidation product of stibnite as cervantite, which may occur as pseudomorphs as well. This identification has not been confirmed by the present study (see below).

According to KUN (1985) fine acicular stibnite aggregates were found in the southeastern section of the +467 m and +515 m levels of the Mátraszentimre vein, filling fissures that cross the vein. KÁROLY NAGY (personal communication, 1996) reported stibnite from the +864 m level and from the ventillation shaft.

Based on museum samples (HOM) the largest (3-4 cm long) documented individual stibnite crystals of Hungary, although without terminal faces, were found at Mátraszentimre. Secondary antimony oxides in various shades from white to yellow frequently occur in the specimens. A yellowish crust on a sample from the MÁFI collection (inv. # 11677) from the left drift proved to be stibiconite according to the XRPD pattern (sample # C3, Fig. 4).

On the southern slope of the Teréz Hill exploration trenches were driven by Aladár Vidacs in the 1950s (VIDACS, 1961b). On the basis of the (MÁFI) museum samples stibnite was found abundantly in these trenches. The mineral usually formed typical radial-fibrous aggregates in the quartz veins of the altered andesite. One sample of this vein-filling (MÁFI, inv. # 2946) contains a 7–9 cm thick aggregate of stibnite and white and butter yellow antimony oxides. Another specimen contains stibnite pockets 1–3 cm in diameter, rimmed by white to light yellow antimony oxide coatings 1–2 cm thick, with pseudomorphs 2-5 mm long, after stibnite in the cavities. The secondary antimony oxide of these specimens proved to be stibiconite on the basis of the XRPD patterns (samples D10 and D12). Characteristic reflections are 5.88 (80), 3.084 (70), 2.956 (100), 1.809 (+quartz), and 5.92 (55), 3.09 (70), 2.963 (100), 2.568 (20), 1.820 (40), 1.546 (+quartz) [d(Å) (I_{rel})], respectively. Reflections of stibnite and/or quartz have also appeared on the patterns.

Asztag-kő Hill, Gyöngyössolymos, antimony mineralisation in silicified rhyolite tuff

In Hungary antimony oxides have been found the most abundantly on the Asztag-kő Hill at Gyöngyössolymos in the upper horizon of the hydrothermally silicified rocks related to a steam-heated alteratation zone of a low-sulphidation type epithermal system. The siliceous rock is dark grey due to embedded stibnite on the western side of the steeply dipping kaolin vein near the benchmark on the top of the hill. Stibnite crystals up to 5 cm long used to be found near the surface (SZUROVY, 1940). KISS (1960) noted that stibnite is usually coated "by yellow antimony-ochre, cervantite". KOCH (1966) added that the cervantite pseudomorphs in small vugs are dark straw-coloured, whereas those after stibnite embedded in the rock are light yellow. Koch also reported the rare occurrences of sénarmontite. Small octahedral crystals with diamond lustre were found associated with cervantite pseudomorphs in small vugs. In a brief report on the paragenesis SZAKÁLL (1989) described stibiconite on the basis of XRPD data, and postulated the presence of tripuhyite indicated by EDS analyses.

The appearances of the antimony oxides was highly variable in the several hundred samples examined by optical microscope. The colours ranged from white thorugh butter yellow, lemon yellow, orange and light brown shades to reddish brown and dark brown,

sometimes even to black. EDS analyses revealed a definite relationship between iron content and colour; viz. darkes shades correspont to higher iron content (cf. VITALIANO and MASON, 1952). The hardness of the antimony oxides varies between 2 and 4 Mohs' scale. The morphology is also varied: thin to thick crusts with smooth to rough surfaces (*Fig. 5.*), globular, stalactitic or irregular aggregates. Every intermediaries from fresh stibnite to crystals that completely altered to antimony oxides (stibiconite, tripuhyite) including common pseudomorphs after stibnite (Fig. 6) can be observed. From among antimony oxides only sénarmontite forms well-developed crystals; colourless or white octahedral of 1–3 mm size and crusts composed of octahedral of 0.05–0.1 mm size also occur (*Fig. 7*). A pale purple aggregate of 0.1 mm-long acicular crystals was also observed once. The habit and the qualitative EDS data (Sb+, S+; O cannot be detedted due to the experimental conditions) suggest kermesite but in lack of enough material it was impossible to confirm by XRPD.

About half of the examined samples were difficult to identify by XRPD, as they are poorly crystalline, their reflections are diffuse. In other cases sharp peaks of stibiconite can be observed (e.g. sample V204). Well and poorly crystalline phases proved to be indistinguishable by their appearance. Cervantite and valentinite have not been detected undoubtedly in any sample.

As far as the presence of tripuhyiite is concerned, it has already been suggested on the basis of the high iron content of some reddish brown and dark brown antimony oxide phases (SZAKÁLL, 1989). One of the XRPD patterns made during the recent study (sample D37) showed broad reflections of tripuhyite accompanied by those of quartz. On other patterns a few, ambiguous, low-intensity peaks of tripuhyyite appeared together with strong reflections of stibiconite.

Antimony oxides of the antimony-bearing paragenesis of the Asztag-kő Hill are associated with quartz, barite, calcite, pyrite/marcasite, sphalerite, cinnabar, galena, anatase, goethite, hematite, manganese oxides, pharmacosiderite, scorodite (?) and sulphur.

Parádsasvár, stibnite occurrence in rhyoite tuff

NAGY and SZENTES (1969) found thin quartz veins with fine needles of stibnite about 500 m east from the village, in the cut of the Parád-Gyöngyös road. The surface of stibnite was reported to have been covered by cervantite according to the XRPD data (unpublished). On the original sample (MÁFI 10399), 2–4 mm long radial-fibrous stibnite aggregates appear in thin quartz veinlets in intensively weathered rhyolite tuff, which contains lemon yellow spots of jarosite. A film-like, greyish-white weathering crust rims the stibnite crystals. According to the XRPD investigations (sample D13), the weathering product is stibiconite rather than cervantite. Characteristic reflections are 5.92 (60), 3.06 (+stibnite), 2.962 (100), 2.564 (80), 1.811 (+quartz) [d(Å) (I_{rel})].

Gyöngyös-Mátraháza, stibnite occurrence in andesite

The HOM collection holds a stibnite sample (inv. # 22661) collected by Péter Badinszky, its locality is given as "Mátraháza, road cut". This occurrence doesn't correspond to the above-described one, since the host rock of the stibnite-bearing quartz veins is altered, pyretic andesite and not rhyolite tuff. In some parts of the quartz veins, columnar stibnite crystals are embedded in calcite. Calcite is black due to another fine acicular stibnite generation. A brown film of antimony ochre covers the surface of some stibnite crystals. The weathering product cannot be identified by XRPD due to its poor crystallinity.

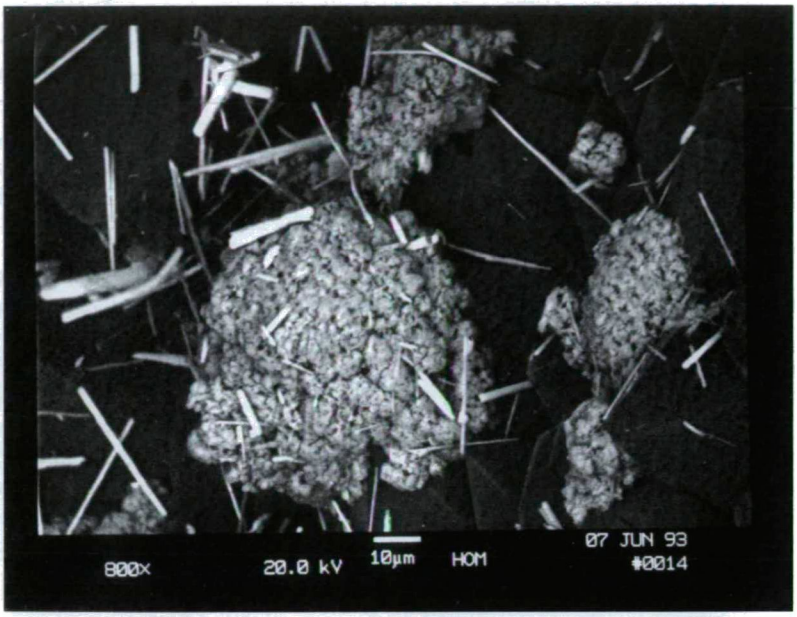

Fig. 5. Tripuhyite aggregates (grey) with stibnite needles (white) on quartz (dark grey) from Asztag-kő Hill, Gyöngyössolymos, SEM image

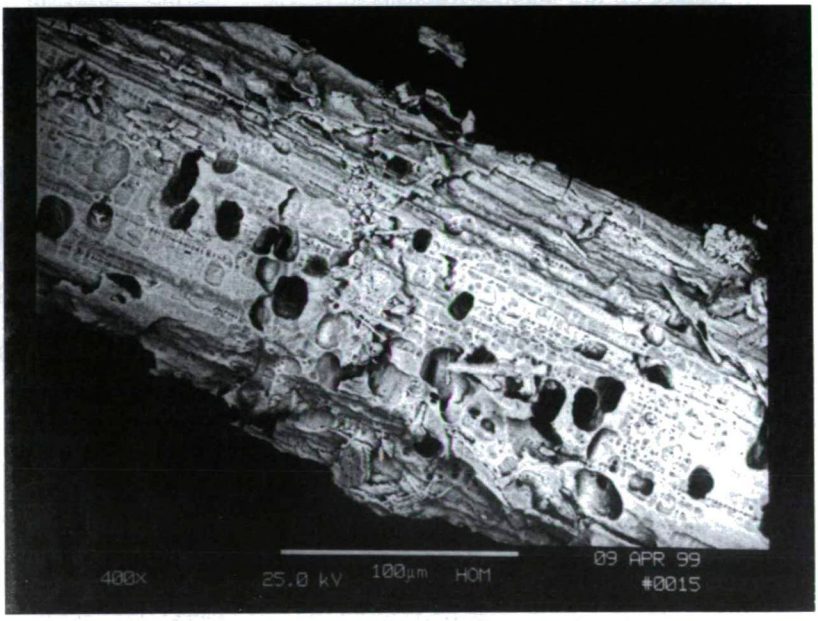

Fig. 6. Stibiconite, pseudomorphs after stibnite, Asztag-kő Hill, Gyöngyössolymos. SEM image

Fig. 7. Sénarmonite crystals, Asztag-kő Hill, Gyöngyössolymos. SEM image

Rudabánya Mts.

The Rudabánya Mts. forms the Eastern part of the Aggtelek–Rudabánya Mts., which is one of the most complex regions of Hungary considering its geology and structural development. The Rudabánya Mts. Is built up by four dislocated segments and itself is separated from the Aggtelek Mts. By a lateral dislocation zone. In the basement an Uppermost Permian and Lowermost Triassic evaporitic sequence is found, which is followed by Lower Triassic to Jurassic shallow to deep marine formations (marl, limestone, dolomite, etc.). The cover formations are Miocene to Pliocene sediments. There are several metasomatic iron ore occurrences in the Middle Triassic formations of the mountain.

Rudabánya, iron ore deposit

The large siderite body at Rudabánya, which is exposed in some 4 km length by the huge open pits was formed by the metasomatism of a Triassic sedimentary series built up by Lower Triassic marl and limestone and Middle Triassic (Gutenstein) dolomite. Subsequent hydrothermal events produced a multiphase sulphide mineral paragenesis. The amount of sulphides can be estimated from the historical fact that Rudabánya used to be a rich silver and copper mine in the Middle Ages.

The ore-forming phases and their products are reconstructed as follows (see PANTÓ, 1956; JANTSKY, 1966; HERNYÁK, 1977 for further details and references). In the first phase a hematitic and slightly sideritic ore formed with some chalcopyrite along the main overthrust planes. During the second (main iron producing) phase tectonised dolomite and limestone turned into a so-called sparry iron ore (siderite, ferroan dolomite, tha latter also called incorrectly "ankerite"). In the third phase vein- and stockwork-like bodies were

formed. A peculiar product is a 0.5 to 3 m thick barite zone ("marginal barite") with abundant sulphides, which was formed a on the margin of the marl. The ore formation is terminated by later large-scale weathering processes producing ochreous, siliceous and brown iron ore. A peculiar secondary product is the so-called spherosiderite ore (from the radial–spherical texture of siderite grains under the microscope), which was formed by the reprecipitation of dissolved iron.

As a result of analyses and field observations made in the last decade, minerals such as stibnite, stibiconite, valentinite, bindheimite and a red, unidentified antimony oxide phase were detected from several outcrops of the deposit.

Stibnite was found in two different parageneses in Rudabánya. It appears in radial aggregates of 1–3 mm long crystals in the outcrops of the spherosiderite ore (Polyánka area and Andrássy III mines) together with siderite, calcite, malachite and realgar. (It is to be noted that the miner's term to the spherosiderite ore is "scoriaceous ore" because of its porous nature, see PANTÓ, 1956.) This stibnite-bearing paragenesis belongs to the last sulphide phase of the ore formation. Secondary antimony oxides have not been found in this paragenesis. Stibnite of the second paragensis forms sheaf-like aggregates of 1–2 mm long crystals in the galena- and sphalerite-bearing ores of the large baritic zones in the Polyánka area. Here stibnite is covered by white crusts composed of valentinite (see below).

Bindheimite occurrences are of two types. Bindheimite is ubiquitous in the weathered galena-sphalerite ore of the large barite bodies. Lemon yellow to orange, powdery crusts covering up to 10–20 cm^2 areas, as well as earthy, irregular aggregates of 1–2 mm size were discovered in the Polyánka, Andrássy I, Andrássy II, Villanytető and Vilmos mining areas. It was also found rarely as yellow, acicular crystals and radial-fibrous aggregates, which may be pseudomorphs after heteromorphite, which was also observed here. Associated minerals (Villanytető area) are cerussite and barite according to and XRPD record (sample L55). The second type of occurrence is in the silicified limonite of the Adolf area. Here bindheimite forms yellow, earthy crusts in the fissures of the ore. Parent sulphide minerals have not been found even in the wider environment of bindheimite. It is to be noted that KERTAI (1935) mentioned native sulphur crusts 0,5–1 mm thick usually covered with a cinnabar film associated with cerussite. We think that this "sulphur" occurrence may have been bindheimite in fact.

Stibiconite is also widespread, although it occurs in much smaller amounts. It forms radial-fibrous aggregates of white colour and diamond lustre after stibnite in fissures of quartz veins in the siliceous limonite of the Adolf area. Every important reflection of stibiconite appeared on the XRPD pattern (sample G163) 2.978 (100), 1.822 (+quartz), 3.11 (35), 5.95 (30), 2.578 (30), 1.554 (30) etc. [d(Å) (I_{rel})]. It is also connected to the fissures of intensively silicified zones of limonite at the upper horizons of the Villanytető area, where stibiconite forms white, 0.5 to 1 mm thick crusts and globular aggregates. Acicular pseudomorphs after stibnite are found in the cavities of the spherosiderite ore of the Andrássy III mine. The most abundant accompanying minerals in these outcrops are malachite, azurite, goethite and cinnabar. In a sample from the Villanytető area white spherules 0.2–0.4 mm in diameter of an antimony oxide (by EDS) are found on azurite crystals associated with calcite in cavities of limonite.

Partzite forms olive green powdery aggregates or friable coatings in the cavities of the so-called spherosiderite ore of the Andrássy III mine. SEM micrographs revealed that the coatings are composed of isometric graisn up to 1-2 μm without any apparent crystal forms (*Fig. 8*). Only the strongest reflection of partzite is observalble on the XRPD pattern

(sample K281) as a broad peak at 2.96 Å. Cu and Sb content was proved by EDS. Associated minerals are malachite, cuprite, native copper, siderite and quartz in the samples. Its formation may be related to the weathering of chalcostibite and other Cu, Sb sulphides that are present in the spherosiderite ore.

Valentinite is known only from the Polyánka area as a rarity. It forms crusts of white euhedral crystals with diamond lustre on acicular stibnite aggregates. The crusts are composed of 0.1–0.3 mm long bipyramidal crystals according to the SEM observations (*Fig. 9*). The identification was confirmed by XRPD (*Fig. 10*). It is to be mentioned that this is the first report of valentinite from Hungary based on XRPD and EDS results. Further members of the secondary mineral paragenesis that appears in the weathering zone of the Polyánka galena-sphalerite-bearing barite body are cerussite, gypsum, mimetite, jarosite, goethite, acanthite, barite, bindheimite and smithsonite.

Based on EDS analysis, an antimony- and sulphur-bearing secondary mineral appears also in a secondary baritic fissure filling in the Polyánka area, forming red, earthy crusts and, very rarely, irregular aggregates up to 0.1 mm size. SEM images shows that the aggregates consist of foraminous spherules 5-10 μm in diameter (*Fig. 11*). An X-ray study was attempted using Gandolfi camera without interpretable results.

Martonyi, iron ore deposit, doubtful stibnite occurrence

A small iron ore deposit, similar to that at Rudabánya is found near to Martonyi. Middle Triassic Gutenstein dolomite was replaced metasomatically by the main "primary" minerals including siderite, quartz, barite, pyrite, chalcopyrite, bornite, tetrahedrite and galena; secondary products are goethite, hematite, chalcocite, covellite, malachite, azurite and cerussite, etc. (JANTSKY, 1966).

Maderspach (1880) listed stibnite among the minerals of Martonyi. Although stibnite really occur in the above-described Rudabánya deposit of similar origin, the size of the Rudabánya stibnite suggests that Maderspach probably confused manganese oxides with stibnite as it had happened earlier in the case of the Úrkút pyrolusite (cf. PAPP, 1990).

Tokaj Mts.

The main mass of the mountain is made up by Badenian to Lower Pannonian andesite-rhyolite volcanic rocks related to horst/graben structures with interbedded remnants of small andesite stratovolcanoes, dacite extrusive domes and extensive rhyolite pumice tuff horizons with flow-dome complexes in volcanic centres. There are geophysical evidences of diroite porphyry intrusions. Volcanic rocks rest upon Middle Miocene sedimentary rocks, Hercynian to Late Palaeozoic basement is exposed on horsts. Ore deposits and showings are bound to intrusions-related Au-Ag±Sb low-sulphidation epithermal veins and stockworks and steam-heated alteration zones. See MOLNÁR et al. (1999) for details and further references.

Erdőbénye, antimony showings in lacustrine siliceous sediments (limnoquartzite)

Between Erdőbénye and Sima a limnic sequence, composed from rhyolite tuff, tuffite, sand, sandstone, diatomite and quartzite, is found. The limnic sequence is exposed by boreholes and diatomite open pits. The quartzite used to have been quarried for millstones. (See MÁTYÁS, 1979, for further details.)

SZABÓ (1870) described a stibnite vein in limnoquartzite from a millstone quarry west from Erdőbénye in the valley of the Sás Stream. PAPP (1982) investigated a museum specimen (ELTE) in detail. He observed thin, light brown crusts of antimony ochre

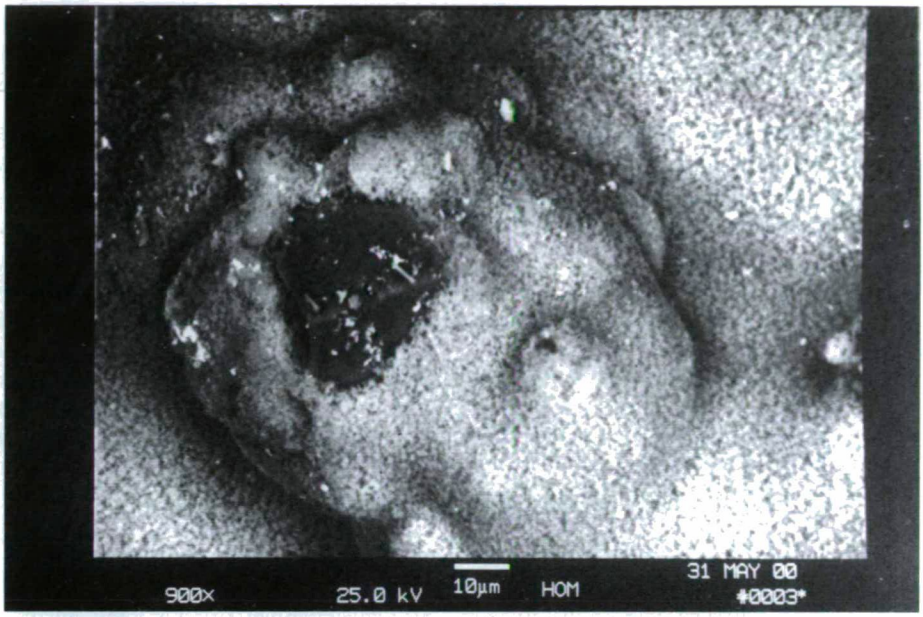

Fig. 8. Partzite crust on siderite rhombohedra, Andrássy III mine, Rudabánya. SEM image

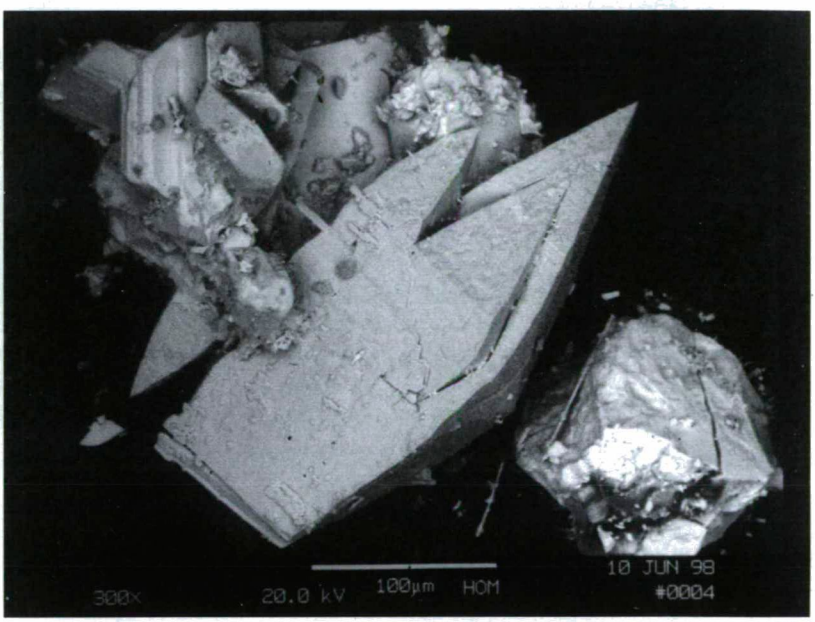

Fig. 9. Valentinite, bypiramidal crystals, Polyánka area, Rudabánya, SEM image

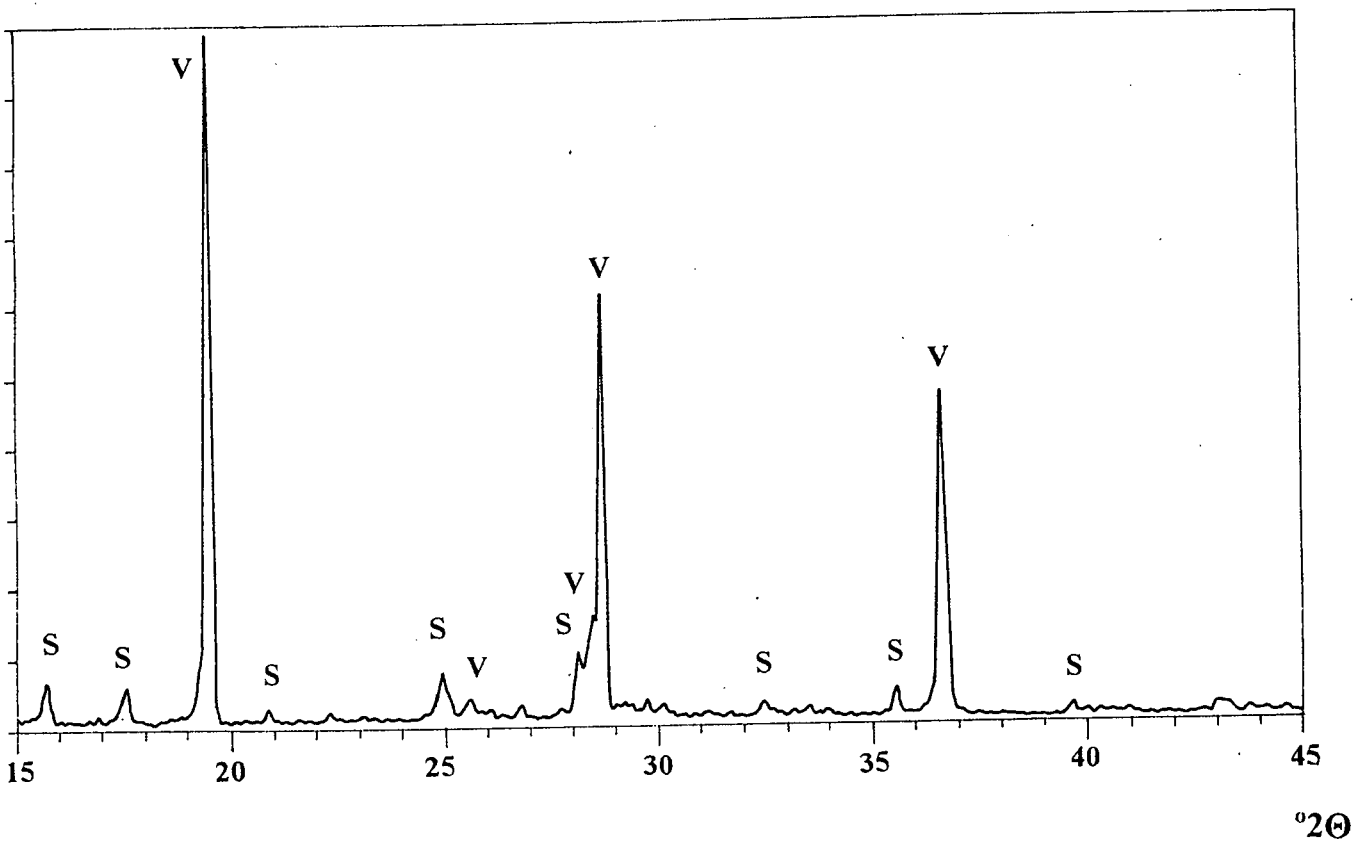

Fig. 10. XRPD pattern of valentinite, Polyánka area, Rudabánya. Symbols: S: stibnite, V: valentinite

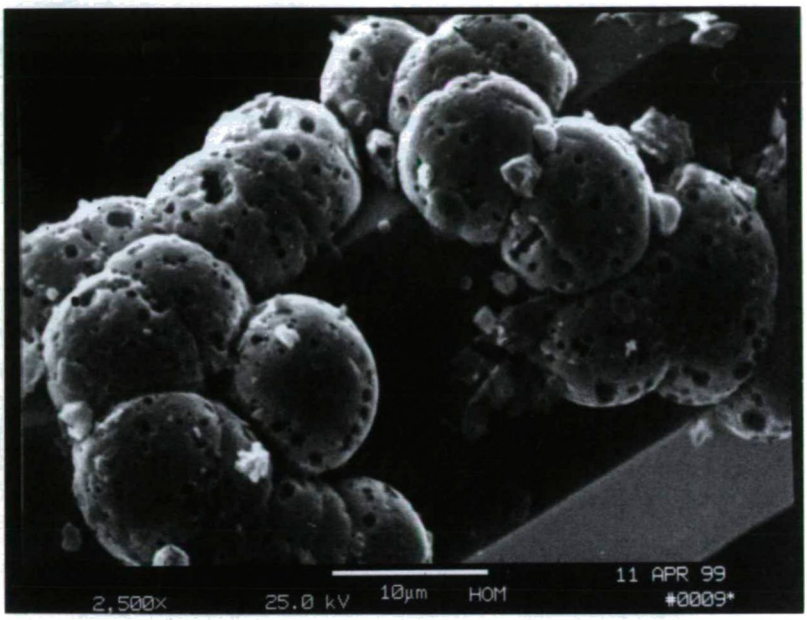

Fig. 11. Foraminous aggregate of an unidentified secondary antimony mineral, Polyánka area, Rudabánya

rimming the stibnite vein, which was embedded in silica minerals, quartz (chalcedony) and opal. In polished sections, the antimony ochre appeared as pseudomorphs after stibnite, forming white, radial aggregates of acicular crystals up to 1 mm long. The mineral is probably stibiconite on the basis of the XRPD patterns. Framboidal pyrite aggregates were also observed as two concentric strings along the inner part of the stibnite vein.

ENDES (1988) found a similar occurrence in the debris of a temporary steam on the western slope of the Mogyorósok Hill; most of the stibnite enclosed in blocks of limnoquartzite is exposed in the bed of a temporary stream between the Liget and Mogyorósok areas. Stibnite veins 1-2 cm in thickness are found on the bedding planes of the thin-bedded limnoquartzite. Peripheral parts of the veins are usually covered by yellowish white to light brown antimony oxides. In more disturbed zones, where weathering proceeded along the joints, the alteration of stibnite is more pronounced. Stibiconite was identified by XRPD; weak but characteristic reflections were observed in addition to those of stibnite (sample G2). Sb, Pb, and Cu were detected on the XRF spectrum. In another sample (EBSZ-1S) the broad reflections of stibiconite (5.91 (50), 3.09 (60), 2.95 (100), 2.56 (25), 1.81 (30) [d(Å) (I_{rel})]) were accompanied by quartz and opal peaks. The samples contained pyrite framboids similarly to those found in the sample from the Sás Stream valley. All stibnite occurrences associated with limnoquartzite near Erdőbénye are supposed to have been formed by epithermal processes. Later stibnite altered more or less to stibiconite at near-surface conditions. It should be mentioned that according to ERNŐ MÁTYÁS (personal comm.) small amounts of stibnite were found several times in limnoquartzite beds traversed by the prospect boreholes of the Ligetmajor diatomite deposit.

Herczegköves and Koldu open pits, Rátka, antimony showings in lacustrine siliceous sediments (limnoquartzite)

Between Mád and Rátka a sedimentary sequence of a lacustrine basin crops out over an approx. 8 km^2 area (see MOLNÁR et al., 1999 for details and further references). The limnic sequence of the basin is underlain by a pyroxene andesite lava flow. In the lacustrine sequence 3 major consolidated siliceous layer occur. The siliceous layers show bedding from few cms up to 1–2 m. Bentonite, bentonitic tuffite, rhyolite tuff etc. are interbedded. Siliceous beds show high concentration of Sb and less As and Hg, as well as some Ag (VETŐ, 1971).

A stibnite occurrence, similar to those around Erdőbénye, is known from the limnoquartzite cover of the bentonite open pit of the Hercegköves area (misnamed for Koldu by JÁNOS and PAPP, 1985). Radiating circular or spherical aggregates up to 3 and 1-cm diameter, respectively, are found on the bedding planes of the rock and in the irregular cavities within the beds. Stibnite clusters have usually been altered to whitish to ochre or brownish yellow stibiconite (investigated by XRD and EDS by JÁNOSI and PAPP, 1985).

MASON and VITALIANO (1953) suggested that "the brown or black colour of some stibiconites is generally due to the presence of admixed tripuhyite". Recent XRF studies showed that the darker stibiconite samples from Hercegköves have a higher iron content than that of the lighter ones. The XRPD pattern of the darker samples corresponded to that of stibiconite but the increase of width and relative intensity of the peaks at 2.56 and 1.72 Å suggested the presence of a poorly crystalline tripuhyite-like phase (the strongest tripuhyite reflection at 3.28 Å was overlapped by the large quartz peak at 3.33 Å). A brown, friable, earthy substance filling a cavity showed the highest iron content. The sample gave an XRPD patterns with broad reflections of tripuhyite, some small peaks of stibiconite, opal and quartz, and probably some poorly crystalline goethite (*Fig. 12a*). After heating to 1000 °C tripuhyite peaks became sharp and well defined, the crystallinity of opal also increased (*Fig. 12b*). The most intensive reflections of hematite appeared on the pattern, whereas no traces of stibiconite were visible. In a parallel experiment an iron-free sample of stibiconite + quartz gave identical XRPD patterns before and after heating.

It is to be noted that pyrite hexahedra, cinnabar and realgar have also been found in the close environment of the stibiconite.

There are similar specimens in the MÁFI collection (collected by ORSOLYA KÁKAY SZABÓ in 1971) from the near Koldu open pit, suggesting an occurrence identical to that at Hercegköves.

Telkibánya, Au-Ag ore deposit

The most renowned ore deposit of the Tokaj Mts. is that at Telkibánya. The mining flourished in the Middle Ages with a short-term revival in the 18th century. Badenian volcanic rocks host small veinlets of the older stockwork-type mineralisation (sphaerlite, galena, pyrite, chalcopyrite, and arsenopyrite). A younger and more important near-surface mineralisation with abundant pyrite dissemination in the hydrothermally altered Sarmatian volcanic rocks and noble metals in siliceous veins consists the major part of the low-sulphidation type epithermal deposit.

"Antimony ochre" was mentioned from Telkibánya by ZIPSER (1817) and by COTTA and FELLENBERG (1862). This piece of information has been republished in several monographs in a rather confusing way. ZEPHAROVICH (1859) at first simply adopted Zipser's data on antimony ochre but later (ZEPHAROVICH, 1873) he reclassified it as cervantite without any any further investigation, referring to the studies of Blum on

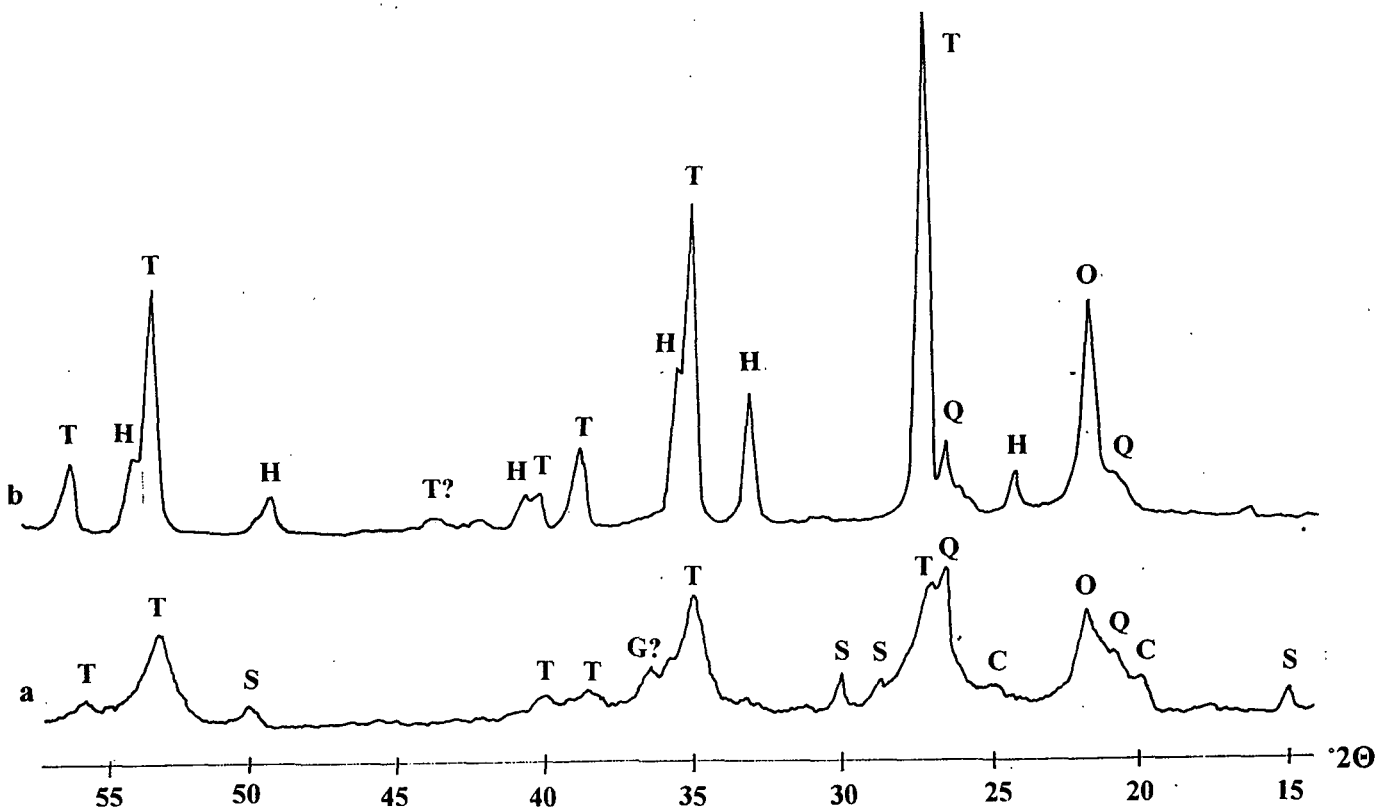

Fig. 12. XRPD pattern of tripuhyite, Hercegköves open pit, Rátka (a) before and (b) after heating to 1000 °C.
Abbrevations: C: a clay mineral (d001≈7.1 Å), G: goethite, H: hematite, O: opal, Q: quartz, S: stibiconite, T: tripuhyite

antimony ochre from other localities. TÓTH (1882) published the data of Zipser and of COTTA and FELLENBERG (together with those from other Hungarian occurrences) under the heading "antimony ochre", noting that he used this general term for the mineral because it was not known which one is cervantite and which is stiblite [=stibiconite]. LIFFA (1955) gave antimony ochre, cervantite and stiblite alike. In the first edition of this monograph KOCH (1966) pointed out that "one failed to find the antimony ochre mentioned by earlier authors" but, curiously enough, he included cervantite in the paragenesis referring to TÓTH (1882). Antimony ochre has not been found even during the detailed study of the ore deposit by SZÉKY-FUX (1970). Cervantite and antimony ochre were then omitted from the Telkibánya chapter of the second edition of the monograph of KOCH (1985). MOLNÁR and SZAKÁLL (1994) were also unable to find any antimony oxides in the part of Telkibánya mining area, except for a light yellow, unidentified iron- and antimony-bearing oxide from a pit on the Fehér Hill. They suggested that early authors might have been mistaken acanthite for stibnite and jarosite for antimony ochre.

For only documented stibnite specimen form the Telkibánya area was collected from the spoil heap of the Nyíri gallery on the Fehér Hill, west from Nyíri (HOM collection, inv. # 24 404). Fibrous aggregates of 1–3 mm long crystals were found in cavities of vuggy vein quartz. A yellowish antimony oxide coating covers the surface of the crystals. The poorly crystalline material cannot be identified by XRPD.

A forgotten antimony occurrence from the Tokaj Mountains (?)

Some mineral collections (HOM, Pannonhalma Abbey and a former old private collection) hold similar stibnite specimens collected presumably in the 18–19th century; strangely enough, neither of them has exact locality data. On an old label attached to one of the specimens (HOM, formerly Pál Kriván's collection), the word "Tokaj" may be rad (with a later question mark pencilled after the name). Another autograph label by Kriván reads: "perhaps Tokaj Mountains?". The outward appearance and the paragenesis of the host rock suggest that the locality was somewhere in the Eperjes–Tokaj Mountains (Slanské Mts. in Slovakia and Tokaj Mts. in Hungary).

Main features of these samples are as follows: stout, columnar stibnite crystals, which as a rule form radial aggregates, are embedded in white to light brown common opal. The crystals are well formed; even their terminal faces are frequently developed. (It is to be mentioned that all other stibnite specimens from the Eperjes–Tokaj Mountains, at least those known by us, consist of fine acicular aggregates.) A white, thin film of antimony oxide may cover the surface of the stibnite crystals; due to its low crystallinity, XRPD results were not interpretable. A yellow powdery material obtained from one of the specimens proved to contain poorly crystalline sphalerite.

Supposing that these samples were really collected from an obsolete occurrence of the Tokaj Mountains, the only locality (to our knowledge) where a considerable amount of stibnite is mentioned from is the antimony mine at the former Klauzúra or Szigord (now Sigord) E from Kokošovce near Prešov (cf. MADERSPACH, 1875; FOULLON, 1884).

SUMMARY AND CONCLUSIONS

General conclusions

Stibiconite proved to tbe ubiquitous among antimony ochre minerals of Hungary. On the other hand, cervantite, which is frequently mentioned in the literature (usually without any reference to analytical data), is actually rare. VITALIANO and MASON (1952) reached a

similar conclusion during their global research on antimony oxides from different localities. It can also be stated that in some cases "cervantite" or "antimony ochre" reported in the Hungarian mineralogical papers is in fact jarosite. This misinterpretation may be due to the similarity of appearance and paragenesis of jarosite and of antimony oxides.

Bindheimite is the second most widespread antimony-bearing alteration product. It is usually formed by the weathering of fahlore or galena containing antimony (as sulphosalt or other inclusions). Bindheimite was frequently associated with cerussite and stibiconite.

Valentinite was unambiguously detected only in one (stibiconite-free) sample from Hungary but, as stibiconite strongly prevails in the examined samples, the presence of small amounts of valentinite in other occurrences cannot be excluded (cf. VITALIANO and MASON, 1952).

Sénarmontite and partzite occur as a rarity.

Tripuhyite was found in iron-rich dark parts of stibiconite-dominated associations in two localities.

Antimony oxides rarely form monomineralic aggregates. The weathering product usually contains relics of stibnite, or other admixed minerals, such as quartz, opal, pyrite, marcasite, iron oxides (goethite, hematite), gypsum and jarosite. Sometimes antimony oxides are intermixed, e.g. bindheimitie + stibiconite, stibiconite + cervantite, stibiconite+tripuhyite assemblages have been detected.

The colour of antimony ochres varies from white to dark brown. According to our semi-quantitative electron microprobe (EDS) analyses, the colour of the weathering product practically depends on the iron content: the higher is the iron content, the darker is the antimony ochre (cf. VITALIANO and MASON, 1952).

X-ray powder diffraction (XRPD) analyses indicated that the antimony ochres show different degrees of crystallinity. About one third of the studied samples hasn't produced any interpretable reflections.

Summary of occurrences

Microscopic stibnite grains that occur in the Kőszeg–Vashegy area and in the Sopron Hills are not accompanied by antimony oxides.

In the Velence Hills stibnite is known from two ore deposits (Kőrakás Hill and Szűzvár, both at Pátka) and also from one ore mineralisation (Meleg Hill, Lovasberény). The weathering products of the Kőrakás Hill and Meleg Hill stibnite are stibiconite, presumably as a weathering product of Pb, Sb-bearing sulphides.

In the Börzsöny Mountains stibnite was found as a rarity at Nagybörzsöny (Nb-13 borehole), and a small amount of as yet unidentified antimony oxides was found at Nagybörzsöny ore deposit (Felső Rózsa gallery).

In the Mátra Mountains stibnite is known from the upper horizons of the Gyöngyösoroszi and Mátraszentimre ore deposits, its weathering products such as stibiconite and, in a single case, cervantite were found in some heavily tectonised zones. The stibnite-rich siliceous formations of the Asztag-kő Hill near Gyöngyössolymos hold one of the most varied paragenesis of antimony oxides in Hungary, due to its shallow position. Stibiconite and bindheimite were detected in the rich secondary mineral paragenesis of the outcrops of veins on Fehér-kő Hill at Parádfürdő. Small stibnite occurrences were found in fissures or rhyolite tuff and andesite of the Mátra Mountains and also in the deep-seated parts of the Recsk ore deposit.

In the Rudabánya ore deposit antimony oxides are found in the weathering zone of the sulphide (galena, sphalerite, stibnite, Ag-sulphides) –rich barite bodies (bindheimite, valentinite) or accompany the stibnite of the so-called spherosiderite ore (stibiconite, partzite).

In the Tokaj Mountains near Rátka and Erdőbénye limnoquartzite bodies that were formed during the post-volcanic activity of Miocene volcanism include a characteristic stibnite + framboidal pyrite + stibiconite ± tripuhyite mineral assemblage. Stibnite occurs only in minor amounts in the eastern part of the Telkibánya mineralised are (Nyíri adit); a weakly crystallised antimony oxide phase was found here as a weathering product.

ACKNOWLEDGEMENTS

Several X-ray diffraction records were made at the Dept. of Mineralogy of the Eötvös University, in the X-ray Laboratory of the MOL Rt. and at the former Dept. of Mineralogy of the Veszprém University. MELINDA JÁNOSI, GYÖRGY LOVAS, TAMÁS WEISZBURG, ÉVA MARGATICS-SIPŐTZ and VENDEL OLASZI are thanked for the investigations.

Thanks are extended to collectors and researches who provided us samples for study: GÁBOR GYOMBOLa (Budapest), ISTVÁN HORVÁTH (Miskolc), TIBOR HORVÁTH (Budapest), SÁNDOR KLAJ (Pécs), GÁBOR KOLLER (Törökszentmiklós), BÉLA KUN (Gyöngyös), ÁRPÁD MÓRICZ (Székesfehérvár), KÁROLY NAGY (Gyöngyösoroszi), LÁSZLÓ TAVAS (Miskolc), SZABOLCS TÓTH (Recsk), ANDRÁS VARGA (Gyöngyöshalász) and GYŐZŐ VÁRHEGYI (Budapest).

The help of TIBOR NAGY (Eötvös Loránd University, Budapest) and ORSOLYA KÁKAY SZABÓ (Hungarian Geological Institute, Budapest) during the survey of the specimens of the ELTE and MÁFI collections and in the selection of samples for analysis is gratefully acknowledged.

Valuable suggestions and critical remarks of GYÖNGYI LELKES-FELVÁRI (HNHM) and FERENC MOLNÁR (ELTE) are heartily thanked.

REFERENCES

BENDEFY, L. (1963): Az egykori Vas-megyei antimonércbányászat [One-time antimony ore mining in Vas county]. Bány. Lapok, 96, 537–545. (In Hung.)

BENDEFY L. (1968): A Bányászati Kutató Intézet antimonérc kutatásai Velemszentvid környékén [Antimony ore prospecting of the Mining Research Institute in the environs of Velemszentvid]. Bány. Koh. Lapok, 101, 312–314. (In Hung.)

BÉRCZI, I. & JÁMBOR, Á. (1998) (eds.): Magyarországi geológiai képződmények rétegtana [Lithostratigraphy of the geological formations of Hungary]. Budapest, MOL-MÁFI, 517 p.

COTTA, B. and FELLENBERG, E. (1862): Die Erzlagerstätten Ungarns and Siebenbürgens. Engelhardt, Freiburg, 226 p.

CSÁSZÁR, G. (ed.) (1998): Magyarország litosztratigráfiai alapegységei, táblázatok és rövid leírások (Basic lithostratigraphic units of Hungary. Charts and short descriptions). MÁFI, Budapest, 114 p. (Bilingual)

CSONGRÁDI, J. (1969): A mátraszentimrei új ércelőfordulás ásványtani, kőzettani és teleptani vizsgálata [Mineralogical, petrographical and ore deposit study of the new ore occurrence at Mátraszentimre]. M. Sc. Thesis, manuscript, Eötvös L. University, Budapest. (In Hung.)

CZAJLIK, Z., MOLNÁR, F. and SOLYMOS, G. (1995): Angaben zur spätbronzezeitlichen Metallrohmaterial-versorgung am Velem/St-Veit-Berg, Westungarn. Archäol. Österr., 6/2, 30–35.

DÓDONY, I. (1986): A gyöngyösoroszi antimonit ásványtani újdonság (A new stibnite-like mineral from Gyöngyösoroszi). Ásványgy. Figy., 3/2, 19–23. (In Hung. with English abstr.)

ENDES, M. (1988): Antimonit, antimonokker és nemesopál Erdőbényéről [Stibnite, antimony ochre and precious opal from Erdőbénye, NE-Hungary]. Ásványgy. Figy., 3/4, 7. (In Hung.)

FAZEKAS, V., KÓSA, L. and VINCZE, L. (1972): Szulfidos ércesedés a fertőrákosi palasziget területén [Sulphidic ore mineralisation in the territory of the Fertőrákos Schist Isle]. Research report, manuscript, Archives of Mecsek Ore Mining Company (MÉV), Pécs. (In Hung.)

FÖLDVÁRI, A., NOSZKY, J., SZEBÉNYI, I. and SZENTES, F. (1949): Földtani megfigyelések a Kőszegi hegységben [Geological observations in the Kőszeg Hills]. Jel. Jövedéki Mélykút. 1947-48. évi munk., 5–31. (In Hung.)

FOULLON, H. von (1884): Ueber Antimonit von Czerwenitza. Pseudomorphose von Hyalit nach Antimonit von ebanda, von Chalcedon nach Antimonit vom Josephistollen in Klausenthal bei Eperies. Verh. kais.-k. Geol. Reichsanst., 34, 142–144.

GATTER, I. (1986): Fluid inclusion studies in polymetallic ores at Gyöngyösoroszi (North Hungary) – spatial and temporal evolution of ore-forming fluids. Chem. Geol., 61, 169–181.

HERNYÁK, G. (1977): A Rudabányai-hegység szerkezeti elemzése az elmúlt 20 év kutatásai alapján (Structural analysis of the Rudabánya Mountains in the light of the last twenty years of research). Földt. Közlöny, 107, 368–374. (In Hung. with English abstr.)

JANTSKY, B. (1952): A Velencei-hegység hidrotermális ércesedése [Hydrothermal ore mineralisations in the Velence Hills]. MTA Műsz. Oszt. Közlem., 5, 69–83. (In Hung.)

JANTSKY, B. (1957): A Velencei-hegység földtana (Géologie de la Montagne de Velence). Geol. Hung. Ser. Geol., 10, 1–179. (In Hung. with French and Russian abstr.)

JANTSKY, B. (1966) (ed.): Ásványtelepeink földtana [Geology of our mineral deposits]. Műszaki Könyvkiadó, Budapest, 315 p.

JÁNOSI, M. and PAPP, G. (1985): Sztibikonit és antimonit Rátkáról [Stibiconite and stibnite from Rátka]. Ásványgy. Figy., 2/4, 18-21. (In Hung.)

KASZANITZKY, F. (1959): A pátkai kőrakáshegyi érckutatás jelenlegi állása (Der gegenwärtige Stand der Erzforschung bei Pátka). Föld. Közl., 89, 133-142. (In Hung. with German asbstr.)

KERTAI GY. (1935): Rudabánya oxidációs övének új ásványai (Neue Vorkommen aus der Oxydationszone von Rudabánya). Földt. Közlöny, 65, 21-30. (In Hung with German abstr.)

KISS J. (1954): A Velencei-hegység É-i peremének hidrotermális ércesedése (La minéralisation hydrothermale du bord septrentrional de la Montagne de Velence). Magy. Áll. Földt. Intézet Évi Jel. 1953-ról, 1/111-127. (In Hung. with French abstr.)

KISS J. (1960): A new ore occurrence in the environment of Nagygalya, Nagylipót and Aranybányafolyás, Mátra Mountains, NE-Hungary, Ann. Univ. Sci. Bp. Rolando Eötvös Nom., Sect. Geol., 3, 55-81.

KOCH, S. (1943): Das Bleierzvorkommen auf dem Szárhegy im Komitat Fejér. Acta Mineral.-Petrogr., 7-12.

KOCH, S. (1954): Minerals of Gyöngyösoroszi. Acta Mineral.-Petrogr., 7, 1-23.

KOCH, S. (1966) Magyarország ásványai [Minerals of Hungary]. Akadémiai Kiadó, Budapest, 419 p. (in Hung.)

KOCH, S. (1985): Magyarország ásványai [Minerals of Hungary]. 2 nd rev. End, ed by J. MEZŐSI. Akadémiai Kiadó, Budapest, 562 p. (in Hung.)

KUBOVICS, I. (1958): A sukorói Meleg-hegy hidrotermális ércesedése (The hydrothermal ore genesis of the Meleg Hill, Sukoró, Velence Mountains, Hungary). Földt. Közlöny, 88, 299–314. (In Hung. with English abstr.)

KUN, B. (szerk.) (1985): Gyöngyösoroszi és környéke ércbányászata [Ore mining at Gyöngyösoroszi and in ist environment]. Documentation for the closing of the mine, manuscript, Archives of the MGSZ (Hungarian Geological Survey), Budapest.

LENGYEL E. (1953): Mangánércnyomok a Kőszegi-hegységben (An occurrence of manganese ore in the Kőszeg Mountains). Földt. Közl., 83, 360–368. (In Hung. with English abstr.)

LIFFA, A. (1955): Telkibánya bányaföldtani viszonyai (Conditions géologiques des gites métalliques des environs de Telkibánya). Magy. Áll. Földt. Intéz. Évkv., 42/4, 211 p. (In Hung. with French abstr.)

MADERSPACH, L. (1875): Antimontelep Eperjes vidékén [Antimony deposit in the vicinity of Eperjes]. Bány. Koh. Lapok, 8, 52–53. (in Hung.)

MADERSPACH, L. (1880): Magyarország vasércfekhelyei. Királyi Magy. Termtud. Társ., Budapest, 111 p. (in Hung.)

MASON, B. and VITALIANO, C. J. (1953): The mineralogy of the antimony oxides and antimonates. Mineral. Mag., 30, 100–112.

MÁTYÁS, E. (1979): Az erdőbényei kovaföld-előkészítő üzem nyersanyagbázia [Raw material for the diatomite plant at Erdőbénye]. Bány. Koh. Lapok (Bányászat), 112, 190–202. (In Hung.)

MIKÓ, L. (1964): A Velencei-hegységi kutatás újabb földtani eredményei (New geological results of prospecting in the Velence Mountains). Földt. Közlöny, 94, 66–74. (In Hung. with English abstr.)

MOLNÁR, F. (1995): Mineralization in a Variscan monzogranite intrusion, Velence Mountains, western Hungary: Fluid inclusion evidence of polystage metallogeny. In PAŠAVA, J., KRIBEK, B. and ŽÁK, K.

(eds.): Mineral deposits: From their origin to their environmental impacts. Proc. Third biennial SGA Meeting, Prague, Czech Republic, 28-31 August 1995. Balkema, Rotterdam-Brookfield, 487-490.
MOLNÁR, F. and SZAKÁLL, S. (1994): A telkibányai ércesedés oxidásványai (Oxide minerals of Telkibánya ore deposit). Topogr. Mineral. Hung., 2., 181–199. (In Hung. with English abstr.)
MOLNÁR, F., LEXA, J. and HEDENQUIST, J. W. (1999) (eds.): Epithermal mineralizations of the Western Carpathians. Soc. Econ. Geol. Guidebook Ser., Soc. Econ. Geol., Littleton, Vol. 31. 274. p.
NAGY, B. (1983): Adatok a nagybörzsönyi Rózsabánya ércesedésének genetikai ismeretéhez (Contribution to the genesis of the Rózsabánya ore mineralization in Nagybörzsöny). Magy. Áll. Földt. Intéz. Évi Jel. 1981-ről 129–145. (In Hung. with English abstr.)
NAGY, B. (1984): A Börzsöny-hegységi hidrotermális ércesedések komplex ércföldtani és geokémiai vizsgálata [Complex ore geological and geochemical study of the hydrothermal ore mineralisations in Börzsöny Mts.]. C. Sc. thesis manuscript, Library of the Hungarian Academy of Sciences (MTA), Budapest. (In Hung.)
NAGY, B. (1985): Arany-, ezüst- és bizmutteluridok a parádfürdői ércesedés ásványparagenezisében (Gold-, silver- and bismuth tellurides in the paragenesis of the Parádfürdő mineralisation). Magy. Áll. Földt. Intéz. Évi Jel. 1983-ról, 321–357. (In Hung. with English abstr.)
NAGY, B. (1986): A gyöngyösoroszi ércesedés ásványtani felépítése (Mineralogy of the ore mineralization of Gyöngyösoroszi). Magy. Áll. Földt. Intéz. Évi Jel. 1984-ről, 403–423. (In Hung. With English abstr.)
NAGY, B. and BARBÁCSI, Á. (1966): A mátraszentimrei ércesedés ásványparagenetikai vizsgálata (Untersuchung der Mineralparagenese der Hydrothermalen Vererzung von Mátraszentimre). Magy. Áll. Földt. Intéz. Évi Jel. 1964-ről, 403–421. (In Hung. with German and Russian abstr.)
NAGY, B. and SZENTES, GY. (1969): Új antimonit előfordulása a Mátrában (A new occurrence of antimonite in the Mátra Mountains). Földt. Közlöny, 99, 384–386. (In Hung. with English abstr.)
NAGY, E. (1972): Vizsgálataink a Kőszegi-hegységben (Untersuchungen im Kőszeg-Gebirge). Magy. Áll. Földt. Intéz. Évi Jel. 1970-ről, 197–207. (In Hung. with German abstr.)
PANTÓ, G. (1956): A rudabányai vasérctelep földtani leírása [Geological description of the Rudabánya iron ore deposit]. In: Pantó, E., Pantó, G., Podányi, T. and Moser, K. (eds.): Rudabánya ércbányászata [Ore mining of Rudabánya]. OMBKE, Budapest, 222–275.
PAPP, G. (1990): XVIII. századi adatok a bakonyi mangánásványokról (18th century data about the manganese minerals of Bakony Mts.). Fol. Mus. Hist.-Nat. Bakonyiensis, 9, 7–9. (In Hung. with English abstr.)
PAPP, G. (1992): Az erdőbényei antimonitról (On the stibnite from Erdőbénye (Tokaj Mts., Hungary). Földt. Közlöny, 122, 39–50. (In Hung. with English abstr.)
SZABÓ, J. (1870): Antimonit opal-érben Erdőbényén [Stibnite in an opal vein at Erdőbénye]. Magy. Földt. Társ. Munkálatai, 5, 194–195. (In Hung.)
SZAKÁLL, S. (1989): Adatok a Mátra ásványainak ismeretéhez I (On minerals of teh Mátra Mts. I). Fol. Hist.-nat. Mus. Matr., 14, 9–13. (in Hung. with English abstr.)
SZAKÁLL, S. (1991): Ásványtani vizsgálatok még le nem írt gyűjteményi mintákon a Bodrog és Bódva közé eső területen [Mineralogical studies of unidentified collection specimens from the area between the Bodrog and Bódva rivers]. Manuscript, Herman Ottó Museum, Miskolc. (In Hung.)
SZAKÁLL, S., MOLNÁR, F., KOVÁCS, Á. and DÓDONY, I. (1994): A telkibányai ércesedés szulfidásványai (Sulphide minerals of Telkibánya ore deposit). Topogr. Mineral. Hung. 2, 149–179. (In Hung. with English abstr.)
SZAKÁLL, S., HORVÁTH, L. and ZSÁMBOKI, L. (in prep): Classical mineral localities: Rudabánya (Hungary). Mineral. Rc.
SZUROVY, G. (1940): Ásvány-kőzettani megfigyelések a Mátra-hegység déli részéből (Mineralogisch-petrographische Beobachtungen am südlichen Abhang des Mátragebirges in Ungarn). Mat. Termtud. Ért, 59, 701–721. (In Hung. with German abstr.)
TÓTH, M. (1882): Magyarország ásványai [Minerals of Hungary]. Hunyadi M. Intézet, Budapest, 568 p. (In Hung.) A reprint edition was published in 2000 in Miskolc by the HOM, 568 + 49 P.
VENDEL, M. (1969): Die mineralogischen, petrographischen und lagerstättenkundlichen Forschungen in unserem Institut. Publ. Hung. Min. Res. Inst., 12, 15–20.
VETŐ, I. (1971): A Tokaji-hegység szarma hévforrástavi képződményeinek ritkaelem-indikációi (Rare element indications in the hydrothermal –lacustrine formations of the Tokaj Mountains). Magy. Áll. Földt. Intéz. Évi Jel. 1969. évről, 77–84. (In Hung. with English abstr.)
VIDACS, A. (1961a): A gyöngyösoroszi ércbánya hidrotermális telérei (Filons hydrothermaux de la mine de Gyöngyösoroszi). Magy. Áll. Földt. Intéz. Évi Jel. 1956/57 évről, 77–84. (In Hung. with French and Russian abstr.)
VITALIANO, C. J. and Mason, B. (1952): Stibiconite and cervantite. Am. Mineral., 37, 982–999.

ZEPHAROVICH, V. von (1859): Mineralogisches Lexicon für das Kaiserthum Österreich. [Vol. 1]. Braumüller, Wien, 627 p.
ZEPHAROVICH, V. von (1873): Mineralogisches Lexicon für das Kasierthum Österreich. Vol. 2. Braumüller, Wien, 436 p.
ZIPSER, A. (1817): Versuch eines topographisch-mineralogischen Handbuch von Ungarn. Wigand, Oedenburg, 440 p.
ZSIVNY, V. (1951): Mineralogische Beiträge. Földt. Közlöny, 81, 161–167.

Manuscript received: 18. Oct. 2000.

Acta Mineralogica-Petrographica, Szeged, XLI, 63–77, 2000

GENESIS OF LOW SULFIDATION TYPE EPITHERMAL ORE INDICATIONS AT ARANYOSBÉRC (MÁTRAKERESZTES), MÁTRA MTS., NORTH HUNGARY

PÉTER SIPOS
Laboratory for Geochemical Research, Hungarian Academy of Sciences[1]

ISTVÁN GATTER
Department of Mineralogy, Eötvös Loránd University[2]

ABSTRACT

Indications are situated at the western border of the low sulfidation type western Mátra ore field, representing a characteristic part of the polymetallic-epithermal zone of the Inner Carpathian Volcanic Belt. The host rock shows intense silicification and K-metasomatic alteration. The poor, original sulfide mineralization (marcasite and arsenic pyrite) is accompanied by silicification, in form of stockworks and little veins with banded structure. Later these minerals were transformed into goethite and jarosite (gossan formation), indicating the high potassium content (13% K_2O) of the host rock. In the area there is an As-Sb-(Hg-Ba) anomaly (8500ppm As, 1000ppm Sb) belonging to the secondary minerals. The mineralization proceeded at 190-200°C. Two types of fluids could be distinguished of different salinity and composition (vein-forming and "apophysis" stage). The dilution of solutions by meteoric water was characteristic. Consequently, the upper region of the vein system of a low sulfidation type mineralization can be identified, which is located in shallower depth than the vein system of the western Mátra mineralization.

INTRODUCTION

Aranyosbérc is the largest continuous and most intensely K-metasomatized area of the Mátra Mts., and is situated at the western border of the K-metasomatized belt surrounding the western Mátra ore field (Fig.1.). Many scientist studied the genesis of this potassium-rich rock: according to VARGA (1966a, 1966b, 1992) and VARGA et al. (1975) this rock crystallized from potassium rich lava. On the other hand, KUBOVICS (1965, 1966, 1970) and MEZŐSI (1968, 1970) are of the opinion that this rock obtained its high K_2O (12-13%) content during an intense K-metasomatism. This later view is corroborated by the investigations accomplished in the Mátra Mts. by BAKSA et al. (1982), and in the Tokaj Mts. by SZÉKY-FUX (1970) and by MOLNÁR (1993).

The hydrothermal indications in these rocks were described by KUBOVICS (1966). He found 10 ppm Ag, and in traces Pb, Zn and Cu in the intensely pyritized quartzite at Aranyosbérc, generated by low temperature silicification. VARGA (1992) recognized three

[1] H-1112, Budapest, Budaörsi út 45., e-mail: sipos@sparc.core.hu
[2] H-1088, Budapest, Múzeum krt. 4/A

types of silicification here. According to MEZŐSI (1970) the silicification is closely related to the K-metasomatism.

Our purpose was the genetic study of the epithermal indications of this hydrothermally strongly altered area.

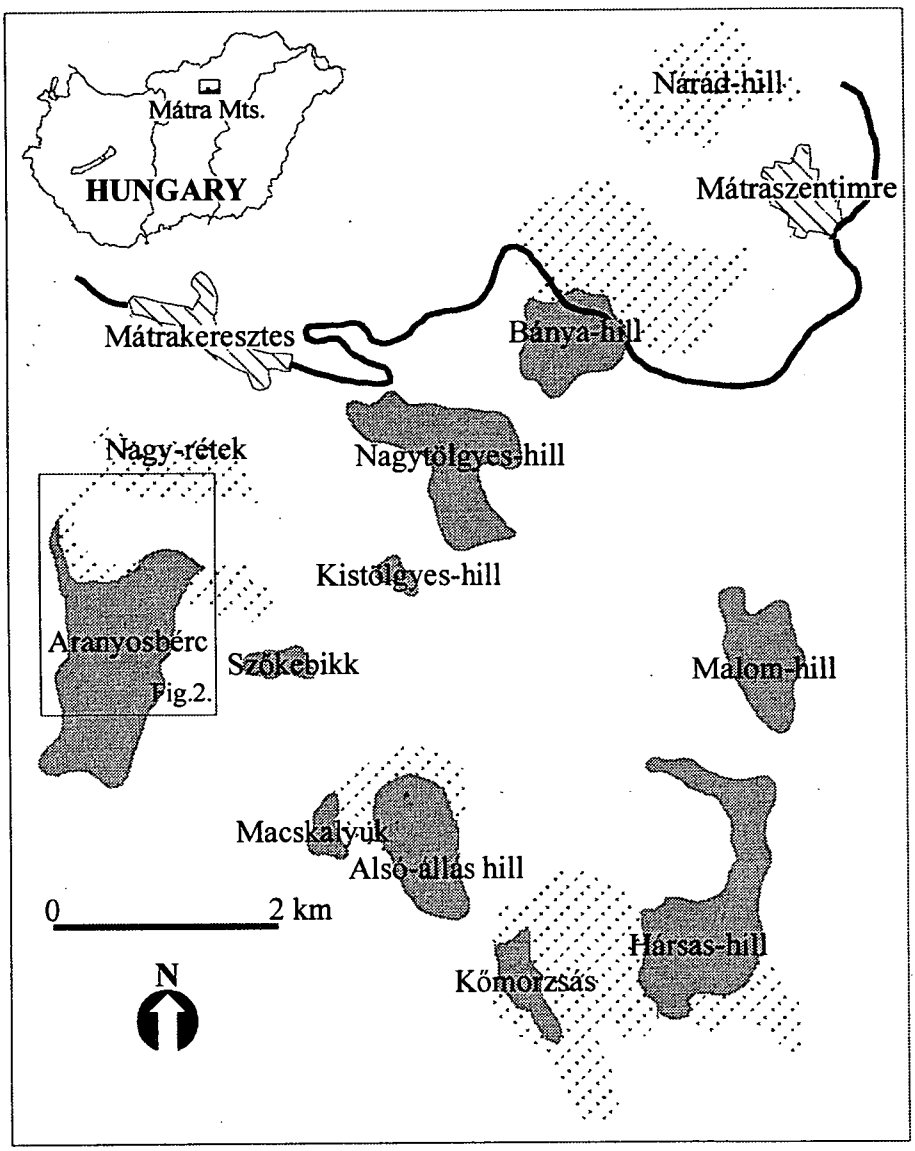

Fig.1. Important potassium metasomatite occurrences in the Mátra Mts. after Varga (1992).

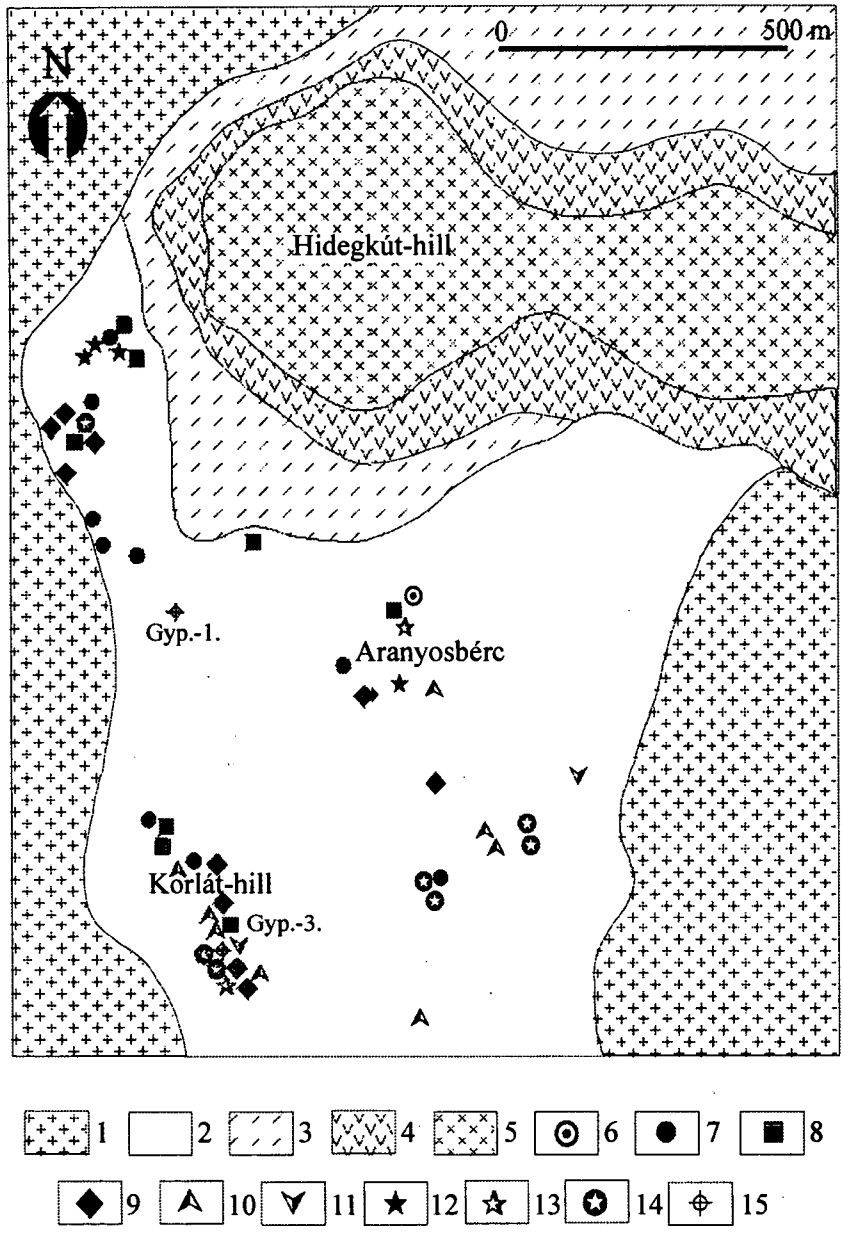

Fig.2. Generalized geological map of Aranyosbérc and its surroundings after Varga (1966b) showing the sites of collected samples.
1 pyroxene-andesite ("middle-andesite"), 2 K-metasomatized lava rock, 3 K-metasomatized tuff, 4 andesite agglomerate and tuff ("upper-andesite"), 5 pyroxene-andesite ("upper-andesite"), 6 fresh andesite, 7 K-metasomatized lava rock, 8 K-metasomatized tuff, 9 breccia, 10 gossan, 11 spoil, 12 quartzite, 13 vein quartz, 14 "apophysis" quartz, 15 borehole

GEOLOGICAL SETTING

The low sulfidation type (GATTER, 1997) western Mátra ore mineralization represents a characteristic part of the epithermal-polymetallic zone of the Inner Carpathian Volcanic Belt. It developed in close relation with the caldera structure in the middle part of the Mátra andesitic stratovolcano, which is characterized by three eruption cycles. According to the K/Ar data, the age of the whole volcanic sequence is about 12-16 Ma (HÁMOR et al., 1978). The last section of stratovolcanic series was strongly altered by hydrothermal fluids after the caldera formation (BAKSA et al., 1982). This potassium rich rock belt (average 8.50% K_2O) surrounds the uniform western Mátra vein system from western direction (VIDACS, 1965). The K-metasomatite is underlain by pyroxene andesite (so-called "middle andesite"), and overlain by more basic andesite tuffs and lavas (so-called "upper andesite"). The geological map of the studied area is shown in Fig.2.

The K-metasomatized rocks of Aranyosbérc and its surroundings are mainly of vesicular texture, but subordinately they appear as massive and brecciated types, as well. Separation of these rock types is not possible in the field. According to KUBOVICS (1965) the high frequency of the vesicular texture is due to the K-metasomatism of the originally vesicular andesites. In the late stage of K-metasomatism an intense silicification proceeded with the formation of quartz of stockwork structure (MEZŐSI, 1970). The second and third generations of silica consist of concentric or radial chalcedony, red jasper and cristobalite of low temperature origin (KUBOVICS, 1966). From the Hidegkút-hill south-southwestwards the rate of silicification and argillization (illite, celadonite, and montmorillonite) decreases, and the rate of K-metasomatization increases, because the low temperature silicification displaces the potassium feldspar from the rock (VARGA, 1992).

In the studied area two boreholes were drilled (Fig.3.), both of them penetrated the K-metasomatized lavas and tuffs. The thickness of the potassium rich rock sequence is between 27 and 64 m. It is built up by two eruption cycles, and interrupted by three younger andesite apophyses (VARGA et al., 1975 and VARGA, 1992).

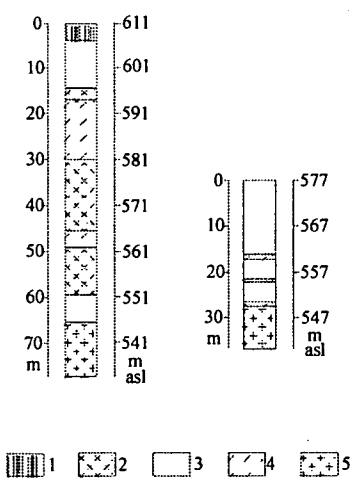

Fig.3. Boreholes drilled in the studied area (Gyöngyöspata-1. And Gyöngyöspata-3.) after Varga et al. (1975) and Varga (1992). 1 soil, 2 pyroxene-andesite ("upper-andesite"), 3 K-metasomatized lava rock, 4 K-metasomatized tuff, 5 pyroxene-andesite ("middle-andesite") asl = above the sea level

ANALYTICAL METHODS

To distinguish the different rock and ore types and to recognize their alteration characteristics the polarization microscope was used.

The identification of constituents of ore mineralization, the distinction between SiO_2 phases and identification of clay minerals were accomplished by XRD analysis (Siemens D-5000 type X-ray diffractometer, Department of Mineralogy, Eötvös Loránd University).

Chemical analyses were performed by neutron activation (Canberra model, Technical University of Budapest) and by electron microprobe analysis (Amray 1830 I/T6, Department of Petrology and Geochemistry, Eötvös Loránd University).

Microthermometric studies were carried out by means of Chaixmeca freezing-heating stage on 0,1-0,5 mm thick sections of quartz (Department of Mineralogy, Eötvös Loránd University).

RESULTS

1. Rock types

VARGA (1992) distinguished five different rock types on the basis of the mineralogical and petrological study of K-metasomatites in the Mátra Mts. We recognized the massive, the vesicular, the brecciated, and the scoriaceous types at Aranyosbérc and in its surroundings. Each of these rock types was silicified in different rate.

The metasomatized rock consists almost solely of potassium feldspar and quartz. Mafic minerals are absent in the lava rocks, their previous presence is indicated by the limonitized and argillized nodes. These rocks are of flow texture: pilotaxitic or hyalopilitic, and subordinately perthitic. According to KUBOVICS (1966) this latter texture type is due to the ringwise precipitated opaque and clay minerals. Among the K-metasomatized tuffs the dust tuffs are prevailing. They contain a few little lapillis only very rarely, and we found pumice only in one case. However, in the tuffs the mafic minerals appear in form of fresh biotite. Both the lavas and the tuffs are often brecciated, their matrix consists mainly of quartz, and of limonite (goethite and jarosite).

The K-feldspar phenocrysts are often sericitized, and rarely limonitized (Fig.4a.). Moreover, fresh generation of hydrothermal K-feldspars (adularia) appears in the open vesicles and in fractures of the host rock (Fig.4b.). MOLNÁR (1994) recognized two generations of K-feldspars in the K-metasomatites of the Telkibánya ore deposit, as well. This indicates the increase of pH of the hydrothermal fluid, which is the result of loss of the acid dissociation gases, or of silicic acid release. The first process is due to the decrease of pressure by the opening of fracture system in the host rock, the second one to the sericitization of potassium feldspars. At Aranyosbérc the K-feldspars of metasomatites do not contain any fluid inclusions.

2. Alteration of the host rock

70-80% of the rocks consists of potassium feldspar, which is the result of strong metasomatism. The K-feldspar phenocrysts which displaced the primary plagioclases are often spotted and inhomogeneous. The fresh K-feldspars of the metasomatized rock underwent strong sericitization caused by acidic fluid migration. During this process silicic acid could be released in large quantities. According to the investigations of Mezősi

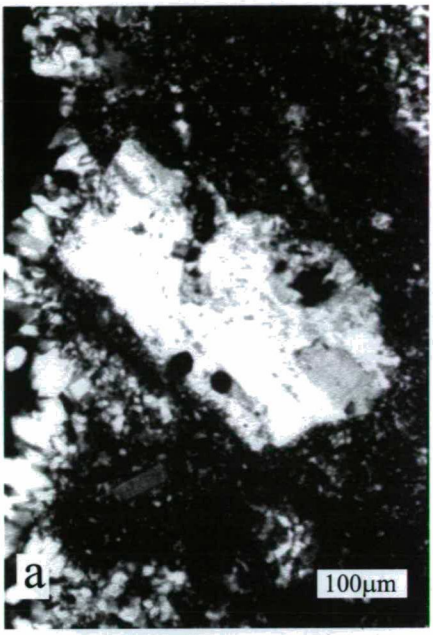

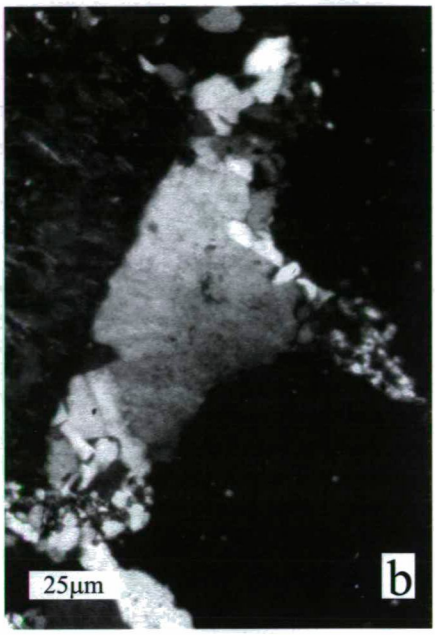

Fig.4a. Strongly sericitized K-feldspar phenocryst.
Fig.4b. Fresh hydrothermal K-feldspar in the vesicle of the host rock.
Fig.4c. Totally silicified metasomatite with mosaic structure quartz and chalcedony encrustation.

(1968) at Mátraszentistván, in the initial stage of metasomatism the mafic minerals and the groundmass were dissolved and replaced by K-feldspar, this process was followed by the displacement of plagioclase. In the late stage of metasomatism intense silicification proceeded, which resulted in quartz crystals in the leached vesicles and in fractures of the rock (stockwork structure) as well as dispersed in the groundmass.

Several generations of the strong silicification consisting solely of quartz can be observed in the fractures or in the vesicles of the host rock. Usually, the oldest quartz generation of mosaic structure is followed by idiomorphic quartz grown loose in the vesicles. The youngest chalcedony generation forms sheets and incrustations. The hydrothermal K-feldspar (adularia) appears in these quartz veins, indicating the boiling, and the "quasi" neutral pH in the epithermal systems (HEDENQUIST, 1995). Limonite sheets are often between quartz generations. This silicification is characteristic of the whole area, and its grade extends from the weakly silicified rock to quartzite (Fig.4c.). In addition, at the Korlát-hill we found typical vein formations: saccharoidal quartz and amethyst.

Argillization and hematitization are of secondary importance. According to the X-ray diffractometric analyses, this argillization is indicated by sericitization of K-feldspar phenocrysts, and by montmorillonitization of the groundmass.

3. Ore mineralization

In the metasomatites of Aranyosbérc poor secondary limonitic ore mineralization appears in form of vesicle and fracture fillings as well as of massive ore (gossan). The primary sulfide mineral, the pyrite is in microscopic form, disseminated in the silica veins and displaced by goethite in the oxidized ore. The original ore minerals are indicated by the pentagonal and the hexagonal pseudomorphs after pyrite (Fig.5a.) and the pseudomorphs with rhomb-shaped cross section after marcasite (Fig.5b.). The pseudomorphs after pyrite are often built up by alternating limonite and jarosite zones. We recognized two generations of goethite: the older generation is of boxwork or radial-spherolitic texture (Fig.5c.), the younger one is of incrusting, colloform texture (Fig.5d.). In these ores the two texture types of limonite suggest their formation from weathering of pyrite to boxwork habit or aqueous precipitation to botryodal-colloform habit (SANGAMESHWAR and BARNES, 1983). The structure pattern of the boxwork habit goethite is not homogeneous: the porous and the massive rhomb-patterned zones alternate often symmetrically. This phenomenon suggests rhythmic precipitation, or the zoned quality of the primary fracture filling phase. The spherolitic structure is characteristic of the thin encrustations. Jarosite occurs in form of fine-grained radial mass, mainly associated with goethite.

At Aranyosbérc and its surroundings the rock altered by hydrothermal fluids consisted of K-feldspar, quartz, and pyrite (marcasite). Close to the surface these minerals reacted with the O_2-rich groundwater, which resulted in acid solutions as well as goethite and jarosite. During the weathering of pyrite, the first reaction product is always goethite. The sequence of reaction products following goethite varies with the irreversible flux of Fe and Al to the solution from dissolving minerals: reactions with molar ratios of Fe/Al greater than 1.0 precipitate jarosite. The formation of jarosite depends on the quality of both the sulfide phase and the K-bearing phase (BLADH, 1982).

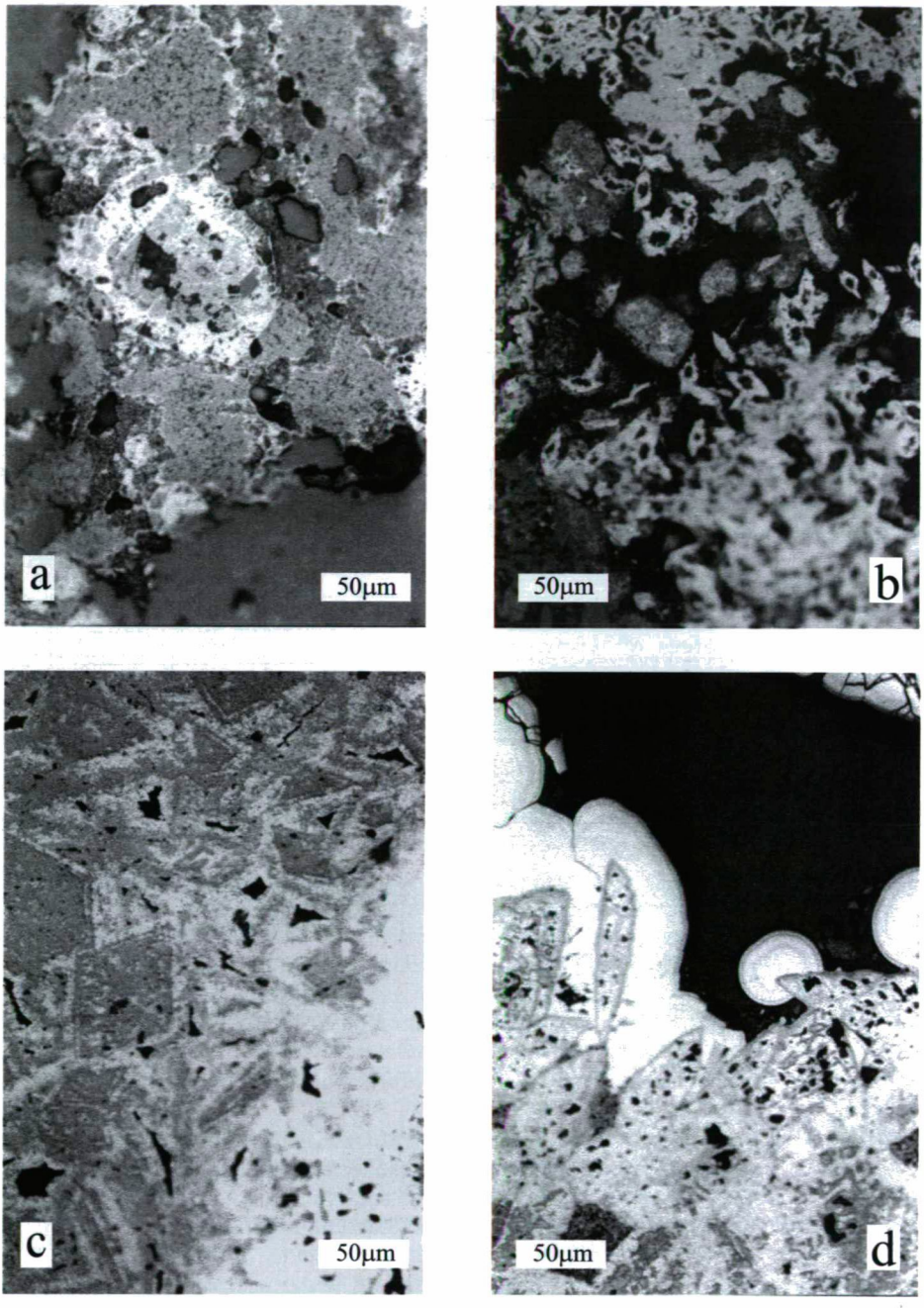

Fig.5a. Hexagonal-shaped goethite and jarosite pseudomorphs after pyrite.
Fig.5b. Rhomb-shaped goethite pseudomorphs after marcasite.
Fig.5c. The older goethite generation of boxwork texture.
Fig.5d. The younger goethite generation of colloform texture.

4. Geochemistry

In the studied area there is an extended As-Sb-(Hg-Ba) anomaly, which is associated with Zn, as well (Tab.1.). The large quantity of Fe belongs to goethite and jarosite. In certain samples there is large quantity of potassium, which derives from the host rock. According to HEDENQUIST (1995) the As, Sb, Ba, Hg, Zn and K are the typical element association of the low sulfidation type epithermal systems. SZÉKY-FUX (1970) recognized that the K-metasomatism promotes the mobilization and accumulation of Ba, As, Hg, Pb, Zn, and Ni. The high arsenic content of these rocks is due to their high pyrite content. Accordingly, the geochemical anomaly, the ore mineralization and the silicification may be the result of processes linking with the potassium metasomatism at Aranyosbérc.

TABLE 1

Important anomalies at Aranyosbérc and its surroundings (ppm).

1 jarosite (Aranyosbérc), 2 breccia (Aranyosbérc), 3 limonitic breccia (Hidegkút-hill), 4 limonite (Korlát-hill), 5 limonite (Korlát-hill), 6 limonitic metasomatite (Aranyosbérc), 7 silicified metasomatite (Aranyos-brook), 8 vein quartz (Korlát-hill), 9 soil (Boc-brook)

	1	2	3	4	5	6	7	8	9
As	1386	6078	98	596	6526	8589	510	34	15
Ba	1423	604	578	369	352		450		190
Hg		10		5	7	7			
Sb	117	1181	84	71	739	1052	36	96	54
Zn	79	103	78	118	157	229		20	
Fe (%)	16.7	31	4.1	14	45	38	4.8	1.4	0.4
K (%)		11.2			7.8	13.6			
Na	4514	3822	6800	1020	7140	3920	750	540	630

The quantities of As, Sb, Hg and Zn correlate well with one another, and they belong to the Fe-bearing minerals (Tab.2.). According to microprobe analyses, the distribution of arsenic is not homogeneous in the ore samples, thus it does not belong solely either to goethite or to jarosite. The same investigations verified 2wt% arsenic content of pyrite (Fig.6.). Some sulfide minerals contain the largest quantities of arsenic as trace element. According to KISS (1982) the pyrite may contain 110-20000 ppm As and 25-1160 ppm Sb.

TABLE 2

Correlation matrix of As, Sb, Hg, Zn, and Fe at Aranyosbérc and its surroundings.

	As	Sb	Hg	Zn	Fe
As	1				
Sb	0.95	1			
Hg	0.84	0.90	1		
Zn	0.89	0.89	0.90	1	
Fe	0.94	0.86	0.84	0.88	1

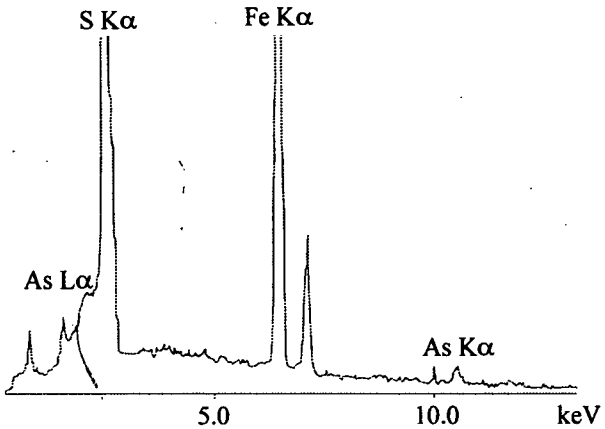

Fig.6. Result of the microprobe analysis of arsenic-bearing pyrite from the gossan at Aranyosbérc. This sample contains 2wt% arsenic.

The limonite ore mineralization was formed by the weathering of the primary ore minerals under oxidizing conditions. At low temperature the iron and manganese were separated, and the anions were adsorbed by iron-hydroxide, and the cations rather by manganese-hydroxide (WEDEPOHL, 1972), so the limonite phase could strengthen significantly the original anomaly.

TABLE 3

Chemical composition of potassium metasomatites at Aranyosbérc and its surroundings after Varga (1992) (wt%).

1 borehole, Gyöngyöspata-1., 5 m, 2 Southern slope of Hidegkút-hill, 3 South-western slope of Hidegkút-hill, 4 Southern slope of Aranyosbérc, 5 South-western slope of Aranyosbérc, 6 Korlát-hill, 7 Southern slope of Korlát-hill, 8 Northern slope of Korlát-hill

	1	2	3	4	5	6	7	8
SiO_2	54.97	68.01	65.25	67.64	66.79	66.46	66.00	65.79
TiO_2	0.97	0.58	0.70	0.46	0.54	0.45	0.57	0.54
Al_2O_3	18.81	16.02	14.23	12.09	15.83	15.58	15.46	15.57
Fe_2O_3	6.27	1.97	5.04	4.75	3.34	0.01	1.48	1.00
FeO	0.40	0.24	0.33	0.47	0.56	0.42	0.45	0.40
MnO	0.10	Trace	0	0.09	0.02	0.04	0.06	0.04
MgO	2.90	Trace	0.27	0.91	0.91	0.52	0.74	0.37
CaO	1.45	Trace	0.71	0.90	0.72	1.03	0.63	1.26
Na_2O	0.49	0.34	3.56	0.39	0.92	0.21	036	0.25
K_2O	7.73	8.18	6.07	10.23	7.35	12.05	13.08	11.75
H_2O^+	4.41	3.31	2.08	2.19	2.41	1.56	0.93	1.65
H_2O^-	1.00	1.22	0.83	0.10	0.19	0.83	0.57	1.37
CO_2	0	Trace	0.19	0	0	0.50	0.34	0.32
P_2O_5	0.16	0.05	0.71	0.16	0.07	0.02	0.06	0.12

In the analyzed samples the large quantities of potassium are due to their high jarosite content, which indicates also the high K content of the host rock as weathering product. According to VARGA (1992) 76-77% of the metasomatites consists of K-feldspar at Aranyosbérc, so the K_2O content of these rocks may be as high as 12-13% (Tab.3.). The jarosite may contain larger quantities of lead (plumbojarosite) and silver (argentojarosite), too (BROWN, 1970). The presence of lead and silver was not verified in the jarosite at Aranyosbérc, which indicates that either these elements were not present in the original ore mineralization, or they were completely leached during the weathering.

5. Genesis

According to fluid inclusion studies the homogenization temperatures determined from two-phase inclusions of hydrothermal quartz fall between 160 and 250°C (Fig.7.). The average density of fluid is 0,873g/cm^3. The low salinity fluids are site-dependent: the salinity of fluid is 2-2,5wt% (NaCl eqv.) at the Hidegkút-hill and Korlát-hill, while at Aranyosbérc the salinity is 0,1-0,5wt% (NaCl eqv.). The development of fluids varies also with different sites: according to the T_h/c diagrams the low salinity fluid was fully diluted and depleted with decrease of the temperature at Aranyosbérc. Cooling and dilution took place at the Hidegkút-hill. The development of fluid was more complicated at the Korlát-hill, but small number of data do not allow sure conclusions (Fig.8.).

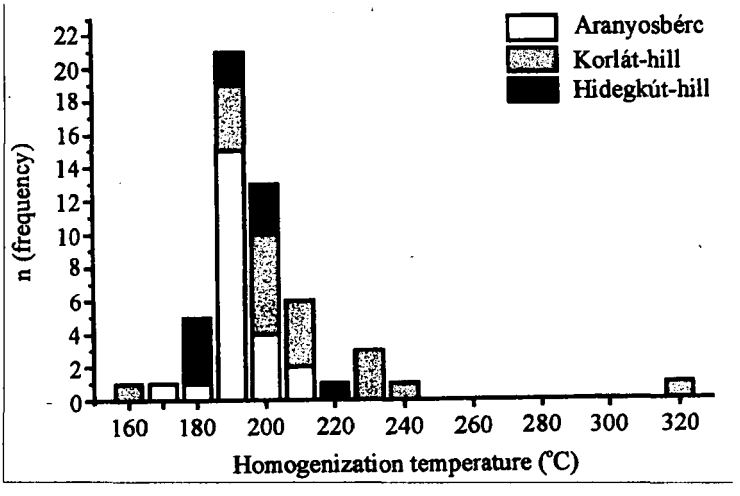

Fig.7. Homogenization temperatures measured from the fluid inclusions of quartz at Aranyosbérc, Hidegkút-hill, and Korlát-hill.

The composition of fluids differs, too: the composition of vein forming fluid is Ca-Na-chloride type, and that of "apophysis" quartz forming fluid is alcaline bicarbonate/sulfate type (GATTER, 1983). These two types were recognized in the measured data as well, which verify the presence of chloride type fluid at Aranyosbérc (it proves the dilution of fluid), and the presence both chloride and bicarbonate/sulfate type fluid at the Hidegkút-hill and Korlát-hill. The chloride type fluid predominates at the whole area suggesting the greater role of the vein forming stage.

DISCUSSION AND CONCLUSION

The epithermal mineralization at Aranyosbérc consists of strong silicification, which took place at the late stage of potassium metasomatism, and of poor secondary limonite mineralization (gossan). The original sulfide minerals were the arsenic-bearing pyrite and marcasite, which were transformed into goethite and jarosite under oxidizing conditions (gossan formation). The extended As-Sb-(Hg-Ba) anomaly belongs to the secondary Fe-bearing minerals, and it could be increased during the weathering. The primary ore mineralization is accompanied by strong silicification in form of stockworks. In these rocks the hydrothermal potassium feldspar (adularia) is frequent. The argillization (sericitization of the K-feldspar phenocrysts, and montmorillonitization of the groundmass of host rock) and the hematitization are of secondary importance. The mineralization proceeded at 190-200°C. The salinity of the fluids was low, and the composition was mainly Ca-Na-chloride type. The dilution of solutions was characteristic, since the originally mixed fluids could be diluted-cooled by the direct influence of the meteoric water.

According to the alteration characteristics, the stockwork-type structure, the geochemical element association and the fluid characteristics obtained by the fluid inclusion studies the presence of a low sulfidation type epithermal system can be identified at Aranyosbérc. This system is located in shallower depth than the western Mátra vein system (Gyöngyösoroszi-Mátraszentimre) and at greater distance from the main upwelling channels, and represents the stockwork zone of the low sulfidation type systems, which forms above the vein zone (Fig.9.). Later this system was exposed on the surface, and was transformed under oxidizing conditions, therefore the original element association was enriched. According to Fig.9., the Pb, Zn and the Cu enrich in the vein zone below the brecciated zone. Above it is the zone of boiling, where Au and Ag accumulate. The western Mátra polymetallic vein type mineralization corresponds to the vein zone.

According to the boreholes drilled in the studied area, the thickness of the hydrothermally altered zone is small here. From the Aranyosbérc westwards important hydrothermal alteration zones are absent. The studied area is located vertically and horizontally at the greatest distance from the center of the western Mátra ore mineralization.

REFERENCES

BAKSA, CS, J. CSILLAG, J. FÖLDESSY, T. ZELENKA (1981): A hypothesis about the Tertiary volcanic activities of the Mátra Mountains, NE Hungary. Acta Geologica Hungarica, 24, 337-349.

BLADH, K. W. (1982): The formation of goethite, jarosite, and alunite during the weathering of sulfide-bearing felsic rocks. Economic Geology, 77, 176-184.

BROWN, J.B. (1970): A chemical study of some syntethic potassium hydronium jarosites. Canadian Mineralogist, 10, 696-703.

CLARKE, D. S., G. J. S. GOVETT (1990): Southwest Pacific epithermal gold: geochemistry perspective. Journal of Geochemical Exploration, 35, 225-240.

GATTER, I. (1983): Folyadék-gáz zárvány vizsgálatok a nyugat-mátrai érces képződményekben. Egyetemi Doktori Értekezés, ELTE Ásványtani Tanszék, 85 p.

GATTER, I. (1987): Fluid inclusion studies in the polymetallic ores of Gyöngyösoroszi (North Hungary) - Spatial and temporal evolution of ore-forming fluids. Chemical Geology, 61, 169-181.

GATTER, I. (1997): Fluid inclusion characteristics of the epithermal style mineralizations of the central Mátra Mts. (NE Hungary). In: M. C. Boiron, J. Pironon (Editors): Proceedings of the XIVth European current research of fluid inclusion, Volume de Resumes, Nancy, 121-122.

HÁMOR, G., K. BALOGH, L. RAVASZ-BARANYAI (1978): Az észak magyarországi harmadidőszaki képződmények radiometrikus kora. MÁFI Évi Jelentés 1976-ról, 61-72.

HEDENQUIST, J. W. (1995): Origin of and exploration for epithermal gold deposits. Eötvös Loránd University, Budapest.

KISS, J. (1982): Ércteleptan. Tankönyvkiadó, Budapest.

KUBOVICS, I. (1965): The role of Potassium metasomatism on volcanic rock genesis in the Western Mátra Mountains. Acta Geologica Hungarica, 9, 193-213.

KUBOVICS, I. (1966): A kálimetaszomatózis szerepe a nyugat-mátrai kőzetképződésben. Földtani Közlöny, 96, 13-26.

KUBOVICS, I. (1970): Északkelet és nyugat Mátra ásvány-kőzettani vizsgálata. In: I. Kubovics, Gy. Pantó: Vulkanológiai vizsgálatok a Mátrában és a Börzsönyben. Akadémiai Kiadó, Budapest.

Mezősi, J. (1968): Potassium metasomatism in the neighbourhood of Mátraszentistván. Acta Mineralogica-Petrographica, 18, 79-86.

MEZŐSI, J. (1970): Metasomatic phenomena in the Mátra Mountains. Acta Mineralogica-Petrographica, 19, 143-157.

MOLNÁR, F., (1993): Tokaji-hegységi ércesedések és indikációk genetikája folyadék zárvány vizsgálatok alapján. Egyetemi Doktori Értekezés, ELTE Ásványtani Tanszék, 177 p.

MOLNÁR, F. (1994): Káliföldpátok a telkibányai ércesedésben. Topographia Mineralogica Hungariae, 2, 225-232.

SANGAMESHWAR, S. R., H. L. Barnes (1983): Supergene processes in zinc-lead-silver sulfide ores in carbonates. Economic Geology, 78, 1379-1397.

SZÉKY-FUX, V. (1970): Telkibánya ércesedése és kárpáti kapcsolatai. Akadémiai Kiadó, Budapest

VARGA, GY. (1966a): A Mátra hegység fejlődéstörténetének vázlata. MÁFI Évi Jelentés 1964-ről, 389-401.

VARGA, GY. (1966b): Magyarázó a Mátra hegység földtani térképéhez, 10000-es sorozat, Hasznos (Mátrakeresztes). MÁFI, Budapest.

Varga, Gy. (1992): Kálitrachit és káliumdús kőzetek a Mátrában. MÁFI Évi Jelentés 1990-ről, 241-276.

VARGA, GY., E. CSILLAG-TEPLÁNSZKI, ZS. FÉLEGYHÁZI (1975): A Mátra hegység földtana. MÁFI Évkönyve, LVII.

VIDACS, A. (1965): A Mátra hegységben 1963-ban végzett ércföldtani vizsgálatok eredményei. MÁFI Évi Jelentés 1963-ról, 189-195.

WEDEPOHL, K.H. (ed.) (1972): Handbook of geochemistry, Spriger-Verlag, Berlin.

Acta Mineralogica-Petrographica, Szeged, XLI, 79–91, 2000

PETROGRAPHICAL CHARACTERISTICS OF THE GYÓD SERPENTINITE BODY, SOUTH–EASTERN TRANSDANUBIA

G. KOVÁCS*

Department of Mineralogy, Geochemistry and Petrology, University of Szeged

ABSTRACT

The Gyód serpentinite body consists mainly of serpentinite, in addition, ultramafics and tremolite, anthophyllite schists are also present. Based on textural investigations the relic enstatite and olivine–bearing ultramafics constrain a harzburgitic protolith for the serpentinites. Low CO_2–content fluids penetrated the body and serpentinised the, resumably, ocean mantle-derived, depleted harzburgites. The serpentinization resulted in a new, lizardite, chrysotile–magnetite–talc–chlorite mineral assemblage. The tremolite and anthophyllite schists occur just certain parts of the sequence suggesting that their development was caused by localised impacts. The tremolite could have formed from a higher CO_2–content fluids. The anthophyllite schists appear adjacent to the aplite dyke which, locally, thermally metamorphosed the serpentinite. The formation of bastites after talc, tremolite and anthophyllite demonstrates that serpentinization is a multi–stage process. Subsequently, carbonate minerals were formed.

INTRODUCTION

In the search for radioactive substances geophysical reconnaissance work started in the early 1960s in southern Transdanubia. Field magnetic, aerogamma and aeromagnetic investigations indicated strong magnetic anomalies in the crystalline basement and, subsequently, some of these anomalies were penetrated by boreholes (boreholes of G–2 and He–1,–2). This resulted in the discovery of a serpentinised body in the region of Gyód and Helesfa. In the 1970s and 1980s more detailed research was carried out on the Gyód serpentinite to identify its mineralogy and geochemistry. Attempts were also made to determine the protolith and the metamorphic evolution-path of the serpentinite. These results are, in many cases, contradictionary. The aim of this paper is to clarify the mineralogy and texture of the sequence penetrated by the Gyód–2 borehole.

PREVIOUS WORKS ON THE GYÓD SERPENTINITE BODY

According to SZEDERKÉNYI (1974a,b, 1976, 1977) the Lower Paleozoic Gyód serpentinite can be regarded as a vertical neck or dyke, representing the root–remnant of an ancient volcanic event. The main part of the body consists of pyroxenite, weakly

*H–6701 Szeged P.O. Box 651, Hungary
e-mail: kovacsg@sol.cc.u-szeged.hu

serpentinised pyroxenite and serpentinite, all of them showing a laminar texture, caused by the lineation of large clinopyroxene crystals. This rock assemblage was later cut by Carboniferous aplite–microgranite veins. The composition of the pyroxenite is predominantly clinoenstatite a smaller quantity of olivine, basic plagioclase and chromite–magnetite. The ferromagnesian suite was altered to lizardite and clinochrysotile during serpentinization. The microstructure of the serpentinised rocks exhibits an undisturbed mesh structure without traces of any shearing or cataclasis.

ERDÉLYI (1974), using X–ray analysis on particular mineral concentrates, attempted to reconstruct the complex metamorphic evolution of the Gyód serpentinite. He invoked a hot basic magma intrusion into a serpentinised rock complex which transformed lizardite to olivine and enstatite above 800°C, while talc and clinoenstatite were generated from enstatite above 700°C. With further cooling chlorite was formed between 500–600°C whereas the serpentine minerals (mainly lizardite and chrysotile) were crystallised around 400°C. He also detected dolomite, ankerite, calcite, brucite, boehmite, montmorillonite, apatite, tourmaline, muscovite, biotite, magnetite and plagioclase feldspar (albite, bytownite). He concluded, that the protolith of the serpentinite was probably an olivine–rich ultramafic rock such as olivine–diabase.

GHONEIM (1978) distinguished three rock types in the Gyód rock complex including pyroxenite, amphibolite and serpentinite. According to his results the pyroxenite consists of 75 % clinoenstatite, 7 % olivine, 16 % basic plagioclase and 2 % opaque minerals. This composition is in agreement with the results of SZEDERKÉNYI (1977). Hornblende is the dominant mineral in the amphibolite, accompanied by minor amounts of quartz, plagioclase and laminar serpentinite (bastite). Chrysotile and lizardite builds up the mesh texture after olivine. Opaque minerals are chromite, magnetite and pentlandite. The presence of relic minerals suggests that the original rock might have been lherzolite and pyroxenite which were slightly serpentinised.

BALLA (1983, 1985) recognised four metamorphic events. The olivine and enstatite–bearing oceanic harzburgite underwent a granulite facies metamorphism (T>700°C), followed by an amphibolite facies cataclasis (T=600–650°C) which resulted in the formation of an enstatite$_2$–antophyllite–talc–magnetite paragenesis. A subsequent greenschist facies metamorphism produced antigorite, talc$_2$, magnetite and carbonate. During the final stage with serpentinization (T=200–300°C) lizardite, chrysotile and iddingsite were developed. According to his tectonic interpretation the serpentinite body was formed by the Upper Devonian–Lower Carboniferous collision of an older continent with island arc and obduction, followed by a post–collisional thermal and isostatic equilization which moved it into its present position.

PAPP (1989), using a microscope, an X–ray powder diffraction, and transmission electron microscope, carried out a detailed investigation of the serpentine minerals of the Gyód body and identified lizardite with little clinochrysotile and polygonal serpentine as the main serpentine minerals. Common accessories include chlorite and magnetite. The appearance of talc indicates the impact of the granite–aplite and veins. The serpentinite shows a dominantly pseudomorph texture but some altered, non-pseudomorphic texture can also be recognised.

GEOLOGICAL SETTING

The Gyód magnetic anomaly is situated along the Szilvás–Keresztespuszta–Aranyosgadány line with 5–7 km in length and 300–500 m in width. The strike of the

diapir–like body is WNW–ESE and is similar to that of the country–rocks (*Fig. 1*). The geometric depth of the body is 400 m and it wedges out no deeper than 700–800 m. The borehole of Gyód–2 was drilled into the geometric centre of the serpentinite body, penetrating it between 65.2–131.3 m under the overlying Pleistocene and Lower Pannonian sediments (*Fig. 2*). The boreholes of Gyód–3 and Gyód–4 were drilled into the country–rocks which are mainly amphibolite and gneiss. However, Gyód–4 did not reach the proximity of the serpentinite contact which is probably in a tectonic zone.

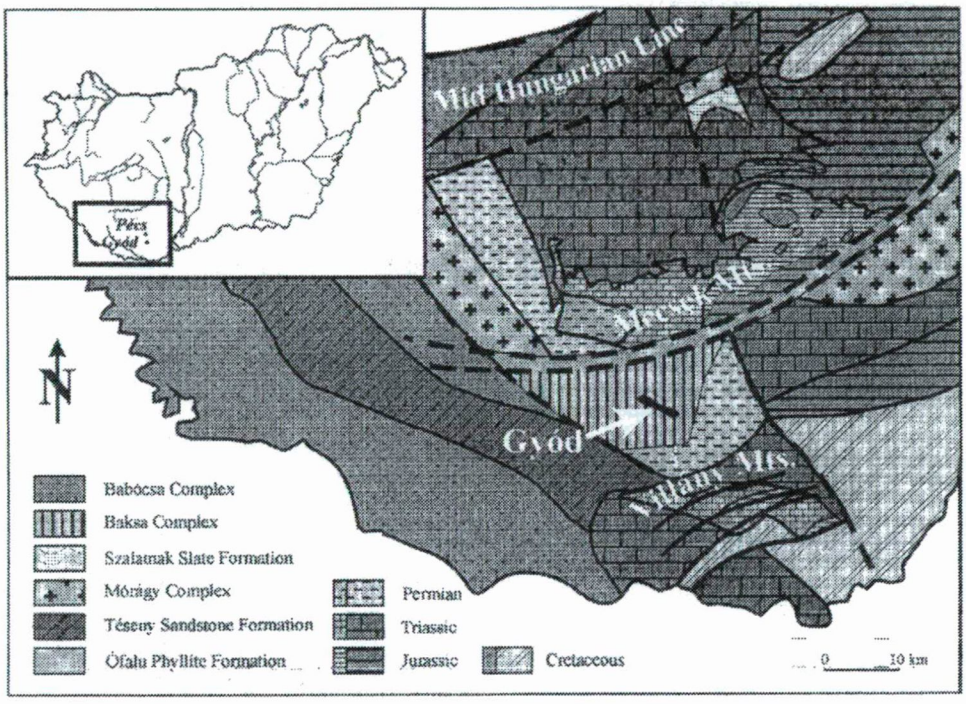

Fig. 1 Geological sketch map of South Transdanubia showing position of Gyód serpentinite (after SZEDERKÉNYI, 1994b and CSÁSZÁR, 1997).

TEXTURAL CHARACTERISTICS OF THE SERPENTINITE BODY

A new set of samples were collected for the current study from the entire Gyód–2 borehole sequence. These were examined both by macroscopy and microscopy, together with the previously analysed samples. According to the macroscopic observations three rock types could be distinguished: serpentinite, an ultramafic rock and an amphibole schist. 150 pieces of thin sections were described which were made from almost every metre of the serpentinite body in borehole. Detailed textural investigations permitted the subdivision of the three main rock types into the following:

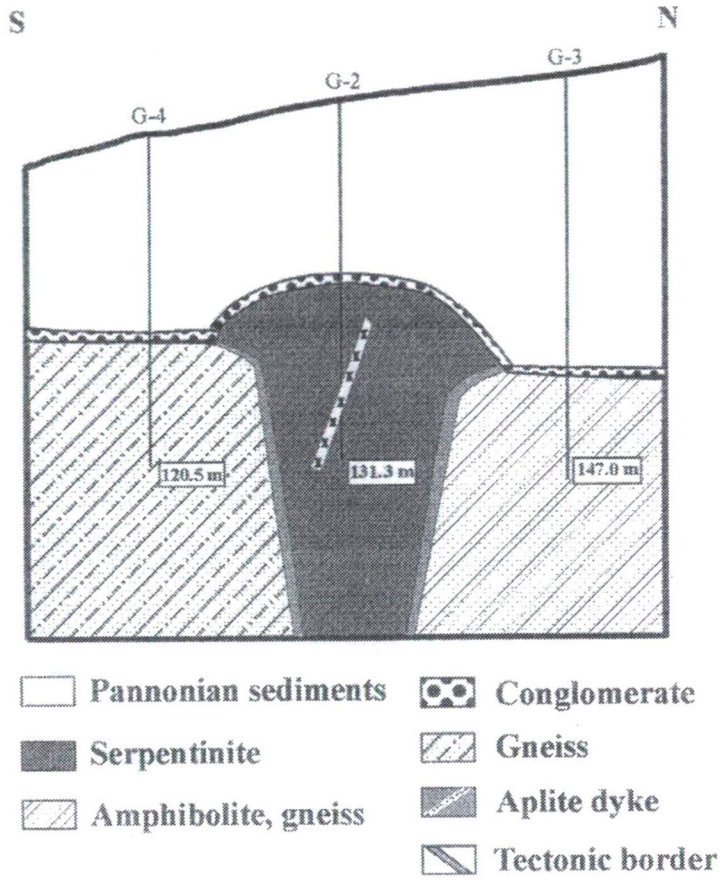

Fig. 2. Position of Gyód serpentinite within the sketchy cross–section.

Serpentinite

The Gyód body comprises mostly serpentinite which, according to structural characteristics and mineral composition is made up of several types, such as ultramafic rocks, amphibole schists and an aplite dyke which is known only from the borehole log (c.f. SZEDERKÉNYI, 1977). It may compartmentalise into the following types:

– between 65.2–68.1 m, in the uppermost part of the examined body a strongly sheared, tectonised serpentinite can be found which is cut by white and greenish carbonate veinlets. Oriented silvery grey mica grains can be recognised in it (*Fig. 3a*).

– between 70.0–78.6 m a massive dark grey serpentinite is intermingled with lighter grey units (*Fig. 3b*). This pattern resembles a cataclastic texture where the clasts appear to be the darker units, showing a mesh texture of serpentine minerals and magnetite. The lighter units represent the matrix which contains talc, chlorite, little serpentine minerals and minor amount of opaques. The mesh texture is often irregular because its centre is not well developed, instead of it short bipartite mesh and rim-like stages occur in a so called curtain texture (WICKS and WHITTAKER, 1977). This can be interpreted as an alteration of the mesh texture by shearing.

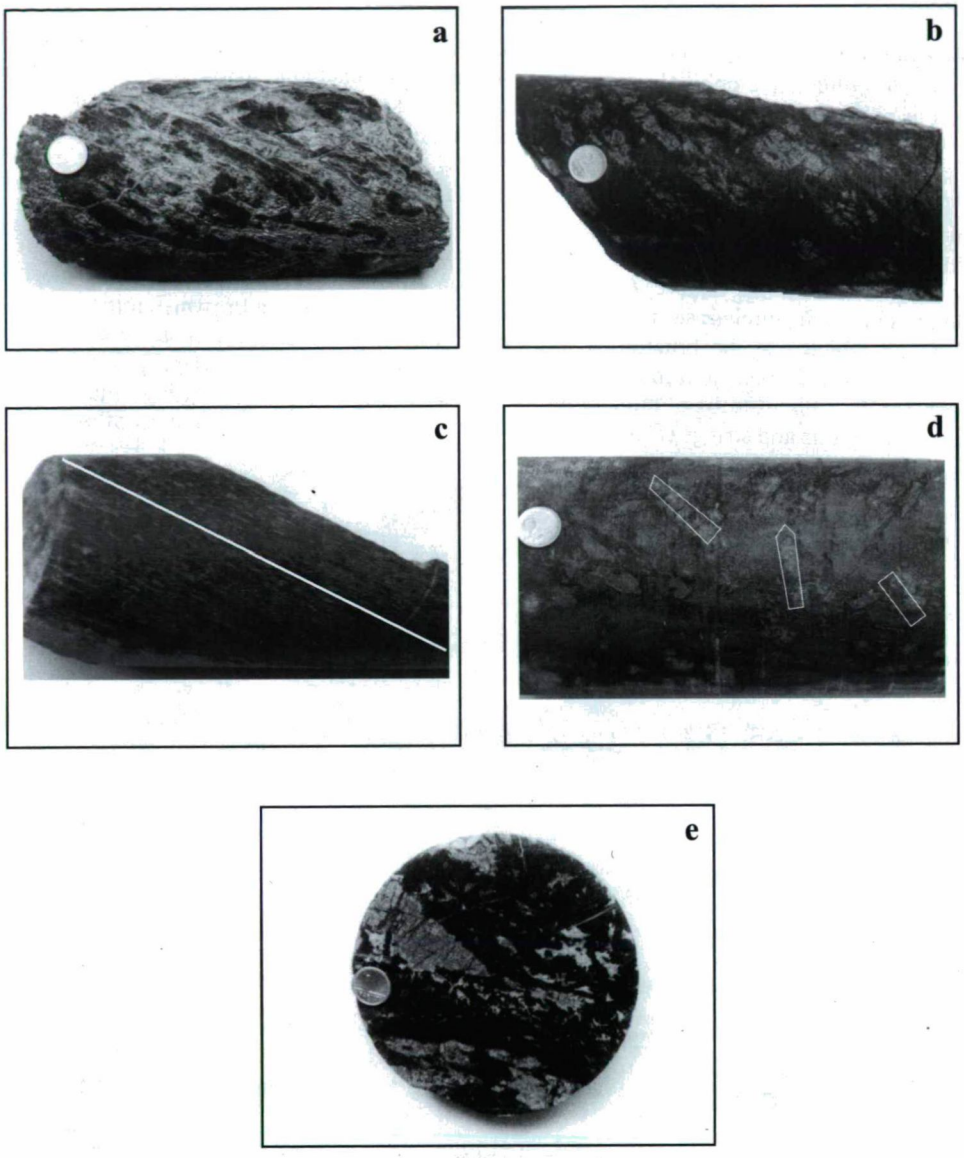

Fig. 3. The main rock types of the Gyód serpentinite (the size of the coin is 1.5 cm). a, ÁGK–7004 sample. Strongly sheared serpentinite from the uppermost part of the body; b, ÁGK–7017 Cataclastic serpentinite; c, ÁGK–7019. Serpentinite with 60-80 degree foliation plane (white line represents the foliation); d, ÁGK–7037 Non–foliated, bastite–bearing serpentinite; e, ÁGK–7083B Relic ultramafic rock (light) in serpentinite (dark).

– between 85.3–131.3 m a greenish dark grey serpentinite with 60–80 degree foliation can be found (*Fig. 3c*). Greenish-white, several mm wide veins cross cut it. The wider veins are complex, built up by alternating layers of serpentine and carbonate. Silvery, 1–2

mm sized micas (chlorite and/or talc) are abundant in the plane of foliation. 2–4 cm long oil green, columnar amphibole or enstatite–bastite with unctuous lustre occurs in them without any orientation. There is a non–foliated, massive serpentinite in this part of the drilling sequence which contains the same minerals as the previous type but they occur in smaller proportions (*Fig. 3d*).

The main rock–forming minerals of the serpentinites are lizardite, chrysotile magnetite, chlorite and/or talc, and/or carbonate, similar to those identified by PAPP (1989). Their textural features are as follows: The serpentine minerals appear in three textural units (i) in the mesh or mesh–like texture, (ii) in the pseudomorphs and (iii) in the veins. The mesh centre contains featureless serpentine. In the upper part of the mass a brownish mineral can be found which may be brucite (WICKS et al., 1977), however, its minute size would necessitate a high–precision microanalytical equipment for its accurate identification. The mesh rim is a bipartite type, built up by an α-serpentine. The central parting consists of magnetite grains and strings (*Fig. 4*). The relationship between the distribution of magne-

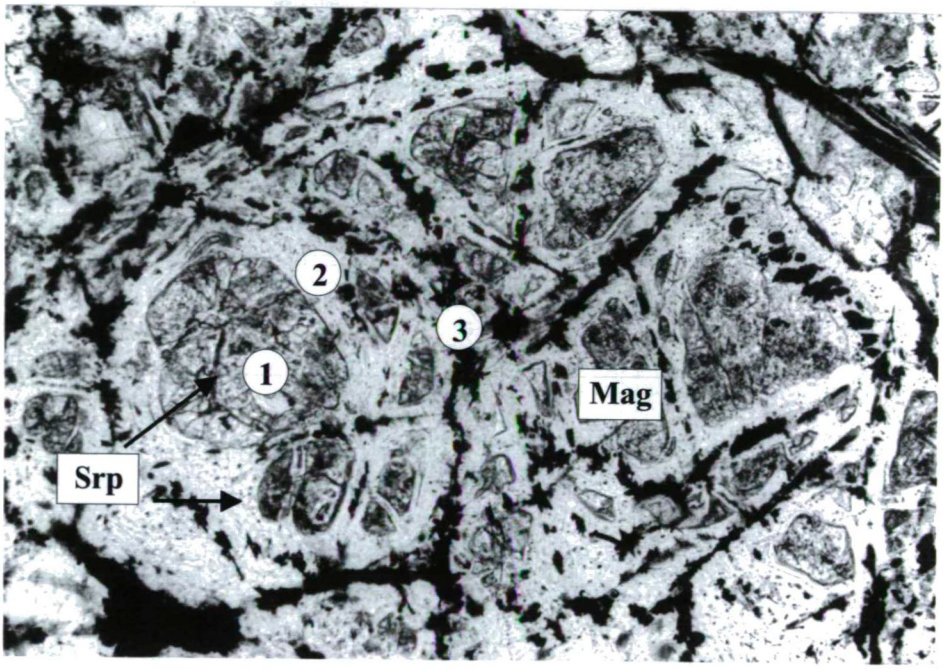

Fig. 4 . No. 400412 sample. The basic unit of mesh texture from 79.7 m, 1. mesh centre, 2. mesh rim, 3. central parting, ||N, 100x (The abbreviations were introduced by KRETZ (1983)).

tite grains and the ratio of serpentinization is well-documented (e.g. WICKS, WHITTAKER, 1977). Fine discrete grains of magnetite become coarser as the serpentinization progresses, concentrating in the mesh centre and in the central parting from which they migrate out into the cross–cutting lenses and veinlets at later stages. The second type of serpentine minerals occur as pseudomorphs (*Fig. 5*). Orthopyroxene, amphibole and talc–bastites are present in the whole sequence of the borehole. The altered, columnar enstatite type is similar to the bastite after amphibole. The original minerals of bastites cannot be

determined accurately under the microscope (DUNGAN, 1979, WICKS, WHITTAKER, 1977). The serpentine pseudomorphs consist of χ–serpentine which is usually fibrous, but may also appear in form of nearly featureless plates. The final appearance of the serpentine minerals is in the cross–cutting veins. The thickness of the veins is between 0.1 mm and 4 cm. The simple veins contain fibrous χ–serpentine which is chrysotile, as revealed by XRD analysis. Carbonate and serpentine minerals can also be recognised in the complex veins.

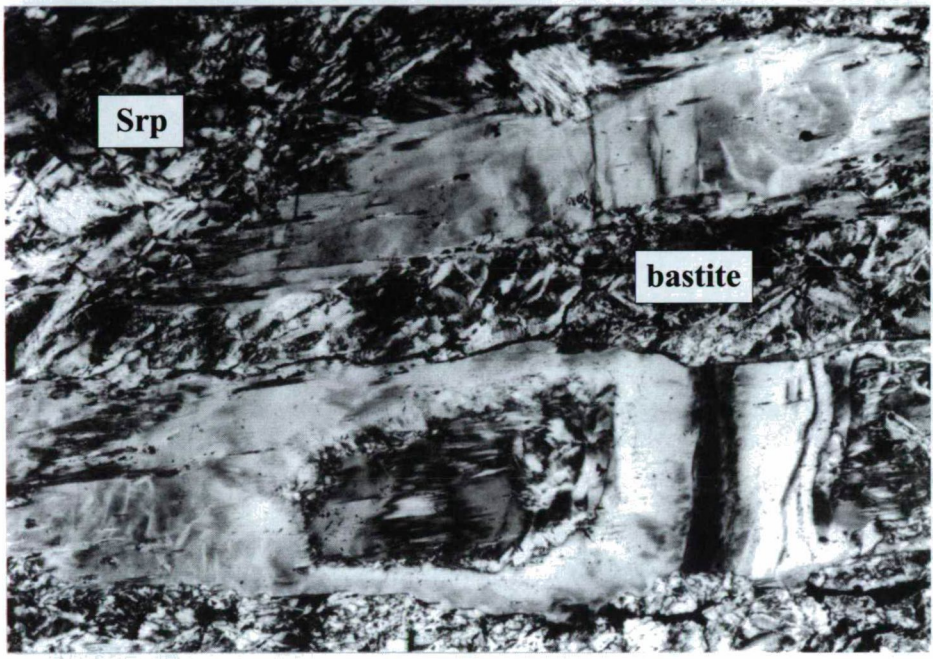

Fig. 5. No. 400398 sample. Bastites with altered texture from 98.0 m, +N, 50x.

Hypidiomorphic chlorite, with an average 0.2 mm size, is a rather frequent component in all rock types. Its crystals are often deformed and are optically zoned. Carbonate minerals are common in the cleavage faces of the chlorite and are rarely surrounded by opaque minerals. An altered, xenomorphic chlorite also occurs within the serpentine minerals, forming in resorption embayements. Its brownish interference colour indicates that it is probably a Mg–chlorite.

Talc is hypidiomorphic, often deformed (kink–banded) and its size ranges from 0.1 mm to 0.5. It is absent in some parts of the drilled sequence but may be the main rock–forming mineral in other places, thus it is not limited to the shear zones (c.f. with SZEDERKÉNYI, 1974a,b and PAPP, 1989). During the serpentinization process talc forms from enstatite, suggested by its textural position, as it can be found on the periphery of the enstatite crystals in the ultramafic rocks (*Fig. 6*). Rarely it occurs together with olivine or opaques. Talc can also be generated by CO_2 metasomatism of serpentine minerals (NALDRETT, SCHANDL, 1992). In this case talc occurs together with carbonates (*Fig. 7*). The development of talc–bastites demonstrates that serpentinization is a complex, multi–stage process.

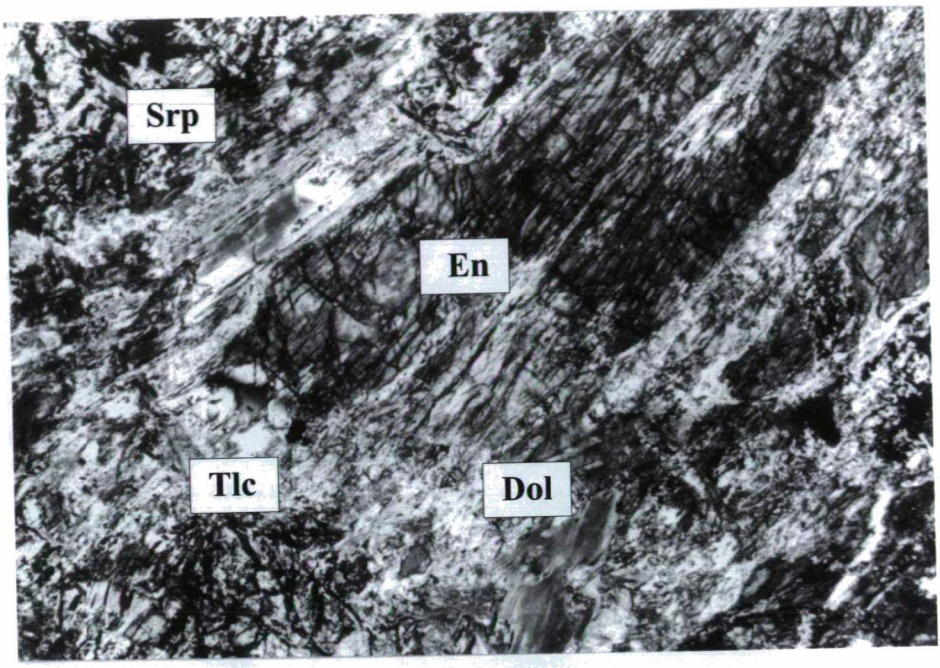

Fig. 6. ÁGK–7084 sample. Serpentinised grain of the enstatite surrounded by talc, +N, 50x.

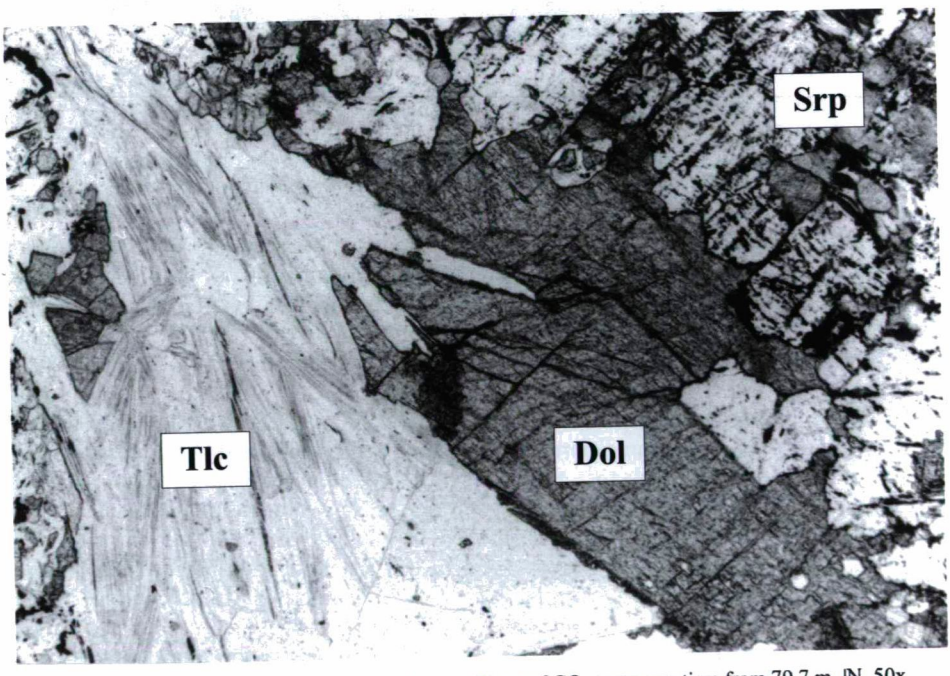

Fig. 7. No. 400412 sample. Talc–carbonate assemblage of CO_2 metasomatism from 79.7 m, |N, 50x.

The carbonate grains can be found between the relic minerals of the ultramafic rocks and in two different textural positions in the serpentinites. Carbonate staining (EVAMY, 1963) has revealed that the examined carbonate grains are low Fe–bearing dolomite. The individual grains and aggregates are characteristic of the ultramafic rocks where they often engulf serpentine minerals and enstatite. Fine grained, diffused carbonate can be seen in the mesh centre and along the central parting. As mentioned earlier, carbonate can also be detected in the veins.

Ultramafic rocks

Between 78–90 m in the Gyód–2 borehole several foliated, relic mineral–bearing, light–grey lenses and strings can be found. These are also ultramafic rocks but they do not form a continuous mass but rather appear as sheared lenses, enclosed in the serpentinites (*Fig. 3e*). The main rock–forming minerals here are enstatite, olivine, serpentine minerals, Mg–chlorite, talc and dolomite. Based on grain size, two types of ultramafics can be distinguished: one is a dominantly fine grained, relic enstatite and olivine–bearing rock and the other is a coarse grained ultramafic rock. The original igneous textures can be no longer recognised in these rocks because it has been obliterated during serpentinization.

Enstatite found in these rocks is hypidiomorphic, often shows undulatory extinction and is sheared, caused by deformation. Its size ranges from 0.2–0.5 mm in the fine grained type (*Fig. 8*). Elongated, columnar enstatite of 1–4 cm size characterises the course grained type. Enstatite often composes monomineralic layers or lenses which might reflect the original feature of the ultramafic rock (COLEMAN, 1979), but can also be the effect of serpentinization. Fresh olivine is rare because it is less resistant than enstatite, consequently, the description of its original textural features is problematical. Olivine alters along fractures and grain boundaries to form the easily recognisable pseudomorphs, composed of mesh and hourglass textures (*Fig. 8.*). Xenomorfic olivine remnants occur mostly in the centre of the mesh unit. Serpentinization of enstatite is similar to that of olivine; it begins at grain boundaries and fractures, then follows along cleavages and parting. However, it alters to χ–serpentine-bastite which usually appears in form of fibrous or nearly featureless plates. In the stages of alteration, talc is the first mineral phase which forms at the rim of enstatites but at the later stages it alters to serpentine (*Fig. 6*).

Between the ultramafic lenses and the surrounding serpentinite a courser grained band can be observed. This is composed of serpentine minerals (bastite), chlorite, talc, carbonate and some magnetite. This zone reflects the primary textural features of serpentinization. However, this band is rather narrow, compared with the mesh textured serpentinite and its mineral content is different. It is highly probable that almost the whole pseudomorphic texture has been modified.

Amphibole schists

Amphibole–bearing, light grey rocks are present at three intervals in the Gyód–2 borehole. The thickness of these rocks does not exceed 1 m but their position is not fully understood. On the basis of their mineralogy these rocks can be divided into tremolite and anthophyllite schists.

Tremolite schists occur at 82.9 and 112.2 m in the Gyód–2 borehole. The main rock–forming minerals here are tremolite, serpentine minerals, chlorite, talc and opaques. Tremolite occurs in form of hypidiomorphic, zoned needles, ranging between 0.4 mm and 2 cm and is imbedded into the fine grained serpentine matrix (*Fig. 9*). Its undulatory extinction is indicative of deformation. Tremolite often alters to bastite which consists of χ–serpentine. Talc occurs in small amounts in the contact with tremolite. Chlorite is zoned and its size reaches 1–2 mm. Occasionally it is surrounded by opaque grains. Carbonate can be found only in the veins.

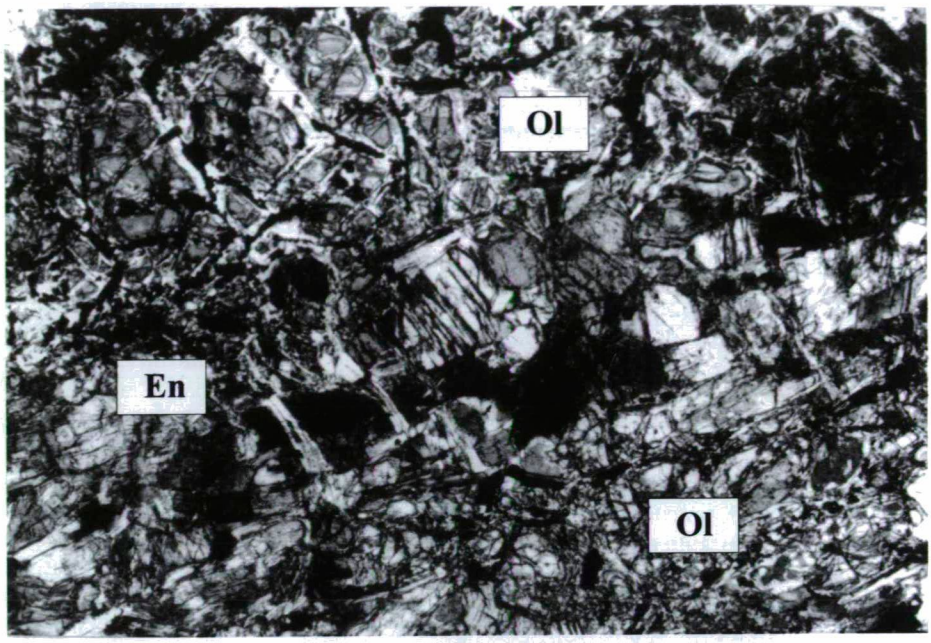

Fig. 8. ÁGK–7083B sample. The relic rock forming minerals in ultramafic rock, +N, 50x.

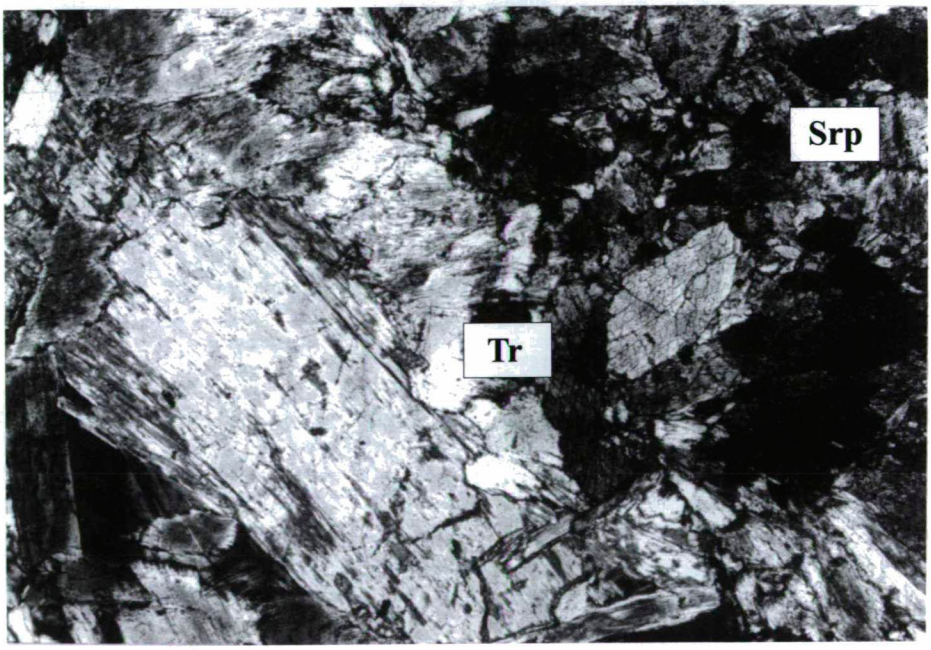

Fig. 9. No. 400381 sample. Tremolite schist from 112.3 m, +N, 200x.

Anthophyllite–bearing schists occur only at 105.0 m in the borehole and show two kinds of appearance: (i) as radiated or parallel 0.2–0.4 mm size fibrous crystals (*Fig. 10*), (ii) elongated, 0.5 mm–1.5 cm prismatic forms. Chlorite and talc are present in remarkably high amounts. The serpentine minerals are preserved as some kind of bastite, thus they are not as dominant here as in the other parts of the sequence. All of the rock–forming minerals are strongly deformed.

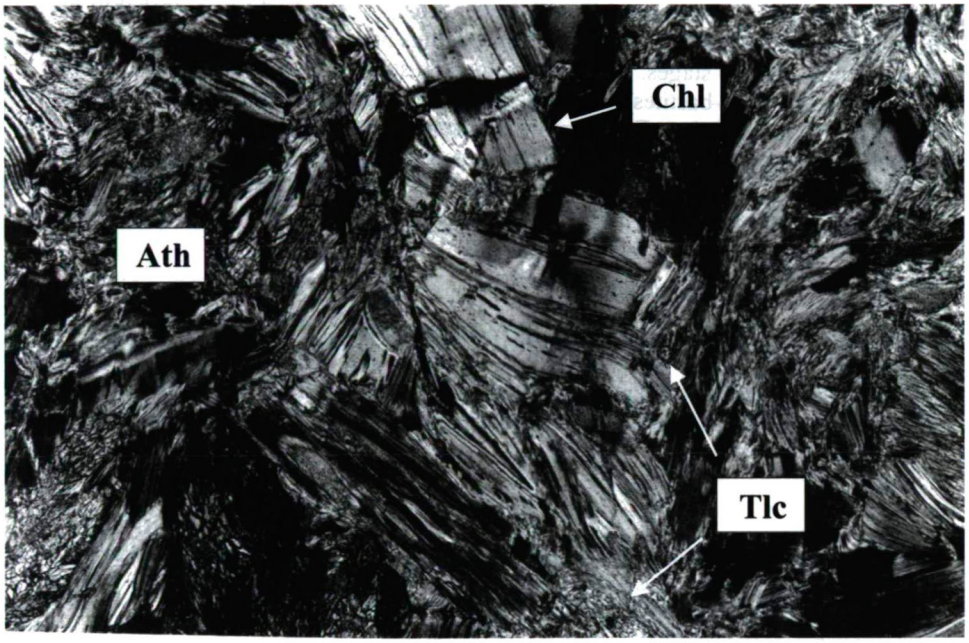

Fig. 10. No. 400389 sample. Anthophyllite schist from 105.0 m, +N, 100x.

SUMMARY

The principal rock types of the Gyód serpentinite complex are serpentinite, ultramafic rocks and tremolite and anthophyllite schists. The main rock–forming minerals of the ultramafics are enstatite and olivine. Other common minerals of ultramafic rocks are not present in the examined complex. Such a simple mineral composition indicates that the examined ultramafic rock is a harzburgite which, presumably, was also the protolith of the serpentinite. Harzburgite was derived from a depleted oceanic mantle, a conclusion made on the basis that it contains only enstatite and olivine whereas Ca and Al–bearing minerals (such as clinopyroxene, plagioclase, spinel, garnet) are absent. However, detailed geochemical analyses are necessary to support this statement.

Resulting from serpentinization and a subsequent recrystallization, generated by a metamorphic event, the primary textural features of the ultramafics can be no longer recognised. During the serpentinization process enstatite and olivine altered to serpentine

Acta Mineralogica-Petrographica, Szeged, XLI, 93–103, 2000

SOURCES OF LEAKAGES AT AL-JUMINE DAM, NW TUNIS, TUNISIA

SAMIR A.AL-GAMAL[1]

National Center for Nuclear Safety, Egyptian Atomic Energy Authority

ABSTRACT

Al-Jumine Dam (90 m high, 600 m long and 60 km NW of Tunis, Tunisia) is constructed on a nonperennial stream, which is storing more than 130 million cubic meters of water (irrigation and drinking for Tunis and Bizerte). Collected data from two drains, piezometers, injected tracers and environmental isotopes were interpreted to determine the possibility and extent of leakage (from the dam) as well as the different types of groundwater intercepted at varying distances from the site. The interpretation of the aforementioned data showed a sizable front of water leaking (at a rate decreasing away from the dam site) and that this fresh water front is being mixed with a local groundwater of higher salinity.The water seepage might constitute a potential risk threatening the integrity of Al-Jumine Dam.

INTRODUCTION

The present work is carried out as a part of the African Regional Co-operative Agreement for Research, Development & Training Related to Nuclear Science & Technology (AFRA).[1]

In Africa, many dams and artificial reservoirs present leakage problems that are expensive to repair because diagnosis of the cause of leakage using conventional means is often inadequate. This investigation demonstrates the importance of using safe tracer methods for precise and rapid determination of sources of leakage, which if ignored might result in great repair costs. The Al-Jumine Dam (*Fig. 1*) is the only hydraulic structure, which controls surface runoff in the Versant Watershed. The whole watershed (418 km^2) is indicated with the punctuated area shown in *Fig. 1*. Dam site is accessible through Tunis – Mateur highway (60 km NW of Tunis) and Tunis - Beja highway (120 km SW of Tunis). Mean annual rainfall over watershed area may amounts to a more than 300 mm. The AFRA (1998) is currently addressing the problem of leaking dams by the utilization of safe tracer techniques.

METHODOLOGIES AND TECHNIQUES

A. Tracer techniques

Tracer techniques involved tracer injection of Rhodamine and Uranine using both point dilution technique (HALEVY et al .1966) and continuous injection techniques (DROST et al.,1974) .However the equation of Turner solely (TURNER et al., 1990) was used for estimating the flow rates in both drains.

[1]National Centre for Nuclear Safety, Nasr City P.O.Box 7551 Cairo 11762.

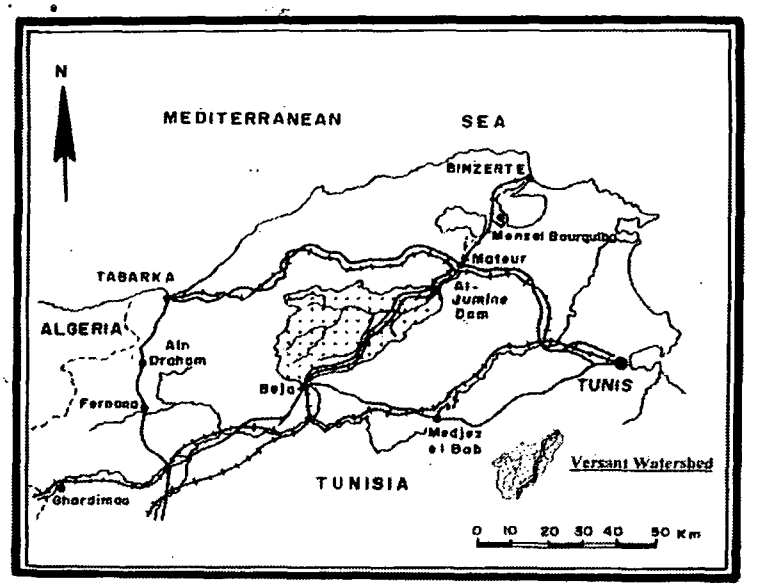

Fig. 1. Location map

B. Environmental Isotope Techniques

Water samples taken from reservoir water, groundwater and seepage water were collected in double capped plastic IAEA bottles . The analysis for environmental isotope; O-18 H-2 and H-3 were carried out in the IAEA Isotope Hydrology Section, Vienna.

INJECTION SITES AND POINTS

The injection sites and piezometers were selected to represent as possible the zone of preferential infiltration at the reservoir and at a selected piezomters *(Fig. 2a)* tapping the riverbed layer (which is made of highly permeable materials) and the composite fault scarp. This situation may enhance a better hydraulic connection between the reservoir and both drains as shown in the geologic cross section of *Fig. 2.* Automatic samplers were used to collect point samples from detection sites.

Injection in the lake

The zone of preferential infiltration is selecteds at the composite fault scarp which corresponds to a level of 65 m a.s.l. and 20 m below surface water near the bottom where seepage current predominates. The injection was carried out upstream to detect underseepage (*Fig.2b*). The philosophy behind injecting the tracer into the reservoir is to find out as possible the zone of preferential infiltration as indicated by the presence of riverbed layer and the composite fault scarp. Before injection and as a prerequisite , the relationship between flow rates in both drains versus the riverbed elevation was constructed (*Fig. 3*) whereas, the variation of conductivity and chloride ion with time for both the reservoir and the sampled waters from the two drains are shown as *Fig.4*. The main reason behined constructing such diagram is to elucidate the difference in the solute chemistry (of the leaked water) expressed as total dissolved solids (TDS) and the most conservative chloride ion (Cl) versus time since the time of dam construction

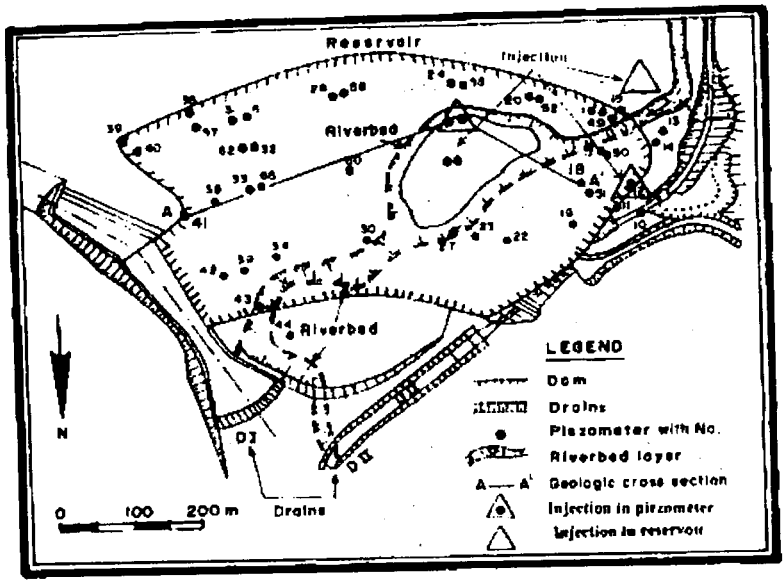

Fig. 2a. Injection sites and points

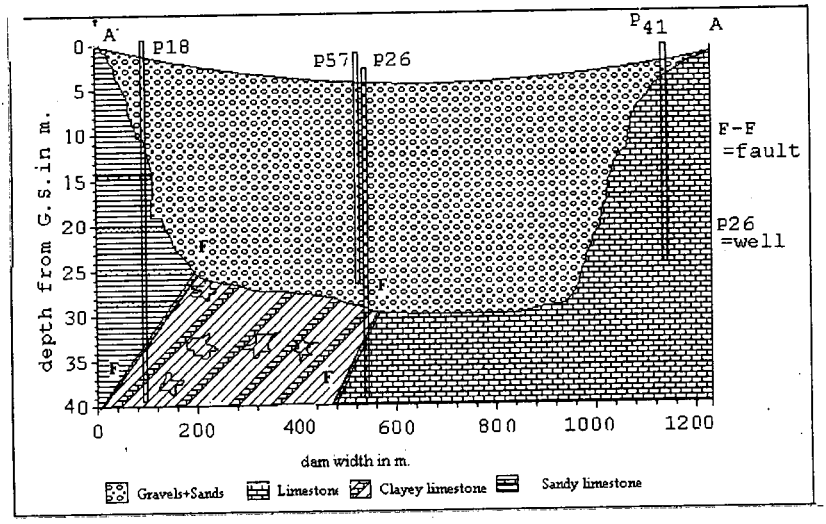

Fig. 2b. Geologic cross section A - A'

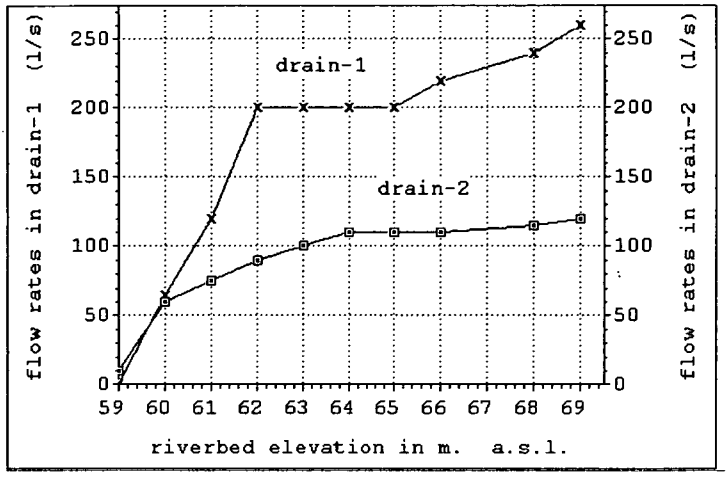

Fig 3. Riverbed elevation and discharge rates at both drains

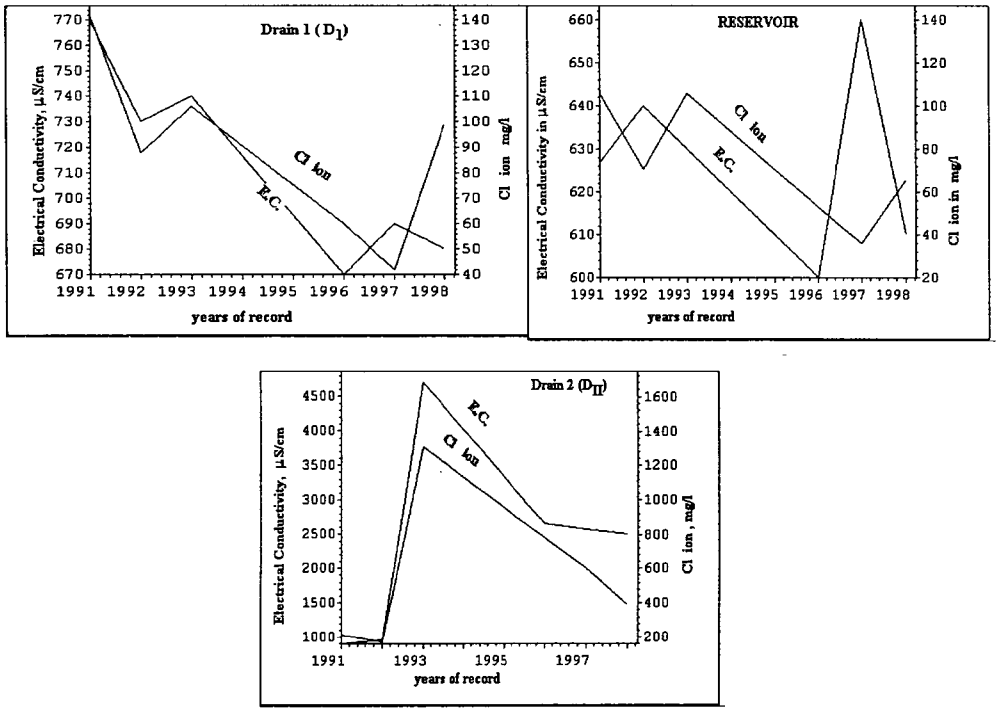

Fig. 4. Variation of conductivity and cl ion with time for reservoir and drains waters

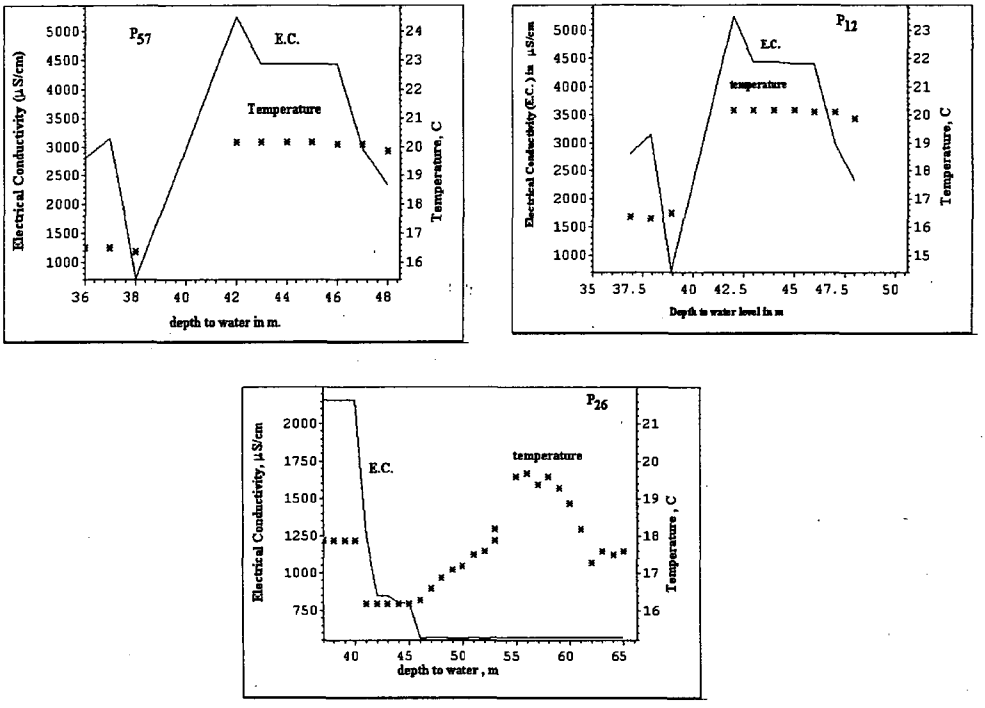

Fig. 5. Vertical flow observed in selected piezometers

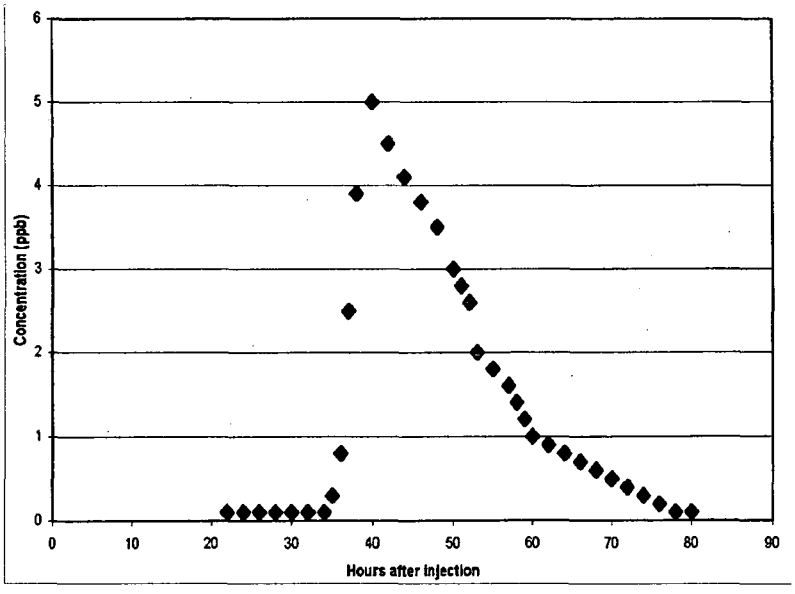

Fig. 6. Breakthrough curve for the detected tracer in drain -1

Injection in the boreholes

Information on the flows existing in the piezometers were collected before injection. Vertical flow was observed in piezometers 57, 12 and 26 (*Fig. 5*) The vertical flow observed in these piezometers (as indicated by salinity and temperature profiles) suggests a better hydraulic connection with reservoir via riverbed and composite fault scarp shown earlier in the geologic cross section of *Fig. 2b*. This hypothesis was tested by injecting the tracers in the aforementioned piezometers. Breakthrough curves for the detected tracers in both drains are shown as *Fig. 6* and *7*.

The diagenesis of emerging water (based on isotopic composition) is shown as *Fig. 8*. Whereas the piezometry of local aquifer, aerial distribution of conductivity, isotherm pattern of emerging water and tritium are displayed as *Figs. 9* through *12* respectively.

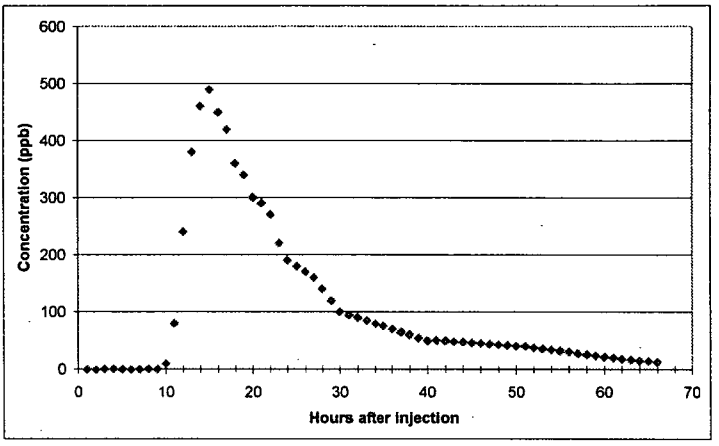

Fig. 7. Breakthrough curve for the detected tracer in drain- 2

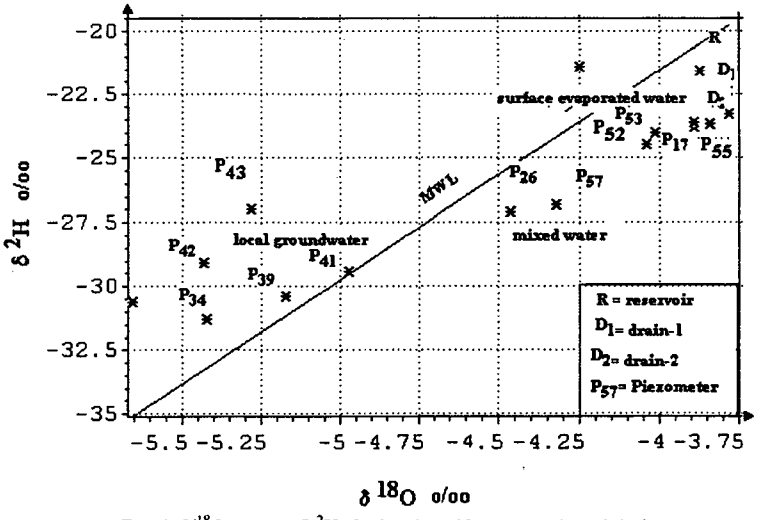

Fig. 8. $\delta\,^{18}O$ versus $\delta\,^{2}H$ for local aquifer, reservoir and drain waters

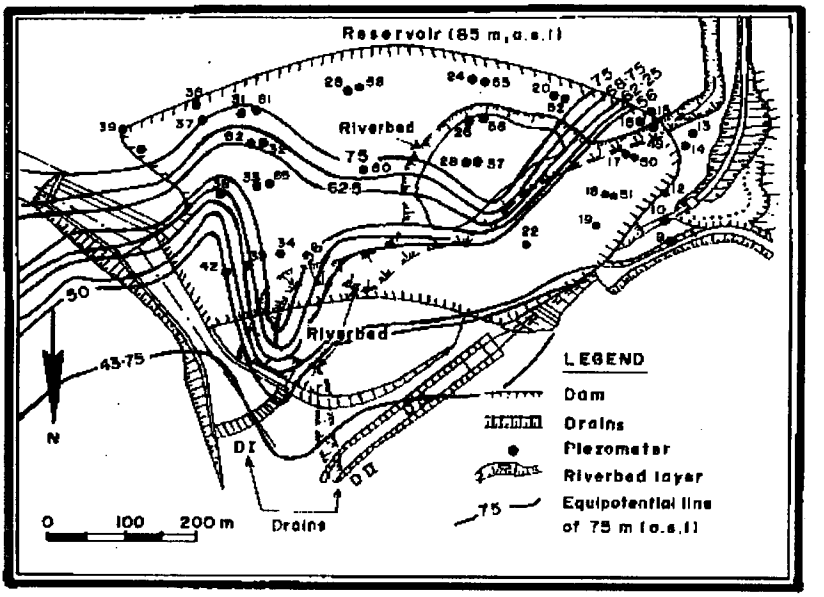

Fig. 9. Piezometry of local aquifer

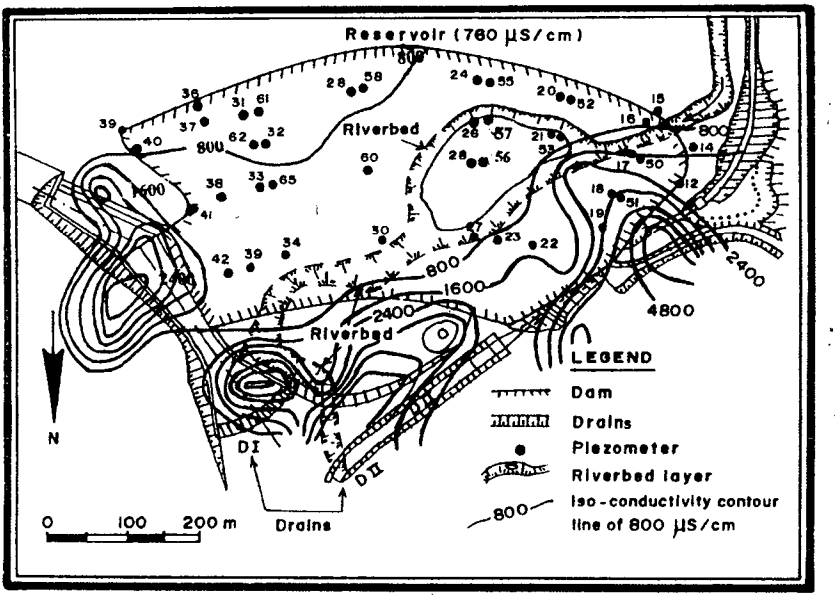

Fig. 10. Conductivity of local aquifer

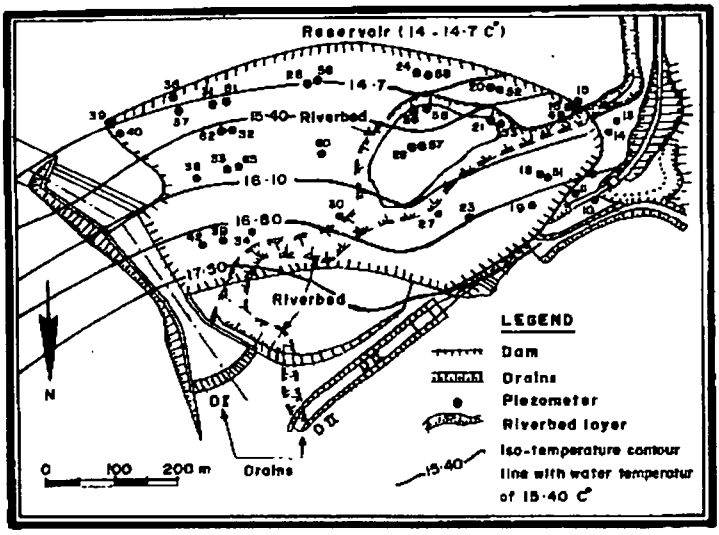

Fig. 11. Isotherm pattern of local aquifer

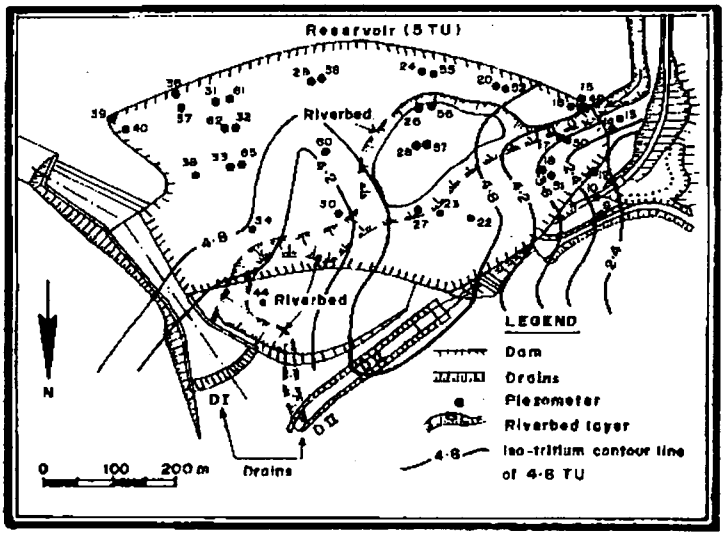

Fig. 12. Tritium distribution of local aquifer

RESULTS

The injection started December 7, 1988 using rhodamine tracer in the reservoir waters (*Fig. 2 a*). The injection was carried out upstream in an attempt to detect underseepage with an average concentration of 0.73µl/m^3 and tracer volume of 12378 milliliter The

stable isotopes (^{18}O and ^{2}H) together with the natural tracer of ^{3}H were used for surface, groundwater and leaked waters .The piezometers (locations shown in *Fig.2a*) were monitored repeatedly for conductivity, temperature and water levels for seepage water and groundwater. The vertical flows in piezometer P_{57}, P_{12} and P_{26} were detected using the conventional piezometric measurements and was confirmed using the tracer and environmental isotope techniques. The main reason for selecting piezometers 57, 12 and 26 for the injection of tracer is to determine their hydraulic connection with rservoir via riverbed layer and composite fault scarp (*Figs. 2a* and *2b*). Flow rate measurements of seepage waters in both drains were carried out using both point dilution technique (HALEVY et al., 1966) and continuous injection technique (DROST et al., 1974). However, the equation of Turner solely (TURNER et al., 1990) for point dilution technique was used for estimating the flow rates in both drains.

The injection and detection time for the injected rhodamine tracer was found to be 92 hours for drain-1 and 68 hours for drain-2. However, the peak of rhodamine representing the most important fraction of tracer has reached drain 1 after about 40 hours and drain 2 after around 15 hours (*Figs 6* and *7*) The flow rates in both drains were estimated as 45 l/s for drain-1 and 57 l/s for drain -2, applying in Turner's equation. Breakthrough curves (*Figs.6* and *7*) which define the relation between the average concentration of the injected tracers (in ppb) and detection times in both drains (in hours) were constructed in order to elucidate the mode of tracer movement and the liquid pathways followed by the tracers. The natural radioisotope tracer of H-3 was analyzed to determine the recent recharge and any groundwater pathways according to ADAR (1994). A cross plot of ^{18}O versus ^{2}H is made to determine the origin of leakage water and the gradation from surface evaporated water trough mixed with groundwater and to eventual groundwater (*Fig 8*).

A piezometric map for the local aquifer in the dam site (Eocene limestone aquifer) is constructed with contour interval of 6.25 m and a piezometric head that ranges from 75 m a.s.l. and 43.75 m a.s.l. (*Fig. 9*) .A waterfront can be seen emerging from the reservoir to the dam site.

The implication of the aforementioned interpretive steps together with the aerial distribution of: 1. Electrical Conductivity (*Fig. 10*), 2. Isotherm pattern (*Fig. 11*) and 3. Tritium distribution (*Fig. 12*) shall be discussed in detail.

CONCLUSION

A piezometric head of a magnitude reaching 43.75 m is noted by the inspection of *Fig. 9*. In addition, a difference of 10 m in water level at both the reservoir (85 m) and the maximum height of water at the local aquifer in dam site (75 m) suggest a hydraulic connection between the aquifer and the reservoir. This fact is supported by the dependance of flow rates in both drains on riverbed layer which in turn, has a better hydraulic connection with the reservoir (*Fig. 3*) It is shown (*Figs 10* and *11*) that the flow of seepage water (retrieved from both drains) diminishes monotonously away from the dam site. An intrusive thrust of fresh water leaking (between 38 and 45 m) from the reservoir might be inferred (*Fig. 5*) The electrical conductivity of waters, in these piezometers (which are tapping the riverbed layer), decline at a depth ranging between 38 and 45 m (*Fig. 5*).

The suggested front (*Fig. 10*) is found to be characterized by abnormally low conductivity (800µS /cm) in contrast with much higher values in both drains (2500 – 4800 µS/cm). The graph (*Fig. 4* Cl-EC) showing the most conservative chloride ion and the electrical conductivity for the reservoir water and the two drains (particularly drain 1) as a

function of time for the interval between 1991-1998 suggest a leaked front emerging from the dam. This front was being soaked with salts driven away from the riverbed.

The isotherm pattern (*Fig. 11*) of the suggested fresh waterfront, which overlies the riverbed, is characterized by lower temperature value (14.7 C°) than those distant from the riverbed. However, the rate of temperature rise is higher towards drain 2. In contrast, the reservoir water is shown to have consistent temperatures with depth (14.1- 14.7 degree Celsius).

The plot of $\delta^{18}O‰$ versus $\delta^{2}H‰$ is shown in *Fig. 8*. An inspection of this figure reveals that ground water close to the reservoir has a stable isotopic composition which is indicative of an appreciable contribution of reservoir water (P53, P17, P52 and P55). Moving away from the reservoir the δ -values become more depleted, owing to the contribution of infiltrating precipitation which also recharges the local groundwater system of piezometers P42, P41, P34 and P39. Seepage water in D1 and D2, in addition to reservoir water (R) with piezometer noose; P53, P17, P52 and P55 that show a similar isotopic composition and hence, reflecting the same origin. Regression line that best fit the aforementioned group has a slope of 4.36, which reflect the effect of evaporation and/or mixing on δ-values. This cluster (P53, P17, P52 and P55) represents the first end member (which is the surface water suffering from partial evaporation). The second end member (P42, P41, P34 and P39) (which is more depleted in δ -values) is the local groundwater system which shows a different isotopic composition that has ruled out the theory that the reservoir water is the only source of water in the piezometers (*Fig. 8*). This separate cluster plot to the left of Meteoric Water Line (MWL) is indicative of isotopic exchange with CO_2 issued from the local carbonate aquifer. The plots in between the two end members (P26, P57) represent a mixture of the reservoir water and the local groundwater with different mixing proportion (*Fig. 8*).

Tritium was used as natural tracer in order to delineate seepage flow pathways and any recent recharge to the groundwater from reservoir (JØRGENSEN et al., 2000). Aerial distribution of tritium for the local aquifer is shown in Fig 12.The prevailing tritium concentration in reservoir water amounts to 5 TU at a depth of 20m. Whereas, tritium in the ground water and in seepage water ranges between 1.24 and more than 4.8 TU. Tritiated water is emerging from the reservoir in the form of tritium front (*Fig. 12*) having tritium value of about 5 TU, following the same direction of riverbed layer and confirming the above-mentioned fact that the reservoir water is the main source of seepage water. This tritiated water when emerging from the reservoir is mixed with tritium devoid water (local ground water) and gives rise to lower tritium concentration water resulted from the mixing of the above-mentioned two end members.

ACKNOWLEDGEMENT

The authors would like to acknowledge support from the International Atomic Energy Authority (IAEA) Vienna where the project was entirely funded by IAEA as part of the African Regional Co-operative Agreement for Research, Development & Training Related to Nuclear Science & Technology (AFRA) and from Republic of Tunisia, Center National Des Sciences Et Technologies Nucleaires (CNSTN)-Tunis-Cartage without which this work would not have been completed. The manuscript was considerably improved by the very critical reading of Prof. M. KHATTAB, Faculty of Engineering, Suez Canal University, EGYPT.

REFERENCES

ADAR, M. E., (1994): Application of Tracers in Arid Zone Hydrology: Proc.Symp. IAHS Publication No.232, PP 451.

DROST, W. and F. NEUMAIER (1974): Application of Single Borehole Methods in Groundwater Research, Isotope Techniques in Groundwater Hydrology, Proc.Symp. Vienna, IAEA, 11-15 March 1974, P.241.

HALEVY, J.A. (1967): Borehole Dilution Techniques: Critical review, Isotopes in Hydrology, Proc. Sympo. Vienna IAEA, 14-18 Nov. 1966) IAEA, Vienna 1967, P.531.

JØRGENSEN, N.O. and T.K. SØRENSEN (2000): Stable isotope studies of artificial recharge in glaciofluvial sediments at Arrenaes, Denmark, Proceed. Of the Int.Conf. On Groundwater Research, Copenhagen, 101-102.

TURNER, E. (1990): Flurometric Facts, A Practical Guide to Flow Measurement, Turner Design, p.21.

Manuscript received: 19. Oct. 2000.

Acta Mineralogica-Petrographica, Szeged, XLI, 105–118, 2000

STRUCTURAL EVOLUTION OF EL-ATAWI AREA, CENTRAL EASTERN DESERT, EGYPT

AHMED M. HEGAZI

Geology Department, Suez Canal University*

ABSTRACT

El-Atawi area is covered mainly be metasediments, metavolcanics serpentinites, cataclastic granodiorites, El-Atawi alkali granite, which are intruded in many places by post-granite dykes and late volcanics (mainly trachites).

The geometric analysis and the cross-cutting and overprinting relationships of the mesoscopic structural elements reveals that the metasediments and metavolcanics have been subjected to three folding phases. The F1-fold generation is the oldest one and was refolded by a widely distributed system of isoclinal overturned F2-folds. The F3 isoclinal, reclined folding system represents the youngest folding phase which are recorded at the study area.

The folding pattern of El-Atawi area could be evolved through the superimposing of three successive folding phases. The geometry of the interference pattern produced by the superimposing of two folding generations depends on the values taken by angles α and β. At El-Atawi area the superimposing of F1 and F2 has α and β angles which are compatible with that of the condition suitable to produce type-2 interference pattern of RAMSAY (1967). The overprinting of F3-folding has resulted in the formation of type-1 interference pattern. Due to this superimposing process, El-Atawi area was folded into a series of sharply elongated domes and basins which is well-developed in the metasediments exposed at the area.

INTRODUCTION

El-Atawi area is a part of the Precambrian basement complex exposed in the Central Eastern Desert, and it is bounded by latitudes 25°35' and 25°40' N and longitudes 34°07' and 34°15' E. It is a mountainous terrane characterized by high peaks such as G. El Sibai, G. Um-Luseifa, and G. Andia. The highest two triangulation points in the area occur in the granite mass of G. El-Atawi (1062 m), at the southeastern part, and in the metavolcanics of G. El-Hameir (829 m), at the southwestern corner. The area is traversed by two main wadis, namely Abu-Garadi and El-Atawi. The southern parts are drained by W. E-Miyah and W. Sitra.

El-Atawi area has been the subject of many studies, particularly as being a part of G. El-Sibai area. Most of the studies are mainly concerned with metamorphism, geochemistry, and regional tectonic setting. Structurally, El-Atawi area belongs to the major upper tectonic units (Suprastructure), which include serpentinites, metavolcanics and their equivalent volcaniclastics (SABER, 1993). The present work aims at analyzing the mesoscopic fabrics and structures, and describing their geometric style, orientation, ad overprinting relationships. Resolving the spatial and the temporal relationships of the mesoscopic structures helps deciphering the tectonic history of the deformed rocks. Eventually, the structural evolution of the study area, based on the geometric and kinematic analyses, it also simulated.

* Ismailia 41522, Egypt

GEOLOGIC SETTING

The metamorphic belt of El-Atawi area is bounded at the north and easy by the red and pink alkali granite masses of G. El-Sibai and G. Um-Luseifa, and at the south by the red, coarse- to medium-grained, alkali granite of G. El-Atawi. The granite-gneiss and the other metamorphic rocks are the oldest rock units, whereas the alkali granites are the youngest ones. The metamorphic rocks of El-Atawi area are intensively folded and regionally metamorphosed assemblage of volcanics and volcaniclastic sediments that range in metamorphism from green schist to amphibolite facies. Furthermore, the volcaniclastic sediments contain dismembered ophiolitic masses of serpentinite and related rocks, together with spilitic pillow lava (EL-SHAZLY and SABET, 1955, and EL-BAHARIYA, 1988).

The metasediments include meta-mudstones, meta-greywakes, schists, phyllites, and hornselfes, (Plate Ia). The main metavolcanics are represented by fine- and coarse-grained meta-basalts, meta-andesites, meta-dacites and rhyodacites, (Plate Ib). Other rock units exposed in the study area are serpentinites, cataclastic granodiorites, diorites, Hammamat metasediments, El-Atawi alkali granite, (Plate Ic), post-granite dykes, and late volcanics (trachytes), (SABET, 1961, RAGAB, 1971 and EL-GHAWABY, 1973).

Three main alkali granites outcrop in El-Atawi area; namely, G. El-Atawi, Abu-Garadi and the northern gneissose granite. Many apophyses are intruded from the first two granite bodies into the older metamorphic rocks. Moreover, G. El-Atawi is a part of a granite batholith which is located at the southeastern part of the area (KHAWASIK, 1968).

SABER (1993) revealed that G. El-Sibai area is characterized by the presence of two major structural units separated by a shear zone. The lower tectonic unit is referred to as the infrastructure, whereas the upper tectonic unit is defined as the suprastructure. The infrastructural rocks are differentiated into amphibolite-migmatite association, quartz-feldspar gneiss, and gneissic granites. The suprastucture is exposed in two belts overlaying the infrastructure, and is made up of weakly metamorphosed basic to intermediate volcanics and their equivalent volcaniclastics.

Accordingly, the El-Atawi metasediments and metavolcanics belong to the Pan-African suprastructure island-arc volcanics and volcaniclastics which are thrusted over the infrastructural units located to the north.

The areal distribution of different lithologic units exposed in El-Atawi area, as verified during the field work, is shown in *Fig. 1*. Their relative ages are arranged from the oldest to the youngest as follows: metasediments, metavolcanics, serpentinites, cataclastic granitoids, El-Atawi alkali granite, and post-granite dykes.

MESOSCOPIC STRUCTURES AND FABRICS

Conventionally, the simple mesoscopic structures and fabrics are treated geometrically as planes or lines. Hence, the field orientation data, i.e., the mesoscopic structures which have been measured and recorded in the field will be treated under the following topics:

1. Planar structures

These structures include the bedding planes and the cross- and graded-bedding in the metasediments, the relic banding in metavolcanics, as well as the foliation and fracture cleavage in both rock units (Plate Id).

Linear structures:

These structures encompass minor fold hinges, intersection lineations, and pencil and rod structures in both metasediments and metavolcanics (Plate Ie).

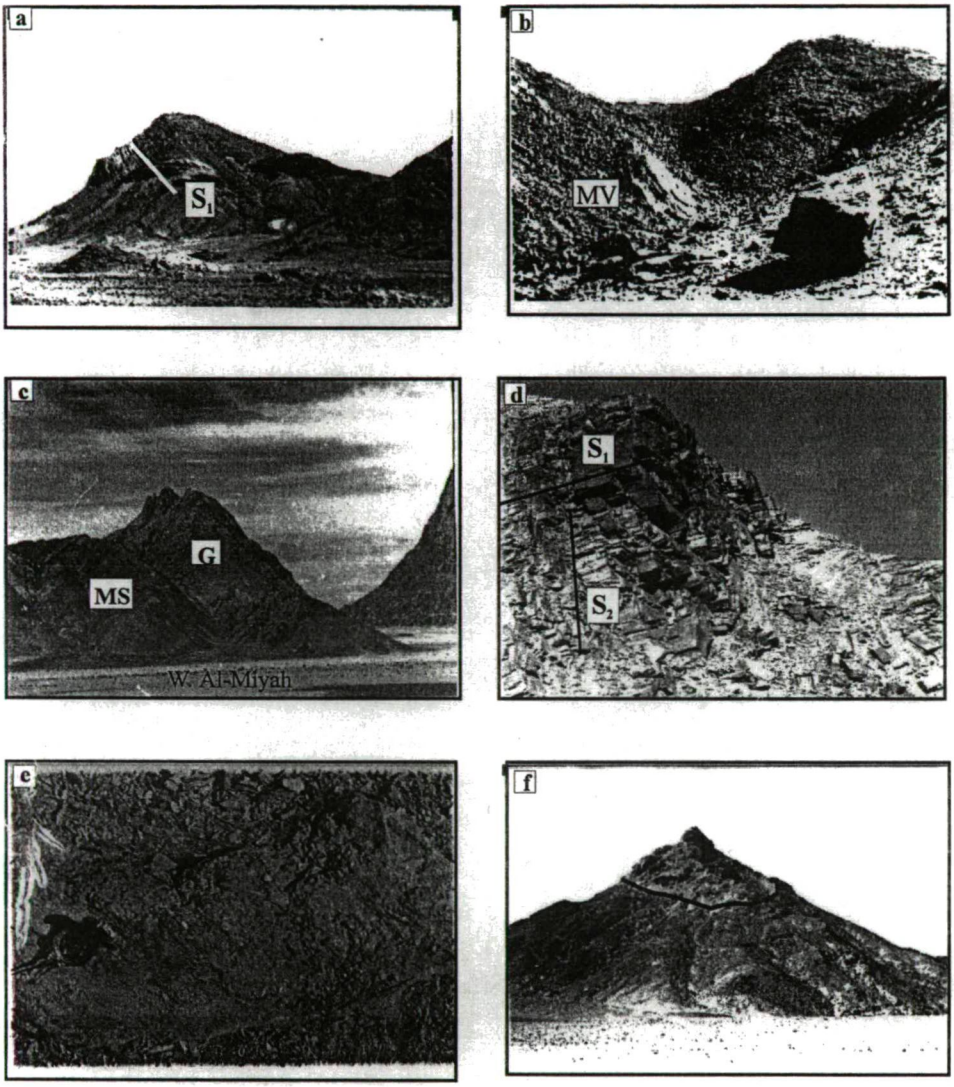

Plate I.

(a): Isoclinally F2-folds in Metasediments, El-Atawi area, looking SE
(b): Metavolcanics of G. Al-Hameir.
(c): G. El-Atawi alkali granite (G) intruding Hammamat metasediments (MS), W. Al-Miyah, looking north.
(d): S1-foliation and S2-fracture cleavage in metasediments, W. Abu-Garadi, looking NW.
(e): Pencil structure in metasediments, El-Atawi area.
(f): Elongated basin-pattern which is a part of type-I interference pattern in metasediments, El-Atawi area (looking NW).

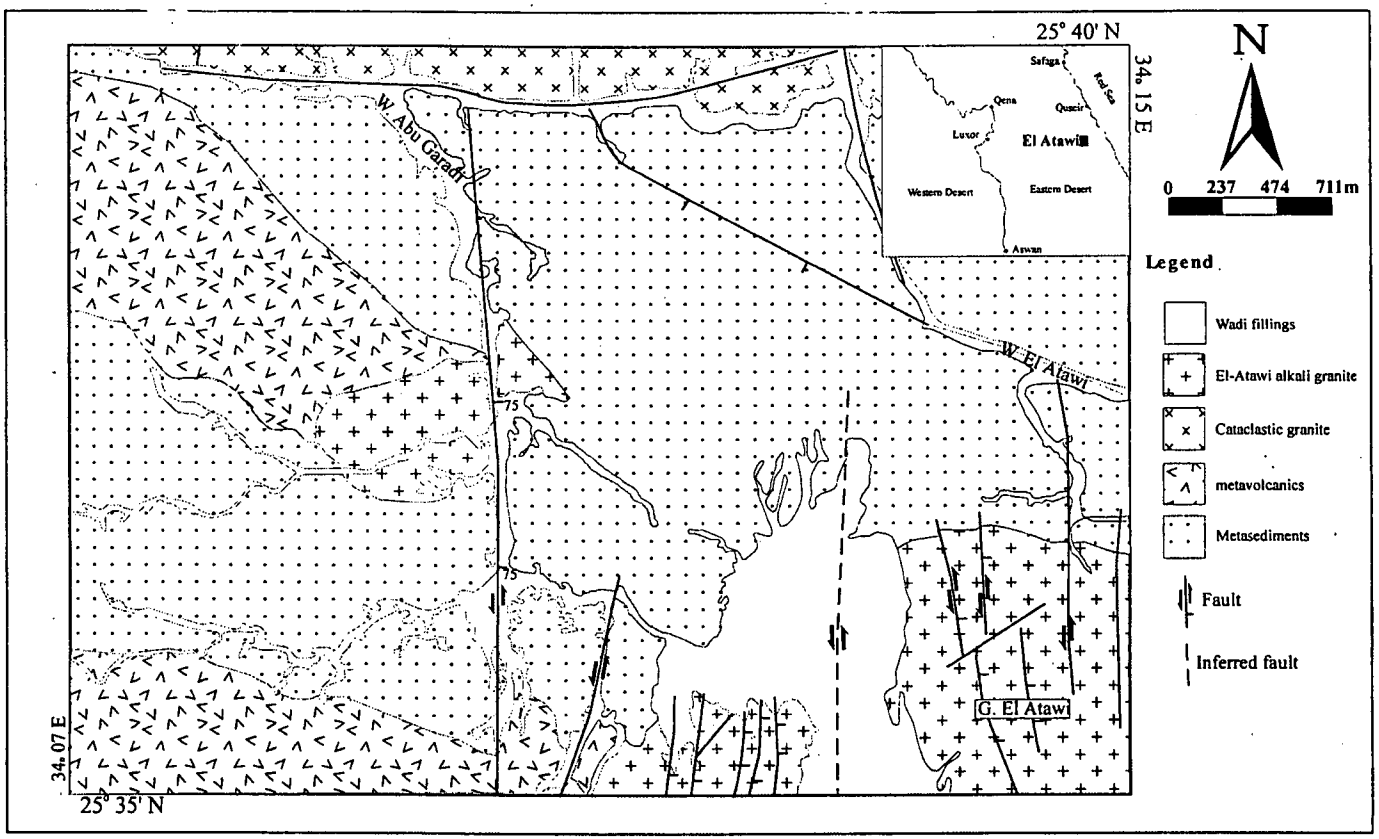

Fig. 1. Geological map of El-Atawi area, Central Eastern Desert

The mesoscopic structures which are measured and recorded in El-Atawi area are plotted on the structural map (*Fig. 2*) and their geometrical and genetical relationships are exhibited in Table 1.

TABLE 1

The genetic relation of the mesoscopic structures in El-Atawi area

Relative age	Symbol	Type of structure	Mesoscopic structures in the field
Primary structures	S_0	Primary S-surfaces	- Bedding, cross-, graded-bedding in metasediments - Banding in metavolcanics.
Secondary structures associated with the first folding phase (F1)	S_1	Axial planes of F1	- Foliations. - Fracture cleavage.
	B_1	Axes of F1 in S_0 with S_1 as axial plane	Hinges of minor folds belong to F1
	L_1	Lineations parallel to the S_0-S_1 intersections	- Cleavage-bedding intersection - Pencil and rod structures
Secondary structures associated with the second folding phase (F2)	S_2	Axial plane of F2	- Foliations. - Stay cleavage - Fracture cleavage.
	B_2	Axes of F2 in S_0 & S_1 with S_2 as axial plane	Hinges of minor folds belong to F2
	L_2	Lineations associated with F2	S_0-S_2 & S_1-S_2 intersection lineatons
Secondary structures associated with the third folding phase (F3)	S_3	Axial plane of F3	- Slaty cleavage
	B_3	Axes of F3 in S-surfaces with S_3 as axial plane	Hinges of minor folds belong to F3
	L_3	Lineations associated with F3	Intersection lineations of S3 with different S-surfaces

GEOMETRICAL ANALYSIS

The conventional geometrical analysis is carried out by plotting the poles to a given structural planar element or the plunge of a linear element on an equal area net, then the geometrical interpretation of these data can often be done by inspection, assisted by contouring methods.

In the present work the mesoscopic structural elements are plotted and contoured using "SPHERISTAT", an orientation analysis and plotting program for MSDOS Computers, Version 1.1.

1. Planar elements:

The contour diagram of poles to S0-surfaces represented by bedding planes in metasediments and banding in metavolcanics is shown in *Fig. 3*. This diagram shows that the poles are distributed along a girdle and they posses a bimodal distribution. The attitude of the axial plane is predicted to be S55°W/50°, and the axis is plunging 36° towards N70°W. Although the poles to the bedding are generally configurated into a great circle (*Fig. 3*), it is evident that these poles attend to arrange along another girdle whose

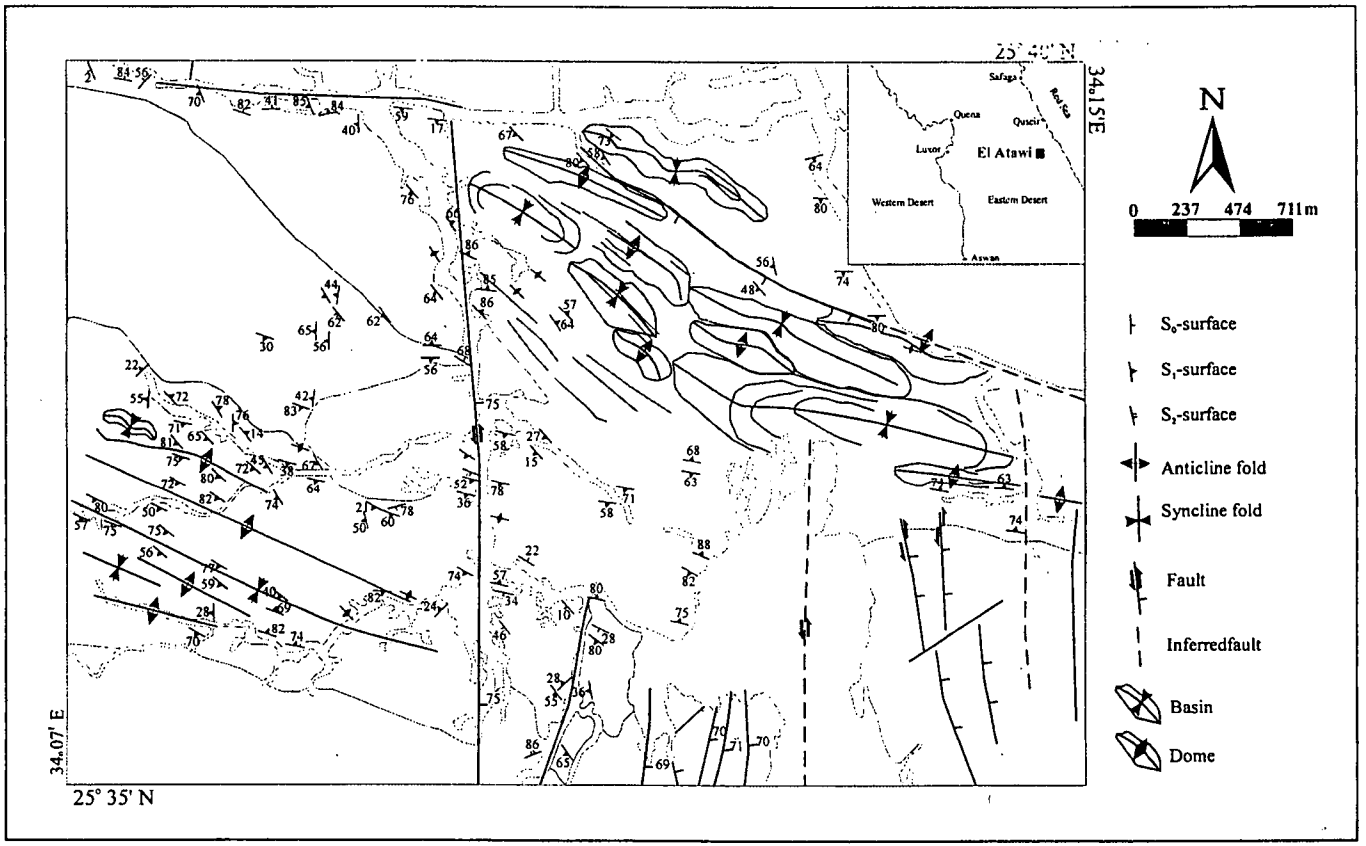

Fig. 2. Structural map of El-Atawi area, Central Eastern Desert, showing the predicted closed elongated interference patterns Resulted by the superimposing of the folding phases.

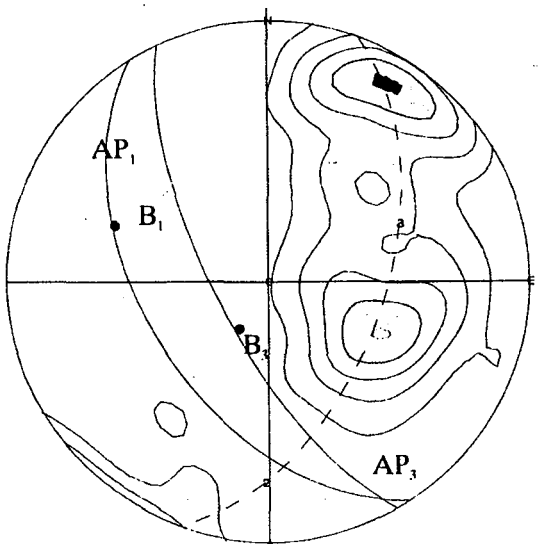

Fig. 3. Stereogram of poles to bedding and banding in metasediments and meta volcanics, El-Atawi area.
AP_1: Axial plane and B_1: geometric axis of the first phase of folding.
AP_3: Axial plane and B_3: geometric axis of the third phase of folding.

geometric axis plunging 70° due S36° W and the attitude of its axial plane is S58°W/74°. WOODCOCK (1977) introduced K- and C-ratios as useful indicators of the fabric shapes of folding. The K-ratio is an estimate of both girdle and cluster tendencies of the directional data, whereas, the C-ratio is a measure of their strength of preferred orientation. The K- and C-ratios of the plottered S0-surfaces are estimated 0.76 and 1.2, respectively, indicating a weakly developed girdle and cluster pattern of folding which also has a weak preferred orientation.

The poles to foliations also suggest a girdle distribution whose axis is horizontally trending in N55°W direction, whereas the attitude of the axial plane is S35°W/70° (Fig. 4). The K- and C-ratios of the plotted foliation surfaces are respectively estimated 0.95 and 1.38, indicating a weakly-developed girdle and cluster pattern of folding which is characterized by a weak preferred orientation. The folding in foliations surfaces seems to have an isoclinal overturned style. Furthermore, the diagram shows that the poles tend to spread along another great circle whose geometric axis plunges 70° to S36°W, and the attitude of its axial plane is S58°W/74°.

The geometric analysis clearly indicates that there are three generations of folding. The first one has a geometric axis plunging 36° to N70°W and an axial surface (S55°W/50°). The second generation of folding has a horizontal geometric axis trending N55°W-S55°E and an axial surface (S35°W/70°). The third one has a geometric axis that plunges 70°, S36°W, and an axial surface (S58°W/74°).

FLEUTY (1964) suggested a useful geometrical classification scheme for folds based on the relative orientation and the absolute inclinations of hinge lines and axial surfaces. According to this classification, the three folding phases that affected El-Atawi area are listed in Table 2.

TABLE 2

Geometrical classification of folds (FLEUTY 1964)

Generation	Axial surface	Hinge	Type of fold
1st	moderately inclined	moderately plunging	moderately inclined, moderately plunging
2nd	steeply inclined	horizontal	horizontal, steeply inclined
3rd	steeply inclined	steeply plunging	steeply plunging, steeply plunging

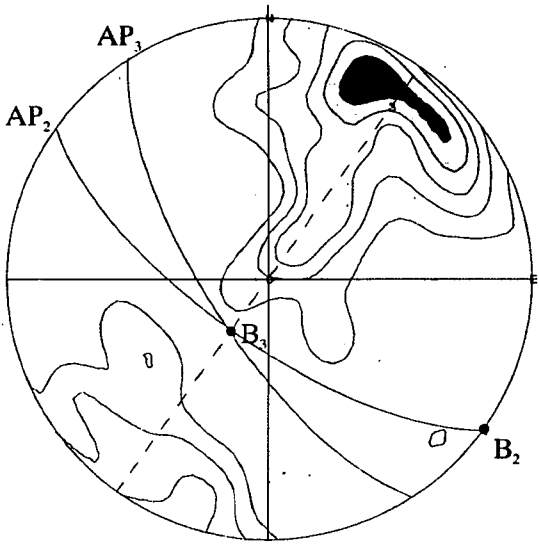

Fig. 4. Stereogram of poles to foliations in metasediments and meta volcanics, El-Atawi area.
AP_2: Axial plane and B_2: geometric axis of the second phase of folding.
AP_3: Axial plane and B_3: geometric axis of the third phase of folding.

2. Linear structures:

a) $L_{1\text{-}a}$-intersection lineations:

These lineations are represented by the intersection of the bedding S_0-surfaces and the first foliation S_1-surfaces. The intersections are plotted on stereogram (*Fig. 5a*), which exhibits that the measurements are hovering around the B1-geometric axis, i.e., they are more or less parallel to it, with a tendency to spread along a small circle due to the effect of subsequent refolding.

b) $L_{1\text{-}b}$ pencil structure:

The pencil structure is a very distinctive linear structure associated with folded and cleaved mudstones and siltstones which are widely exposed at El-Atawi area, (Plate Ie). It is formed by the intersection of bedding fissility surfaces (S_0) and cleavage surfaces (S_1). It is predicted from the stereogram of the pencil structures (*Fig. 5b*) that these linears are

distributed in a bimodal pattern, and they hover around an average attitude with maximum plunging 16° to N86°W. Moreover, the plot shows a tendency to spread along a small circle whose center is found to be concomitant with the B3-geometric axis.

c) L3-intersection lineations:

The linear structures produced by the intersection of the S_3-foliations with the previously formed S-foliations. These linear structures are projected on a stereogram (*Fig. 5c*). The distribution of data on the stereogram suggests a unique average plunging 68°, S26°E, which is more or less parallel to B3-geometric axis.

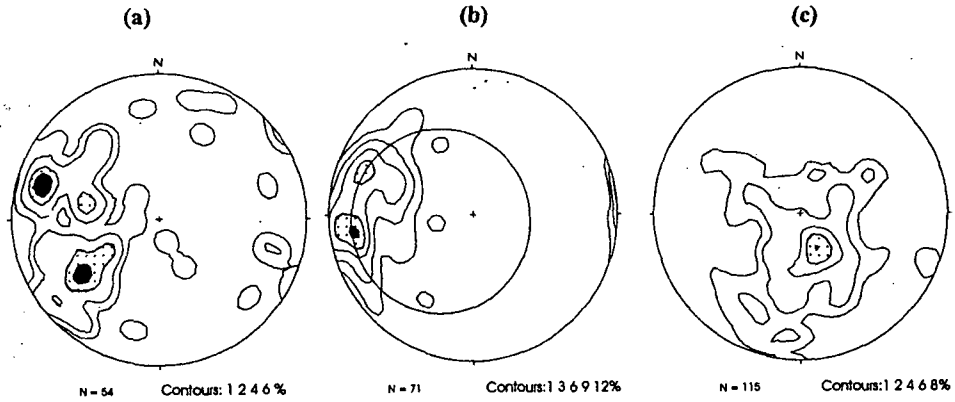

Fig. 5. Stereogram of L1-a intersection lineations (a), L1-b pencil structures (b), and L3 intersection lineations (c) in metasediments and metavolcanics, El-Atawi area.

d) Fold hinges:

The hinges of the different fold generations are plotted on a stereogram (*Fig. 6*), that shows distinctive maxima which could be related to the three folding phases. Two maxima; 1a and 1b, whose attitudes are 24° due West and 32° to N26°W respectively, re-

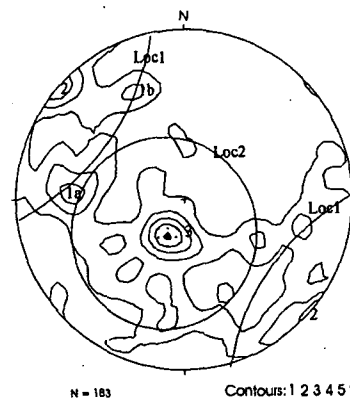

Fig. 6. Stereogram of fold hinges in metavolcanics and meta sediments, El-Atawi aea. (Loc1: is the locus of B1 about B2-geometric axis and Loc2 is the locus of b1 about B3-geometric axis)

present the locus of rotation of B1-geometric axis through a small circle about B2-geometric axis. The stereogram also shows another maximum, denoted as "2" in *Fig. 6*, coinciding with B2-geometric axis. This maximum is horizontal and trends to N46°W-S46°E. Moreover, the B3-fold hinges are represented by a pronounced maximum designated as "3" plunging 68° to S18°W. This maximum have the highest contour value (5%) indicating that the F3-fold hinges are more or less coaxial. This means that F3-hinges have not been subjected to subsequent refolding events. In addition to that, the stereogram exhibits a subordinate clustering of fold hinges that could be interpreted in terms of the locus of rotation of different geometric axes about a subsequent refolding axis.

STUCTURAL EVOLUTION

The structural evolution of El-Atawi area, based on the foregoing geometric and kinematic analyses, could be simulated in terms of the superimposing of three successive folding phases. The geometric analysis of the preserved bedding planes (S0) and the different foliation surfaces (S_1, S_2 & S_2) reveals that the metasediments and metavolcanics have been subjected to three folding phase. The cross-cutting and overprinting relationships of the mesoscopic structural elements have verified that F1-fold generation is the oldest one and are refolded by a widely distributed system of isoclinal overturned F2-folds. Representative measurements of S1-foliations (*Fig. 7a*) are distributed along a girdle whose geometric axis plunges 18° towards S39°E. The axial plane, which is measured directly in the field, has an attitude S27°W/70°. Also, representative measurements F2-fold hinges (*Fig. 7b*). show bimodal distribution, which is a clue for refolding process. The F3-folding system represents the youngest folding phase recorded at the area. This is confirmed by selective measurements reveals that the F3-folding is isoclinal and having axial plane whose attitude is S58°W/77°, whereas the geometric axis plunges 74° to S23°W. The characteristic feature of F3-fold hinges, is its clustering in the SW quadrant of the plot (*Fig. 8b*), indicating their tendency to be coaxial. This means that they are more or less parallel and show no signs of refolding process.

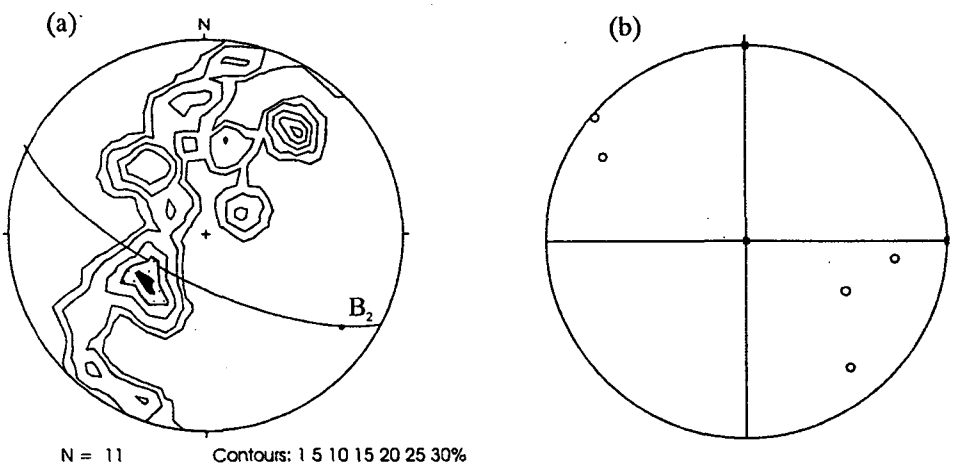

Fig. 7. Stereogram of poles to S1-foliations (a), and the F2 hinges (b)

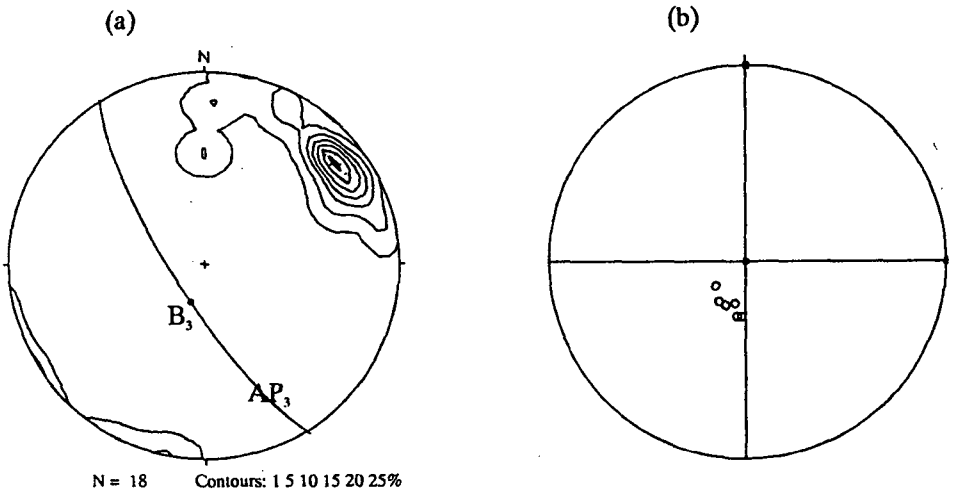

Fig. 8. Stereogram of poles to S2-foliations (a), and the F3 hinges (b)

The folding pattern of El-Atawi area (*Fig. 2*), could be evolved through different successive steps which began with original S0-surfaces represented by the bedding surface in the metasediments and banding in metavolcanics. These surfaces were initially horizontal and later on, they were tilted and their attitude became N70°W/36° (*Fig. 9a*). The original layered materials were subjected to an inhomogenous strain due to a compressive stress regime whose maximum principal axis plunged 44°, N66°E. This compressive stress resulted in the formation of the first folding phase F1, whose geometric axis plunges 36° to N70°W direction and the S1-axial surface (S55°W/50°), (*Fig. 9b*). If the nature and orientation of strain increments change, any previously folded rock layers may be subjected to refolding about different axial directions, and the axial surfaces of the original folds may take up some folded forms (RAMSAY, 1967). This is clearly exhibited at the study area, where the first folding generation F1 is superimposed by a second phase of folding F2, which related to subhorizontal compressive stress trending N35°E. F2-folds are generally isoclinal overturned folds and its B_2-geometric axis is horizontal one trending N55°W, whereas the attitude of S_2-axial surface is S35°W/70° (*Fig. 9c*). The geometry of the three-dimensional form produced by the superimposing of the first and second folding generation depends on the values taken by angles α and β. Where α is the angle between the two axes of successive folding, and β is the angle between the pole to the first axial plane and the direction of flow (a_2) of the second fold generation (RAMSAY, 1967). At El-Atawi area the superimposing of F1 and F2 has α and β equal to 36° and 69° respectively. These values are found to be compatible with that of the condition suitable to produce type-2 interference pattern of RAMSAY (1967) (*Fig. 9d*). The F3-folds are isoclinal, reclined fold (*Fig. 9e*) which took place by the influence of NW-SE-oriented horizontal compressive stress axis. The overprinting of F3-folding on the widely distributed F2-folds resulted in the formation of type-1 interference pattern (*Fig. 9f*) and the values of angles α and β are 77° and 75° respectively. Due to this superimposing process, El-Atawi area is folded into a series of elongated domes and basins, (Plate If), which is well-developed in the metasediments exposed at the area (*Fig. 2*). The sharply inflected and elongated domes and basins could be attributed to the very tightly nature of the interfering folds (TURNER and WEISS, 1963).

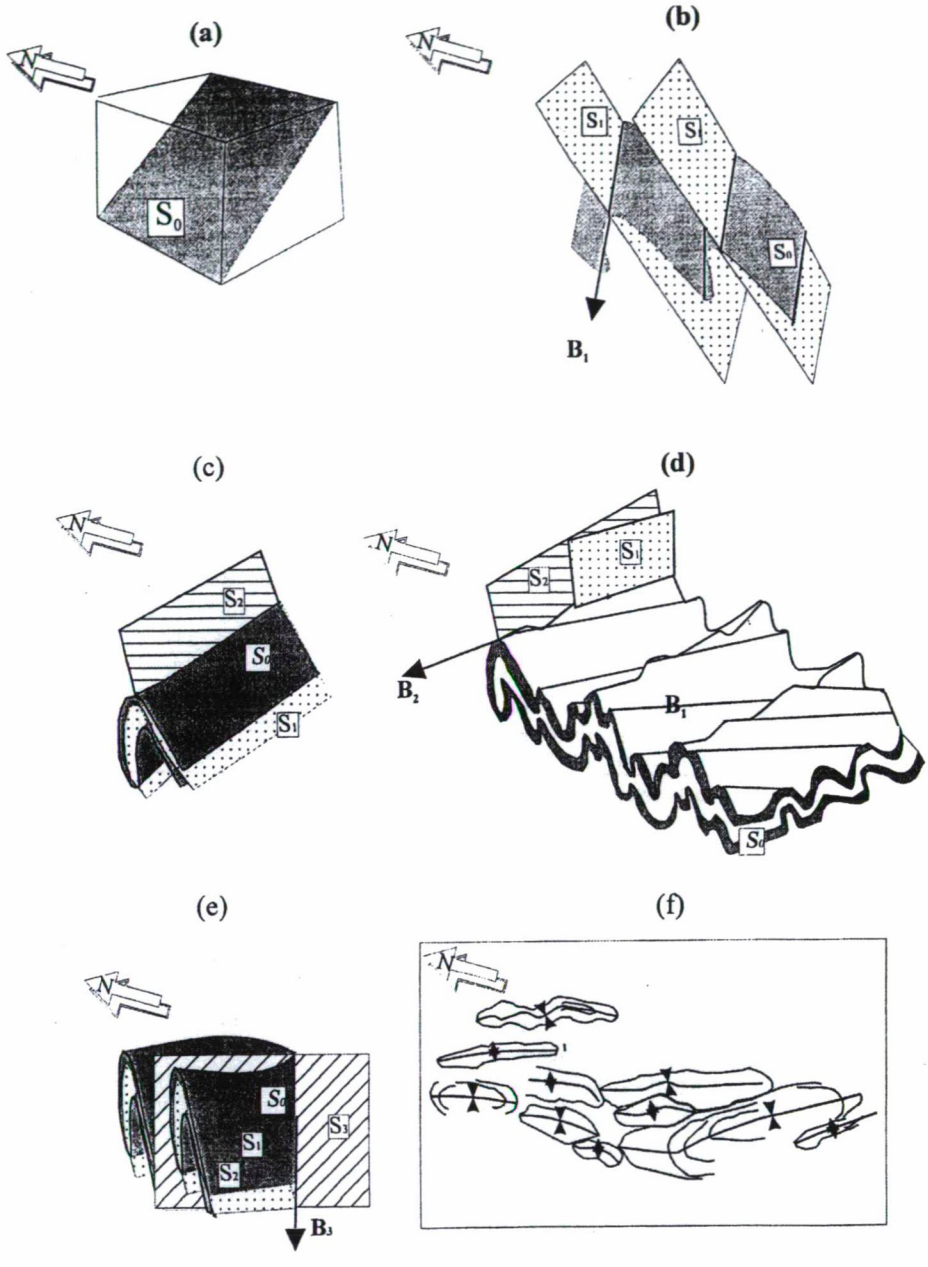

Fig. 9. A proposed structural evolution model of El-Atawi area, Central Eastern Desert. (S_0: bedding and banding, S_1, S_2 & S_3: first, second and third axial surfaces. B_1, B_2 and B_3: first, second and third geometric axes.)

SUMMARY AND CONCLUSIONS

The metasediments and metavolcanics of El-Atawi area are intensively folded and regionally metamorphosed assemblage of volcanics and volcaniclastic sediments of green schist and amphibolite facies. They belong to the Pan-African suprastructure island-arc volcanics and volcaniclastics thrusted over the infrastructural units located to the north.

The metasediments include meta-mudstones, meta-greywakes, schists, phyllites, and hornfelses. The main metavolcanics are represented by fine- and coarse-grained meta-basalts, meta-andesites, meta-dacites and rhyodacites. Other rock units exposed in the study ara are serpentinites, cataclastic granodiorites, diorites, Hammamat metasediments, El-Atawi alkali granite, post-granite dykes, and late volcanics (trachytes). Futhermore, the volcanoclastic sediments contain dismembered ophiolitic masses of serpentinite and related rocks, together with spilitic pillow lava.

The geometric analysis and the cross-cutting and overprinting relationships of the mesoscopic structural elements reveals that the metasediments and metavolcanics have been subjected to three folding phases. The F1-fold generation is the oldest one whose geometric axis plunges 36° to N70°W direction and the S_1-axial surface (S55°W/50°). They are refolded by a widely distributed system of F2-folds. F2-folds are generally isoclinal overturned folds and its B2-geometric axis is horizontal one trending N55°W, whereas the attitude of S2-axial surface is S35°W/70°. The F3-folding system represents the youngest folding phase recorded at the area. These F3-folds are isoclinal and having axial plane whose attitude is S58°W/77°, whereas the geometric axis plunges 74° to S23°W.

The folding pattern of El-Atawi area could be evolved through different successive steps which began with original S0-surfaces represented by the bedding surfaces in the metasediments and banding in metavolcanics. These surfaces were subjected to a compressive stress regime whose maximum principal axis plunged 44°, N66°E which resulted in the formation of the first folding phase F1. The previously folded rock layers may be subjected to refolding about different axial directions, and the axial surfaces of the original fold may take up some folded forms. This is exhibited at the study area, where the first folding generation F1 is superimposed by a second phase of folding F2, which related to subhorizontal compressive stress trending N35°E. The geometry of the interference pattern produced by this superimposing depends on the values taken by angles α and β. At El-Atawi area the superimposing of F1 and F2 has α and β angles which are compatible with that of the condition suitable to produce type-2 interference pattern of RAMSAY (1967). The F3-folds took place by the influence of NW-SE-oriented horizontal compressive stress axis. The overprinting of F3-folding has resulted in the formation of type-1 interference pattern. Due to this superimposing process, El-Atawi area is folded into a series of elongated domes and basins which is well-developed in the metasediments exposed at the area.

ACKNOWLEDGEMENTS

The author is gratefully indebted to Prof. Dr. SAMIR M. KHAWASIK, Head of Geology Department, Suez Canal University (SCU), Prof. Dr. MOHAMED A. EL-GHAWABY, (SCU), Dr. NABIL N. EL-MASRY, (SCU) and Dr. T. J. FOWLER, Geology Dept., La Trobe University, Australia, for reading, valuable discussion and constructive criticizing the typescript of the present work.

REFERENCES

EL-BAHARIYA, G. A. (1988): Geology of the District southwest of Gabal El-Sibai, Eastern Desert, Egypt. M. Sc. Thesis, Faculty of Science, Tanta University, 198.

EL-GHAWABY, M. A. (1973): Structure and radioactivity of Wadi Zeidun area, Central Eastern Desert, Egypt. Ph. D. Thesis, Faculty of Science, Ein Shams University, Cairo.

EL-SHAZLY, E. M. and SABET, A. H. (1955): A preliminary report on El-Atawi copper deposits, Eastern Desert. Geological Survey of Egypt, Paper No. 2, 5.

FLEUTY, M. J. (1964): The description of folds: Geological Association Proceedings, 75, 461-492.

KHAWASIK, S. M. (1968): Geology of radioactive localities of Abu Garadi area, Easter Desert. M. Sc. Thesis, Faculty of Science, Ein Shams University, 157.

RAGAB, A. I., (1971): Geology of Gebel El Atawi area, Eastern Desert, Egypt. Ph. D. Thesis, Ein Shams University, Cairo, 196.

RAMSAY, J. G. (1967): Folding and fracturing of rocks. McGraw-Hill Book Company, New York, 560.

SABER, G. M. (1993): Geochemistry and tectonic significance of the Pan-African El-Sibai Window, Central Eastern Desert, Egypt. Forschüngszentrum, Julich GmbH, Scientific Series of the International Bureau, 19, 154.

SABET, A. H. (1961): Geology and mineral deposits of Gebel El Sibai area, Red Sea hills, Egypt, U.A.R. Ph. D. Thesis, Leiden State University, The Netherlands, 187.

TURNER, F. J. and WEISS, L. E. (1963): Structural analysis of metamorphic tectonites. McGraw-Hill Book Company, Inc., 545.

WOODCOCK, N. H. (1977): Specification of fabric shapes using an eigenvalue method. Bull Geol. Soc. Am., 88, 1231-1236.

Manuscript received: 5. March 2000.

Acta Mineralogica-Petrographica, Szeged, XLI, 119–128, 2000

GEOCHEMICAL ANALYSIS OF SUSPENSION LOAD OF WHITE KÖRÖS

CS. SZABADOS*, A. KISS**, L. KURILLA**

Department of Mineralogy, Geochemistry and Petrology, Attila József University of Szeged, and Hydrology Institute of Gyula

ABSTRACT

Few studies are available concerning the Hungarian river load. Previously mainly qualitative measurements were performed and as well as is being performed more recently. In the literature chemical analysis of flapping river load is not common (BALLÓ M. L873: TAKÁTS T- L930: MEZŐSI J-DONÁTH É. 1951: BOGÁRDI J.). More papers are available regarding the characteristics of catchment areas of rivers Berettyó and Körös. Workers of Hydrology Institution are continuously measuring the hydrographic measurement. The complex mineralogical and geochemical analysis of suspension load of the rivers have been never done. During our study we are addressing the following questions:

The quality and quantity of the suspension load of the river

When and why does the river deliver the largest amount of load?

What is the flapping particles roundness?

Which part of the catchment area are these particles coming from?

What difference can be found between the particles in the river and the mineral composite of the catchment area?

To answer these questions we analyze the suspension load.

INTRODUCTION

The river load is composed by organic and inorganic compounds. The organic load comes from urban, industrial and agricultural waste, its appearance is random, and its movements is unorganized. The inorganic load originates from the decomposing of rocks. So it contains different kind of pebble and minerals which can be characteristic of river. The size of the river load varies from hundreds kilograms to very small flapping particles, so most of the time the load is a mixture of particles of different size. Particles over 0.002 mm are considered as a load. Their shape can be sharp or spherical depend on how long way they take in the river.

In the catchment area a complex water erosion produce load. The rocks are eroded, delivered affected by chemical and physical effects.

Two different kind of load can be distinguished by their origin. One comes from the catchment area other comes from the river bed and bank. Thus the development of the load influenced by geological and topographical characteristics of the catchment area, the

* H-6701 Szeged, P. O. Box 651.
** H-5700 Gyula

soil (agriculture) and the climate (quantity and distribution of rainfall, yearly and monthly mean temperature, evaporation and specific amount of water). The river load is different in different part of the river and different cross section of the river, so the place of the sample-taking is very important.

The water moves the load as a carrier. Three different kind of load can be distinguish:

1) Rolling or bottom load (rubbing, sliding movements)
2) Suspension load (flapping in the water, moves the same speed as the river)
3) Dissolved salts and colloids (continuously present independent from the movement of the water)

During the study of the load we make two groups:

I. The characteristics of catchment area: studying the geological and topographical conditions, the soil composition, and the climate conditions (rainfall, temperature, evaporation),

II. Characteristics of the water-flow: determination of the quality and quantity of traction and suspension load, and their changes through cross section and depth of the river. Hydrographic measurements (data on water level, fall, speed, seed dispersion, discharge, quality and quantity of water and river channel.

Samples were taking every 3 months (spring and summer flood, low water at the end of fall and flood in spring after snow thaw). We drew 10 liters of sample in the current of the river, form 1-1.5 meters deep using special vessel, and after centrifugation we got g dried material. After special treatment and size measurement the specimens were analyzed by binocular and polarization microscope and x-ray difractoraph and x-ray fluorescent technic.

THE WHITE KÖRÖS

This river originate from south-east side of mountain Apuseni at 980 meters high. The length of the river is 236 kilometers, the catchment area is 4275 km^2. The falls of the river is changing: at the upper course it is a running stream (fall: 17.5 meters/kilometer), slows at the middle course (fall: 1 meter/kilometer), and even slower at the lower course in the plane, It is bordered by Transylvanian Érc Mountains (Mt. Auriferi) and Zarándi (Mt.Highis, Mt. Drocea) Mountains from the south and Béli (Mt. Codru, Mt. Moma) Mountain from north.

Table 1 shows the hydrographic measurements of White Körös in 1999. This table indicates the correlation of the mean water level, the water discharge and the suspension load in year 1999. During the spring measurements we found average load discharge at 3 centimeters water level and 27,7 m^3/s water discharge. However, sample from the summer flood the suspension load was 13763,93 g/s at the 43,8 m^3/s water discharge.

TABLE 1

Shows the hydrographic measurements of White Körös in 1999.

Date	Mean water level (H) cm	Water discharge (Q) m^3/s	Mean speed (v_k) m/s	Suspension load discharge G. g/s	Suspension mean concentration Ck g/m^3	Average diameter of the load d_g mm
1999.04.15.	3	27.7	0.61	576.256	20.789	0.045
1999.06.24.	151	43.8	0.45	13763.93	314.441	0.044
1999.12.03.	-104	8.12	0.36	87.439	10.771	0.034

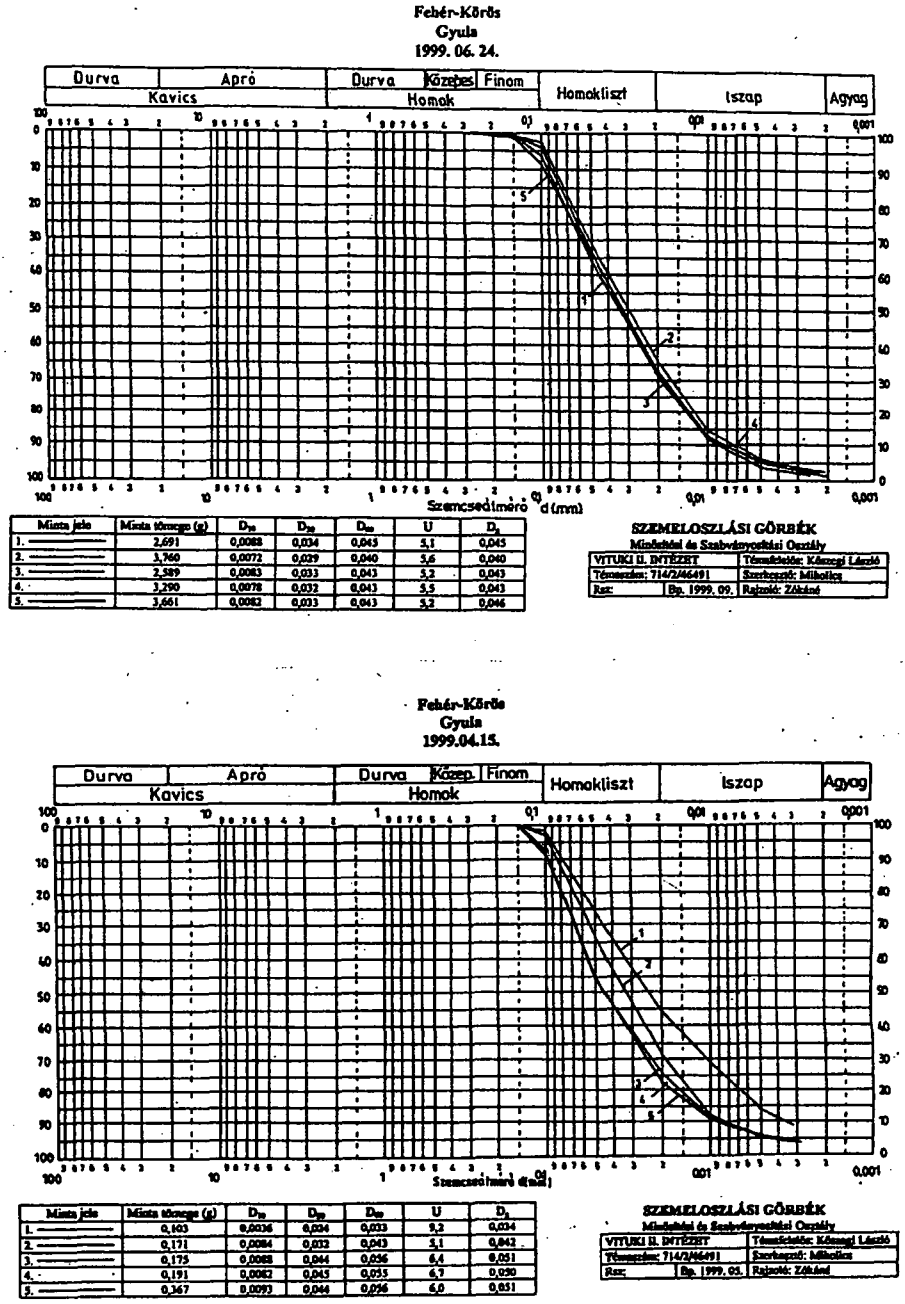

Minta jele	Minta tömege (g)	D_{10}	D_{30}	D_{60}	U	D_k
1.	2,691	0,0088	0,034	0,045	5,1	0,045
2.	3,760	0,0072	0,029	0,040	5,6	0,040
3.	2,589	0,0083	0,033	0,043	5,2	0,043
4.	3,290	0,0078	0,032	0,043	5,5	0,043
5.	3,661	0,0082	0,033	0,043	5,2	0,046

Minta jele	Minta tömege (g)	D_{10}	D_{30}	D_{60}	U	D_k
1.	0,103	0,0036	0,034	0,033	9,2	0,034
2.	0,171	0,0084	0,032	0,043	5,1	0,042
3.	0,175	0,0088	0,044	0,056	6,4	0,051
4.	0,191	0,0082	0,045	0,055	6,7	0,050
5.	0,367	0,0093	0,044	0,056	6,0	0,051

Fig. 1. The results of the size measurements of White Körös in 1999.

The river comes through different geological strata. It originates from Mesozoic limestone, then come through crystalline slate and granite for a while and then rum through Paleozoic, Mesozoic volcanic area at the end. Between Brad, Honctő and Borossebes it runs through Neogene (Badenian-Sarmatian) andesite area. The only barrage can be fond at Körösbökény, so the water coming from the mountains delivers the load continuously. After reaching the Plane the river slows down (after Borosjenő and Kisjenő) and delivers smaller load, but during the flood it can deliver sandy load up to Gyula.

The results of the size measurements were the following. The suspension load of the river at Gyula does not contain gravel. The suspension load contains 68.1% sand, 28.9% silt and 3% clay. Samples taken different season (spring, summer, fall) are different (*Fig. 1.*). In spring (subside rivers, smaller water discharge, but higher mean speed) the river load contains 69.8% sand, 26.2% sandy-silt and 3% clay. The load size of the blank and the current is different, the curve is changing. The samples from the bank indicates that the river delivers more fine slit and sand there then in the current, where the faster waterflow delivers greater sandy load coming from distant cachment area. Samples from the summer flood, the river load is more uniform, 66.4% sand, 32.1% silt and only 1.5% clay. Thus at lower water level, lower water discharge, but faster mean speed the White Körös has much more sandy load in the current. While at higher water level, at greater water discharge, but slower mean speed the load size is more unified in the cross section of the river, and delivers relatively less sandy sediment. We conclude that like other plane rivers (Tisza, Maros) average size of suspension river load decrease with the elevation of water level.

During the sediment-petrography measurements, minerals greater then 2. 75 specific gravity were separated by bromophormic procedure. The suspension loads of the river can be distinguished by the light (95-99%) and heavy (1-5%) fraction of minerals. In the samples from the White Körös the heavy fraction minerals are the following: pyroxene , hyperstene (30%), brown amphibole (25%), hematite-magnetite-ilmenite (13%), augite (7%), green amphibole (7%), and garnet (6%). The rest is made up by chlorite, biotite, epidote, rutil and limonite minerals. The most of the minerals remain in their original shape, which means that the time while the minerals take their way from the geological layers to Gyula is short, and there was no time for shaping. The amphiboles can be found in every flood. Their shape are columnar and less shaped. Brown and green version can be found either. Amphiboles are probably products of Neogene andesite volcanoes around Brad. Between the pyroxenes the hyperstene a general component with columnar shape. Sometimes its color changes to greenish. The quantity of iron-contain minerals (hematite, magnetite) is not significant, their shape are roundest. The monoclinic shape of augite can recognize easily. It is common in samples from flood. The heavy mineral content of the suspension load originates from decomposing the basic-intermediate rocks. That is indicated by the components mentioned above. The garnet are rare, they are spherical in shape, pink or colorless in color. The garnet is probably originated from the Crystal slate, granite belt at the origin of the river. The epidote and biotite are rare, and originate also from the Crystal belt (Bihar South). The quantity of the lighter specific gravity compounds (quartz, feldspar, mica) and clay granule) is much higher then heavy minerals. The quartz, feldspar, muscovite content are likely elevated in the summer samples. The feldspar are much less common, they are spherical in shape and hard to differentiate in microscope. They are supposed to be plagioclase. Calcium and chlorite can be found in the base material and hard to separate them. The most common mineral is the quartz. It is present in all flood samples and samples from lower level water also.

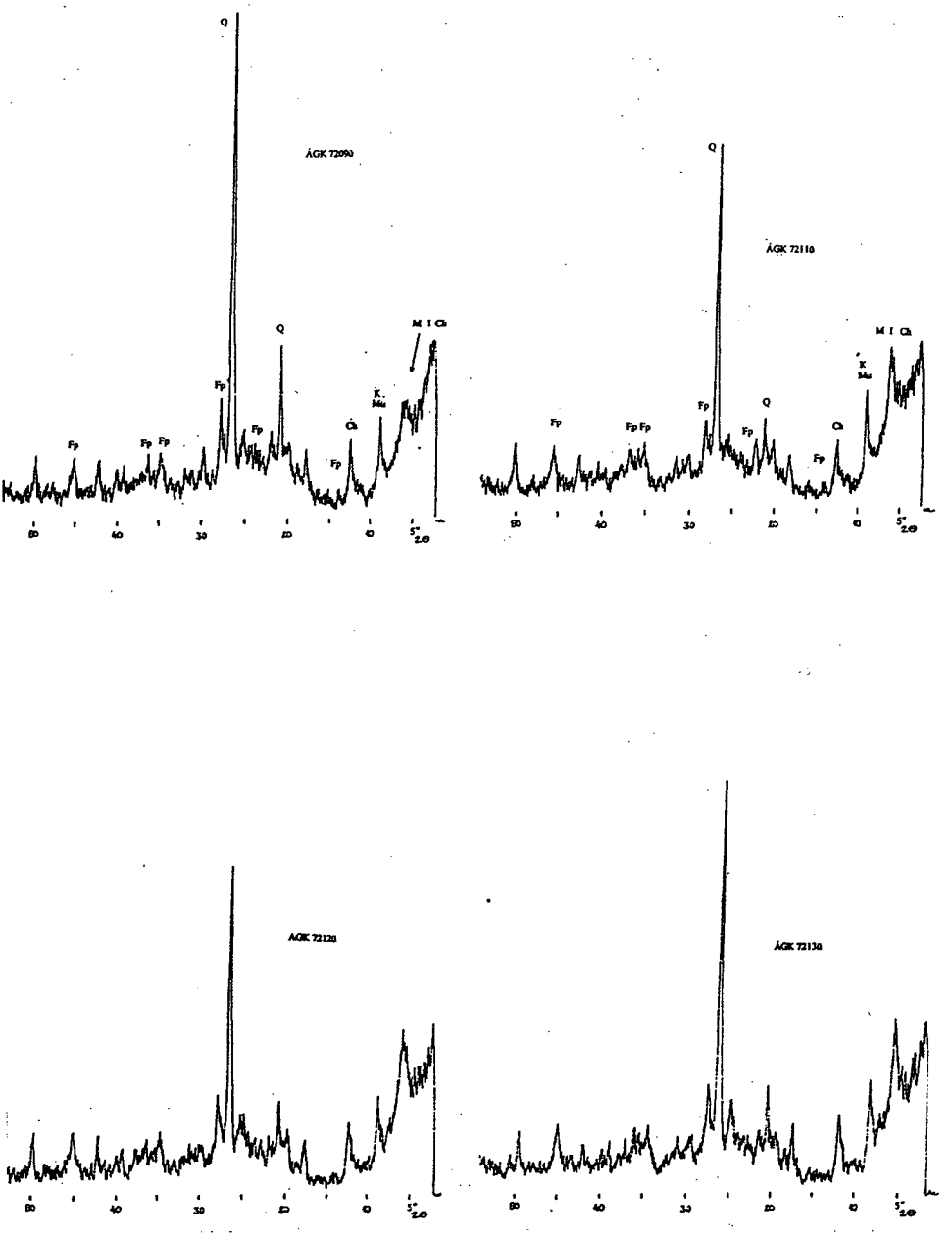

Fig. 2. X-ray difractograms (AGK 7209-7215) of the suspension load are reflect their mineral contents

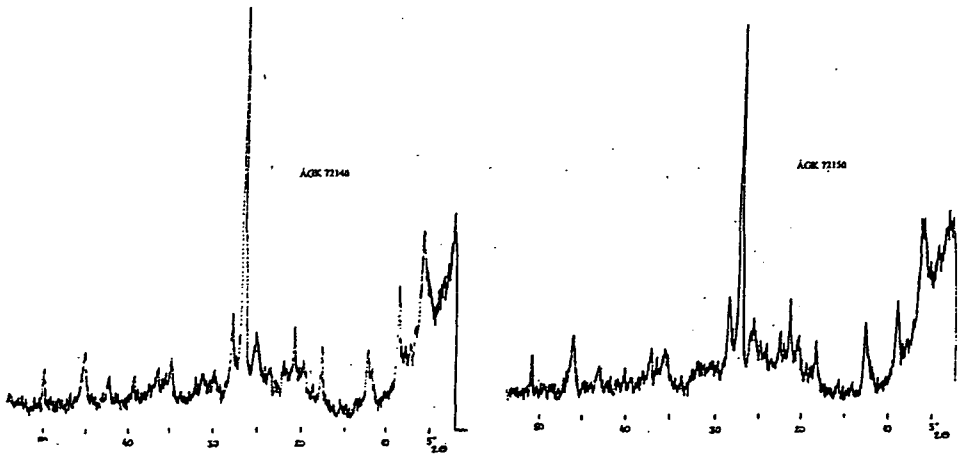

Fig. 2b.

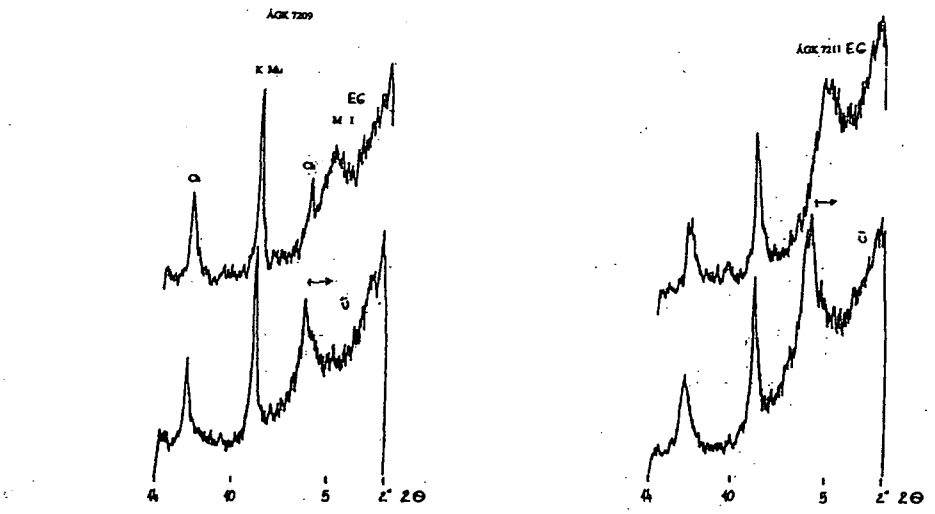

Fig. 3. X-ray difractograms shows the clay mineral fraction in normal case (AGK 7209) and shows the different clay minerals in ethylene-glycol case.

The x-ray difractograms of the suspension load are reflect their mineral contents well as shown in *Fig. 2*. Differences of the composition were found in spring samples (snow thaw 12 March, 2000) flood samples and summer flood samples (rainy flood). The summer sample AGK 7209 contains much more quartz and feldspar (approximately 1/3 more) then spring sample AGK 7211). However the contents of the clay-minerals smaller then 10 micron (between 5-10 on the 2 φ scale) (illite-montmorillonite-chlorite) is lower in the spring samples. Thus the x-ray difractograms shows that mineral composition of the

river does not change significantly in the summer and spring samples, but the quantity of the minerals is different. While the Q and Fp contents are higher in the summer flood samples, the proportion of clay mineral contents (I,M, Ch) is increased.

In the spring flood samples (March 12, 2000) we studied the load in the current throughout the deepness of the river. We analyzed 5 samples (AGK 7211-7215) in every meter from the surface to the river bed. Between the samples, the Q contents show small differences, but no conclusion can be drawn from the mineral composition. The Fp and clay mineral part are almost the same too. The x-ray difractograms of the samples indicate in the current of White Körös there is no differences in the composition of suspension load in the upper 5-6 meters of the water. Thus the composition of suspension load is relatively stable.

We also examined the clay-mineral fraction (size under 10 micron, from the fine silt to the fine clay). On the difractogam (scale 2 φ) the 14 and 7.08 peaks indicate chlorite (Ch), 9.96 peak indicate muscovite, caolinite (K, Mu), 15.5 and 4.5 peaks indicate montmorillonite-illite (M,I) as shown on *Fig. 3*. The different clay minerals can be separated by ethylene-glycol (EG). Samples treated with EG, the muscovite chlorite and kaolin peaks are stable while the peaks of montmorillonite-illite are shifted. So the samples treated with ethylene-glycol the differences between the summer and spring load can be easily recognized. While in the summer samples concentration of chlorite and muscovite is higher and illite-montmorillonite is lower, in the spring samples contain mainly montmorillonite-illite and lower concentrations of muscovite and chlorite.

The chemical elements of the load were analyzed by energy-disperse x-ray methods (*Fig 4.*). In the summer samples (7209) the concentration of SI, Fe are higher and K, Ca, Ti, Mn are lower then in the spring samples (7211). In the sample 7211 and 7215 the distribution of the elements are difference. When the Si concentration is higher the K, Ca, Ti is lower and vica versa. The Fe and Ca concentration is high constantly. The trace elements are pushed into the background. The levels of Rb, Sr, Y, Zn are negligible. However in the 7214 sample we detected low concentrations of Si, K and Ca and high levels Ti, Fe, Cu, Cuβ and Sr. It is likely that a mineral particle with high concentration of Ti, Cu and Sr was detected by chance. The differences between the main and trace element of summer spring samples caused by alteration of minerals in the suspension load.

During the spring thaw of the snow the continuos erosion deliver enormous amount of rubble from the catchment area. Since the upper and middle reaches, the river runs through mainly basic-intermediate rock-layer (Neogene andesite: around Brád and Honctő-Borosjenő), the composition of minerals, main and trace elements reflects composition of this area. During the continuos physical chopping minerals from heavy mineral containing rock are released into the load of the river. This phoneme course higher Ti, Fe, Cn, K, Ca (amphibole, pyroxene, biotite) in spring. Flood caused by summer rainfall does not reflect the composition of andesite-rich area. Because the river is short and low number of bend low amount of rain can course flood in the plane. The sudden rain can elevate the water levels in streams and river, but does not result such a hard physical chopping then ice, snow and water in winter. So the river delivers less primer load. The fast water stirs up the sandy river bed and wash its sediment from the bank. This is indicated by the composition of sandy, high levels of Q and Fp in the summer samples.

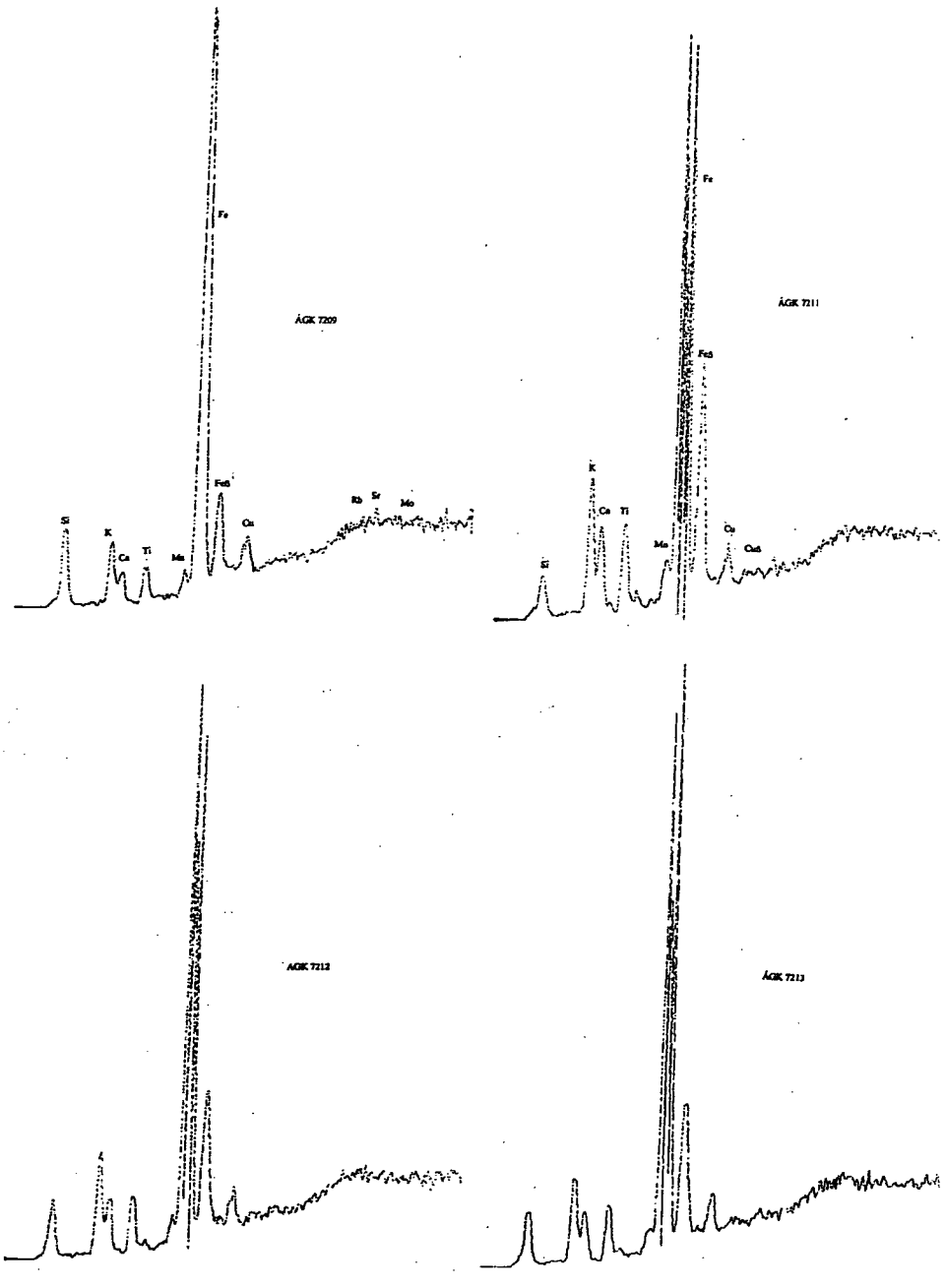

Fig. 4a. The chemical elements of the load (AGK 7209-7215) were analyzed by energy-disperse x-ray methods

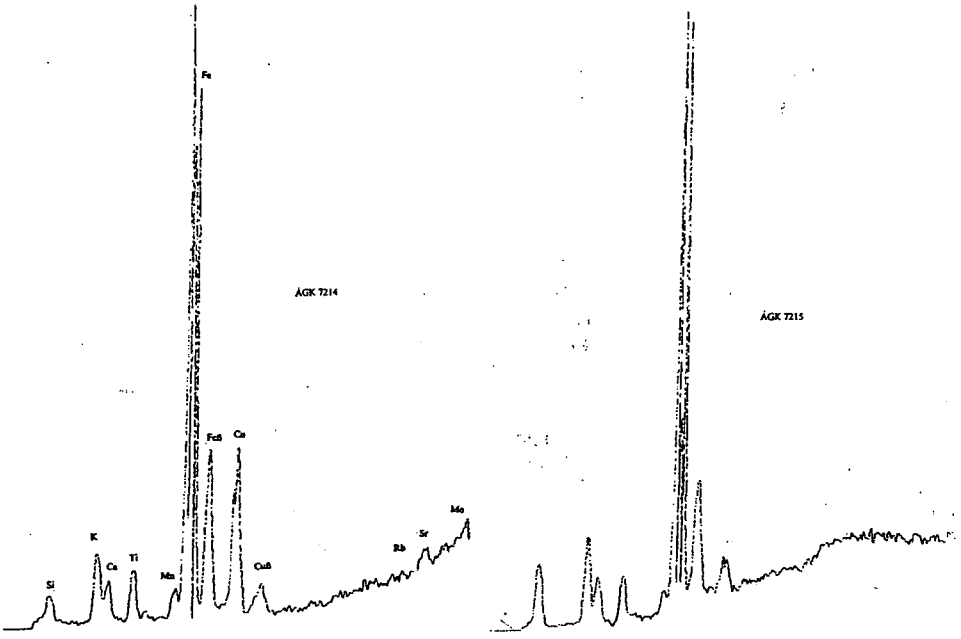

Fig. 4b

SUMMARY

From the study of the suspension load of the White Körös can be concluded that the river deliver relatively constant alluvial deposits either in the spring and summer. The highest levels of flapping contents was at the summer flood (1999): 13763.93 g/s. Calculating this to one year (with the same discharge) it delivers 434059296.5 kg alluvial deposits, which far less then the average discharge of river Maros (715236480 kg in 1951, MEZŐSI) or river Tisza (7978608000 kg in 1936, MIHÁLTZ) Thus the White Körös is not saturated even at highest discharge. The size of the suspension load is decreased parallel to the water level. In the samples the heavy minerals are the following: pyroxene (hyperstene), brown amphibole, hematite, magnetit-ilmetit, muscovite, augit, green amphibole and garnet. The minerals can be found in their original shape, which means that the speed of the transfer from the original geological layer to Gyula is fast and there was no time to reshape. The x-ray difractogram indicates that the mineral compositions do not change in the summer and spring samples, just the quantity of the minerals are different. While in the summer flood samples contains more Q and Fp, the in the spring samples the concentrations of clay minerals are (I, M, Ch) are higher. In the current of the river, in the upper 5-6 meters there is no significant differences in the mineral composites of suspension load. So the vertical composition of the load is identical. In the suspension load andesite can be found which probably product of the Neogene andesite volcano of Brad. The lower content of garnet-epidot-biotit complex originate from Crystal slate and granite of the source of the river (Bihar South).

ACKNOWLEDGMENT

This work was supported by Bolyai János research grant. I thank the Department of Mineralogy Geochemistry and Petrology and the Hydrology Institute of Gyula for their help in my work.

REFERENCES

BOGÁRDI J.(1955): A hordalékmozgás elmélete

GEDEONNÉ RAJETZKY M. (1973): Fosszilis folyóvízi üledékek mikromineralógiai spektrumának értelmezése recens hordalékvizsgálatok alapján. Földtani Közlöny.103.

MEZŐSI J., DONÁTH É.(1952): A Maros és Tisza lebegtetett hordalékának ásványtani és vegyi vizsgálata. Acta Mineralogica, Petrographica. Tomus V.

MEZŐSI J., DONÁTH É. (1954): A Tisza és Maros oldott és lebegtetett anyagának vizsgálata. Hidrológiai Közlöny. 34.

MIHÁLTZ I. (1938): A Tisza lebegő és oldott hordaléka Szegednél. Hidrológiai Közlöny. XVIII.

NAGY L. (1958): A Román Népköztársaság Földtana I-II.

PETHŐ GY. (1887): Fehér Körös. MÁFI 56-85.

SCHICK K. (1933): A Tisza , Körös, Maros, Zagyva vizeinek elemzése. Hidrológiai Közlöny

VITUKI (1956): Magyarország Hidrológiai Atlasza I.Folyóink vízgyûjtője 6:A Körösök.. Bp.

Manuscript received: 2. Sep. 2000.

Acta Mineralogica-Petrographica, Szeged, XLI, 129–140, 2000

THE RADIOACTIVE ELEMENT CONTENT OF LAKE MUD OF SEVERAL HYPERSALINE LAKES OF THE DANUBE-TISZA INTERFLUVE, SOUTH HUNGARY

T. SZEDERKÉNYI*, E. PÁL MOLNÁR*, B. KÓBOR*

Department of Mineralogy, Geochemistry an Petrology, University of Szeged

ABSTRACT

According to sparse samples, the radioactivity of young sediments of some lakes on the Danube-Tisza Interfluve was remarkably high compared to that of their environment and the average of such formations. Many of these lakes are utilized by tourism and fisheries, that is why it is important to examine how reliable the results of previous measurements are.

We have performed in situ and laboratory analyses on two typical lakes. Our aim was to determine the degree of radiation and the areal distribution of the radioactive element content in their sediment.

INTRODUCTION

In 1985 analyses of eutrophication on the Vadkerti Lake, Soltvadkert, Hungary, revealed several times occasionally an order higher radioactivity in case of some samples (mainly from areas covered by reeds) originating from the thick, organic matter rich mud layer of the bottom than that of the background value (KEDVES, SZEDERKÉNYI 1985, 1987). Based on preliminary analyses, the radioactive element content was believed to be in correlation with the decaying vegetal debris and the pollen content. Trial analyses on some other hypersaline lakes have reinforced these results.

The two lakes which were chosen to examine more detailed regarding radiological features, the permanent Vadkerti Lake (Soltvadkert) and the temporary Kolon Lake (Izsák) are located on the blown sand covered Danube-Tisza Interfluve, where in the lakes, according to MOLNÁR (1980), in an alkali environment hypersaline carbonate formation takes place. This process is characteristic in the first place in case of the bottom of the Kolon Lake, which is covered by water temporarily. A more than 0.5 m thick sediment with a fairly rich carbonate content can be observed some 10 cm under the muddy-sandy water of the lake. Under this sediment a thick layer of blown sand can be found. In the Vadkerti Lake this carbonate-rich layer is thin and it can be observed only sporadically. Hidrodynamically, the basin of the Vadkerti Lake is a part of the territory dominated by ascending ground waters, consequently, it is filled with water permanently and there is even an outflow for the excess water (ERDÉLYI 1990). Years ago in the SW corner of the lake on the territory of the beach the lake mud was dredged.

* H-6701 Szeged, P. O. Box 651, Hungary

METHODS

Double samples were collected from each point of sampling with an instrument constructed especially for this occasion. One of the samples was taken from the surface of the bottom, the other was collected from a position 40-50 cm deeper. Samples were collected from points 25 m far from each other along the longitudinal and the cross axis of the lake by divers due to the 1.4-3.0 m depth of the water. Since the past two years have brought a rainy weather the basin of the temporary Kolon Lake was pretty full, therefore, only its shores could be handled as areas of periodic water cover, and sampling was restricted to these areas. In all, 75 samples were collected from the two sites. The samples weighting 1-2.5 kg were dried on free air, then 800 g of each was ground to a grain size of 100 μ. Measures were performed on samples processed like above.

For the laboratory radiometry NP-424P, four channelled, nuclear spectrometer, ND-424L scintillation detector, NZ-490 lead tower, and Marinelli bowl were used. In case of every 10th sample a control measure was performed at the Mecsekurán Ltd. Deviations remained under 5%.

Field measurements were carried out with an NC-483, portable, nuclear analyzer equipped with an ND-493 scintillation detector. Field measurements were made only in the narrow shore zone of the Kolon Lake, because the currently high level of water did not allow other possibilities. Field measurements provided less information than those made in laboratory, therefore, the results of these will not be published.

DISCUSSION

Based on the gamma spectrometric analysis of the specific activity and the U, Th and K concentrations of the samples (*Fig.1.*) taken from the Vadkerti Lake's (Soltvadkert) North-South and West-East cross-sections, the following statements can be made:

A) The mean specific activity of the so-called lower samples, collected from under the mud along the N-S cross-section is 45.38 Bq/kg. The variation of results is considerable, the minimum value is 16.78 Bq/kg, the maximum is 114.31 Bq/kg. The summed gamma values increase northward along the profile (*Fig. 2.*). The only exception is the local anomaly – reason is unknown yet – in sampling point 2. The specific activity of upper samples (71.13 Bq/kg in average) which were collected along the same axis but from the bottom of the lake exceeded that of lower samples in almost all cases, nevertheless, their organic material content was generally higher, too. The minimum of specific activity in their case is 22.95 Bq/kg, while the maximum is 215.82 Bq/kg, and there is a significant increase in the values along the profile toward the North. At the border of the dredged area and the vegetated water surface the value of specific activity increased by one and a half times in average. Parallely with the northward increase of specific activity the concentration of U to some extent also increases. Similarly to the value of specific activity a remarkable change can be detected in U concentration at the border of the dredged area with open water surface and the vegetated area with higher organic material content.

The U concentration values of lower samples are lower than that of upper samples: 1.82 and 2.01 g/t in average. These average U concentrations correspond to that of the average of arenaceous-argillaceous-carbonate sediments. Results are quite disperse in value (lower samples: 0.58-3.83 g/t, upper samples: 0.45-4.03 g/t), real difference can only be experienced in the number of samples with high U concentration, which is higher in case of the upper sequence (*Fig. 3.*).

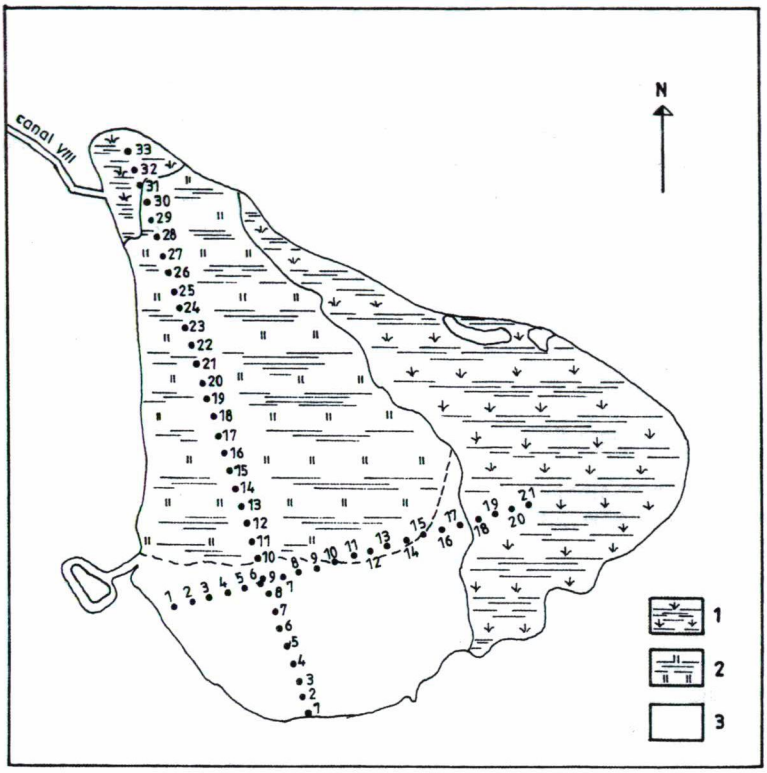

Fig. 1. Vadkerti Lake, sampling points per 25 m (M: 1:7500)

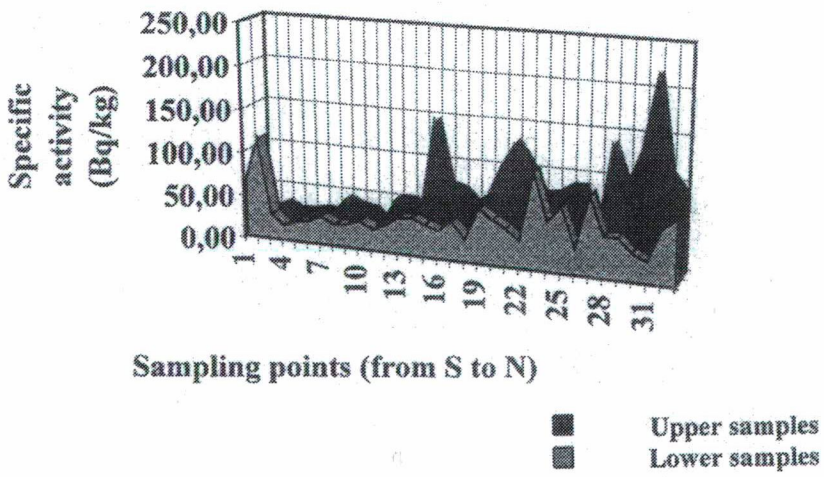

Fig. 2. Soltvadkert, S-N profile, specific activity (Bq/kg)

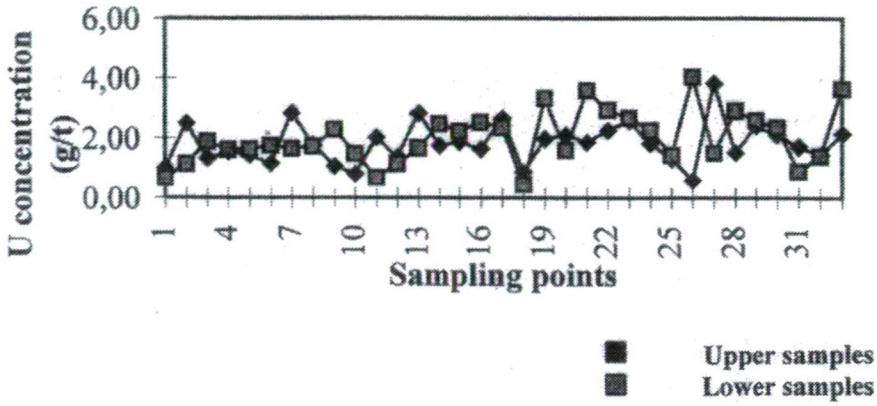

Fig. 3 Soltvadkert, S-N profile, U concentration (g/t)

The Th concentration along the N-S section is quite balanced. Only the upper sequence shows an increasing tendency of concentration from sample No. 10 northward, at the same time the Th concentration of lower samples is practically constant. The mean Th concentration of upper samples (rich in organic material) is almost twice as much (3.29 g/t) than that of lower ones (1.73 g/t). To explain this tendency further researches would need. Similarly, more thorough examinations might throw light on the unusually high Th concentration of the 2nd sampling point's lower sample (11 g/t) which is perhaps responsible for the relatively high specific activity (*Fig. 4.*) of this sample.

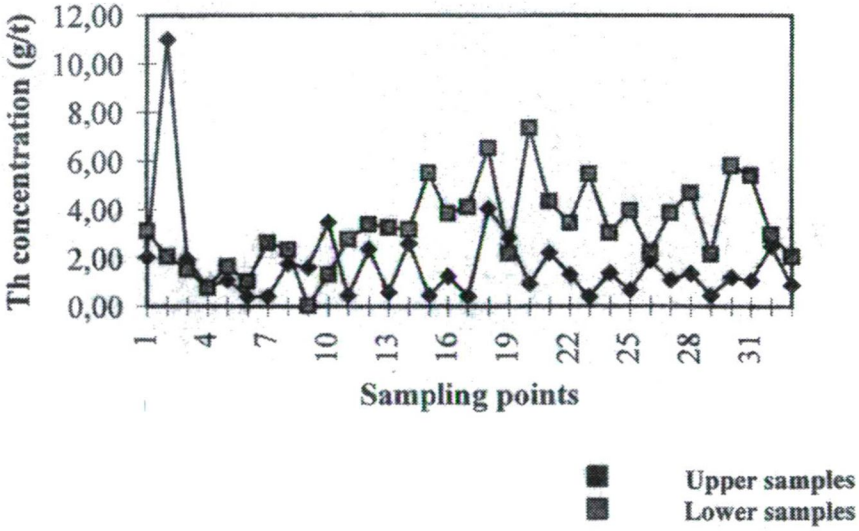

Fig. 4 Soltvadkert, S-N profile, Th concentration(g/t)

The mean K concentration of samples along the N-S axis corresponds well to the mean K concentration of feldspar-poor calcareous-argillaceous marly sediments. There is no considerable difference between the K concentration of lower and upper sequences (0.86 and 0.78 g/t), and no real tendency can be defined along the section either. Disregarding some extreme results the values vary between 0.6 and 1.1 g/t. No significant changes were detected at the border of areas of high and low organic material content (*Fig. 5.*).

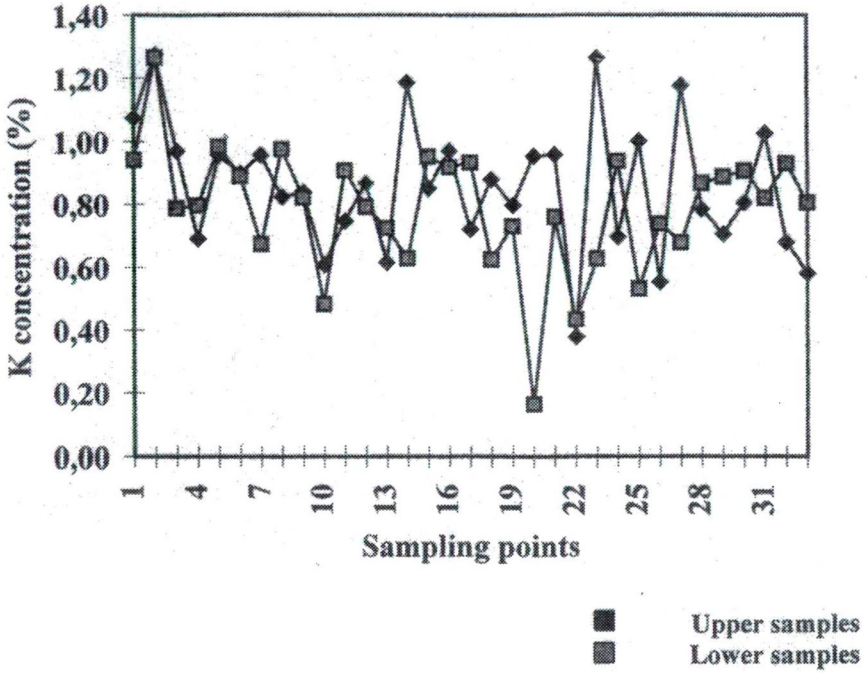

Fig. 5. Soltvadkert, S-N profile, K concentration(%)

B) Regarding the samples of the W-E profile of the Vadkerti Lake also the upper samples show the higher specific activity (49.99 Bq/kg in average), the lower samples' specific activity is slightly lower (37.14 Bq/kg). The axis of sampling mostly ran along the border of the opened and the vegetated water surfaces, that is why from the West to the East till the sampling point No. 15 the variation of specific activity is relatively low, and the upper samples originating from the dredged bottom provided low values as well. The specific activity of the upper sequence booms (maximum: 180 Bq/kg) at areas of high organic material content, i.e. areas of rich vegetation, reeds. Although by lower values, lower samples follow this tendency too (*Fig. 6.*).

Along the W-E profile the samples' mean U concentration is 1.73 and 1.88 g/t in average (*Fig. 5.*). Samples from the dredged zone (samples No.1-5) can be characterized with a lower concentration, while those originating from the vegetated zone – both the lower and the upper sequence – have a slightly higher U concentration. Samples from areas of rich vegetation have a remarkably high U concentration (maximum: 4.20 g/t) (*Fig. 7.*).

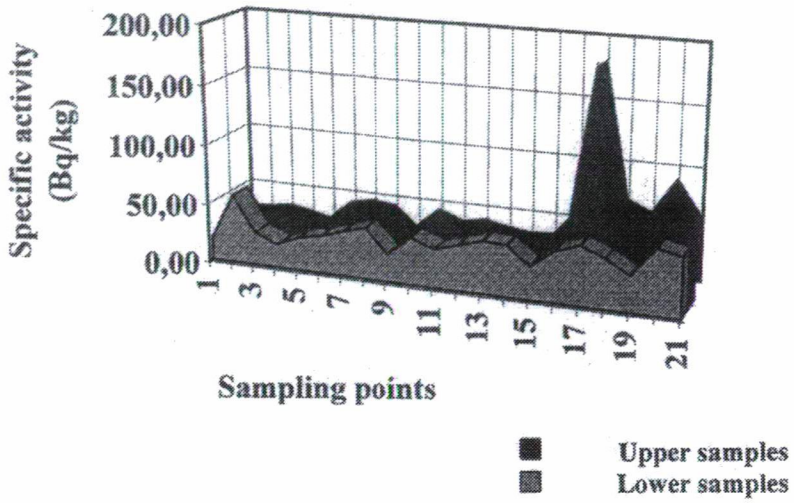

Fig. 6 Soltvadkert, W-E profile, specific activity (Bq/kg)

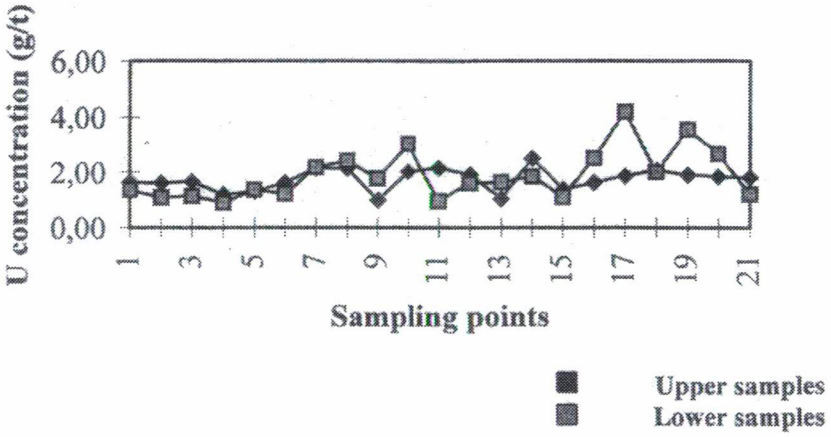

Fig. 7 Soltvadkert, W-E profile, U concentration(g/t)

The Th concentration also increases along the profile eastward, though, this tendency is striking only in case of the upper sequence, the Th distribution of lower samples can be regarded even. (The Th concentration is at its maximum at the edge of reeds: 3.5-3.8 %.) The Th content of the lower sample in sampling point No. 2 – similarly to sampling point No. 2 of the N-S axis – is remarkably high (4.1 g/t). Further examinations would need to determine whether there is a connection between these two anomalies, and whether there is a higher concentration of Th everywhere in the 25-30 m zone of the beach (*Fig. 8.*).

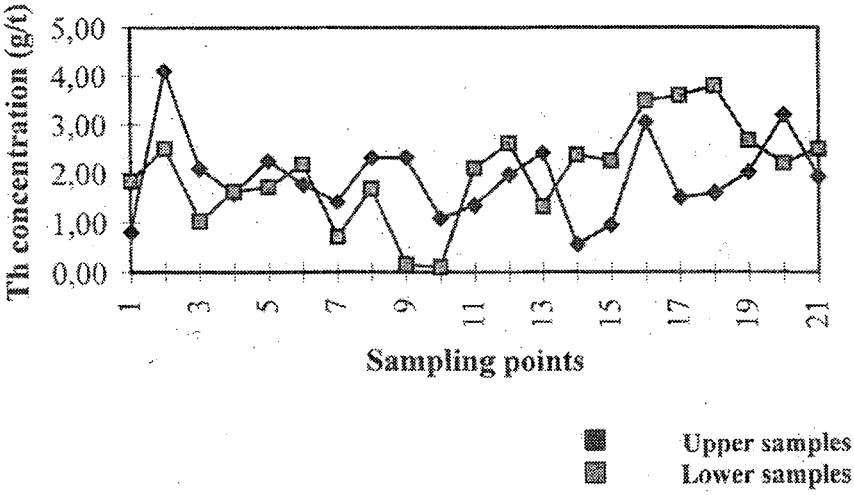

Fig. 8 Soltvadkert, W-E profile, Th concentration(g/t)

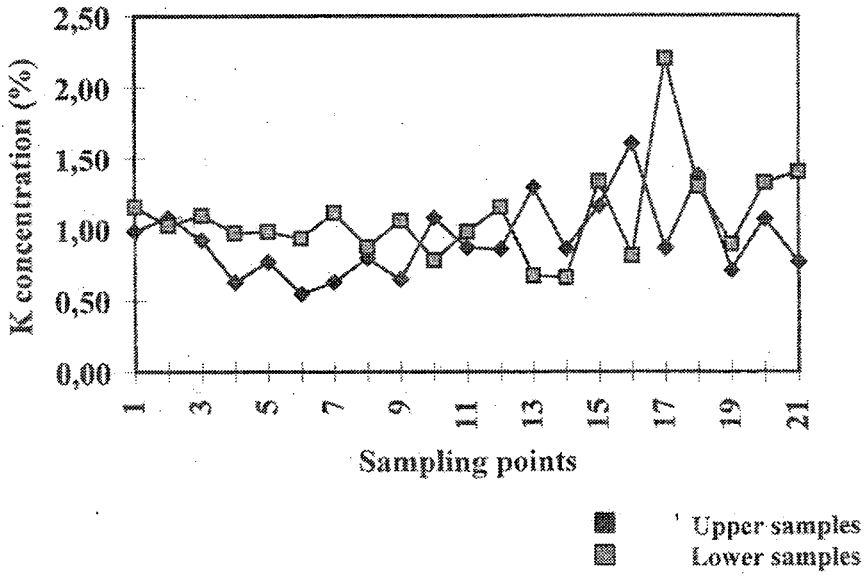

Fig. 9 Soltvadkert, W-E profile, K concentration(%)

The concentration of K along the W-E section is relatively even (mean value of lower samples: 0.93 g/t, of upper samples: 1.08 g/t). To the East the dispersion of values increase (*Fig. 9.*).

The area related mean concentration of radioactive elements are presented in Table 1., 2. and 3. and on *Fig. 10.*

TABLE 1

The mean values of radioactive elements in the samples collected from the SW part of the Vadkerti Lake, Soltvadkert (based on 16 samples)

Samples	U (g/t)				Th (g/t)				K (%)			
	min.	max.	mean	disp.	min.	max.	mean	disp.	min.	max.	mean	disp.
Lower samples	1,0	2,84	1,67	1,84	0,4	11	2,24	10,6	0,54	1,28	0,87	0,74
Upper samples	0,66	2,41	1,48	1,75	0,71	3,14	1,79	2,43	0,67	1,27	0,97	0,6

TABLE 2

The mean values of radioactive elements in the samples collected from the middle part of the Vadkerti Lake, Soltvadkert (based on 12 samples)

Samples	U (g/t)				Th (g/t)				K (%)			
	min.	max.	mean	disp.	min.	max.	mean	disp.	min.	max.	mean	disp.
Lower samples	0,8	2,83	1,7	2,03	0,46	3,5	1,63	3,04	0,61	1,19	0,85	0,58
Upper samples	0,67	3,01	1,81	2,34	0,02	5,53	2,32	5,51	0,48	1,15	0,85	0,67

TABLE 3

The mean values of radioactive elements in the samples collected from the NW, N, E part of the Vadkerti Lake, Soltvadkert (based on 26 samples)

Samples	U (g/t)				Th (g/t)				K (%)			
	min.	max.	mean	disp.	min.	max.	mean	disp.	min.	max.	mean	disp.
Lower samples	0,58	3,83		3,25								
Upper samples	0,45	4,2		3,75								

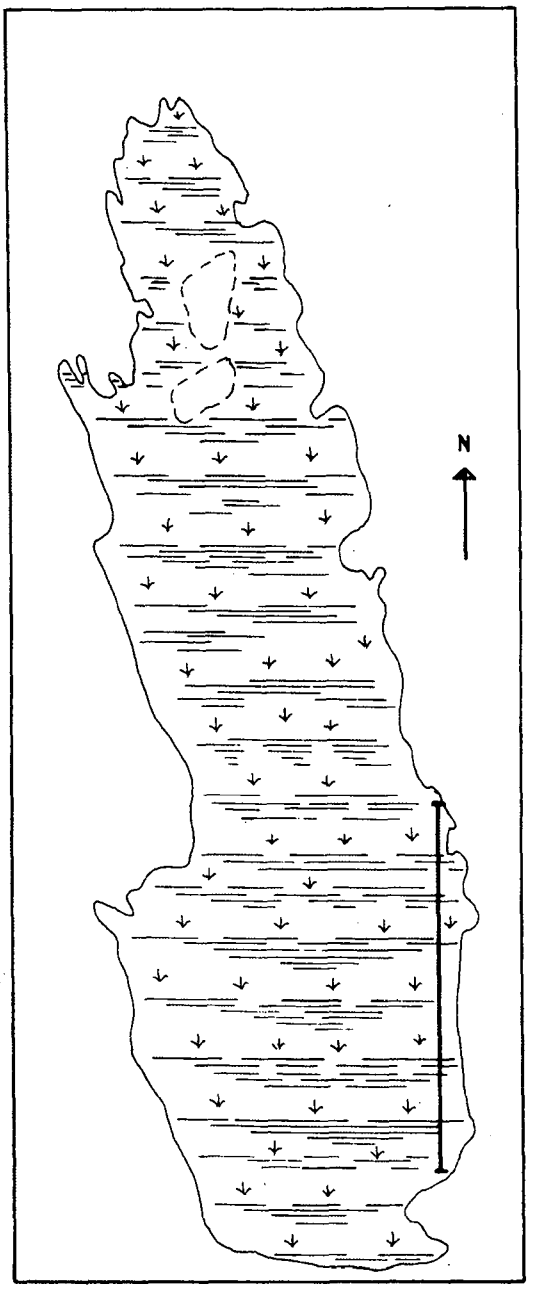

Fig. 10. Kolon Lake ——————— sampling profile (M: 1:15.000)

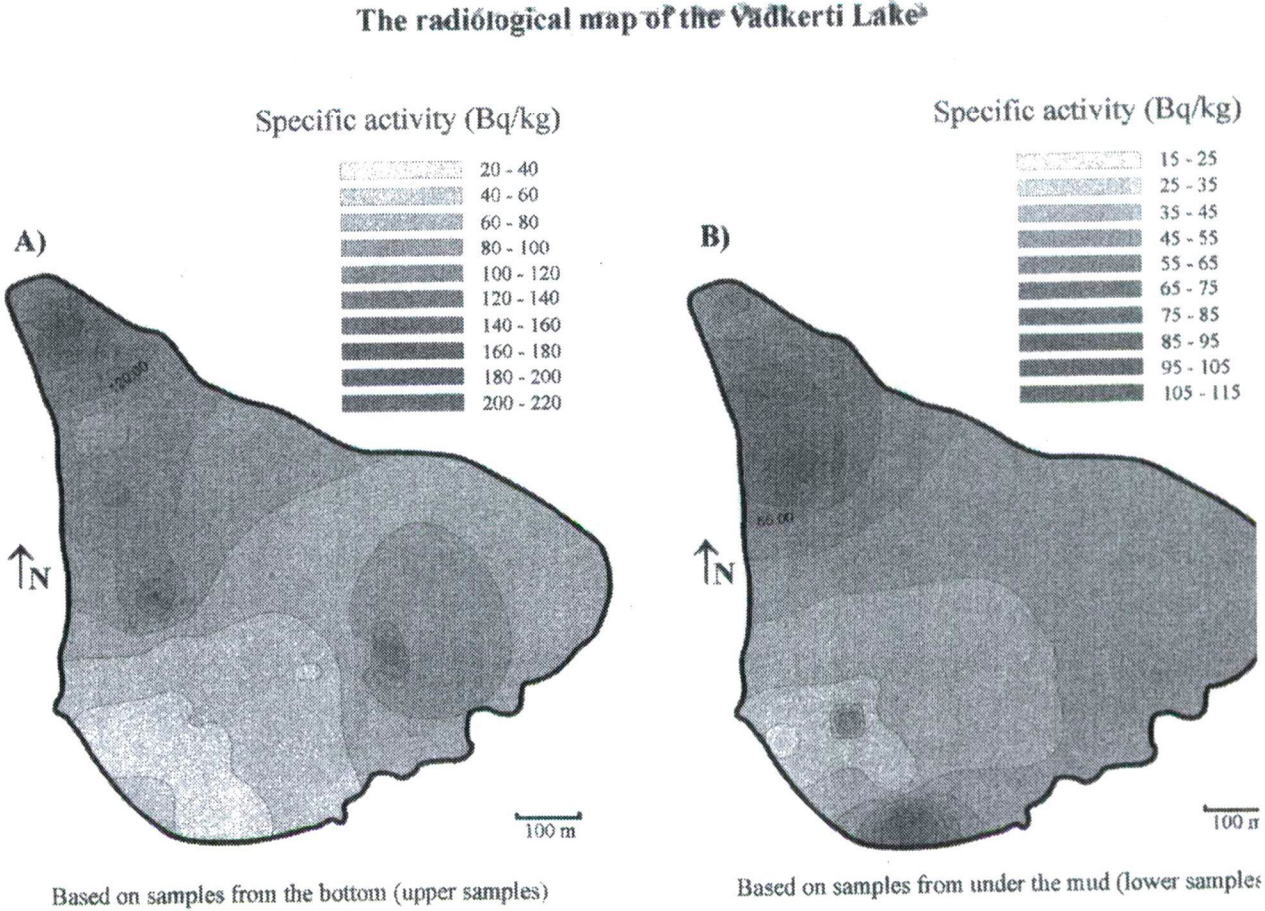

Fig. 11 Radiological map of Vadkerti Lake

Since in the case of the Kolon Lake the samples (*Fig. 11.*) were collected along the present shore line their radiological results are monotonous. Surface samples have a higher activity but it is slightly lower than the similar data of the Vadkerti Lake. Deeper level samples have also a lower activity than the corresponding Vadkerti results, thus, it is characteristic that the radioactive element content of surface samples is higher than that of samples from a deeper position. The reason of this character is explained by the difference in carbonate content. Samples under the surface represent organic material poor carbonate sediments characterized by low activity. Both in case of the surface and the deeper level samples it is characteristic in the Kolon Lake as well as in the Vadkerti Lake that the U concentration exceeds the Th concentration (Table 4.).

TABLE 4

The mean values of radioactive elements in the samples of the shore section of the Kolon Lake, Izsák (based on 21 samples)

Samples	U (g/t)				Th (g/t)				K (%)			
	min.	max.	mean	disp	min.	max.	mean	disp	min.	max.	mean	disp
Surface	0,8	2,34	1,56	3,2	0,78	2,48	1,5	3,42	1,02	1,38	1,18	2,26
40cm depth	0,92	1,87	1,17	2,8	0,8	1,77	1,21	2,78	0,6	0,88	0,7	1,76

CONCLUSIONS

The essential result of this research is that it has been proved that in the mud of hypersaline lakes of the southern part of the Danube-Tisza Interfluve even 4-5 times higher U and Th concentrations can be detected than that of the formational average. On the other hand, an order or much higher concentrations have not been found. Nevertheless, because of the fact that these lakes are actively used by tourism (beaches) and fisheries, dosimetric analyses seem to be necessary.

Th and U are bound to organic material and clay minerals, thus, their amount is in direct proportion to the amount of these components.

In the mud of hypersaline lakes the Th/U ratio is mainly dominated by the U, which fact has not been explained yet. Probably, ascending ground waters transport U here in a dissolved form.

Based on our researches at the two typical lakes, we suggest that the radiological analysis of the sediments of lakes, temporarily water covered areas, dead and outflowing waterflows which are located on the territory influenced by the ascending waters of the deep hydrodinamic water system would be important. According to the results of this research, on the above mentioned territory there is a real chance for the formation of much higher radioactive element concentration than those we have detected currently.

ACKNOWLEDGEMENT

This work has been supported by the AKP (No. 97 -144.).

REFERENCES

ERDÉLYI, M. (1990): The hydrogeology of arsenic artesian waters of the Transtisza Region (A tiszántúli arzénes rétegvizek hidrogeológiája). In: SZAB kiadványai 1990., 71-86. Szeged.

KEDVES, M., SZEDERKÉNYI, T. (1985): The importance of the spore-pollen investigations in the recognition of the radioactive element content of the lake mud. Acta Biol. Szeged. 31, 215-216

KEDVES, M., SZEDERKÉNYI, T. (1987): Importance of sporomorph-pollen investigations in the detection of radioactive elements (U, Th, Ra) of lucustrine mud. Acta Biol. Ac. Sci. Hung. 36, 45-48.

MOLNÁR, B. (1980): Hypersaline dolomite formation on the Danube Tisza Interfluve (Hiperszalin tavi dolomitképzõdés a Duna-Tisza közén). Földt. Közl. 110, 45-64.

Manuscript received: 16. Nov. 1999.

Acta Mineralogica-Petrographica, Szeged, XLI, 141–145, 2000

THE MINERAL COMPOSITION OF LAKE MUD IN SEVERAL HYPERSALINE LAKES OF THE DANUBE-TISZA INTERFLUVE, SOUTH HUNGARY

T. SZEDERKÉNYI*, E. PÁL MOLNÁR*, Á. BERTALAN*, B. KÓBOR*

Department of Mineralogy, Geochemistry an Petrology, University of Szeged

ABSTRACT

The radioactivity of young sediments of some lakes on the Danube-Tisza Interfluve is remarkably high compared to their environment. We have performed X-ray diffractional and bulk chemistry analyses on two typical examples to determine their mineral composition and major element content, and to examine how close the relation between the radioactive element content and the mineral composition of the lake mud is.

We have found that the boundaries of radioactive element rich areas are in accordance with the changes in mineral composition. Thus, mineral composition is also responsible for radiological conditions. In both lakes the mineral set originates from the break down of rocks of granitoid composition.

INTRODUCTION

The two lakes which were chosen to examine more detailed regarding radiological features, the permanent Vadkerti Lake (Soltvadkert) and the temporary Kolon Lake (Izsák) are located on the blown sand covered Danube-Tisza Interfluve, where in the lakes, according to MOLNÁR (1980), in an alkali environment hypersaline carbonate formation takes place. This process is characteristic in the first place in case of the bottom of the Kolon Lake, which is covered by water temporarily. Here a more than 0.5 m thick sediment with a carbonate content higher than 50% can be observed some 10 cm under the muddy-sandy water of the lake. Under this sediment blown sand can be found. In case of the Vadkerti Lake this carbonate-rich layer is thin and it can be observed only in some places. Hidrodinamically, the basin of the Vadkerti Lake is a part of the territory dominated by ascending ground waters, therefore, it is filled with water permanently and there is even an outflow for the excess water (ERDÉLYI, 1990). Years ago in the SW corner of the lake on the territory of the beach the lake mud was dredged.

METHODS

Two samples were collected from each points of sampling with an instrument constructed specially for this occasion. One of the samples was taken from the surface of

* H-6701 Szeged, P. O. Box 651, Hungary

the bottom, the other from beneath the surface from a depth of 40-50 cm. Samples were collected from points 25, 50 and 100 m far from each other along the longitudinal and the cross axis of the lakes, from under a 1.4-3.0 m deep water. Since the past two years have brought a rainy weather the basin of the temporary Kolon lake was pretty full, therefore, only its shores were handled as areas of periodic water cover, and sampling was restricted to these areas. In all, 75 samples were collected from the two sites.

Radiographs were taken with DRON-UM 1 diffractometer in a 3-63 degree 2θ angular field to determine mineral composition. The radiation source (Cu-tube) was operating with a LiF monochromator, with a 35 KV excitation voltage and with a 20 mA anode current. We appraised the results by measuring peak heights and peak areas with a software named Super Visor. All samples were X-rayed.

Since major element examinations have never been done yet in the case of these formations, we performed these examinations on the average samples of the two stratigraphic levels. Average samples were derived from samples of similar mineral composition on the basis of X-ray diffractional analyses. Bulk chemistry examinations were made in the Geological Institute of Hungary.

DISCUSSION

On the basis of radiographs, made of all collected samples, we could separate 7 mineral groups and as an eighth group an X-ray amorphous fraction due to both its quality and quantity features. Separated minerals (groups) are the following: dolomite, calcite, feldspar in general, quartz, kaolinite-chlorite, muscovite-illite, montmorillonite-chlorite and the amorphous fraction composed of ferrioxihidroxides, humin acids and vegetal debris.

The examined territories can be characterized both by the vertical and the horizontal spread of each mineral (group). Boundaries displayed by the mineral compositional changes correspond well to the boundaries drawn with the help of radiological analyses, i.e., mineral composition is also responsible for radiological conditions. Radiologically active components of the sediment are feldspars, clay minerals and the amorphous fraction.

The vertical difference between diffractionally measured sediment components is represented (with only a few exceptions) in all areas by the higher radioactive element content of samples collected from a deeper layer. The reason for this is the more compact form of deeper sediments than that of the mud of the bottom. According to mineral composition, the bottom of the Vadkerti Lake can be divided into three units. However, the ratio of minerals is not the same in different parts of these units:

a) The Vadkerti Lake has a characteristic floor of blown sand, thus, the dredged SW beach area can be separated easily from the blown sand floor by its higher quartz-content and by its unusually high feldspar-content. In the middle unit of the lake (have not been dredged) the major role of blown sand have remained. Areas North and East (mainly covered by reeds) of the previous unit differ in their higher clay mineral and amorphous fraction content. In the sediments, similarly to other hypersaline lakes of the Alföld region, carbonate minerals formed by evaporation processes are presented evenly in a 1:1 dolomite-calcite ratio. Nevertheless, the total carbonate-content is less than in the case of other hypersaline lakes. This can be explained with the temporal water exchange (outflow) of the Vadkerti Lake.

TABLE 1

Average mineral composition, based on X-ray diffractional analyses (in %)

Area			Sampling point	Dolomite	Calcite	Feldspar	Quartz	Chlorite, Kaolinite	Illite, Musco-vite	Montmoril-lonite Chlorite	Amor-phous
Vadkerti Lake (Soltvadkert)	**SW unit**	upper samples	16	7,5	6,4	5,0	69,9	0	5	0	7,2
		lower samples	16	7,8	7,0	5,5	71,9	0	3,2	0	4,6
	Middle unit	upper samples	12	7,3	6,6	6,5	65,6	0	4,4	0	9,6
		lower samples	12	7,6	7,2	4,8	72,5	0	3,0	0	4,9
	NW, N and E unit	upper samples	26	5,5	5,2	3,6	53,6	3,2	3,8	2,5	22,6
		lower samples	26	6,8	6,5	3,8	58,1	2,4	3,5	2,8	16,1
Kolon Lake (Izsák)		upper samples	21	19,3	10,6	2,2	51,1	0	3,7	2,7	10,4
		lower samples	21	33,5	17,1	2,8	34,5	0	1,8	1,6	8,7

Note: methods provided base data with 5% limit of errors, thus, there was no point in examining dispersion

b) Due to the rainy weather of the past two years, the basin of the temporal Kolón Lake is almost full of water. Thus, we could find areas of temporal water cover (still not flooded) only along a 2 km long section of the Eastern shore. That is why all measurements provided only linear, not areal results, and these hardly differ from each other in a mineralogical and radiological sense. However, a significant difference can be observed vertically in the sediments' carbonate-content. Under the soil level carbonate-rich sediments can be found, which, according to MOLNÁR (1980), is the result of hypersaline sediment formation under arid climate.

The major element content of average samples of the bottom sediments of each examined lakes is presented in Table 2. If the results are converted into a volatile-free form and the extreme carbonate-content is smoothed as well, then the major element composition of sediments of the Vadkerti Lake and the Kolon Lake is closest to that of very acidic granite.

TABLE 2

The mean major element content of examined sediments

Major Element	Vadkerti Lake		Kolon Lake	
	upper	lower	upper	lower
SiO_2	58,1	59,81	53,16	49,10
TiO_2	0,45	0,50	0,18	0,10
Al_2O_3	12,8	13,04	11,02	8,69
ΣFe_2O_3	3,22	3,32	1,82	1,10
MnO	0,05	0,05	0,04	0,04
MgO	2,16	2,20	3,82	9,96
CaO	4,54	4,55	7,29	8,77
Na_2O	3,18	3,30	2,64	3,16
K_2O	2,96	3,01	1,82	0,54
P_2O_5	0,08	0,09	0,05	0,15
Loss of Ignition	14,32	10,7	18,10	18,25
Σ	99,86	100,04	99,94	99,86

appraised by: ***Mrs Nagy I.***

We have found that the boundaries of radioactive element rich areas are the boundaries of mineral compositional changes at the same time. Namely, mineral composition is also responsible for radiological conditions. In both lakes the set of minerals originates from the break down of rocks of granitoid composition.

ACKNOWLEDGEMENTS

This work has been supported by the AKP (No. 97 -144.)

REFERENCES

ERDÉLYI, M. (1990): The hydrogeology of arsenic artesian waters of the Transtisza Region (A tiszántúli arzénes rétegvizek hidrogeológiája). In: SZAB kiadványai 1990., 71-86. Szeged.

KEDVES, M., SZEDERKÉNYI, T. (1985): The importance of the spore-pollen investigations in the recognition of the radioactive element content of the lake mud. Acta Biol. Szeged. 31, 215-216

KEDVES, M., SZEDERKÉNYI, T. (1987): Importance of sporomorph-pollen investigations in the detection of radioactive elements (U, Th, Ra) of lucustrine mud. Acta Biol. Ac. Sci. Hung. 36, 45-48.

MOLNÁR, B. (1980): Hypersaline dolomite formation on the Danube Tisza Interfluve (Hiperszalin tavi dolomitképzõdés a Duna-Tisza közén). Földt. Közl. 110, 45-64.

Manuscript received: 10. Oct. 1999.

Acta Mineralogica-Petrographica, Szeged, XLI, 147–150, 2000

THE TRACE ELEMENT DISTRIBUTION OF LAKE MUD IN SEVERAL HYPERSALINE LAKES OF THE DANUBE-TISZA INTERFLUVE, SOUTH HUNGARY

T. SZEDERKÉNYI*, E. PÁL MOLNÁR*, Á. BERTALAN*, B. KÓBOR*

Department of Mineralogy, Geochemistry an Petrology, University of Szeged

ABSTRACT

Trace element analyses on the sediments of the Vadkerti Lake and the Kolon Lake (southern part of the Danube Tisza Interfluve) have shown that the amount of certain trace elements is abnormally high. The Cu and the As content is several times higher than the allowed value, and the Pb content is just acceptable. These anomalies have anthropogene origin and they are the results of intensive grape and fruit cultivation in the region.

INTRODUCTION

The two lakes which were chosen to examine more detailed regarding radiological features, the permanent Vadkerti Lake (Soltvadkert) and the temporary Kolon Lake (Izsák) are located on the blown sand covered Danube-Tisza Interfluve, where in the lakes, according to MOLNÁR (1980), in an alkali environment hypersaline carbonate formation takes place. This process is characteristic in the first place in case of the bottom of the Kolon Lake, which is covered by water temporarily. Here a more than 0.5 m thick sediment with a carbonate content higher than 50% can be observed some 10 cm under the muddy-sandy water of the lake. Under this sediment blown sand can be found. In case of the Vadkerti Lake this carbonate-rich layer is thin and it can be observed only in some places. Hidrodinamically, the basin of the Vadkerti Lake is a part of the territory dominated by ascending ground waters, therefore, it is filled with water permanently and there is even an outflow for the excess water (ERDÉLYI, 1990). Years ago in the SW corner of the lake on the territory of the beach the lake mud was dredged.

METHODS

Two samples were collected from each points of sampling with an instrument constructed specially for this occasion. One of the samples was taken from the surface of the bottom, the other from beneath the surface from a depth of 40-50 cm. Samples were collected from points 25, 50 and 100 m far from each other along the longitudinal and the

* H-6701 Szeged, P. O. Box 651, Hungary

cross axis of the lake by divers due to the 1.4-3.0 m depth of the water. Since the past two years have brought a rainy weather the basin of the temporary Kolon lake was pretty full, therefore, only its shores could be handled as areas of periodic water cover, and sampling was restricted to these areas. 22 pairs of samples (44 samples in all) were collected from the four sites.

Radiographs were taken with an NZA-8500 X-ray analyzer in order to determine the samples' trace element content (Pb, Cu, Zn, As, Sr, Cd, Ag, Cr, Co, V, Zr, K, Ca, Ti, Fe). The Mo K radiation source operated with a 29 KV excitation voltage and with a 4 mA anode current. Measurements were performed in a He atmosphere of 0.1 mbar pressure from boric acidic pastilles weighing 500 mg, compacted with a 6 ton pressure. In order to receive more proper data the 13.5-16 KeV interval was remeasured under a 33 KV excitation voltage. XRF analysis was carried out on 62 samples in all. These measurements were verified in the Soil Science and Agrochemistry Institute of the Hungarian Academy of Sciences. Deviations stayed under 8%.

DISCUSSION

Table 1. presents the mean element-content of the 22 pairs of samples which can be chosen on the basis of the results of radiological and X-ray diffractional analyses. Based on the results of XRF examinations, we could not make areal distinctions regarding the mud of the two lakes. However, differences in trace element distribution of the two sampling levels is inevitable. Values of K and Ca concentrations correlate well to the mineral composition. Naturally, the amount of Sr follows precisely the changes of Ca concentration.

Regarding the base metal content of the sediments of the Vadkerti and the Kolon Lakes, the high amount of arsenic, copper, lead (and zinc) is striking. Compared to the concentrations determined by the MI-08-1735-1990 directive regarding arenaceous soils *the Cu and the As content is several times higher than the allowed value, and the Pb content is just acceptable.* These anomalies have antropogene origin and they are the results of intensive grape and fruit cultivation in the region. In the exact vicinity of the examined territories huge vineyards and fruit farms can be found.

CONCLUSIONS

In case of each area of examination the enrichment of Cu As and Pb in the sediment is several times higher than the threshold value. For the metal contamination the surrounding large scale vineyards and fruit farms are responsible.

Based on our researches at the two typical lakes, we suggest that the radiological analysis of the sediments of lakes, temporarily water covered areas, dead and outflowing waterflows which are located on the territory influenced by the ascending waters of the deep hydrodinamic water system would be important. According to the results of this research, on the above mentioned territory there is a real chance for the formation of much higher radioactive element concentrations than those we have detected currently.

TABLE 1

The mean trace element content of the four examined sites, data are based on XRF analyses

Site		sample	Min. Max. Mean	Pb	Cu	Zn	As	Sr	Cd	Ag	Cr	Co	V	Zr	K	Ca	Ti	Fe^{tot}
				ppm											%			
Vadkerti Lake	upper samples	14	min.	50	140	5	0	120	0	0	0	0	50	100	0,6	1,7	0,06	0,66
			max.	90	300	40	220	870	trace	trace	30	5	150	130	1,4	9,3	0,12	1,35
			mean	80	201	16	53	448	-	-	4	0,7	104	113	0,94	6,2	0,09	1,05
	lower samples	14	min.	45	130	5	0	170	0	0	0	0	55	105	0,7	1,8	0,09	0,8
			max.	100	240	50	170	670	trace	trace	25	5	155	135	1,2	9,0	0,2	1,36
			mean	71	191	14	39	398	-	-	3	0,7	110	118	0,95	5,5	0,11	1,13
Kolon Lake	upper samples	8	min.	7	22	4	0	150	0	0	0	0	50	90	0,45	4,3	0,01	0,88
			max.	46	100	45	80	920	0	0	8	0	130	135	1,15	10,6	0,1	2,56
			mean	12	85	17	46	560	-	-	2	-	102	121	0,78	7,5	0,05	1,13
	lower samples	8	min.	5	10	0	0	480	0	0	0	0	10	20	0,05	6,9	0	0,15
			max.	26	40	16	55	1250	0	0	0	0	75	84	0,53	14,6	0,01	0,56
			mean	7	23	10	18	855	-	-	-	-	27	33	0,32	12,8	-	0,38

ACKNOWLEDGEMENTS

This work has been supported by the AKP (No. 97 -144.)

REFERENCES

ERDÉLYI, M. (1990): The hydrogeology of arsenic artesian waters of the Transtisza Region (A tiszántúli arzénes rétegvizek hidrogeológiája). In: SZAB kiadványai 1990., 71-86. Szeged.

KEDVES, M., SZEDERKÉNYI, T. (1985): The importance of the spore-pollen investigations in the recognition of the radioactive element content of the lake mud. Acta Biol. Szeged. 31, 215-216

KEDVES, M., SZEDERKÉNYI, T. (1987): Importance of sporomorph-pollen investigations in the detection of radioactive elements (U, Th, Ra) of lucustrine mud. Acta Biol. Ac. Sci. Hung. 36, 45-48.

MOLNÁR, B. (1980): Hypersaline dolomite formation on the Danube Tisza Interfluve (Hiperszalin tavi dolomitképződés a Duna-Tisza közén). Földt. Közl. 110, 45-64.

Manuscript received: 10. Oct. 1999.

Acta Mineralogica-Petrographica, Szeged, XLI, 151–154, 2000

THE MEASURING METHODOLOGY OF EXCESS RADIOACTIVE LOAD CAUSED BY COAL MINING IN THE VICINITY OF PÉCS (MECSEK MTS. - HUNGARY)

B. KÓBOR*

Department of Mineralogy, Geochemistry and Petrology, University of Szeged

ABSTRACT

Beside several other harmful effects of coal mining on the environment (destroying landscape, dust and noise pollution), we must lay a great emphasis on dealing with its excess radioactive load as well, since it is widely known that some coal types have a remarkably high radioactive element content. In Hungary the coal of the Tatabánya Coalfield (ZETHNER, 1958), the Cretaceous coal of Ajka (BODROGI ET AL., 1959) and the Liassic coal of the Mecsek Mts. are of that character. It is getting to be necessary to develop a measuring methodology that can be authoritative in land reclamation plans, environmental geological surveys on other Hungarian territories with similar problems and that corresponds to the directives of the IAEA (International Atomic Energy Agency). This measuring system involves "in situ" and laboratory analyses, and as a result of this, beside the actual environmental impact analysis it provides further information on the geological setting of the territory. With an informative purpose we also publish the preliminary results of the measurements that are performed on the coalfields of the Mecsek Mts.

INTRODUCTION

In Pécs and in its vicinity as a result of coal mining, that started two hundred years ago, a great amount of waste material has been already extracted. The excess radioactive load of this waste on the people of the area has not been examined in every detail yet. The high radioactive element content of these coals and their wastes is well-known for a long time. High values can be explained by the uranium accumulating effect of organic material and by the granitoidic base level of the clastic, sedimental rocks of the coal formation (PÁL MOLNÁR et al., 1999). The mean uranium-content of previously examined Liassic coal samples is 25 g/t, but in case of clay shales 150-220 g/t values are not rare either (SZALAY et al., 1959). According to estimations, the coal mining in the Mecsek Mts. has raised the radioactivity of the surface of the area approximately by 60 % (VADOS et al., 1999).

We can receive a total view of the radioactivity of the environment only by measurements that last at least for a year, since several parameters (e.g. falling dust, radon exhalation, aerosol activity) significantly depend on the meteorological situation. Thus, measurements are of full value only if the examination of variable parameters is extended to a whole year period.

* H-6701 Szeged, P.O.Box 651, Hungary

DISCUSSION

"IN SITU" MEASUREMENTS

In order to be able to make comparisons we have carried out field measurements at three locations of different character: a still working open cast mine, a covered waste heap and a reclaimed waste heap. Nevertheless, we examined geologically different areas that are not involved in mining to determine threshold values characterizing the wider surroundings.

Gamma dosage intensity measurements

We examine the intensity of gamma rays, that has the greatest penetrating ability regarding components of radioactive radiation, independently from the energy of the radiation components. On the examined territory measurements are carried out in a grid of 25x25 m frequency, 1 m (standardized height) above the ground, for 12 sec, with an energy independent analyzer (Eberline E6000, equipped with a plastic scintillation measuring head)(SZEDERKÉNYI ET AL., 1994).

Mean values of dosage intensities exceed the Hungarian average by 15-20 % (87 nGy/h)(xxx, 1991). On reclaimed waste heaps 100-140 mean values, while on heaps that are not reclaimed and in case of active mines one and a half times higher values are expected.

Field measurements of gamma-spectrometry

Measurements of this kind help in determining the main radioactive element content - K, U(Ra), Th - of the soil among field circumstances. (Actually, instead of the U-content the Ra-content is determined, and by assuming a radioactive equilibrium the concentration of the mother element is countable.)

Elements and decay families mentioned above emit photons of different energy level, thus, by the selective dating of these, concentrations can be determined.

At the measurements in the vicinity of Pécs we apply a device that is in accordance with the IAEA standards. The device is operating with a four channeled analyzer (NK484P) and with a scintillation detector containing a NaI(Tl) crystal. Measurements are carried out in the same points as in the case of gamma dosage intensity measurements, they last for one minute, whilst the detector is placed on the ground. Results are averaged from three measures.

On the basis of measurements carried out so far, the radioactive element concentrations on the uncovered waste heaps of the examined territory are the following: Th: 18-35 ppm, U(Ra): 5-10ppm, K: 1.8-2.25%. On reclaimed heaps we have got 25 % lower results, still, these are often two times higher than the results of the wider surroundings.

Determination of ^{222}Rn concentration and exhalation

The ^{222}Rn-content of free air can be explained by the Rn production of decaying U in the soil. In case of an average concentration the activity is 1-20 Bq/m^3, though, it varies quickly and whimsically as soil types, hydrogeological and atmospherical features change (VADOS et al., 1999). In order to determine concentrations we apply a low background radiation device, operating with a passive diffusional chamber. The device measures Rn concentrations in every ten minutes due to quickly changing influencing factors.

During Rn exhalation analyses we measure the activity of ^{222}Rn that is exhaled through a given surface during a given time (mBq/m^2s). In an average situation the value of Rn

exhalation is 20-60 mBq/m^{2}s, however, due to the above mentioned factors there can be significant deviations.

Analysis of falling dust

Dust particles get back on the ground in a solid form or in the form of solution by precipitation. For measurements a funnel-shaped measuring bowl, that has a 0.5 m^2 opening and that is filled with distilled water, has to be placed at least in a 1.5 m height in a vegetation-free area. The sample, that is gained through a long collecting period (1-2 months), is put under gamma spectrometric analyses after evaporation and ignition. The measuring time is long (100-200 thousand sec) due to the small concentrations.

The analysis of the radioactivity of aerosols

Aerosols can easily enter the body, thus, they can be responsible for a large proportion of radioactive load on humans. On the basis of the measuring technique, the components affecting biological life can be divided into two groups:

- short term ^{222}Rn components
- long term alpha radiation components

After filtering out the aerosol-content of air with the adequate filter disk both groups can be determined. The radioactivity of components of quick decay has to be measured right after the preparing of the sample, while that of components of slow decay has to be measured after the required length of time.

LABORATORY MEASUREMENTS

Determination of specific activity and gamma-spectrometry of solid samples (coal, waste, soil)

The collection of samples, weighing 2 kg, is carried out in a grid of 25x25 m frequency in order to exclude significant deviations of point-like sampling that is caused by the inhomogenousness of waste heaps. After drying and grinding the collected samples are kept in a so called Merinelli-bowl to ensure their radioactive equilibrium. For measurements a highly sensitive scintillation detector that is attached to a NP424 analyzer is used (SZEDERKÉNYI et al., 1994). Results are values of radioactivity (Bq/kg) of the mass unit of a given sample.

On the basis of results received so far, on the coalfields of the Mecsek Mts. the mean specific activity of covering soils, sandstones - aleurolites and coals - coaly clays is 140-190, 180-190 and 220-380 Bq/kg, respectively.

Gamma spectrometric measurements are performed on samples prepared the same way as mentioned above with a multi-chanelled nuclear amplitude analyzer. These measurements on Mecsek samples have provided the following results:

- covering soils: U(Ra): 5-10 ppm, Th: 15-22 ppm, K: 1.8-2.2 %
- coals, coaly wastes: U(Ra): 13-18 ppm, Th: 12-38 ppm, K: 0.5-1.6 %

Analyses of specific beta radioactivity of plant samples

During the radiological examination of an area there is a good reason for analyzing plant samples, since the vegetation can easily absorb radioactive elements from the soil, water and air. It is important that the plant has to be collected after a year long growing period when it is fully developed. Samples collected from surfaces of the same size are washed an burnt to ashes. This is followed by the measurement of beta activity, which is expressed in ^{226}Ra equivalent.

REFERENCES

BODROGI, F., UPOR, E., VADOS, I. (1959): Zárójelentés az ajkai szénmedencében 1956-57. években végzett földtani és radiológiai kutató munkáléatokról. MÉV adattár, Kővágószőlős, J-0143.

PÁL MOLNÁR, E., VADOS, I., GERZSON, I., KÓBOR, B. (1999): Natural radioactiv element content of the old crystalline rocks in Southern Transdanubia (SW Hungary). Acta Miner.Petr., XL., 121-138. Szeged.

SZALAY, S., ALMÁSSY, GY., PESTY, L., LOVAS, I. (1959): Magyarország egyes fontosabb kőszénterületeinek átvizsgálása uránium nyomelőfordulás szempontjából. ATOMKI Közl., 1, 7.

SZEDERKÉNYI, T., PÁL MOLNÁR, E., VADOS, I.(1994): A radioaktivitás környezetvédelmi vonatkozásai, Egyetemi jegyzet, JATE, Szeged.

VADOS, I., VÁRHEGYI, A. (1999): Pécs-Nagybányarét tervezett külfejtési terület és környezete radiológiai vizsgálata. Jelentés a P.E. Rt. részére.

ZETHNER, GY. (1958): Jelentés az 1957. évben a tatabányai szénmedencében végzett radiológiai kutatásokról. MÉV Adattár, Kővágószőllős, J-0028.

xxx (1991): OSSKI. Tanulmány a MÉV külszini rekultivációja sugárvédelmi követelményeinek meghatározásáról, az ezzel kapcsolatos elméleti és gyakorlati feladatokról. Budapest.

Manuscript received: 10. Oct. 2000.

Acta Mineralogica-Petrographica, Szeged, XLI, 155–173, 2000

ON THE THERMODYNAMICS OF METEORITES AND PARENT BODIES III: BASALTIC ACHONDRITES IN AN INCREASING SiO_2 SEQUENCE AND COMPARISON OF THE ROLE OF DIOGENITES AND KOMATIITES IN PLANETARY EVOLUTION

SZ. BÉRCZI[1], Á. HOLBA[2] and B. LUKÁCS[2],

[1]Eötvös University, Faculty of Science, Department of G. Physics, and Dept. of Petrology and Geochemistry, Cosmic Materials Space Research Group
[2]Central Research Institute for Physics RMKI

ABSTRACT

After chondritic thermal metamorphism the thermal evolution of a primitive achondritic mineral assemblage continued by partial melting and outflow of the metal-sulfide components and of the low melting point basaltic components. Metal-sulfide assemblage migrated toward the center, basalt migrated toward the surface of the asteroidal parent body. In our paper the HED basaltic achondrites are arranged into a sequence by their increasing SiO_2 content: diogenites, howardites and eucrites. Comparing this sequence with that of terrestrial basalts of komatiites, picrites and tholeiitic basalts we found a similar bulk thermal evolution trend for them. We give an overview about both of these sequences as a long term planetary evolutionary differentiation sequences by inserting them into the thermal evolution of a solid body. General main trends in planetary differentiation are also discussed.

INTRODUCTION

During the last seven years our Cosmic Materials Space Research Group had excellent opportunities to study and compare different basalts and related rocks from the Solar System (BÉRCZI et al, 1997). Over the rich set of terrestrial basalts and andesites from both Hungary and from elsewhere on the Earth we had lunar basalts from the NASA Lunar Sample Thin Section Set, (12002, 12005, 70017 basaltic and 74220 picritic samples, MEYER, 1987), achondritic HED basalts from the NIPR Antarctic Meteorite Thin Section Set, (Y-74097 and ALHA-77256 diogenites A and B, Y-7308 howardite and Y-791195 and Y-74450 eucrites A and B, YANAI, KOJIMA, HARAMURA, 1995), Martian basalt samples from both NIPR and NASA Antarctic Meteorite Thin Section Sets: ALHA-77005 (NIPR), EETA-79001 (NASA). Over these samples of four planetary bodies (Earth, Moon, Mars, and Asteroid - probably Vesta) we know compositional data from the Venera and Vega Venus lander spacecraft (KARGEL, KOMATSU, 1992) and temperature measurements of Galileo in the vicinity of Io (KESZTHELYI et al, 1998, MATSON et al, 1998, WILLIAMS et al, 2000) which also refer important early Solar System type volcanic rocks. In our statistical comparisons all these planetary bodies and data sources were considered and studied.

[1] H-1117 Budapest, Pázmány Péter sétány 1/a., Hungary
[2] H-1152 Budapest 114. P.O. Box 49. Hungary

Basalts play the role of the "common denominator" among rocky planetary bodies of terrestrial type because partial melting of various chondritic precursor materials give basaltic partial melts. Over their common basaltic nature all these melts preserved stamps of the thermal history of their source parent body, too. In general: our expectation is that if the body was small, thermal history was short and the time scale for basaltic volcanic events resulted in not so various differentiated melts. At the same time stamps by small gravity could be deciphered in the crystallization history of basaltic achondrites of an asteroidal sized body. But contrary to the scale differences between parent bodies common trends in the sequence of basalt compositions were revealed when the whole range of thermal history span of the basaltic volcanism of different sized bodies had been studied (LUKÁCS, BÉRCZI, 1997, 1998).

In this work we focus on the common characteristics of the evolution of basaltic partial melts on a solid rocky body. Gravitational separation less affects the smaller body then the larger, but during the crossing of basaltic melts across thicker and thicker crust layers on any body characteristic changes for this basaltic melt composition will be similar: for example on both large and small bodies they would become more and more Ca-Al rich in the later and later eruptions (from deeper and deeper sources).

In our paper we compare the similarities and differences of basaltic magmatisms on rocky planetary bodies. We consider two main trends basically: the terrestrial evolution and an asteroidal evolution. Other planetary bodies will be interpolated between the two wedges, and will be considered as various branchings from or levels of the common evolutionary trend. Because the terrestrial compositional separation in the atmosphere had got a name after the barometric height formula, we give such name to the compositional separation in the solid part of the rocky planetary bodies. Therefore we call it barometric basaltogenesis on rocky planetary bodies when we study planetary differentiation.

RECAPITULATION: EARLY THERMAL EVOLUTION OF CHONDRITIC PARENT BODY

Before studying the basaltic period of the chondritic body evolution we summarize some key events from the earlier two periods. Starting from parent bodies with different initial composition (E, H, L, LL, C) we formulated evolutionary paths of these parent bodies in the Fe+FeS vs. Fe-oxides compositional field. In this earlier statistical investigations (BÉRCZI, LUKÁCS, 1995, BÉRCZI et al, 1996, LUKÁCS et al, 1997) we calculated the main paths of thermal evolution for chondritic parent bodies of E, H, L, LL, C projected to the UREY-CRAIG (1953) Fe-compound field and VAN SCHMUS-WOOD (1967) table. This part of the thermal history of chondritic parent bodies began with thermal metamorphism, some diffusion processes and slow transformations of the chondritic texture, and advanced forward iron accumulation and outflow to form a core. In the evolutionary path projections in the UREY-CRAIG (1953) field (given by the Van Schmus-Wood type-numbers of metamorphism, as a degree of diffusion) the compositional sequences showed *first reduction then oxidation* transformations (E, H, L, LL, C chondrites). Reduction and C loss, between 3-4 petrologic types, was also recognized earlier (LUX et al, 1980, HUSS et al, 1981, SCOTT et al, 1984), the oscillation between oxidized and less-oxides states, which occurred between the 4-5-6 middle petrologic types, this was our groups's recognition (BÉRCZI et al, 1998, LUKÁCS et al, 1998).

After thermal metamorphism further heating results in segregations in the chondritic asteroidal body. Partial meltings begin and the primitive achondritic assemblage segregates two types of materials. First is the metallic/sulfide melt which migrates toward the depths to form a core (or to collect into great blocks). Second is the melt of lower melting point silicates, which form basaltic melts which migrate toward the surface. We studied these two stages of the chondritic body evolution in our last year paper (BÉRCZI et al, 1999). There we extended the chondritic thermal metamorphic transformation sequence till the basaltic achondrites. The gradual transition from chondritic mineral assemblages (and compositions) through different primitive achondritic stages to the most differentiated basaltic achondritic meteorites was divided into two main stages. Stage A was the earlier partial melting and outflow of iron-sulfide stage (acapulco, lodranite, winonaite), stage B was the later partial melting of a low melting point basaltic like component and its outflow toward the surface (leaving ureilites and some lodranites in their less primitive achondritic state). This division of the chondrite to primitive achondrite range made it possible to distinguish different types of primitive achondrites (BÉRCZI ET AL, 1999). The flow-chart of the chondritic body evolutionary stages is given on *Fig. 1.* Now we study the segregated basaltic achondritic rocks, originating from the surface or near surface layers of an evolved asteroidal body, probably Vesta.

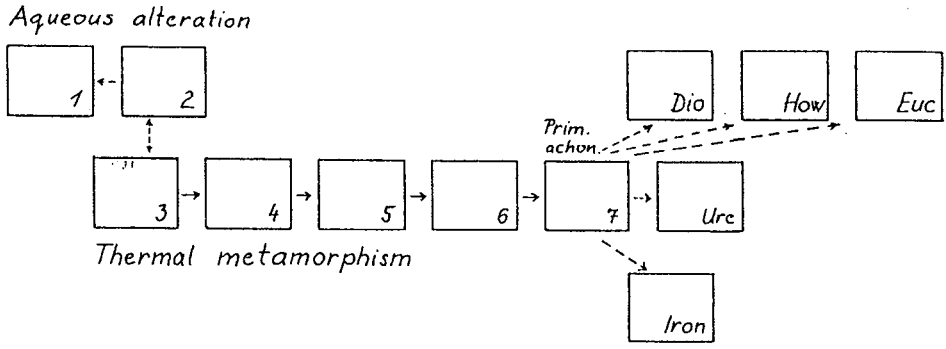

Fig. 1. Summarizing flow chart about the main blocks of thermal evolution of a chondritic parent body. The process starts on left with thermal metamorphism where milestones are the van Schmus-Wood types from 3 to 6, then primitive achondritic stage A and Stage B follows, finally separation of the partial melts in the form of a metallic iron+sulfide component, and a basaltic component follows. Our paper deals with the last period observable on the surface of an evolved parent body: the diogenite-howardite-eucrite sequence.

DIOGENITES, HOWARDITES, EUCRITES

Among meteorites the basaltic achondrites compose a complex series of mafic and ultramafic rocks. They represent a crust rock series with magmatic origin but frequently suffered brecciation on or near the surface of a larger asteroidal body. (According to the **H**owardite, **E**ucrite and **D**iogenite names they are shortly mentioned as HED meteorites.) Essentially the diogenite-howardite-eucrite series consists of rocks mineralogically composed of pyroxenes and feldspar. In the case of the diogenitic endmember the dominant pyroxene is Mg-rich orthopyroxene, the texture is a recrystallized granular. The

other endmember in the series is the cumulate eucrite with pigeonite+plagioclase mineral components.

Along the diogenite-howardite-eucrite (DHE) series we find non-brecciated and brecciated types of textures with monomict and polymict breccias of the later. After a decade of classification debate about the detailed distinction between the groups finally the weight of the diogenitic component (orthopyroxene) became the distinctive component in separating the groups.. Howardites are transitional between the diogenitic and eucritic endmembers of the series (DELANEY et al, 1983). The howardite/eucrite separating line is at the 10 weight percent diogenitic (magnesian-orthopyroxene) component in the polymict basaltic achondrites. Above this value the polymict basaltic achondrites are howardites, below this line the basaltic achondrites are polymict eucrites (DELANEY et al, 1983).

New discoveries of basaltic achondrites in Antarctica triggered a new period of studies of basaltic achondrites (i.e. MITTLEFEHLDT, LINDSTROM, 1992). Granular orthopyroxenitic diogenites were classified to a Diogenite A group. Brecciated pigeonite-plagioclase diogenites were classified to Diogenite B group (TAKEDA, MORI, 1985). Today that is the accepted boundary between the two endmembers and the howardites in between that if a brecciated diogenite or eucrite contains less then 10 percent foreign breccia (so it contains more then 90 % of its original diogenitic or eucritic mineral assemblage) then its category would be polymict diogenite or polymict eucrite, otherwise all polymict basaltic achondritic breccias are howardites.

As a summary, according to the textural characteristics the DHE sequence contains 5 representatives. Along the series, starting from Diogenite A (monomineralic opx crystalline texture) from Diogenite B, (brecciated, mostly monomineralic opx texture) the participation of the pigeonitic monocline-pyroxene in the mineral composition increases, while the hypersthene component decreases, and the Fe-content of the pigeonite also increases through howardites (brecciated opx+cpx+plagioclase texture) toward the eucrites (brecciated eucrite B), till the microgabbro textured Eucrite A endmember. So considering the textural sequence a more detailed Diogenite A, Diogenite B, Howardite, Eucrite B and Eucrite A series is the object of our studies. But because we study mainly the chemical compositional data, mostly we restrict our formulations for the DHE series

The continuous sequence of these brecciated rocks of basaltic achondrites allows magmatic deduction and comparison only for endmembers. Diogenitic orthopyroxenites of pigeonite+plagioclase basaltic eucrites can be the representatives of the basaltic volcanism of an evolved asteroidal body. Diogenites represent those magmatic ultramafic rocks which were segregated from a chondritic precursor asteroidal mantle and migrated to the near surface region. Even if they were exposed as an early volcanic rocks, they were later overlapped by the younger eucritic basalts. In a thermal model of the following sections we shall show that earlier large scale (larger degree) partial melts (diogenites) might have been followed by the lower degree partial melts (eucrites) as we find it in the terrestrial case. The fact that at least two different magmatic rocks can be found in an asteroidal sized body shows that thermal evolutionary process may have advanced in a smaller rocky type body in the Solar System. Even if impact mixing produced the intermediate howardites, the gradually decreasing Mg-content of the diogenite-howardite-eucrite sequence is a valid characteristic of basaltic achondrites.

KOMATIITES AND RELATED ANCIENT ROCKS FROM EARTH

After recapitulation of the early evolutionary steps in chondritic asteroidal body evolution and overview of the basaltic achondrites we give a short summary about the komatiites and related ancient volcanic rocks on Earth, too. Our hypothesis is that from differentiation historical aspects komatiites from the Earth are far counterparts to the diogenitic type basaltic achondritic volcanism on an asteroid.

Komatiites are ultramafic Archean rocks with high MgO content (VILJOEN, VILJOEN, 1969, NESBITT, SUN, 1976, GLIKSON, 1993,). They were first identified and described in South Africa from the valley of the Komati river (VILJOEN, VILJOEN, 1969). The original Barberton komatiite had, according to the early definition: composition with MgO>9 %, K_2O<0.9 %, TiO_2<0.9% and CaO/Al_2O_3>1. (Spinifex texture is characteristic for Archean komatiites, but it is almost never seen in Phanerozoic rocks of similar chemistry.) Later, the Ca/Al criterion (NESBITT & SUN, 1976) extended the circle of komatiites, and they were identified in Australia, (Pilbara, Yilgarn, i.e. EWERS, HUDSON, 1972), in Canada (Abitibi, Munro Township, ARNDT, NALDRETT, PYKE, 1977), in Siberia, (Norilsk, i.e. NALDRETT, 1997) in the Eastern European Platform (Voronyezs, i.e. KRISTIN, 1980) and many other places. They were found mostly in Archean cratons as ancient multiple layers of thin lava flows, (characteristic to the lunar mare volcanism, too). Dividing the wide MgO range into peridotitic and basaltic komatiites it was shown that on the (Mg,Ca,Al) triangle the komatiites are adjacent to picrites and tholeiites (CONDIE, 1981) and their relations to the picrites (the komatiite-picrite-tholeiite sequence) was also investigated (i.e. JACOB ET AL, 1994, KEAYS, 1995, ANDERSON, 1995). Archean tholeiites are not so Mg-rich as compared to komatiites (Al>Mg), but they would be Mg-rich among modern basalts.

Space probes discovered that komatiites also occur on other planetary bodies of the Solar System. Over the lunar counterparts the interplanetary role of komatiites were strengthened by their probable occurrence on Venus, Mars and Io, on the basis of different measurements. On the Jupiter's Galilean satellite Io the surface temperature was extremely high (KESZTHELYI ET AL, 1998, MATSON ET AL, 1998, WILLIAMS ET AL, 1998, 1999, 2000), on Mars the lava tube and bedrock erosion was suggested by komatiites (BAIRD, CLARK, 1984, WILLIAMS, LESHER, 1996), and also the nakhlite-shergottite petrologic relations to komatiites of martian meteorites were suggested (TREIMAN ET AL, 1996, RUZICKA ET AL, 1998). On Venus the compositional characteristics on two landing sites (Venera 14 and Vega 2 measurements) made it probable that komatiites occur (i.e. KARGEL, KOMATSU, 1992).

PARALLEL RUN OF THE D-H-E AND THE K-P-T SEQUENCES ON THE MgO PLOT

New interplanetary importance of komatiites and related rocks emerged in our petrologic comparison studies carried out on bulk compositions of meteorites and differentiated planetary rocks from the Solar System (LUKÁCS, BÉRCZI, 1997, 1998). We observed on the Mg/Si vs. Fe/Si plots that different komatiitic rocks (from lherzolitic komatiites to komatiites) cover a wide range of MgO composition. The higher MgO range beginning from lherzolites, continues with komatiites and over picrites to the lower MgO containing tholeiitic basalts, too. On the basis of meteorite statistical investigations we observed that this komatiite-picrite-tholeiite sequence (KPT) has a counterpart among the basaltic meteorites (which are very probably the fragments of asteroid Vesta). This

diogenite-howardite-eucrite (DHE) basaltic achondrite sequence covers the similar MgO range in the Mg/Si plot from higher (diogenite) to the lower (eucrite) MgO containing ones. These two very parallel Mg-rich to Mg-poor ranges (of basaltic achondrites and komatiite, picrite, tholeiite sequence) were separated by a gap, which was caused by the great difference in their Fe/Si content (LUKÁCS, BÉRCZI, 1997, 1998). Our explanation was about the gap that the Fe/Si content was sensitive to the gravitational separation of chemical components on the planetary body. The stronger gravity field and long time activity of Earth's magmatic processes "extracted" more iron from the crust and near crust rocks, separated and arranged gravitationally the Fe content of mantle rocks more effectively, then it could have been done by a smaller body. These preliminary results initiated this work. (*Fig. 2.*)

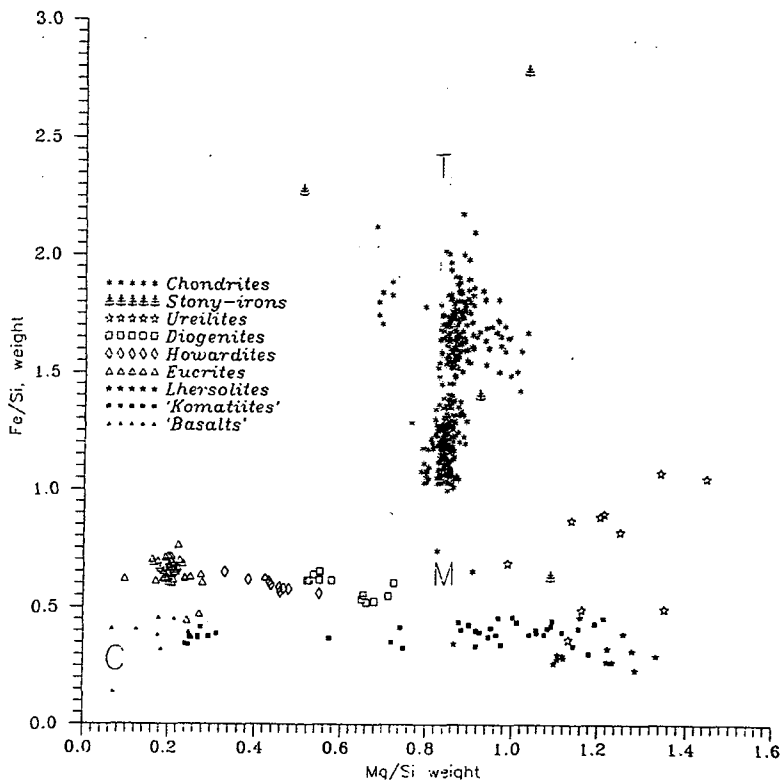

Fig. 2. Si normalized compositional field where chondritic, achondritic and some terrestrial compositions were compared. The Fe/Si vs. Mg/Si plot shows the decreasing Mg content of erupted basaltic magma production both on large and on small rocky body. The chondritic cloud of data (initial condition) can be found at higher total Fe contents because they were not separated yet by iron core forming first differentiation. Iron core formation takes the first distinction between bodies by the mass of the bodies: The higher Fe content of achondritic sequence shows that the separation of Fe compounds on a smaller body could have not been so effective as on a larger body (Earth). The composition of basaltic lava from mantle changes by the thickening of the crust. Crossing thicker crust resulted in lava gradually poorer in Mg as time advanced. Earlier high Mg containing komatiites were followed by later picrites and finally recent low-Mg lava on the Earth. Similarly, we may infer such a sequence of events on a differentiated asteroidal body (Vesta) too. First diogenitic, later howarditic and finally eucritic lava was there erupted onto the surface

We now formulate our conjecture. Since on Earth komatiites rather belong to the geologic past, the analogous diogenites may have been the first lava on Vesta, and when the crust was already substantial, the more aluminous eucrites followed, just before all the Vestan volcanism stopped. These lavas became eucrites, because they contained much Al and Ca (even if assimilated them from the thick crust which they crossed slowly or if they were small degree of partial melting of the asteroidal mantle).

In the following section first we sketch thermal history of Earth by giving parallel cross sectional overview of its main elementary components. Then we do the same for an asteroidal body during its evolution. Then we carry out statistical analysis and comparison of terrestrial and meteoritic data to see the main similarities and differences between the two magmatic rock series, one on the Earth and one on an asteroidal sized body. In this section we project the Si normalized main element bulk compositional data on different compositional fields which characterize evolutionary processes on planetary bodies. (Chondrites and achondrites data were taken from YANAI, KOJIMA, HARAMURA, 1995, those of Earth main rock types from CONDIE, 1981, and NIXON, 1989.) Parallel with our basaltic rock comparisons we sketch a partial thermal evolutionary model for the Earth, too. This emphasizes the role of crust thickening and compositional changes of partial melts in the thermal evolutionary history of Earth.

CROSS SECTION OF THE LAYERED EARTH AND A SIMPLIFIED MODEL OF ITS FORMATION PROCESS DURING THE TERRESTRIAL THERMAL EVOLUTION

We know that some part of Earth's interior is partly molten, and this partially molten material is the source of volcanism. We know that Earth's matter is vertically arranged into zones, mainly via gravitational separation, so around the center there is a dense core (we guess that it is iron), while going outwards the density decreases, mainly with Mg-silicates in the mantle and with mainly Al- and Ca-silicates in the crust. The reason of density zones: Fe's mass density is 7.8 g/cm^3, for the average Mg-silicate this is cca. 3.3 g/cm^3, while for Al-silicates cca. 2.8 g/cm^3. (In these points geophysics and geology treat the questions in more details, but for our present purposes we do not need those details.)

In the upper crust (having much Al-silicates), Al is much more abundant than Mg. At the same time, in the meteorites generally the Al/Mg ratio is opposite, because in the cosmic abundance Mg is one order of magnitude more abundant than Al (NOVOTNY, 1973), and this is also expected from nuclear physics. Namely, in the cosmic nucleosynthesis both Mg and Al (and also Si) form by fusion from the (CNO) triad. Now, Mg is an even-even nucleus and Al is not, so Mg is preferred in the concurrent processes. Therefore we have one more argument that some process enhanced Al content of the crust. It can be conjectured that the enhancement was the result of two selection mechanisms.

The first selecting mechanism is gravity. After accretion the material assemblage forms a sphere, partial melting begins in its interior, and if there is enough time, hydrostatic equilibrium will be achieved with the appropriate gradients of composition. Without convection the change of compositions with radius would be a generalization of the barometric formula known from terrestrial atmosphere (BALÁZS, 1971); if convection is present, then the gradients are smaller.

First we show an ideal layered body arranged according to these density relations. Consider a sufficiently large body with a molten chondritic composition. This body contain some 5-20 % of metallic Fe-Ni and FeS component. This assemblage is expected to flow out, being denser then silicates (and existing separated from the crystalline lattice

of silicates). After flowing out it migrates to greater depths and accumulates around the center to form a core. (This molten metallic and sulfide Fe will contain also some C in solution, too) The overwhelming majority of the remaining material is a mixture of silicates, mainly of Fe-, Mg-, Al- and Ca-silicates.

The second selecting mechanism is melting. Silicates have various densities, and although densities depend on many details, roughly Fe- and Mg-silicates are denser and Al- and Ca-silicates are lighter. Then, in the molten sphere just above the iron core one expects a transition zone where iron is mixed with silicates (pallasites are the meteoritic representatives of this stage) while slightly more above silicates are mixed with iron. Emerging from the iron core along a radius we can observe that upwards the matter is a mixture of silicates, with continuously decreasing Fe and Mg content and with increasing Al and Ca ones. Finally we find the Al-silicate rich outer layers of the crust.

Now, let us repeat our simplified model which shows the great periods how this spherical body evolved while it was cooling. After some time a solid crust appeared, but below this early crust convection was still going on and it broke up crust time to time by volcanism. First probably the molten matter erupted along fissures, later it was possible mainly in spots. (On Earth even now both mechanisms go and mid-ocean ridge basalts do differ from hot spot ones). Anything were the details, the matter of lower density and/or melting point had higher chance to come up. Both density and lower melting point criteria prefer Al- and Ca-silicates; therefore during volcanism the upper crust became more and more enriched in these components. This was an oversimplified sequence of events but first these are the most remarkable steps that came from the principles of thermodynamics of open systems. Obviously, as the molten body cooled the molten zone have got deeper and its temperature also decreased. The crust became wider and wider, and this wider zone must had been crossed by the molten material. These changes have two consequences:

1) The rate of volcanism is decreasing in time (as it is in accord with geologic observations); and

2) The ascension of lava is taking more and more time (crossing thicker and thicker layers).

However, from the second point it follows that the ascending silicate becomes more and more like the crust silicates, which means that the silicates of high melting points "freeze out" from the ascending lava and this indeed leads to Al- and Ca-enrichment.

One can directly see today that the erupting material is not of the mantle composition. Estimated Archean mantle compositions were compared to old lherzolite inclusions, and they resembled each other, and the Al/Mg ratio was 0.1 (CONDIE, 1981). In present volcanism it is well above 1. Also, for the (Archean) mantle Na/Mg$\approx$0.01, while in the present volcanism it is $\geq$1. (The cosmic and terrestrial crust abundance, normalized by weight to Si, are shown on (*Fig. 3.*) until Z=30; the most important elements in the present argumentation are Z=11, 12 and 13, i.e. Na, Mg and Al, respectively. Although it is hard to directly verify, it is obvious that in times when the solid crust was thinner and ascending fluxes higher, the selection for Al and Na (light and of low melting point) must have been more moderate. So as much as Earth is evolving, so much the inner compositional gradients become higher and higher, and the uppermost surface goes farther and farther from the cosmic abundance (and also from the original composition).

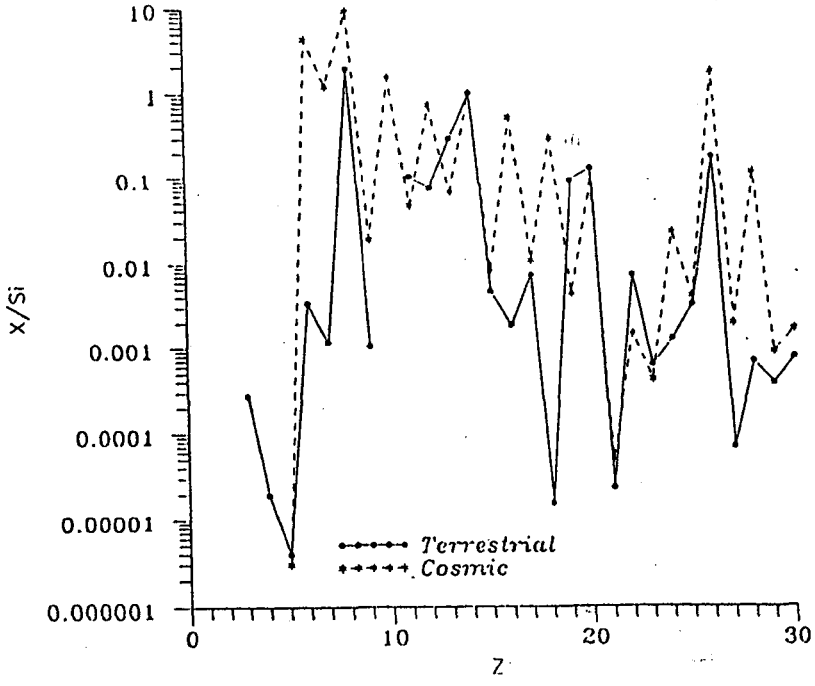

Fig. 3. Cosmic abundance of the first 30 chemical elements compared to the terrestrial abundance in the upper crust.

TERRESTRIAL-TYPE PLANETARY BODIES HAVE SIMILAR THERMAL HISTORY

From planetary surface compositional (and especially from known planetary basaltic) data it can be seen that the general cross section and the bulk thermal history happened similarly on another planetary bodies of the Solar System. Apollo expeditions collected great number of lunar samples, the Venera and Vega probes on Venus, and the Viking and Pathfinder probes on Mars measured surface compositions. All these compositions resemble better the terrestrial one than the cosmic abundance, as a result of planetary differentiation. The Martian sequence was compared to that of Terrestrial one by WANKE ET AL, (1997). They found that Martian rock samples, both SNC meteorites and Pathfinder rocks and terrestrial samples fall to two, almost parallel ranges, both in an MgO decreasing sequence. There the terrestrial komatiites had Martian counterparts in the ALHA-77005 and other high Mg/Si ratio samples (i.e. Chassigny, LEW-88516 and ALHA-84001, for nakhlites see TREIMAN ET AL, 1996), while recent ocean floor basalts had counterparts in Shergotty, Zagami and EETA-79001B samples (WANKE ET AL, 1997). On this Al/Si vs. Mg/Si plot it is clearly shown that Martian samples has lower Al/Si content than that of the terrestrial samples. (This fact may have early Solar System evolution causes, too.)

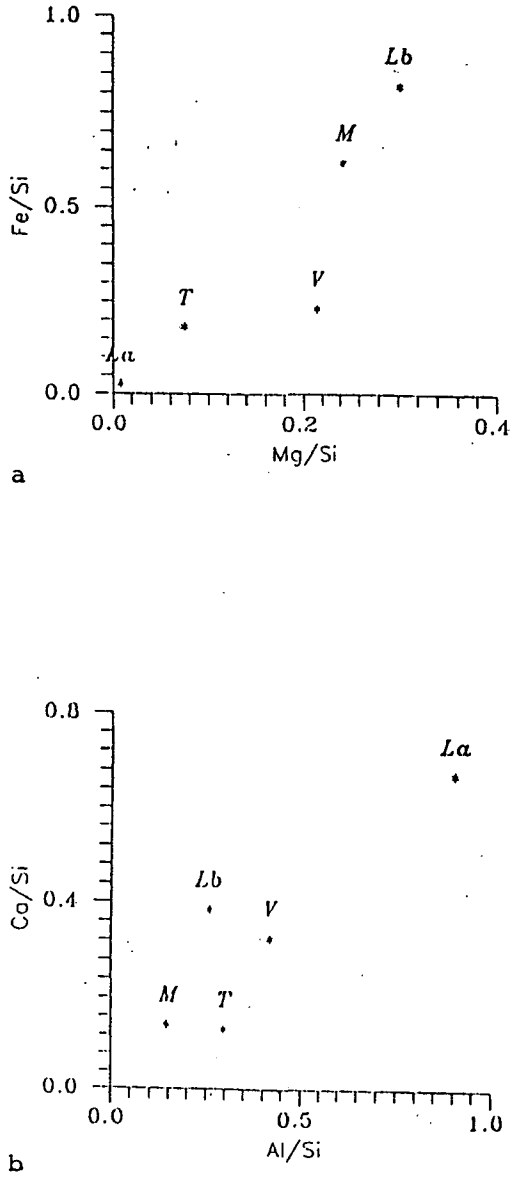

Fig. 4. Two maps for planetary surface rocks. 4a.) The Mg/Si vs. Fe/Si plot, 4B.) The Al/Si vs. Ca/Si plot, where T, V, M, La and Lb marks Earth, Venus, Mars, Lunar anorthosites and Lunar average, respectively.

Among Apollo lunar samples both 12002 and 74220 has picritic Mg/Si ratios (MEYER, 1987). Venera 14 and Vega 2 data, as was mentioned earlier, also refer probably komatiitic composition on Venus surface (KARGEL, KOMATSU, 1992). As for quantitative

data, see *Fig. 4a.* where V stands for Venera 14 data, T is the average Terrestrial crust, M stands for the average of the two Martian Viking lander data, La is the Lunar Apollo 16 anorthosite, and Lb is the average of Apollo 11, 15 and 17 basalts (ENCRENAZ ET AL, 1989 RÖMPP, 1958; CIMBAL'NIKOVA ET AL., 1975, other Martian data in WANKE ET AL, 1997). We may observe on Fig. 4a. (planetary crust Fe/Si vs. Mg/Si plot, ignoring now the completely feldspathic anorthosite) that the Fe content of the surface rocks goes oppositely with the radius or mass of the planet. We guess that the main reason is the more and more successful gravitational separation of iron on these bodies.

The Fig. 4b. Ca/Si vs. Al/Si plot for planetary bodies shows that estimeting from the existing crust data local volcanism distingiushed the 4 planets: it has brought up substantial amounts of Al and Ca to the surfaces. Earth has a fully developed plate tectonics with several types of volcanisms. Mars had no plate tectonics and had shield volcanoes. Venus has volcanism, does not seem to have plate tectonics but some strange crust behavior instead. Finally Moon was too small for any plate tectonics (ILLÉS-ALMÁR, 1994). Still, all above planetary surfaces are far from the cosmic abundance and this cannot be simply the result of static gravitational separation only, because their Ca/Al ratios differ too.

CROSS SECTION OF AN ASTEROID AND THE ASTEROIDAL THERMAL HISTORY

Not only the rocky (terrestrial type) planetary bodies but the larger asteroids are spherical. Therefore they must have had a molten (most probably a partially molten) stage in the past, although their thermal fluxes were small fractions of Earth's one. The probable explanation is the primordial Al^{26} and Pu^{244}, relatively short-living radioisotopes. Ignoring other details for our present purposes, it counts only that the primordial molten stage had probably a chondritic composition. Then gravity can work and forms a minimal energy state sphere, and segragation+migration can rearrange the matter into zones. But in an asteroid, with $R \approx 500$ km at most, silicates cannot separate too successfully from each other. Still its gravity may be enough to collect molten metallic Fe and FeS The observational evidence is the existence of iron asteroids (the first on the list is Psyche 16), and their explanation is an originally zoned asteroid which later has lost the silicate outer layers in collisions.

Applying then the above theoretical scheme for the thermal history of a larger asteroid one can visualize a (hypotethical) totally molten initial stage: first an iron core and around it a more or less homogeneous, zoned onion-shell of the silicates appears. In the outer silicate shell - by cooling the outer parts - a frozen crust appears, and later it gradually grows. As the solid crust becomes substantial, again and again silicates of low melting point (and low density) have better chance to penetrate it. (Now the Fe content of the surface rocks could not decrease on asteroids with larger radius because of its small gravity as compared to the terrestrial planets.) Local volcanism can bring up considerable amounts of Al and Ca containing partial melts and this is shown on the Al/Si and Ca/Si plots, where both of these two components changes proportionally with each other. In the early volcanism the Al/Mg ratio of the asteroidal basalts (diogenites, howardites and eucrites) followed the global picture sketched for the larger bodies (*Fig. 5.*). (Basaltic achondrites, similarly to Mars, also have lower Mg+Al range than that of the Earth.)

Although this is an idealized and simplified theoretical scenario, the basic steps in layer separations could be shown on this model. In a real, chondritic asteroidal system, during the thermal evolution from chondritic to achondritic stage there are no signs of the

totally molten state. In primitive achondritic (acapulcoite-lodranite) mineral assemblages only partial melting of different (low) degree and slow migration of partially molten phases could be observed (i.e. MCCOY ET AL, 1997). In larger asteroids this migration was more effective and resulted in separation of great iron core as the observational evidence of asteroids with metallic spectra have proved, (GAFFEY, BELL, CRUIKSHANK, 1989) and basaltic crust as basaltic achondrites witness it.

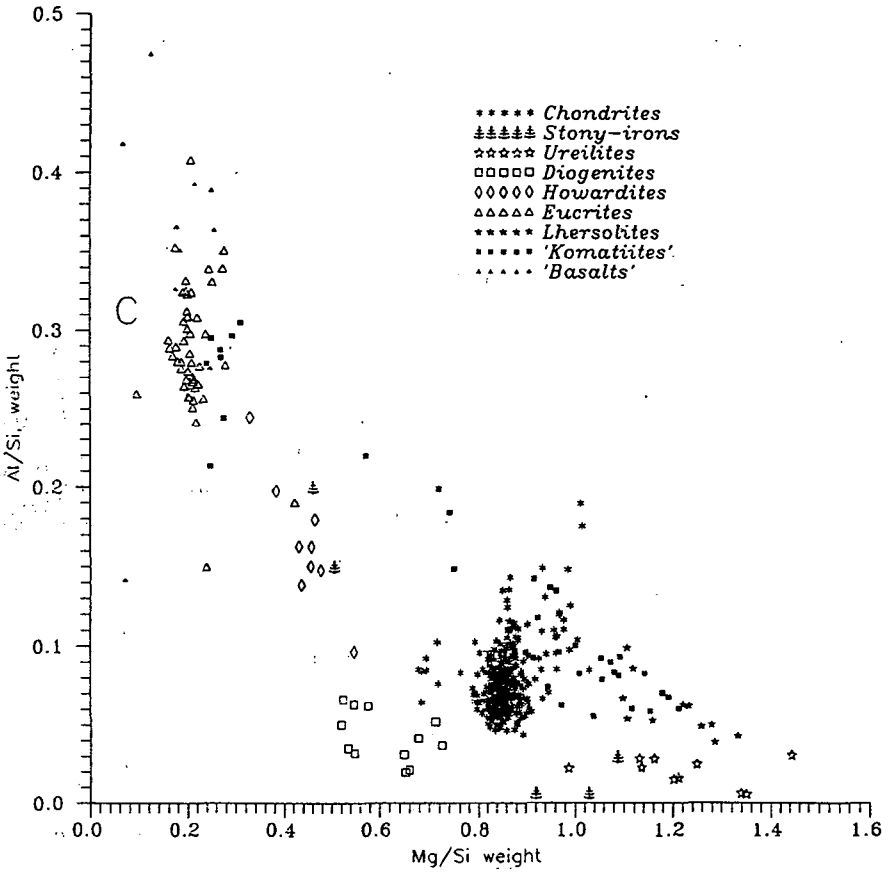

Fig. 5. The Al/Si vs. Mg/Si plot for basaltic achondrites and main terrestrial rocks studied in our work. It shows the main relation between Al and Mg during the long range basaltic evolution. They are essentially in anticorrelation, because differentiation of mantle results in separation of Al containing phases.

EVOLUTIONARY SEQUENCE OF THE TERRESTRIAL ULTRAMAFIC-MAFIC VOLCANISM KOMATIITES-PICRITES-BASALTS AND COMPARISON TO THE DHE SEQUENCE

Evolutionary models of the early Earth adapted the recognition of lunar magma ocean (ANDERSON, 1981). The terrestrial magma ocean model considered that significant fraction of the Earth's mantle was molten. After cooling a thin crust formed and this high

degree of partial melting (with chondritic bulk composition) appeared as a buried magma ocean, (WALKER, 1983), which produced intensive eruptions of Archean komatiitic flows. Therefore komatiites were the surface expressions of the buried magma ocean (NISBET, WALKER, 1982). Our komatiite-picrite-tholeiite sequence fits and continues this model. The cooling Earth later had thicker crust, lower degree of partial melting in its mantle, the partially molten zone withdrawn to greater and greater depths while producing picrites after komatiites, and the recent tholeiites after picritic "middle-period" basalts (LUKÁCS, BÉRCZI, 1997). Our time sequence model also fits to the model of TAKAHASHI, SCARFE (1985) and others (i.e. HERZBERG ET AL, 1988) which explains the origin and rarity of Phanerozoic komatiites. Their model shows that the present Earth's komatiites could come up as partial melts of the mantle peridotite from depths of cca. 175 km, picrites from cca. 100 km, and tholeiitic basalts from 40-50 km. The depth of the source needs great migration time to reach the surface and long transportation time implies great compositional changes. In this respect our model is a 3 parameters system in which depth, transportation time, and transportational compositional changes parameters are involved.

Now we sketch the time sequence of terrestrial basaltic rock starting from the cosmic abundance. Comparing main rock compositions to that of cosmic abundance (Fig. 3.) we can clearly see how far that composition moved from the (hypotethical but very probable) initial composition. (The terrestrial compositional starting point may be the original Barberton komatiite given earlier (CONDIE, 1981). This initial composition at least for silicates was probably very near to that of a chondritic one. (Actually the undepleted terrestrial mantle is that kind of source which could preserved many bulk characteristics of the chondritic primitive Earth, although it segregated iron-and sulfide core, and it also continuously produces crust.) If the most ancient "basalts" were komatiites, (high degree of partial melting of the ancient mantle) then they were rich in Mg (therefore poor in Al and Ca), poor in K (and Na), also poor in Ti, but arbitrary in Ca/Al. These characteristics of komatiitic bulk composition are conform with a less differentiated stage, nearer to the original composition of a mantle after gravitational separation of iron+sulfide to core and at the beginning of thermal separation in volcanism. *Comparing the compositional characteristics of the komatiites and recent tholeiitic basalts to the cosmic abundance we can observe that komatiites point away from the present crust abundance towards the cosmic abundance.* Recent basalts are even farther away from the cosmic abundance.

Let us sketch the basaltogenetic situation caa. 3.5 Ga ago, in order to show a qualitative way about the long term changes in basaltic composition. This will help us in a later comparison of komatiites and diogenites. In Archean times the planetary body is already after the gravitational separation of iron from mantle, but the internal heat production is high and the crust is thin. (Internal heat production then was cca. 3 times the present one, so the heat flux was also threefold and the thickness of the crust was cca. 1/3 of the present; LUKÁCS, 1993.) Large fluxes drive serious convection, so Mg-silicates are still not too much attracted into the depth by gravity. In addition, the crust might have been aluminous, but it was still thin, so the mantle material changed relatively little while crossing through the crust. Then in the average 3.5 Ga basalts we expect much Mg. The reasons are the following: i) the matter just below the crust is still closer to the "chondritic" composition; and ii) not too much Mg freezes out while crossing), alkalia are present cca. in cosmic abundance (what would enrich them in the basalt not stopped by the thin crust). We expect Ti cca. in cosmic abundance because of the same earlier arguments. And just this is seen in the komatiites.

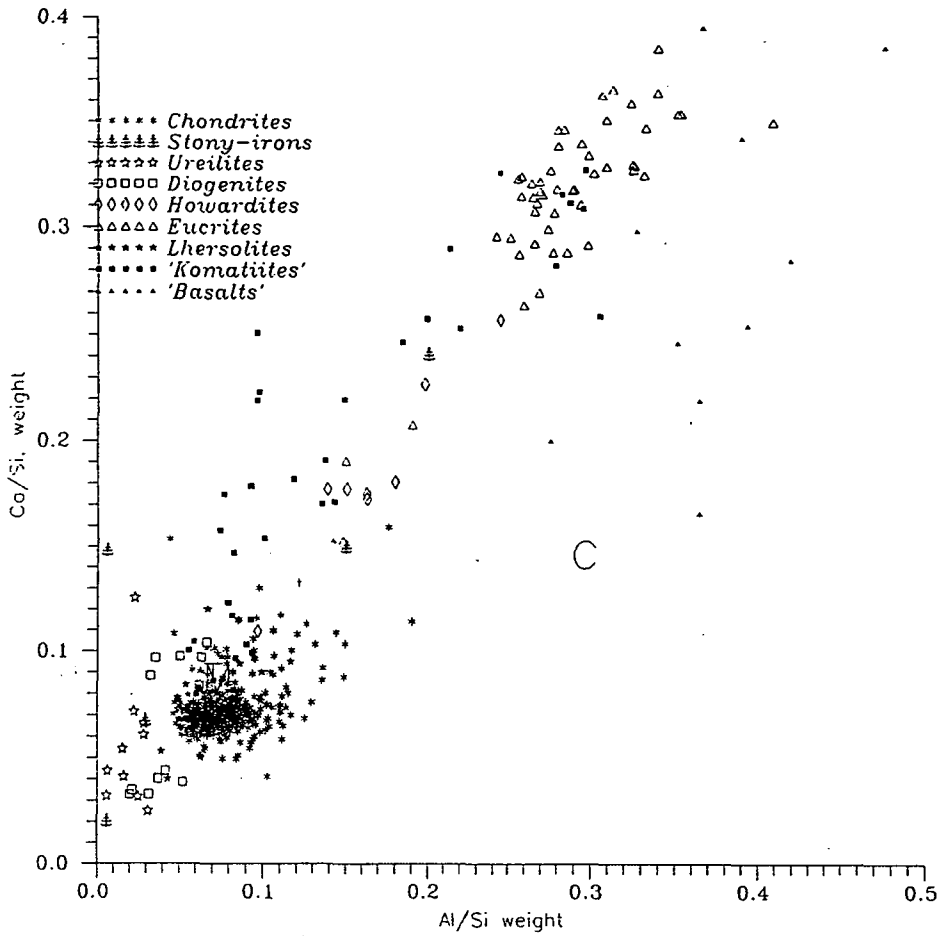

Fig. 6. The Ca/Si vs. Al/Si plot shows that these two elements are strongly correlated in most of the differentiation processes. On the most evolved Earth sometimes Al is more enriched when the outermost layers are considered. This shows that a larger body may reach more detailed, finer "barometric height formula" stratification of the main chemical elements - even if their holders are minerals - then the smaller asteroidal bodies.

Let us compare this evolutionary sequence to those data we know about HED basaltic achondrites (probably from Vesta). On the Fe/Si vs. Mg/Si plot (Fig. 2.) we show 5 types of materials: chondritic meteorites (NIPR data from YANAI ET AL., 1995), diogenite, howardite and eucrite (YANAI ET AL, 1995), and 61 terrestrial basalts of various kind (KRISTIN, 1980, CONDIE, 1981; NIXON, 1987; NEALE, TAYLOR, 1992). We can see that the sequence of the terrestrial ultramafic-mafic volcanic rocks are the most Fe-poor (roughly independently of the widely varying Mg content). Also the figure shows the approximate location of Earth's crust (C), mantle (M) and the whole planer (T). Observe here that:

1) the basaltic achondrite sequence form a line parallel to terrestrial basalts (but with higher Fe content);

2) the most Mg-rich asteroidal basaltic achondrites have the same Mg/Si as that of the chondrites;

3) the chondrites contain more Fe than either terrestrial or asteroidal basaltic-ultramafic rocks.

Fig. 6. shows the Ca/Si vs. Al/Si plots. Chondrites form a dense cluster (hiding among themselves T and M). Almost all the basalts (of any planetary body) fit to a straight line starting from the origo and crossing the chondritic cluster, and all points except for some normal terrestrial basalts lie on a proportionality line where the ratio is the cosmic abundance ratio. It seems that basaltogenesis substitutes indeed Mg with Al and Ca, but cannot prefer one of the latter to the other.

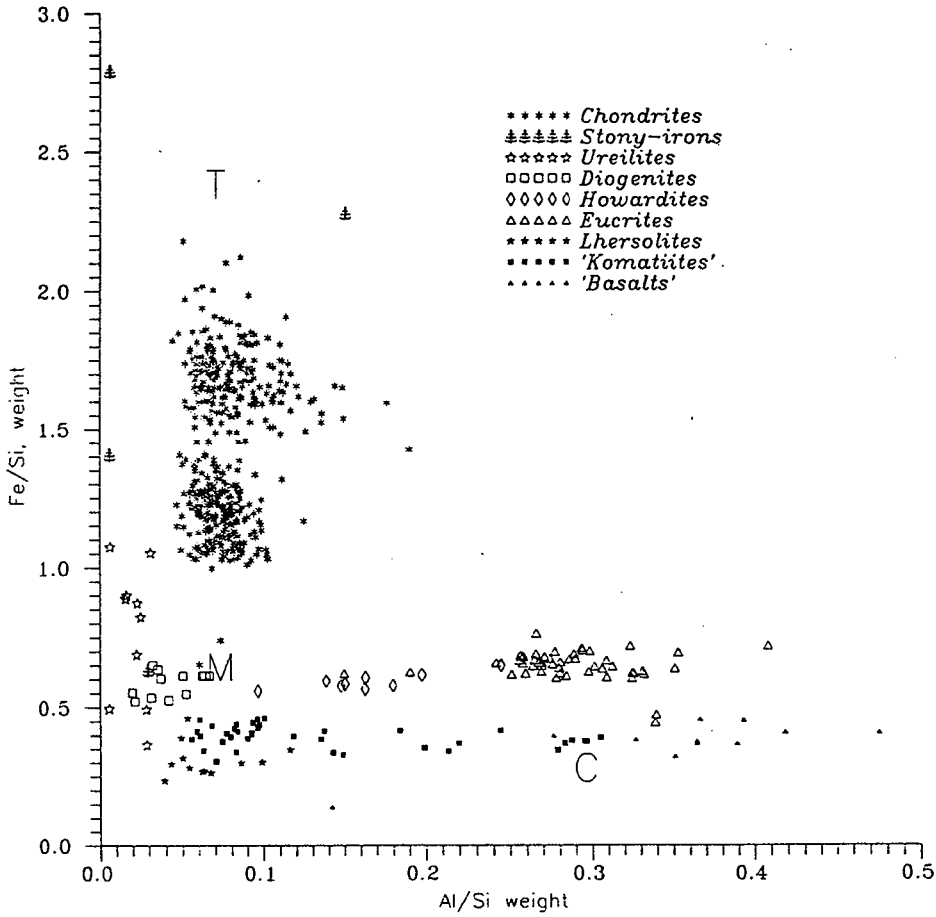

Fig. 7. The Fe/Si vs. Al/Si plot also shows that Fe distinguish different levels of differentiation from the ancient chondritic (highest level of bulk Fe/Si ratio) to the most differentiated terrestrial basalts (the lowest Fe/Si ratio). In the two evolved body dataset we can see to long range of differentiation sequences. One is for achondrites, (upper one) the other from the Earth (the lower one). Both sequences span a wide range of Mg content. The lower Al end basalts of the sequences are the earlier, the greater Al containing basalts are the younger basalts.

All the some element/Si vs. Fe/Si figures (i.e. Fig. 7.) suggest that in the primordial basaltogenetic processes the metallic Fe have been lost by gravitation. All the figures clearly show the analogy between diogenites and some komatiites. At the same time eucrites, (and also lunar basalts), are counterparts to "modern" terrestrial basalts. At this point we return to our original hypothesis, the role of the time sequence of the appearance of these rocks. Since on Earth komatiites rather belong to the geologic past, the analogous diogenites may have been the first lavas on Vesta. This is a profound conclusion of the parallel DHE and KPT sequences on the material maps shown. When the crust was already substantial, the more aluminous howardites might have followed and finally, just before volcanism stopped on Vesta, the lava became eucritic with even higher Al and Ca content. We have another argument in accordance of this hypothesis. We can see in datasets that the Ti content of basaltic meteorites is growing as volcanism becomes more difficult (BÉRCZI ET AL., 1997). The Ti/Si ratio is the smallest in chondrites (hardly above the cosmic abundance), it is growing in the diogenite -> howardite -> eucrite sequence, in lunar basaltic meteorites it is similar to eucrites (and terrestrial basalts), and the last stage is represented in later stage lunar blue basalts (BÉRCZI, LUKÁCS, 1996), not yet found as Antarctic meteorite. Now, remember that a komatiite criterion is the low abundance of Ti.

SUMMARY: MAIN TRENDS IN FRACTIONATION

Comparison of bulk compositional data of basaltic meteorites of evolved asteroidal bodies and those of selected terrestrial volcanic rocks revealed important common thermal evolutionary trend of differentiating planetary bodies, regardless of their size. These trends were shown on Si normalized chemical element level bulk compositional fields of Fe/Mg, Ca/Al and Al/Mg and Al/Fe plots. On these compositional maps we focused on two differentiation sequences: one for achondrites, the other for the Earth. Both sequences spanned a wide range of Mg content. Achondritic sequence had higher total Fe content,. The higher Mg end of the sequences represented the earlier lava formations, the lower Mg containing basalts were the younger differentiates of the mantle. (Without fractionation the chondritic "clouds" of our dataset was found at higher total Fe contents, scattering around the chondritic average value of Mg/Si.)

The higher Fe content of achondritic sequence showed that the separation of Fe compounds on a smaller body (Vesta) could have not been so effective as on a larger body (Earth). Thickening of the crust resulted in lava gradually poorer in Mg as time advanced. Earlier high Mg containing komatiites were followed by later picrites and finally recent low-Mg lava on the Earth. Similarly, we could infer such a sequence of events on the differentiated asteroidal body, Vesta, too. First diogenitic, later howarditic and finally eucritic lava was there erupted onto the surface.

Al-rich phase separation from the mantle was the next period of differentiation, because of the lower density of aluminous minerals. Projections of these compositions onto the Al/Mg map showed parallel trends again both for achondrites and Earth, with lower Mg content of the corresponding achondritic basalts, because iron shared a part of the Mg/Fe mineralogical sites, and in the Earth's case these sites were partly occupied by Ca, too. Ca/Al plots showed that these two elements have been strongly correlated in bulk magmatic processes.

CONCLUSIONS

Comparison of bulk compositional data of basaltic meteorites of evolved asteroidal bodies and those of selected terrestrial volcanic rocks in our paper revealed an important common thermal evolutionary trend of a differentiating planetary bodies, regardless of their size.

The overview about the thermal evolution of a solid body, where the main trends in the basaltic volcanism were modeled gave the following conclusions. There were two types of segregations in planetary bodies: by gravitation and by melting. Partial melting helped segregation of first the metallic components which migrated toward the core. Second basaltic partial melts segregated and they moved toward the surface. Considering size, the early separation of the metal+sulfide bearing components was more effective on the large Earth, then in a small asteroid. The basaltic melts were first high MgO bearing types both on smaller asteroids and the larger Earth. Our comparisons showed that the main characteristics of the parallel evolution in the sequence of volcanic products: from the early high degree of partial melting komatiitic type (probably from a buried magma ocean) throughout the later, gradually lower degree of partial melting picritic type till the recent (on the Earth) stage differentiation of tholeiitic basalts. We conclude that this sequence is partly the result of the gradual separation of chemical elements - similarly to chemical separation according to the barometric height formula in the terrestrial atmosphere - in a gravitationally and thermodynamically affected Earth. We found a similarly MgO decreasing sequence of the diogenite-howardite-eucrite of basaltic achondrites from an evolved asteroid. This similarity indicates that time dependent changes in basalt volcanism have a size-independent scale parameter for different planetary bodies.

ACKNOWLEDGMENTS

Authors thank to NASA JSC Planetary Materials Laboratory and NIPR Antarctic Meteorite Research Center, personally to Drs. S. JÓZSA, K. YANAI, H. KOJIMA, J. GOODING & G. E. LOFGREN, É. PAPP and T. SZEDERKÉNYI for loan of planetary basaltic and andesitic samples and thin sections, and to Dr. T. SZEDERKÉNYI for illuminating discussions. Partly supported by OTKA T/026660.

REFERENCES

ANDERSON, D. L. (1981): Hot spots, basalts, and the evolution of the mantle. *Science,* **213,** 82-89.

ANDERSON, A. T. (1995): CO_2 and the eruptibility of picrite and komatiite. *Lithos,* **34,** 19-25.

ARNDT, N. T., NALDRETT, A. J. & PYKE, D. R. (1977): Komatiitic and iron-rich tholeiitic lavas of Munro Township, Northeast Ontario. *Journ. Petrology,* **18,** 319-369.

BAIRD, A. K., & CLARK, B. C. (1984): Did komatiitic lavas erode channels on Mars? *Nature,* **311,** 18.

BALÁZS N. L. (1971): in *Relativity and Gravitation,* (eds. CH. G. KUPER & A. PERES), p. 17. Gordon & Breach, New York

BÉRCZI SZ., FÖLDI T., KUBOVICS I., LUKÁCS B., VARGA I. (1997): Comparison of planetary evolution processes studying cosmic thin section sets of NASA and NIPR. *LPSC XXVIII,* #1782, (p. 97) LPI (CD-ROM), Houston

BÉRCZI SZ. & AL., (1997): High titanium basalts in the Solar system. *ANTARCTIC METEORITES, XXII,* 9-11. Tokyo

BÉRCZI SZ. & LUKÁCS B. (1995): A comparison among chondrite compositions. *ANTARCTIC METEORITES, XX,* 30-33.

BÉRCZI SZ. & LUKÁCS B. (1996): *On Contacts of High and Low Ti Basalts on the Moon.* KFKI-1996-08/C, Budapest

BÉRCZI SZ. & LUKÁCS B. 1(998): Main Lines and Sidetracks in Basaltogenesis of Terrestrial Planetary Bodies. In: *Side Tracks in Evolution.* (ed. B. LUKÁCS, & SZ. BÉRCZI) KFKI-1998-07/C. 6-12. Budapest

BÉRCZI SZ., HOLBA Á. & LUKÁCS B. (1996): On discriminating chondrites on the basis of statistical analysis of iron-bearing compounds: NIPR Antarctic samples. *ANTARCTIC METEORITES, XXI,* 17-20. Tokyo

BÉRCZI SZ., LUKÁCS B., HOLBA Á., KISS A., PAPP É. (1998): From FeO Reduction to Percolation and Outflow of Iron: Thermal Evolution of Chondrite Parent Bodies. *Acta Mineral. Petrographica, Szeged,* **XXXIX.** 87-105.

BÉRCZI SZ., GÁL-SÓLYMOS K., HOLBA Á., LUKÁCS B., MARTINÁS K. (1999): On the Thermodynamics of Meteorites and Parent Bodies II.: From Chondrites to Achondrites through the Primitive Achondrite Varieties (Stage A and Stage B) to the Basaltic Achondrites. *Acta Mineral. Petrographica, Szeged,* **XL.** 175-198.

BROOKS, J. & SHAW, G. (1973): *Origin and Development of Living Systems.* Academic Press, London

CIMBAL'NIKOVA, A. & AL. (1975): in *Kosmokhimiya Luny i Planet.* Nauka, Moscow

CONDIE, K. C. (1981): *Archean Greenstone Belts.* Elsevier, Amsterdam

DELANEY, J. S., TAKEDA H., PRINZ, M., NEHRU, C. E., HARLOW, G. E. (1983): The nomenclature of polymict basaltic eucrites. *Meteoritics,* **18,** 103-111.

ENCRENAZ, T., BIBRING, J.-P. BLANC, M. (1989): *The Solar System.* Springer, Berlin

EWERS, W. E. & HUDSON, D. R. (1972): An interpretive study of a nickel-iron sulfide ore intersection. *Econ. Geol.,* **67,** 1075-1092.

GAFFEY, M. J., BELL, J. F., CRUIKSHANK, D. P. (1989): Reflectance spectroscopy and asteroid surface mineralogy. (In *Asteroids II,* Eds. R. P. BINZEL & AL.), p. 98-127. Univ. of Arizona Press, Tucson

GLIKSON, A. Y. (1993): Asteroids and early Precambrian crustal evolution. *Earth-Science Review,* **35,** 285-319.

HERZBERG, C. T. & OHTANI, E. (1988): Origin of komatiite at high pressures. *Earth Planet. Science Letters,* **88,** 321-329.

HUSS, G.R., KEIL, K., TAYLOR, G. J., (1981): The matrices of unequilibrated ordinary chondrites: implications for the origin and history of chondrites. *Geochim. Cosmochim. Acta,* **45,** 33-51.

ILLÉS-ALMÁR E. (1994): Planetary Evolution: Comparison of the Tectonics of the Rocky and Icy Planetary Bodies. In: *Evolution of Extraterrestrial Materials and Structures,* (ed. B. LUKÁCS, I. KUBOVICS, L. STEGENA, SZ. BÉRCZI) KFKI-1994-22/C, p. 95-101. Budapest

JACOB, D., JAGOUTZ, E., LOWRY, D., MATTEY, D. & KUDRJAVTSEVA, G. (1994): Diamondiferous eclogites from Siberia: Remnants of Archean oceanic crust. *Geochim. Cosmochim. Acta,* **58,** 5191-5207.

KARGEL, J.S. & KOMATSU G. (1992): The composition of Venus and the petrogenesis of Venusian silicate lavas. *LPSC XXIII,* (Abstract) 655. Houston

KEAYS, R. R. (1995): The role of komatiitic and picritic magmatism and S-saturation in the formation of ore deposits. *Lithos,* **34,** 1-18.

KESZTHELYI, L., MCEWEN, A., KLAASEN, K., & GALILEO SSI TEAM. (1998): High-temperature volcanism on Io: Galileo SSI eclipse observations. (Abstract) *LPSC XXIX.* #1529, LPI, (CD-ROM), Houston

KRISTIN, E. M. (1980): Komatiti zelenokammenüh pojaszov voronyezsszkovo krisztállicseszkovo massziva. *Szovjetszkaja Geologija,* **9,** 84-97.

LUKÁCS B. (1993): On Earth's Thermal History. in *Carpathian Basin: Evolutionary Stages.* (eds. B. LUKÁCS, SZ. BÉRCZI, K. TÖRÖK), KFKI-1993-21/C, p. 2-7. Budapest

LUKÁCS B. & BÉRCZI SZ. (1997): Statistical analysis of the NIPR (Japan) Antarctic chondrites: Paths of thermal evolution of parent bodies? *LPSC XXVIII,* #1137, (p. 853) LPI (CD-ROM), Houston

LUKÁCS B. & BÉRCZI SZ. (1997): Statistical analysis of NIPR meteorite compositions II.: Comparison of sequences of differentiated rocks from an asteroidal sized body and Earth. *ANTARCTIC METEORITES, XXII,* 94-96. Tokyo

LUKÁCS B., & BÉRCZI SZ. (1998): Barometric height formula type fractionation in the stony planetary bodies. *LPSC XXIX.* #1223, LPI (CD-ROM), Houston

LUX, G., KEIL, K., & TAYLOR, G.J. (1980): Metamorphism of the H-group chondrites: implications from compositional and textural trends in chondrules. *Geochim. Cosmochim. Acta,* **44,** 841-855.

MATSON, D. L., BLANEY, D. L., JOHNSON, T. V., VEEDER, G. J. & DAVIS, A. G. (1998): Io and the Early Earth. (Abstract) *LPSC XXIX.* #1650, LPI (CD-ROM), Houston

MCCOY, T. J., KEIL, K., MUENOW, D. W. & WILSON, L. (1997): Partial melting and melt migration in the acapulcoite-lodranite parent body. *Geochim. Cosmochim. Acta,* **61,** 639-650.

MEYER, C. (1987): *The Lunar Petrographic Thin Section Set.* NASA JSC Curatorial Branch Publ. No. 76. Houston, Texas

MITTLEFEHLDT, D. W. & LINDSTROM, M. M. (1992): Geochemistry and Petrology of Yamato HED Meteorites. *Seventeenth Symposium on Antarctic Meteorites*, NIPR, Tokyo, 228-231.

NALDRETT, A. J. (1997): Key factors in the genesis of Norilsk, Sudbury, Jinchuan, Voisey's Bay and other world-class Ni-Cu-PGE deposits: implications for exploration. *Australian Journ. Earth Sci.* **44**, 283-315.

NEAL, C. R. & TAYLOR, L. A. (1992): Petrogenesis of mare basalts: A record of lunar volcanism. *Geochim. Cosmochim. Acta*, **56**, 2177-2211.

NESBITT, R. W. & SUN, S. S. (1976): Geochemistry of Archean spinifex-textured peridotites and magnesian and low-magnesian tholeiites. *Earth Planet. Sci. Lett.* **31**, 433-453.

NISBET, E. & WALKER, D. (1982): Komatiites and the structure of Archean mantle. *Earth Planet. Sci. Lett.* **60**, 105-113.

NIXON, P. H. (1987): *Mantle Xenoliths*. J. Wiley & Sons, New York

NOVOTNY, E. (1973): *Introduction to Stellar Atmospheres and Interiors*. Oxford University Press, New York

RÖMPP, H. (1958): *Chemielexikon*. Franckh'sche Verlagshandlung, Stuttgart

RUZICKA, A., SNYDER, G. A. & TAYLOR, L. A. (1998): The Shergottite-Nakhla connection: Forming nakhlites as cumulates of shergottitic melts. (Abstract) *LPSC XXIX*, #1129, LPI (CD-ROM), Houston

SCOTT, E. R. D., RUBIN, A. E., TAYLOR, G. J., & KEIL, K. (1984): Matrix material in type 3 chondrites - occurrence, heterogeneity and relationship with chondrules. *Geochim. Cosmochim. Acta*, **48**, 1741-1757.

TAKAHASHI E. & SCARFE, C. M. (1985): Melting of peridotite to 14 GPa and genesis of komatiite. *Nature* **315**, 566-568,

TAKEDA H., & MORI H., (1985): The diogenite-eucrite links and the crystallization history of a crust of their parent body. *Proc. Lunar Planet. Sci. Conf. 15th, Part 2.; J. Geophys. Res.* **90**. C636-C6448.

TREIMAN, A. H., NORMAN, M., MITTLEFEHLDT, D., & CRISP, J. (1996): "Nakhlites" on Earth: Chemistry of clynopyroxenites from Theo's flow, Ontario, Canada. (Abstract) *LPSC XXVII*, 1341, Houston

UREY, H.C., & CRAIG, H., (1953): The composition of the stone meteorites and the origin of the meteorites. *Geochim. Cosmochim. Acta*, **4**, 36-82.

VAN SCHMUS, W. R., & WOOD, J. A., (1967): A chemical-petrologic classification for the chondritic meteorites. *Geochim. Cosmochim. Acta*, **31**, 747-765.

VILJOEN, M. J. & VILJOEN, R. P. (1969): *Upper Mantle Project*. Geological Society of South Africa

WALKER, D. (1983): Lunar and Terrestrial Crust Formation. *Journal of Geophys. Res.* **88**. Suppl. B17-B25.

WANKE H. & DREIBUS, G. (1997): New evidence for silicon as the major light element in the Earth's core. (Abstract) *LPSC XXVIII*, #1280, (p. 1495) LPI (CD-ROM), Houston

WILLIAMS, D. A. & LESHER, C. M. (1996): Summary of field evidence for thermal erosionby chanelized Archean and Proterozoic komatiite lava flows. (Abstract) *LPSC XXVII*. 1435, LPI, Houston

WILLIAMS, D. A. & LESHER, C. M. (1998): Analytical/numerical modeling of the emplacement and erosional potential of Archean and Proterozoic komatiitic lavas. (Abstract) *LPSC XXIX*. #1431, LPI, (CD-ROM), Houston

WILLIAMS, D. A., WILSON, A. H. & GREELEY, R. (1999): Komatiites from the Commondale Greenstone Belt, South Africa: a potential analog to Ionian ultramafics? (Abstract) *LPSC XXX*. #1353, LPI, (CD-ROM), Houston

WILLIAMS, D. A., WILSON, A. H. & GREELEY, R. (2000): A komatiite analog to potential ultramafic materials on Io. *Journal of Geophys. Res.* **105.** No. E1. 1671-1684.

YANAI K., KOJIMA H. & HARAMURA H. (1995): *Catalog of Antarctic Meteorites*. NIPR, Tokyo

Manuscript received: 18. Sep. 2000.

ko

Illustrations

Figures should be used only where they are essential to elucidate text.

The illustrations should be numbered according to their sequence in the text, and in the text references should be made to each figure.

All illustrations should be given separately, not stuck on sheets and not folded. The number of the figure and the authors name should be noted on the reverse side of the photographs and on the lower frontside of drawings, indicating at the same time the top of the figure where it necessary.

Captions for all figures should be given typewritten on a separate list at the end of the manuscript. Drawn text in the figures should be kept to a minimum.

Drawings should be made on tracing paper by Indian ink. The thickness of the lines and the size of the lettering should enough to allow a necessary reduction.

Photographs of good contract and intensity on glossy paper are only acceptable. Colour photographs or drawings cannot be accepted.

Use bar scale on all illustrations instead of numerical scales that must be changed if reductions are necessary.

References

All references to publications made in the text should be made by quoting the author's name (without initials) and year of publications in paranthesis.

The list of references at the end of the manuscript should be arranged alphabetically by author's names and chronologically per author.

If the referred publications are written by more than two authors, in the text only the name of the first author should be indicated, the other co-authors are denoted by "et al.", however, in the list of references the names of authors and all co-authors should be mentioned.

In the list of references all references should be written, e. g. Balogh, K., A. Barabás (1972): The Carboniferous and Permian of Hungary. Acta Miner. Petr. Szeged, XX/2, 191–207.

At references to books beside the author's name, year of publicaton, title and the publishing house should also be mentioned.

In the case of references for symposium volumes, special issues or multi-authors books, the following system should be used: Roser, B. P., C. W. Childs, and G. P. Glasby (1980): Manganese in New Zealand. In: I. M. Varentsov and Gy. Grassely (Editors): Geology and Geochemistry of Manganese, Vol. II. Akadémiai Kiadó, Budapest, 199–211.

Manuscripts that are not adequately prepared will be returned to the authors(s).

CONTENTS